Creation, Growth and Stability of Aerated Structures in Chemically Leavened Wheat Flour Dough Systems and Relationships to Mechanical Properties Assessed with Low-intensity Ultrasound

BY

Guillermo Guido Bellido

A Thesis Submitted to the Faculty of Graduate Studies
In Partial Fulfillment of the Requirements of the Degree of

DOCTOR OF PHILOSOPHY

Department of Food Science
University of Manitoba
Winnipeg, MB

THE UNIVERSITY OF MANITOBA

FACULTY OF GRADUATE STUDIES

*****

COPYRIGHT PERMISSION

Creation, Growth and Stability of Aerated Structures in Chemically Leavened Wheat Flour Dough Systems and Relationships to Mechanical Properties Assessed with Low-intensity Ultrasound

BY

Guillermo Guido Bellido

A Thesis/Practicum submitted to the Faculty of Graduate Studies of The University of Manitoba in partial fulfillment of the requirement of the degree

DOCTOR OF PHILOSOPHY

I hereby declare that I am the sole author of this thesis.

I authorize the University of Manitoba to lend this thesis to other institutions or individuals for the purpose of scholarly research.

Guillermo G. Bellido

I further authorize the University of Manitoba to reproduce this thesis by photocopying or by other means, in total or in part, at the request of other institutions or individuals for the purpose of scholarly research.

Guillermo G. Bellido

ACKNOWLEDGEMENTS

I would like to express my sincere gratitude to my thesis adviser, Dr. Martin G. Scanlon, for guiding me throughout my studies, and for showing me that scientific rigor is not meant to be used to establish facts, but rather, to discover them. I would also like to thank Dr. John H. Page for providing direction to my project and for sharing with me his technical expertise on ultrasound. I also want to thank Dr. Harry D. Sapirstein for his advice and support and for serving as a member of my thesis examining committee.

I also want to thank Dr. Guy Della Valle for agreeing to act as the external examiner on my thesis examining committee. My sincere thank you also goes to Dr. Benedikt Hallgrímssson and his staff (University of Calgary) and Dr. Grant M. Campbell (University of Manchester) for allowing me to conduct part of the experiments found in this thesis in their research laboratories.

The advice and encouragement provided by my classmates, Faculty, and staff in the Food Science Department, particularly from Dr. Susan Arntfield and Dr. Erik Liu, throughout my PhD studies is also thankfully acknowledged. The financial support provided by the Canadian Wheat Board Graduate Fellowship, Garson N. (Gerry) Vogel Memorial Award, James W. Barlow Graduate Fellowship, and Natural Sciences and Engineering Council of Canada (NSERC) are gratefully recognized.

I also want to thank my family at home in Peru, my brother Erik in Winnipeg, and my wife's family in France for their unyielding encouragement during my PhD studies. Lastly, I wish to express my appreciation to my wife, Anne-Sophie, for her unwavering support throughout my studies, and for being my source of strength and harmony while pursuing a career path that may often seem chaotic.

Gracias quiero dar al divino Laberinto de los efectos y de las causas
Por la diversidad de las criaturas que forman este singular universo,
Por la razón, que no cesará de soñar con un plano del laberinto,
Por el álgebra, palacio de precisos cristales,
Por el arte de la amistad,
Por el mar, que es un desierto resplandeciente,
Por el lenguaje, que puede simular la sabiduría,
Por el olvido, que anula o modifica el pasado,
Por la mañana, que nos depara la ilusión de un principio,
Por la noche, su tiniebla y su astronomía,
Por los minutos que preceden al sueño,
Por el sueño y la muerte, esos dos tesoros ocultos,
Por la música, misteriosa forma del tiempo,
Por los íntimos dones que no enumero.

Jorge Luis Borges

Un extracto del escrito: *Otro Poema de los Dones*

TABLE OF CONTENTS

LIST OF FIGURES

LIST OF TABLES

LIST OF ABBREVIATIONS

Abbreviation	Description
USDA	United Stated Department of Agriculture
CWRS	Canada Western Red Spring
SAPP	Sodium acid pyrophosphate
ADA	Adipic acid
KAT	Potassium acid tartrate
GDL	Glucono-delta-lactone
NV	Neutralizing value
EMT	Effective medium theory
DDD	Dynamic dough density
D	Diameter
TSE	Total specific energy
ISP	Instantaneous specific power
n	Number of moles
ρ	Dough density
ρ_{gf}	Density of the gas-free dough
γ	Specific volume, surface tension
ϕ	Gas void fraction
β	Longitudinal modulus
μ	Shear modulus, mean bubble size
Subscript m	Matrix
Superscript '	Real part [of the longitudinal/shear modulus]
Superscript ''	Imaginary part [of the longitudinal/shear modulus]
t	Time
k	Reaction rate constant
K	Compressibility
K_L	Overall mass transfer coefficient
X_W	Mass fraction of water in dough
CO_2	Carbon dioxide
C^*	Carbon dioxide concentration at interface
C_∞	Carbon dioxide concentration in dough
Q	Molar rate of transfer
H	Henry's law constant
P	Pressure
R	Universal gas constant
V	Volume
T	Absolute temperature
LL	Low level
ML	Medium level
HL	High level
D_L	Coefficient of diffusivity
FFT	Fast Fourier transform

Creation, Growth and Stability of Aerated Structures in Chemically Leavened Wheat Flour Dough Systems and Relationships to Mechanical Properties Assessed with Low-intensity Ultrasound

Abstract

Identifying and understanding the mechanisms of bubble nucleation, growth and stability in bakery products is of great significance to cereal science and technology since an essential facet of transforming wheat flour into bakery products is the creation of desirable aerated textures. This thesis is a comprehensive investigation of how the aerated structure of chemically leavened dough is created during mixing and bulk fermentation. Low-intensity ultrasound (40 kHz) was used to probe the mechanical properties of the fermenting doughs and the ultrasonic data interpreted in light of the effective medium theory (EMT) proposed by Sheng (1988) with a view to gaining a better understanding of the role of gas bubbles and the dough matrix on the overall mechanical properties of dough in breadmaking.

All experimental lean formula doughs were prepared using flour from bread wheat and with four chemical leavening systems containing sodium bicarbonate and sodium acid pyrophosphate 40 (SAPP), adipic acid (ADA), potassium acid tartrate (KAT), or glucono-delta-lactone (GDL). Their aeration during fermentation was monitored via assessment of void fraction as a function of fermentation time. To determine void fraction (ϕ), the density of the doughs was measured (alongside the ultrasonic experiments) as a function of time using a novel dynamic dough density (DDD) system, while their matrix density (ρ_m), necessary to calculate void fraction from density measurements, was quantified using non-invasive microcomputed tomography (μCT). The development of the mechanical properties of the experimental dough

systems, that in large measure governs their gas retention properties, was measured using a Tweedy 1 mixer operated at a constant energy input (40 kJ kg^{-1}). To measure the actual rates of CO_2 evolved by the chemical leavening systems at ordinary fermentation temperatures (27 and 39 °C), an original methodology that made use of a computerized pressuremeter, the Gassmart apparatus, was developed.

Results showed that the changes in void fraction alone ($0.04 < \phi < 0.66$) could not account for the changes in ultrasonic velocity and attenuation, suggesting that ultrasonic properties were also sensitive to the presence of fermentation by-products (e.g., salts) through the effect of these by-products on the mechanical properties of the dough matrix. The EMT, which made use of the velocity and attenuation data to account for the viscoelastic nature of the dough, was capable of describing the individual contributions of the bubbles and the dough matrix to the overall mechanical properties of SAPP doughs. The EMT had difficulty in doing so in ADA, KAT, GDL doughs, likely because in these highly aerated systems it became necessary to account for higher order scattering contributions associated with the low frequency tail of the resonant interaction of ultrasound with the bubbles. The complex longitudinal elastic modulus $\beta^* \ (= \beta' - j\beta'')$ was used to describe the mechanical behaviour of fermenting doughs containing ADA, KAT, GDL. Changes in viscous losses of mechanical energy (β'' / β') in the experimental doughs as their aerated structure expanded during fermentation followed closely the changes observed in gas retention properties (measured separately), with higher losses of mechanical energy being associated with higher losses in gas retention properties. A remarkable increase in β'' / β' was observed in the experimental doughs when their gas cell walls approached their limit of expansion (i.e., bubble coalescence).

In conclusion, this thesis has demonstrated that ultrasonic velocity and attenuation measurements of fermenting dough could determine non-invasively, non-destructively, and in real time, the mechanical properties of chemically leavened dough. The EMT model showed that even in these simpler chemically leavened dough systems, profound changes in matrix properties occur as a result of the conversion of acid and base to salt and the concomitant effect on the properties of the dough.

CHAPTER ONE

Introduction

1.1. Bubble growth phenomena in breadmaking: *Status quo* and current challenges

With an annual worldwide production of nearly 600 million tons, wheat is currently the world's second most grown and first most consumed cereal crop (USDA, 2006). Much of the success of wheat as a cereal crop stems from its adaptability to a wide range of agronomic growing conditions, high yield, ease of cultivation, and ease of safe storage for long periods of time (i.e., years). However, the prominence of wheat as a staple food resides on its unique ability to produce leavened bread. This uniqueness arises from the unique rheological properties of wheat flour proteins. When appropriately hydrated and developed during mixing, the gluten proteins are able to form a viscoelastic network capable of entrapping and retaining gas during mixing, proving and baking. Baking solidifies the expanded network so that a loaf of bread with high volume and even crumb structure can be fabricated.

Since the objective of breadmaking is to produce a loaf of bread with a light and even crumb structure (Bloksma, 1972a), it is reasonable to conclude that the most important characteristic of bread quality is its cellular structure (Scanlon & Zghal, 2001). Hence, to fabricate bread of good quality or, more importantly, to control the quality of bread, one must have a good control over the formation, subsequent growth and stability of gas bubbles in the dough. Understanding how air bubbles nucleate in the bread dough during mixing is a fundamental first step because it was shown conclusively over 60 years ago that these air bubbles are the only nuclei available for subsequent gas cell

growth (Baker & Mize, 1941). A further reason for studying bubbles in dough is that dough exhibits extremely complex rheological properties (Bagley et al., 1998), and bubble numbers and sizes will affect dough rheology (Bloksma, 1981; 1990a; Carlson & Bohlin, 1978). For example, the rate of disproportionation of air bubbles in the dough is influenced by bubble sizes and by the separation between them (van Vliet, 1999), while the number density of bubbles has a remarkable effect on the rheological properties of the dough (Chin et al., 2005; Elmehdi et al., 2004). Despite the technological and scientific importance of acquiring quantitative data on the bubble size distribution in dough, dough's opacity and fragility have contributed to difficulty in acquiring these data.

Although gas entrainment plays a primary role in breadmaking, the heart and soul of the breadmaking process is leavening (Chiotellis & Campbell, 2003a), as in this stage gas bubbles grow due to CO_2 evolved by yeast fermentation of sugars, causing the dough to leaven and a highly aerated structure to be formed. The stability of gas bubbles in the dough (i.e., maximum dough expansion) is dictated by the limit of expansion of the gas cell walls since their failure leads to bubble coalescence and the eventual loss of the leavening gas (Dobraszczyk et al., 2003). Because the limit of dough expansion with constant gas production is controlled by the rheological properties of the dough, bubble formation phenomena such as bubble growth and stability is typically studied using rheological principles. However, dough rheology is often studied independently of its gas bubble content, an idea that was contended nearly 30 years ago by Carlson and Bohlin (1978), later dismissed by Bloksma (1981), and more recently brought again back into light by Chin et al. (2005).

Chin et al. (2005) found that the physical presence of gas bubbles can disrupt the integrity of the dough structure that is having its rheological properties assessed. Bubbles were found to decrease the strain hardening behaviour of the dough and the resistance of the dough to failure, and to increase the work input of the dough during mixing. The work of Chin et al. (2005) emphasizes not only the importance of gas bubbles to dough rheology but also the need to communicate the gas content of dough when reporting rheological data. One consequence of such an observation is that interpretation of rheological data cannot disregard the presence of bubbles. For example, various studies have found that the baking performance of various wheat flours correlate well with their strain hardening properties – the ability of the high molecular weight proteins to re-orient and form entanglements upon considerable strains of the gas cell walls are achieved (Dobraszczyk, 1997a, 1997b, 2004; Dobraszczyk & Morgenstern, 2003; Dobraszczyk & Roberts, 1994; Dobraszczyk et al., 2003). However, it is questionable whether the non-reported gas contents of the dough samples are not in fact affecting the deformation at which the doughs reached a strain hardening index of 1, which is the basis for explaining gas cell instability (Dobraszczyk et al., 2003).

A technique that has proven to be sensitive to the presence of gas bubbles in dough *in situ*, and thus to the rheological properties of dough is low intensity ultrasound (Elmehdi, 2001; Elmehdi et al., 2003a; Kidmose et al., 2001; Lee et al., 1992; Leroy et al., 2007; Létang et al., 1996, 2001; Scanlon et al., 2002). The ultrasonic technique has also been proven to be useful for measuring the physical and structural properties of the dough and the resulting baked product (Elmehdi, 2001; Elmehdi et al., 2003b; Lagrain et al., 2006). Elmehdi (2001) obtained fundamental rheological information (obtained from

measurements of ultrasonic velocity and attenuation) on dough that had been mixed with no yeast, and in yeasted dough as it underwent expansion due to fermentation. Elmehdi (2001) encountered practical difficulty, however, in determining the absolute attenuation coefficient and the void fraction in yeasted dough. This was so because the biological activity of yeast on fermentable sugar not only generates CO_2 but also a myriad of metabolic by-products whose influence on dough rheology is very difficult to predict (Hoseney et al., 1981, 1988). Measuring the void fraction of yeasted dough is also challenging as it requires knowledge of the density of the gas-free dough. The gas-free dough density is technically difficult to measure because it is affected by the rate and extent to which the various metabolic products of yeast fermentation are produced. Moreover, since the fermentative action of yeast cells depends on glycolysis, a metabolic pathway for which it is impossible to develop a precise analytical description (Bier et al., 2000), it is actually very difficult to reliably predict the gas production characteristics of yeasted dough.

Indeed, while measurements of a dough's gas-retention properties have received a great deal of attention, particularly over the past few years (Campbell, 1991; van Vliet, 1999; Shimiya & Nakamura, 1997; Campbell et al., 1993, 2001; Martin et al., 2004a, 2004b; Mitchell et al., 1999; Shah et al., 1999), actual gas production properties are typically not measured, even though this information is required to model such important breadmaking phenomena as bubble growth during proving of the dough (Chiotellis & Campbell, 2003b). In a recent study, Chiotellis and Campbell (2003b) noted that a technique capable of providing accurate information on the rates of carbon dioxide production in fermenting dough is still needed.

Though yeast is the typical source of carbon dioxide in breadmaking, it is by no means the only source. A viable source of carbon dioxide is contained within chemical leavening systems which are traditionally used only for leavening batters, but that more recently have started to be incorporated in unconventional breadmaking applications. Heidolph (1996) suggested that judicious selection of chemical leavening systems can afford good control over the production of carbon dioxide during dough leavening. Better control over gas production should then translate into better control over the quality of bread. To date, there exist very few comprehensive reports in the cereal chemistry literature on the use of chemical leavening agents to leaven bread dough (Parks et al., 1960; Conn, 1981; Holmes & Hoseney, 1987a, 1987b; Heidolph, 1996).

1.2 Scope of this thesis

This thesis is a comprehensive investigation of the formation of the aerated structure of chemically leavened dough with emphasis on five areas 1) developing techniques to measure the bubble size distribution and void fraction of dough, 2) developing a technique capable of measuring gas evolution from flour-water-salt mixtures containing chemical leavening systems, 3) improving and using a dynamic dough density technique for measuring the gas retention capacity of doughs formulated with chemical leavening systems 4) comparing two novel methods for measuring dynamic dough density in chemically leavened dough 5) measuring mechanical properties of chemically leavened dough using the ultrasonic technique developed by Elmehdi (2001). All experimental lean formula doughs were prepared using Canadian Western Red Spring wheat milled as a straight-grade flour and with four chemical leavening systems containing sodium bicarbonate and one of four leavening acids

(sodium acid pyrophosphate 40 (SAPP 40), adipic acid, potassium acid tartrate (cream of tartar), and glucono-δ-lactone (GDL)). The specific objectives of this thesis were as follows:

1. To evaluate the influence of dough consistency on the size distribution of gas bubbles entrained during standard mixing conditions. The effect of chemical leavening systems on the aeration of dough (gas void fraction) during mixing was also investigated. Dough aeration as well as characterization of the bubble size distributions was accomplished non-invasively using x-ray microtomography, by adapting methodologies developed by medical sciences for studying the skeletal morphology of small animals, to cereal science.
2. To characterize the gas production properties of glucono-δ-lactone, potassium acid tartrate, sodium acid pyrophosphate and adipic acid in wheat flour dough using the Gassmart apparatus, a pressuremeter. In addition, the gas-production activity of selected chemical leavening systems on the basis of the dough rate of reaction (DRR) test was characterized. Gas production rates were discussed in light of chemical kinetics theory to determine rate of reaction constants.
3. To determine the effects of four types and three levels of chemical leavening systems and three fermentation temperatures on the dynamic specific volume of dough made from bread wheat flour, with a view to interpret the experimental results in light of the theoretical model developed by Venerus et al. (1998) for describing diffusion-controlled bubble growth in a viscoelastic medium.
4. To characterize the development of dough with or without the addition of chemical leavening systems and mixed under various headspace pressures using a

high-intensity Tweedy-type mechanical dough development mixer and to monitor and compare the density changes of chemically leavened dough with two internationally recognized techniques to measure changes in dough density dynamically.

5. To evaluate the use of a low-intensity ultrasound (40 kHz) transmission technique to unambiguously assign and model the individual contributions of the gas phase and of the dough matrix to the overall rheological properties of chemically leavened dough.

CHAPTER TWO

Literature Review

2.1. Historical background

Few foods have a history as illustrious and significant to humanity and civilization as bread (Scanlon & Zghal, 2001). There is archeological evidence that einkorn wheat and emmer wheat, two ancestors of today's bread wheat species (Zohary & Hopf, 2000), were growing wild in the Near East "fertile crescent' (e.g., the valleys of the Tigris and Euphrates in the Mesopotamia region; Sarkar, 1993), as far back as the Neolithic era (c.a. 9,000 BC) (Liu & Scanlon, 2003; Orth & Shellenberger, 1988; Zohary & Hopf, 2000). Archeologists believe that the need to make whole wheat more palatable prompted the creation of the first crushing tools to separate the hull from the grain (Delcourt et al., 2006). The discovery that grinding the grain into a coarse meal resulted in an even more appealing food gave birth to the first milling tools (i.e., mortar and pestle and the saddlestone) (Sarkar, 1993). The genesis of bread is thought to have occurred after the coarse meal was formed into a paste that was then baked into a flat unleavened bread (Sarkar, 1993; Delcourt et al., 2006). The people from the mountainous regions of the Near East (e.g., city of Jericho in Palestine) are likely to be the first Neolithic cultures that consumed this form of unleavened bread (Orth & Shellenberger, 1988; Delcourt et al., 2006). However nutritious unleavened bread may have been, it is difficult to imagine bread rising to today's rank of staple food without having an aerated structure. This aerated structure, however, was conceived much later, after the advent of civilization, about 4000 BC in Egypt. At this time, it is thought that the accidental incorporation of

spent yeast from the winemaking process in the dough caused it to rise such that the baked product was found to have a superior quality (i.e., a soft, palatable texture) (Liu & Scanlon, 2003; Scanlon & Zghal, 2001). Since then, bread has been used for nutritional, sociological, linguistic, spiritual, economical, and political purposes to further the progress of humanity and civilization (Elmehdi, 2001; Liu & Scanlon, 2003; Orth & Shellenberger, 1988). The aim of this thesis is to explore yet another facet of bread: a scientific one.

Scientifically, the main focus of cereal science research has been to investigate the molecular basis of the unique viscoelastic properties of wheat dough. For a long time researchers recognized that the unique properties of dough were associated with the gluten proteins of wheat. University of Bologna researcher Beccari is believed to be the first researcher to have isolated the gluten proteins of wheat flour, by washing it with water, in 1745 (Osborne, 1907). However, the unique and yet complex character of wheat flour proteins became better understood only after the work of Osborne in 1907 (Osborne, 1907). In this *magnum opus*, Osborne reported the systematic fractionation of wheat endosperm proteins, and in so doing he laid down the scientific basis for studying plant proteins. Ever since the time of Beccari, wheat proteins have been a continued subject of study which have resulted in the publication of an enormous amount of research from academic, government and private research groups. In fact, gluten proteins are regarded as the most widely and comprehensively studied proteins in the plant kingdom (Shewry et al., 2001). Despite these great efforts, characterization of the structures of the gluten proteins and the molecular basis for their breadmaking properties

have proven a formidable task and are, in fact, still not well understood (Shewry et al., 2001).

More recently, there is increasing interest in understanding the unique properties of dough to make bread from the perspective of aeration processes; in this case, the protagonist is the gas phase of the dough. The importance of aeration to breadmaking can be appreciated from looking at changes in the gas phase in dough during breadmaking. For example, the fraction of gas in dough may constitute up to 20% and 70% of the dough total volume following the mixing (Baker & Mize, 1937) and fermentation (Bloksma, 1990b) stages, respectively. Surprisingly, efforts to understand the role of gas bubbles in the creation of the aerated structure of bread have received very little attention until recently.

Arguably, Campbell (1991) was the first study where the notion that aeration processes are essential to breadmaking was proposed, so that the study and elucidation of these processes are vital to gain a better understanding on the unique properties of dough. Campbell (1991) proposed that breadmaking can be characterized as "a series of aeration stages", wherein "(i) bubbles are incorporated into the dough during mixing; (ii) these bubbles are expanded due to carbon dioxide production during proving (rising); and (iii) the aerated structure is modified and set by baking". Subsequent works by Campbell and coworkers support Campbell's initial view (Campbell & Mougeot, 1999; Chin & Campbell, 2005a, 2005b; Chiotellis & Campbell, 2003a, 2003b; Campbell et al., 1993, 1998; Chin et al., 2004, 2005). Overall, these studies have provided new insight into the influence of processing conditions (e.g., mixing headspace pressure), processing

equipment (e.g., type of mixer), wheat flour quality (e.g., strong versus weak flour), and formula ingredients (e.g., bakery ingredients) on the quality of bread.

The most important studies providing information on the role of bubbles with respect to the physical properties of the dough will be reviewed in the following sections. Chapter 2.2 will deal with the relationships between major dough constituents and the rheology of dough, and will review and discuss the most important literature on conventional and novel techniques to study dough rheology and gas void fractions. Particular emphasis will be placed on low intensity ultrasound as this novel technique has shown sensitivity to both the properties of the gas and the liquid phases of the dough (Elmehdi, 2001; Elmehdi et al., 2003a, 2004; Kidmose et al., 2001; Lee et al., 2004; Létang et al., 1996, 2001; Ross et al., 2004; Scanlon et al., 2002). Chapter 2.3 will review relevant literature on carbon dioxide gas producing agents, with especial emphasis being placed on chemical leavening systems. Methods for measuring gas production will also be critically discussed; relevant factors and the most discriminative techniques found in the literature to measure gas production will be noted. Chapter 2.4 will deal with literature on methods used to characterize the aerated structure of dough and the gas retention capacity of doughs during leavening. An exposition of the most important models available for characterizing the growth of gas bubbles in dough will be discussed. Probable mechanisms controlling bubble growth during proving/fermentation will be discussed.

2.2. Relationship between dough rheology and dough constituents

2.2.1. Dough rheology and dough chemical constituents

The basic ingredients of dough (i.e., a lean formula dough) are flour, water, salt (sodium chloride), and yeast. Typically, French and Italian baguettes are one of the few breads that are made of these four ingredients alone, as other breads, including English and North American breads, contain other ingredients such as dough improvers (e.g., L-ascorbic acid and lipids). The focus of this thesis is on a dough prepared from the basic dough ingredients. Because the yeast ingredient has been replaced by chemical leavening systems in the present work, the emphasis of the literature will be placed on the latter as far as leavening agents are concerned. The typical composition of bread dough and of wheat flour is shown in Table 2.1. Flour is essentially composed of five constituents: proteins, carbohydrates, lipids, moisture, and minor constituents (ash and vitamins). The contributions of lipids and other minor dough constituents to dough rheology will not be reviewed since this thesis will focus on lean formula doughs wherein the said constituents should remain relatively constant as they will not be added or subtracted by formulation or during sample preparation.

2.2.1.1. Carbohydrates

The major carbohydrate in dough is starch. In wheat, starch represents 60-75% of the weight of the grain on a dry basis, which makes starch the main form of energy storage in wheat (Pomeranz, 1988). Hence, much of the energy provided by bread to humans is in the form of starch (Betschart, 1988; Scanlon & Zghal, 2001). Besides serving a nutritional function in bread, starch plays important roles in breadmaking. Firstly, it serves as a source of energy to the metabolic activities of yeast during

Table 2.1. Typical composition of bread flour[1] and dough[2]

Constituent	(%)
Flour	100
Protein	13.7
Carbohydrate	70.8
Fat	1.4
Moisture	13.6
Other	0.5
Sodium chloride	2.0
Water	65
Yeast	3.5

([1])Adapted from Kulp (1988) (excluding dough improvers)
([2]) Adapted from Pomeranz (1988) for hard red wheat patent flour

fermentation (Kulp, 1973; Bier et al., 2000), which is an essential step for making yeasted bread (Hoseney, 1998; Bloksma, 1990b, 1990c; Baker & Mize, 1937; Chiotellis & Campbell, 2003a, 2003b). Secondly, its water absorption is essential in dough development, with native (intact) starch granules having a water absorption capacity as high as 0.45 kg of water per kg of dry matter, and with damaged starch (i.e., due to milling) having this capacity increased up to 2 kg of water per kg dry matter (Bloksma & Bushuk, 1988). Thirdly, its gelatinization is essential in the rigidification of the structure of bread; otherwise, bread will quickly collapse upon baking (Kulp, 1973; Bloksma & Bushuk, 1988; Hayman et al., 1998a, 1998b; Kusunose et al., 1999).

Starch is essentially composed of glucose, which is present in polymeric forms as amylose and amylopectin (Hoseney, 1998). Amylose is essentially a linear polymer (MW ~ 250,000 or 1,500 glucose units) of α-D-glucose linked by α -1,4 glucosidic bonds. Amylopectin is composed of a shorter linear polymer of α-D-glucose (linked by α -1,4 bonds) that is highly branched by α -1,6 bonds (MW ~ as high as $1x10^8$) (Hood & Liboff, 1982; Lineback & Rasper, 1988). The molecular structural description and properties of

the two major polymers of starch are beyond the scope of this work and will not be discussed.

At a microscopic level, wheat starch granules appear to have lenticular or round shape (Hood & Liboff, 1982) and vary widely in their size, with large granules having sizes between 20-35 μm and small granules sizes between 2-10 μm (Bloksma, 1990b; Hoseney, 1998). Reconstitution studies show that wheat starch cannot be replaced by any other cereal starch (Taranto, 1983; Bloksma & Bushuk, 1988). For example, unlike potato starch granules, wheat starch granules do not gelatinize early during baking which has been found to prevent early setting of the dough (Kusunose et al., 1999). Relative to cereal starch granules, including those from barley, triticale, rye oats, corn, sorghum and rice, wheat starch granules have a unique range of gelatinization temperatures, 58-64 °C (Hoseney, 1998), which are also thought to be an important factor in determining their distinctive functionality in breadmaking (Kusunose et al., 1999).

Compared to the protein component, starch has a minor influence on the viscoelastic character of dough, though some researchers recommend that this contribution should not be disregarded (Kusunose et al., 1999). Bloksma and Bushuk (1988) reviewed various flour reconstitution studies and identified two major influences of starch on dough rheology. Firstly, increasing starch content in the flour results in dough with reduced extensibility. Secondly, when the starch content is high, the influence of water on dough rheology is higher. This latter observation highlights the fact that the "continuous" protein phase of dough is actually not continuous, as it contains starch granules. Until the baking stage, these starch granules act essentially as an inert filler of the protein phase because they remain in their native state. However, the concentration of

starch granules in the "continuous phase" of dough is so large (60% in volume) that interactions can indeed become important (Bloksma, 1990b; Bloksma & Bushuk, 1988).

Another important role of starch granules is the one played in dough stability. Bloksma (1990b) proposed that a limit to the expansion of the gas cell walls of bubbles late during fermentation or early during baking is given by the thickness of starch granules. If the wall between two bubbles becomes thinner than this limit (~ 35 μm; Bloksma, 1990b; Hoseney, 1998; Hayman et al., 1998b), the wall would collapse and the bubbles coalesce (van Vliet, 1999; Hayman et al., 1998a, 1998b). Yet, other researchers have postulated that bubbles are lined by a thin aqueous film that enables them to preserve their gas retention properties even after discontinuities form in the starch-gluten matrix (MacRitchie, 1976; Sahi, 1994; Gan et al., 1990; 1995). The existence of such a thin aqueous film is still speculative. Even if the thin aqueous film does exist, further research needs to be conducted in this area to elucidate its role in bubble growth stability.

Another carbohydrate with an important water absorption capacity is pentosans. They constitute 2 to 3% of the weight of the flour (Bushuk, 1966). The high water absorption capacity of pentosans (~10 kg of water per kg of dry mass) make them very important in breadmaking; they are responsible for up to 25% of the total water absorption of dough (Bloksma & Bushuk, 1988; Gan et al., 1989).

2.2.1.2. Proteins

Based on Osborne solubility fractionation, wheat proteins can be classified as soluble in water (albumins), soluble in dilute salt solutions (globulins), soluble in 70% alcohol (gliadins), and soluble in dilute acid solutions or bases (glutenins). Chen and Bushuk (1970) further fractionated the glutenin fraction into two fractions: one soluble in

dilute acid solutions and the other insoluble in this solution. Albumins and globulins are mainly non-storage proteins (i.e., enzymes) which represent about 10% and 5% of the total proteins, respectively (Orth & Bushuk, 1972). Conversely, gliadins and glutenins are storage proteins (contain nitrogen reserves mainly in the form of glutamine) which represent nearly 85% of the total proteins (~ each present at one to one ratio).

The unique properties of dough (i.e., its viscoelasticity) are attributed to the water insoluble fraction (Orth & Bushuk, 1972), with the gliadins and glutenins being responsible for the viscous and the elastic properties of the gluten proteins, respectively. A balance between these two properties is required to make bread of good quality (Bushuk, 1985; Bloksma & Bushuk, 1988; for review see Bushuk & MacRitchie, 1988).

Gliadin proteins are single chain polypeptides with a relatively wide range of molecular weights which can be classified into four groups, based on their separation using polyacrylamide gel electrophoresis: α-, β-, γ-, and ω-gliadins. On the other hand, glutenins are composed of two types of subunits based on molecular weight: the high molecular weight glutenin protein subunits (HMW-GS, M_r = > 100,000) and the low molecular weight glutenin subunits (LMW-GS, M_r = 25,000 to 100,000), linked by interpolypeptide disulfide bonds (Pomeranz, 1988). Wheat flour that has a high concentration of HMW-GS correlates well with good breadmaking performance (Shewry et al., 2001). At the molecular level, the unique characteristics of wheat flour proteins can be investigated in relation to distinctive aspects: the molecular properties of the proteins, the interactions among the proteins, and the interactions between the proteins and other flour constituents (Bloksma & Bushuk, 1988). The first aspect is a subject of extensive research and much debate which is beyond the scope of this thesis. For more information

on this subject the reader is referred to Shewry et al. (2001), Singh and Khatkar (2005), Singh and MacRitchie (2001) and references therein. The second aspect, the type and mechanisms underlying molecular interactions in wheat flour dough, is a complex subject and it will be briefly reviewed next. For extensive information on this topic see Bushuk (1998) and references therein.

Molecular interactions are important because they determine structural conformation of wheat proteins and enable one to understand from a molecular perspective the influence of bakery ingredients on the rheological properties of dough. Disulfide bonds (S-S) are strong molecular bonds (stronger than non-covalent bonds) that are expected to restrict the fluid behaviour of dough (Bloksma & Bushuk, 1988). However, disulfide bonds are capable of entering into interchange reactions with low molecular weight molecules containing free sulfhydryl (-SH) groups (i.e., thiol compounds) (McDermott & Pace, 1961), which explains the ability of dough to undergo permanent deformation while maintaining the integrity of a continuous protein network with disulphide cross-links (Bloksma & Bushuk, 1988). Bloksma (1972b) proposed that only a small fraction of the thiol groups in dough are rheologically active, with L-cysteinylglycine and glutathione making up most of these active thiol groups while only representing about 1% of the approximately 0.5 mmol of thiol groups per kg of dough. The thiol-disulfide interchange reactions enable the protein network to maintain its integrity in spite of being subjected to large stresses (e.g., during mixing) by enabling the dough to be deformed permanently (Blokma & Bushuk, 1988). Glutenins participate in thiol-disulfide interchange reactions because the disulfide bonds they possess form intra- and inter-molecular cross-links within and among polypeptide chains, respectively

(Shewry et al., 2001). Conversely, gliadins are unable to participate in thiol-disulfide interchange reactions as they only have intrapolypeptide disulfide bonds (Shewry et al., 2001). Hydrogen bonding is another type of molecular interaction that contributes to the molecular conformation of wheat proteins (Belton, 1999).

In hydrogen bonding a positively charged hydrogen atom (H^+) is shared between a potential acid (proton donor) and a potential base (protein acceptor) (Eliasson & Larsson, 1993). Hydrogen bonding is important in gluten structure because about 35% of amino acids in wheat proteins are glutamine (Wu & Dimler, 1963a), an amino acid that is capable of hydrogen bonding (Belton, 1999).

Hydrophobic interactions are also important in stabilizing protein conformation as wheat protein contains about 30% nonpolar amino acid residues (Wu & Dimler, 1963a). Hydrophobic interactions explain the solubility of gliadin in 70% ethanol in which protein aggregates dissociate (Bloksma & Bushuk, 1988).

Another type of molecular interaction contributing to the structure of gluten is ionic interactions. The importance of ionic interaction to overall protein structure is controversial. The amino acids that can be ionized at the typical moderately acidic pH of the dough are lysine, arginine, and histidine (Wu & Dimler, 1963b). However, these three amino acids only make up about 2% of the total amino acids in the gluten proteins (Wu & Dimler, 1969a). The strong effects of small amounts of chaotropic salts on the rheological properties of dough nonetheless indicate that ionic interactions are important in the structural conformation of gluten (Preston, 1981, 1984; Fu et al., 1996; Guy et al., 1967; Tanaka et al., 1967).

2.2.1.3. Water

Water is a fundamental ingredient in dough as without it there would be no dough. Water has a plasticizing effect in dough. Doughs with little water lack cohesion, whereas dough with excessive water produces a viscous dough with poor elasticity and that is incapable of retaining gas. Typically, the water content of water makes up 40% of total weight of the dough. Generally, the stiffness of a dough decreases between 5-15% if the water content in the dough is increased by 1% of flour mass (Bloksma and Bushuk, 1988). Similarly, studies using small-strain rheology techniques have found that increasing water content in dough lowers its storage (G') and loss (G'') moduli (Létang et al., 1999; Navickis et al., 1982).

The aqueous phase of dough is essential for the occurrence of many important physical, chemical and biochemical reactions in the dough during breadmaking. For example, carbon dioxide diffusivity in dough is estimated on the basis of the water content of dough, because carbon dioxide is thought to diffuse only in the water fraction (aqueous phase) of dough (de Cindio & Correa, 1995).

2.2.1.4. Salt

Common table salt (sodium chloride) is typically added to the dough at a concentration of 1.5-2.5% (flour basis) (Bloksma & Bushuk, 1988; Eliasson & Larsson, 1993). From a rheological perspective, sodium chloride affects dough rheology by stiffening the dough and making it less sticky. Another important function of sodium chloride is to improve flavour. It has been found that salt affects yeast fermentation, with higher concentrations hampering yeast activity during fermentation.

The report of Hlynka (1962) illustrates the strengthening effect of chloride ions by stating that dough development time (time to reach 500 B.U.) in a Farinograph increases by about 0.5 min for each 1% of salt increased in the dough formula. In general, the influence of sodium chloride or other salts on gluten proteins is explained in terms of lyotropic salt effects via changes in electrostatic and/or hydrophobic interactions (Preston, 1981, 1984; Galal et al., 1978; Guy et al., 1967; Tanaka et al., 1967). This is typically measured in terms of changes in protein extractability and protein aggregation, which implies that measurements of protein properties have been done in dilute solutions (Huebner, 1970; Preston, 1981; 1984; Kim & Bushuk, 1995; Fu et al., 1996; Guy et al., 1967). Hence, interpretation of the effect of salts in dough, which has a water fraction of 0.4, in the light of evidence obtained in dilute solutions is debatable, though it certainly provides a theoretical framework for initial assessments of the effect of salts.

Because of their predominantly high levels of apolar amino acids and low concentrations of charged amino acids (Wu & Dimler, 1963b), gluten proteins have a high density of hydrophobic residues and a low density of charged amino acids on their surface which are expected to promote protein-protein aggregation via hydrophobic interactions when in solution (Preston, 1981). This is so because apolar amino acids are so numerous that they are unable to accommodate themselves in the interior of the protein structure. On the other hand, charged amino acids are almost always located on sites on the protein surface to promote interaction with water, while polar amino acids can reside in the interior or exterior with little difference in free energy (the energy of transfer of apolar residue to water is much higher) (Preston, 1984). There is a good body of evidence supporting the view that flour protein extractability is strongly influenced by

the presence of salts (Huebner, 1970; Preston, 1981, 1984; Kim & Bushuk, 1995; Fu et al., 1996; Guy et al., 1967). These studies have shown that at low salt concentrations, protein interactions decrease (i.e., protein extractability increases) with increasing amounts of salts because the salts interact with oppositely charged groups on the protein surface to form a double layer of ionic bonds (i.e., Helmholtz double layer). Hence, at low salt concentrations (<0.5*M*; Preston, 1984) the extractability and aggregation properties of gluten proteins are chiefly determined by ionic interactions (Preston, 1981). The magnitude of this effect is determined by ionic strength and the charge density and distribution on the protein surface (Preston, 1981). Studies on gluten secondary structure using Fourier transform infrared spectroscopy suggest that protein aggregation arising from the addition of small amounts of NaCl is related to an increase in hydrogen-bonded intermolecular β-sheet structures (Wellner et al., 2003). At higher salt concentrations, extensive ionic shielding causes the neutralization of electrostatic interactions between charged amino acids which makes the protein act as a neutral dipole. In this salt concentration regime, two distinct effects have been identified: an electrostatic 'salting–out' effect and a hydrophobic 'salting–in effect'. The former, where proteins become neutrally charged, is associated with the non-specified binding of salt ions to oppositely charged groups on the protein surface, with chaotropic ions (e.g., iodate) being more effective in this regard than sodium chloride or potassium chloride (Wellner et al., 2003), so that even small amounts of moderately chaotropic ions can be have significant dough strengthening effects (i.e., increasing extensigraph length and dough development time; Preston, 1989). The latter is associated with the effect of neutral salt solutions of the lyotropic series on modifying 'water structure' (Preston, 1981). The anions from the

neutral salts alter the free energy requirements for the transfer of apolar amino acids to the aqueous environment. Preston (1981) explains that increasing salt concentration increases the ordering of water so as to increase the energy requirements for the transfer of apolar amino acids to the aqueous medium. Since, by definition, non-chaotropic salts increase the order of water (Eliasson & Larsson, 1993), these salts are expected to promote hydrophobic interactions because the increased ordering of water structure mean that it would be thermodynamically unfavorable for apolar amino acids to be exposed on the protein surface. A greater degree of hydrophobic interactions is expected to increase the tendency of proteins to aggregate (when in solution). This increase in protein aggregation was observed in the study of Preston (1981) in which the extractability and the turbidity of gluten proteins extracted in dilute acetic acid solutions decreased and increased, respectively, with increasing concentrations of non-chaotropic sodium salts. The just described "salting in" effect (i.e., protein aggregation) depends on the nature of the salt according to the lyotropic (Hofmeister) series (chaotropic order increases): citrate > phosphate > tartrate > sulfate > acetate > chloride > nitrate > bromide > iodide > thiocyanate (Preston, 1981, 1984, 1989; Eliasson & Larsson, 1993; Holmes & Hoseney, 1987a; Kinsella & Hale, 1984; Wellner et al., 2003).

The lyotropic series suggests that, for instance, the ability of phosphate anions to induce protein aggregation is greater than that of chloride anions, at a constant molar concentration. In fact, Holmes and Hoseney (1987a) found that a chaotropic salt like sodium chloride required 339 mg (0.6 mmol) to produce a specified Mixogram pattern, whereas non-chaotropic salts such as sodium tartrate required 194 mg (0.1 mmol), and sodium phosphate only 142 mg (0.1 mmol). The weakening effect observed in dough

when sodium chloride was replaced by sodium sulfate can also be explained in terms of lyotropic effects (Eliasson & Larsson, 1993). Protein aggregation arising from the addition of non-chaotropic salts (e.g., tartrate and phosphate) in dough tends to reduce dough strength (Kinsella & Hale, 1984; Guy et al., 1967) and to hamper dough gas retention capacity (Holmes & Hoseney, 1987a). For example, Holmes and Hoseney (1987a) reported that loaf volume can be reduced by as much as 25% when 2.0% (flour basis) sodium chloride is replaced by sodium phosphate at the same level.

2.2.2. Dough rheology and aeration

2.2.2.1. Influence of gas bubbles on dough rheology

Historically, as mentioned earlier, dough rheology literature disregards the contributions of the gas phase to the rheology of the dough and considers gas bubbles to be an independent variable which is rarely reported (Chin et al., 2005). However, the fraction of gas in dough may constitute up to 20% of the dough total volume following mixing (Baker & Mize, 1937) and up to 70% during the latest stages of fermentation (Bloksma, 1990b). In fact, the view that the breadmaking process can be described as "a series of [aeration] operations" where the objective is "to manipulate the distribution of gas bubbles in dough" (Campbell et al., 1991) has been supported by various studies (Campbell & Mougeot, 1999; Chin & Campbell, 2005a, 2005b; Chiotellis & Campbell, 2003a, 2003b; Campbell et al., 1993, 1998; Chin et al., 2004, 2005). However, the study of gas bubbles and their importance to the rheological properties of dough is far from being a recent subject matter.

Based on a mathematical analysis of the material properties of the gaseous and non-gaseous phases of dough, Carlson and Bohlin (1978) were able to relate dough

rheology with the characteristics of the gas phase (i.e., gas bubble number and sizes) by proposing that the surface tension at the gas-dough interface contributed to the elastic character of dough. Later on, Bloskma (1981) would examine Carlson and Bohlin's (1978) work and determine that the contribution of the surface tension of gas bubbles to the elastic modulus of dough was actually insignificant. Recently, Chin et al. (2005) were able to quantify the effect of aeration on the rheological properties of dough. They used a dough inflation technique, the Dobraszczyk–Roberts Dough Inflation System, to test doughs under biaxial extension at deformation rates comparable to those experienced by the dough during fermentation. Chin et al. (2005) provided experimental evidence suggesting that aeration affects dough rheology due to the contribution of air (which contains oxygen) to the oxidation and development of dough during mixing, and also due to the physical presence of bubbles in dough. The physical presence of gas bubbles was found to promote disruption of the integrity of the dough structure. Bubbles were also found to decrease the strain hardening behaviour of the dough and the resistance of the dough to failure, and to increase the work input of the dough during mixing. The work of Chin et al. (2005) emphasizes not only the importance of gas bubbles to dough rheology but also the need to communicate the gas content of dough when reporting rheological data. Measuring the rheological behaviour of a single bubble during bulk inflation using air as the expansion gas (i.e., using a system such as the Dobraszczyk–Roberts Dough Inflation System), may not truly reflect the actual rheological behaviour of the fermenting dough, wherein an entire population of gas bubbles exists (Chapter 3) that undergoes subsequent expansion (Shah et al., 1998).

2.2.2.2. Conventional measurements of dough rheology

It is widely accepted that the rheological characteristics of dough are of great importance for the quality of the final baked product. As can be expected, the complex composite nature of wheat flour dough–a mixture of flour constituents, water, yeast, salt, and other ingredients– makes it difficult to interpret rheological information (Bloksma, 1990a; Fu et al., 1997), though it is believed that the viscoelastic properties of the dough are dominated by the viscoelastic properties of the wheat gluten proteins (Baird & Labropoulos, 1982; Eliasson & Larsson, 1993; Faubion and Hoseney, 1990; Shewry et al., 2002). Rheological characterization of dough is also important for generating data that can be used to differentiate flour quality and ingredient functionality (Edwards et al., 1999; Uthayakumaran et al., 2000) and to determine the behaviour of dough pieces during mechanical handling (e.g., dividing, rounding, and moulding), dough expansion during baking, and the textural characteristics of the finished loaf of bread (Bloksma & Bushuk, 1988; Amemiya & Menjivar, 1992; Bushuk et al., 1968).

The rheological characterization of dough can be determined using both empirical and fundamental rheological techniques. Empirical rheological instruments such as the Brabender Farinograph, National Mixograph, Chopin Alveograph and Brabender Extensigraph have been widely used in the milling and baking industries since the early 1930's to predict the performance of flour dough. The value of these instruments is that the rheological information they provide usually correlates well with the quality of the final product. However, these correlations are remotely connected to the physical properties of the final product which may explain why these instruments are only valid within a limited range of experimental conditions (Dobraszczyk & Roberts, 1994).

Furthermore, in measuring rheological properties, empirical rheological instruments employ arbitrary units that cannot be readily converted to more useful fundamental dimensions since they do not involve the measurement of a well-defined physical quantity, making fundamental interpretation of the rheological data extremely difficult (Janssen et al., 1996a, 1996b).

Fundamental rheological techniques apply the basic principles of physics to study the rheological properties of dough. Several techniques have been proposed for examining the fundamental rheological properties of wheat flour dough including creep and creep recovery (Hibberd & Parker, 1979; Campos et al., 1997; Edwards et al., 1999), stress relaxation (Launay & Bure, 1974; Fu et al., 1997), and dynamic oscillatory measurements (Menjivar, 1989; Abdelrahman & Spies, 1986; Amemiya & Menjivar, 1992; Faubion & Hoseney, 1990; Faubion et al., 1985; Edwards et al., 1999; Tronsmo et al., 2003). From all these techniques, techniques employing dynamic oscillatory measurements are arguably the most commonly used to study the fundamental rheology of dough.

Dynamic oscillatory measurements use small oscillatory deformations to probe the rheology of the dough in the linear viscoelastic region. In this region the structural integrity of the dough sample is maintained, which allows dynamic oscillatory techniques to make multiple rheological measurements in the same sample as temperature, strain, or frequency are manipulated (Hibberd, 1970a, 1970b; Abdelrahman & Spies, 1986; Faubion & Faridi, 1986; Faubion & Hoseney, 1990; Hibberd & Parker, 1975; Hibberd & Wallace, 1966; Faubion et al., 1985; Smith et al., 1970). The vast majority of these small strain studies have employed shear strains or stresses. One important reason for their

preferred used in dough rheological studies is that dynamic oscillatory techniques have been successfully applied to studies in synthetic polymer systems where a well-developed theoretical framework does exist (Ferry, 1961; Phan-Thien & Safari-Ardi, 1998; Singh & MacRitchie, 2001; Bagley et al., 1998; McKinley et al., 1999). However, unlike in some synthetic polymer systems, attempts to mathematically describe the rheological behaviour of dough through the use of constitutive equations have failed or could not be validated independently (Ramkumar et al., 1996; Wang & Kokini, 1995; Bagley et al., 1998; Phan-Thien et al., 1997), and attempts to establish a credible relationship between small strain dynamic rheological properties and baking performance have also been unsuccessful (Safari-Ardi & Phan-Thien, 1998; Autio et al., 2001; Hayman et al., 1998b; Janssen et al., 1996b; Kokelaar et al., 1996; Mani et al., 1992). A limit to the applicability of dynamic oscillatory techniques is the fact that they test the rheology of the dough at rates and deformations that do not resemble the actual strains experienced by the dough during fermentation and baking. Small strain dynamic rheometers typically operate at small strains of up to 1%, compared to strains of several hundred percent commonly found in bread making. For example, detecting strain hardening, a property that arises from entanglements of high molecular wheat proteins and is thought to be responsible for the baking performance of dough, requires the use of a natural (Hencky) strain of at least 0.75 (~53% strain) on biaxial extensional testing (van Vliet et al., 1992; Dobraszczyk & Roberts, 1994; Wikstrom & Bohlin, 1999). Also, an important consideration when characterizing the behaviour of the dough during breadmaking is to measure its rheology using a suitable deformation mode, e.g., shear is more predominant during mixing, elongation during leavening and both shear and elongation during dough forming.

Another complexity in modelling the behaviour of the dough by the use of rheometry is the difficulty in obtaining batches of dough with homogenous rheological properties, a heterogeneity that becomes more apparent when the doughs are "optimally" mixed than when they are over-mixed (Bagley et al., 1998). Because one major difference between optimally mixed and over-mixed dough is the gas void fraction (Baker & Mize, 1941), it seems logical to examine the extent to which the dough gas phase contributes to the overall rheological behaviour of the dough (Chin & Campbell, 2005a). In fact, the relationship between dough rheology and its gas bubble content is not straightforward and rather it has been the subject matter of numerous studies for many years (Campbell, 1991; van Vliet, 1999; Baker & Mize, 1941; Shimiya & Nakamura, 1997; Campbell et al., 1993, 2001; Elmehdi et al., 2003a, 2004; Mitchell et al., 1999; Shah et al., 1998, 1999; Martin et al., 2004a, 2004b).

2.2.2.3. A novel ultrasonic technique to study dough rheology

2.2.2.3.1. Introduction to ultrasound

Ultrasound is referred to as the study and application of mechanical sound waves propagating at frequencies above those within the hearing range of a human, i.e., at frequencies above 16 kHz (Povey, 1997). The hearing range of young persons, however, is thought to extend beyond 16 kHz, so the lower limit of the ultrasonic range is somewhat arbitrary but is generally agreed to be in the frequency range between 16 to 20 kHz.

2.2.2.3.2. Principles of ultrasound propagation

Since ultrasound represents energy transmitted as stress waves, the modes of vibration associated with the propagation of ultrasonic waves depend on the physical

state of the material through which ultrasound propagates – ultrasound propagation differs in solids greatly from those in liquids (Ensminger, 1973; Povey, 1997). On one hand, liquids attenuate shear waves very rapidly and are capable of transmitting only longitudinal waves and surface waves. Solids, on the other hand, may transmit a wide variety of wave modes, including longitudinal waves, shear waves, surface waves, and Lamb waves (Ensminger, 1973).

Surface and Lamb waves are complex modes of wave motion and have found applicability in systems other than foods (Ensminger, 1973). Shear waves are commonly used to test the properties of solids, but are rarely used to analyze liquids for reasons discussed above. Shear and longitudinal waves are the most commonly used in the food industry since foods generally possess properties intermediate between solids and liquids (Elmehdi, 2001; Javanaud, 1988; McClements, 1995, 1997, 1998; Povey, 1997, 1998; Kidmose et al., 2001; Lee et al., 1992; Lee et al., 2004; Létang et al., 2001). In a shear wave, the particle motion in the medium as the wave travels is normal to the direction of propagation, hence elements of the medium pass ultrasonic energy from one element to another element by shear stresses (McClements, 1997). The longitudinal wave is a compressional wave in which the particle motion is in the same direction as the propagation of the wave (McClements, 1997). In the present thesis (Chapter 7), the ultrasonic technique will use longitudinal waves to probe the properties of fermenting dough.

Because the characteristics of the ultrasonic wave are affected by the structure and composition of the medium through which it propagates (Javanaud, 1988; McClements, 1997; Povey, 1997), ultrasound can be used as an effective means to study the physical

properties of foods. The properties of an ultrasonic wave traveling coherently through a food material can be measured in terms of ultrasonic velocity, attenuation coefficient, and acoustic impedance.

2.2.2.3.3. Ultrasonic velocity

The velocity at which an ultrasonic wave propagates through a material depends on the type of wave, the elastic properties of the medium, the density of the medium, and, in some cases, the frequency (Povey, 1997). The mathematical relationship between the ultrasonic properties of a material and its physical properties has been derived by mathematical analysis of the propagation of a longitudinal ultrasonic wave through a material (Povey, 1997; Elmehdi, 2001; Létang et al., 2001):

$$(k / \omega)^2 = \rho / \beta \tag{2.1}$$

$$\beta = B + 4/3\ \mu \tag{2.2}$$

Here, k is the complex wave number of the material ($= \omega/v + j\alpha$), v is the ultrasonic phase velocity, ω is the angular frequency ($=2\pi f$), f is the ultrasonic frequency, and β is the longitudinal modulus, ρ is the density, B is the bulk modulus (the reciprocal of compressibility), μ is the rigidity modulus (shear modulus), $j^2 = -1$, and α is the attenuation coefficient. These simple two equations clearly illustrate the fundamental relationship between the measurable ultrasonic properties (v and α) and the density and longitudinal modulus of a material; for example, measuring the ultrasonic properties of a material and measuring its density independently can provide information on its mechanical properties. For low-attenuating materials ($\alpha << \omega/v$), Eq. (2.1) can be simplified (Povey, 1997):

$$v^2 = \beta / \rho \tag{2.3}$$

It is worth noting to make the distinction between phase velocity and group velocity and elaborate on the conditions in which they are both equal. The phase velocity of a wave is the rate at which the phase of the wave propagates in space. This is the velocity at which the phase of any frequency component of the wave will propagate. Any particular phase of the wave (e.g., a wave crest) would appear to travel at the phase velocity (Povey, 1997).

$$v_p = \omega / k = f \lambda \tag{2.4}$$

The group velocity of a wave, on the other hand, is the velocity with which the overall shape of the wave's amplitude (also termed "the envelope of the wave") propagates through space. The group velocity is defined in terms of the wave's angular frequency ω and the wave number k (Page et al., 1996):

$$v_g = d\omega / dk \tag{2.5}$$

The function $\omega(k)$, which gives ω as a function of k, is known as the dispersion relation. When the phase velocity varies with frequency, the dispersion curve, $\omega = v_p(\omega)\, k$, is no longer linear, so that the slope $d\omega / dk$, or group velocity, is not equal to the ratio ω / k, so that the group and phase velocities take on different values. In other words, "whenever the dispersion relation ($\omega(k)$) is non-linear, waves of different frequencies travel at different speeds", so that the phase velocity and the group velocity are required to adequately describe wave propagation (Page et al., 1996). Throughout this thesis, the experimental ultrasonic technique uses the phase velocity to measure the properties of fermenting dough.

2.2.2.3.4. Attenuation coefficient

The attenuation coefficient is another important physical property of a material that can be measured using ultrasound. Ultrasonic attenuation is determined by measuring the amplitude of the ultrasonic signal A (V) as a function of the distance L of the material through which it passes:

$$A(L) = A_0 \, exp\left[-\alpha \frac{L}{2}\right] \tag{2.6}$$

where α is the attenuation coefficient (m^{-1}), A_0 is the intensity of the ultrasonic signal at the input face of the sample (at $L = 0$) (V). As implied by Eq. (2.6), the amplitude of the ultrasonic signal drops exponentially as it travels through the material. All materials, including foods, attenuate ultrasound to some degree, the most important sources of attenuation being absorption and scattering (McClements, 1997). Absorption, which occurs indistinctly in both homogenous and inhomogeneous materials, is an important energy loss mechanism that arises from molecular processes that transform acoustic energy into various forms of energy, and ultimately into heat. The main mechanisms of absorption in liquids are thermal conduction, viscosity and molecular relaxation; detailed information on these mechanisms can be found elsewhere, e.g., Povey (1997). Scattering is only important in inhomogeneous material. Scattering occurs because the sound wave interacts with the discontinuities in the material causing it to travel in directions other than its forward direction. In materials where strong scattering occurs, it is difficult to obtain information on the exact location of the scattering units since the direction of the scattered waves are 'scrambled' after traveling multiple scattering paths through the sample (Cowan et al., 2002). These scattered waves would not be part of the leading edge

of the ultrasonic signal detected by a receiver positioned in the forward direction (in which the signal generator and receiver are located on opposite sides of the sample), so that analysis of the information carried by scattered waves requires sophisticated interpretative approaches such as "diffusing acoustic wave spectroscopy" (Cowan et al., 2002; Page et al., 2000, 2003), topics that are beyond the scope of this thesis. Yet, there is often complex absorption mechanisms associated with scattering which can dictate the overall attenuation in the sample (e.g., thermal or viscous loss mechanisms). As is the case of ultrasonic velocity, the attenuation coefficient of a material can provide valuable information on the material's physical and chemical properties as well (Elmehdi, 2001; Javanaud, 1988; McClements, 1995, 1998; Povey, 1997, 1998; Verdier & Piau, 1996; Elmehdi et al., 2003a, 2004; Kidmose et al., 2001; Lee et al., 1992; 2004; Létang et al., 1996, 2001; Scanlon et al., 2002; Verdier et al., 1998).

2.2.2.3.5. Impedance

Acoustical impedance is another important property of a material as it determines the fraction of an ultrasonic wave that is reflected from its surface (McClements, 1997, Kulmyrzaev et al., 2000). The specific acoustic impedance of a material is defined as the ratio of the acoustic excess pressure (ΔP) to the particle velocity (ξ') (Povey, 1997):

$$Z = \frac{\Delta P}{\xi'} = \frac{\omega\rho}{k} \approx \rho v \tag{2.7}$$

In general, Z is a complex quantity ($Z = R_z + jX_z$), which consists of resistive (R_z) and reactive (jX_z) components (Kulmyrzaev et al., 2000). If the attenuation of the material is small (i.e., $\alpha << \omega/v$), then the reactive component can be neglected, so that $Z = R_z = \rho v$, which is called the characteristic impedance. Matching the impedance of the transducer

to the sample is important, as this acoustic mismatch leads to energy losses due to reflection (McClements, 1997). If the acoustic mismatch is large enough, it is possible that no ultrasonic signal would be transmitted to the sample.

2.2.2.3.6. Signal analysis

Besides the importance of ensuring that the ultrasonic signal is transmitted through the sample, the transmitted signal carries information at a broad spectrum of frequencies, the interpretation of which can be difficult in terms of measurements of ultrasonic velocity and the attenuation coefficient. An important tool to analyze the signals detected in ultrasonic experiments is the Fourier transform. The Fourier transform, which has applications ranging from music to telecommunications, is an integral transform that re-expresses a function in terms of sinusoidal basis functions, i.e., as a sum or integral of sinusoidal functions multiplied by some coefficients (also "amplitudes"). In terms of waveforms, the Fourier analysis decomposes an arbitrary wave shape into simple harmonic waves (Wolfson & Pasachoff, 1987). The Fourier analysis depends on the property of any time-varying physical variable (ξ) that can be described mathematically as the sum of sine, cosine, and exponential functions of frequency (Povey, 1997):

$$\xi(t) = \sum_{n=1}^{\infty} \xi_n(\omega) \exp(i\,\omega_n\, t) \qquad (2.8)$$

The coefficients $\xi_n(\omega)$ are referred to as the Fourier coefficients and plotting the relationship between these coefficients and frequency gives rise to the *Fourier transform* of ξ (Povey, 1997). Fourier transforms are particularly useful in analysing ultrasonic

information because it allows us to express such variables as amplitude (or attenuation) and velocity as a function of frequency (Povey, 1997).

The frequency dependence of ultrasonic velocity and attenuation coefficient is complicated but it has been used to study the properties of food. For instance, for a monodisperse sunflower oil-in-water system (20% v/v) at 30 °C it has been found that in the long wavelength region, ultrasonic velocity is independent of frequency while the attenuation scales with the square of the ultrasonic frequency (Povey, 1997). A practical use of such information is that phase volume determinations, for instance, can be made more easily in this frequency region since particle size- and frequency-dependent effects can be neglected. This is so because in the long wavelength limit the wavelength of the probing wave is much larger (~ ten to fifty times larger) than the characteristic size of the scattering unit in the dispersed phase of a two-phase composite (Povey, 1997).

In this thesis, the frequency of the ultrasonic transducers would be carefully chosen so that the ultrasonic pulse would probe the physical properties of dough while in the long wavelength limit. As will be seen in the proceeding Section of this thesis, the experimental transducers produced an ultrasonic signal with a wide range of frequencies. During data analysis of these signals, the Fourier transform was used to determine the frequency dependence of the ultrasonic velocity and attenuation coefficient of the experimental samples. This brief explanation on signal processing will be further expanded in Chapter 7 of this thesis in the context of my experimental results. Nonetheless, the reader is referred to Ensminger (1973), Reid and Passin (1992), or Povey (1997) to learn more about signal processing techniques and their interpretation in relation to the study of the physical properties of multiphase materials.

2.2.2.3.7. Ultrasonic instrumentation

Typically, ultrasonic instrumentation has the following components: (1) signal generator, (2) signal amplifier, (3) oscilloscope, (4) transmitting and receiving transducers, (5) measurement cell (sample holder), and (6) a storage device (PC) with signal analyzing capabilities (i.e., software). The number and configuration of components of the ultrasonic instrument may vary depending on the ultrasonic technique. Broadly and certainly arguably, the ultrasonic techniques fall into one of the following categories (Kaczmarek, 2001): (1) pulse/tone burst ultrasonic techniques, (2) broadband ultrasonic spectroscopy, (3) continuous wave methods, (4) resonance spectroscopy, (5) critical angle reflectometry, and (6) acoustical microscopy. Pulse/burst methods can be further divided into other sub-categories depending on the mode of detection of the sound wave, with ultrasound being propagated in the reflection (echo) mode, transmission mode, and the transmission mode for the study of surface waves (Kaczmarek, 2001).

The ultrasonic technique that will be used in this thesis falls into pulse/tone burst method in the transmission mode. In this ultrasonic technique, one transducer is excited with a short pulse of electrical voltage produced by the signal generator. The piezoelectric ceramic crystal in the transducer converts the electrical signal into a mechanical signal at the fundamental frequency of the transducer. The mechanical signal (sound signal) is propagated through the material (which is coupled between the transducers) and is then received by the second transducer. This transducer converts the mechanical signal back into an electrical signal that is then amplified by the signal amplifier, and acquired and displayed in the oscilloscope and stored in a PC for further signal processing. A trigger pulse from the signal generator is also used to synchronize

timing in the oscilloscope. An excellent discussion of calibration techniques and sources of errors associated with measurements of ultrasonic properties in multiphase materials is provided by Povey (1997 and 1998).

2.2.2.3.8. Ultrasonic studies of doughs

The need for improving our understanding of the relationship between the bulk rheological properties of foods and its molecular/structural properties is clear, as it is the need for developing techniques capable of on-line measurements for monitoring the properties of foods during processing and storage (McClements, 1997) - ideally in a closed loop mode (Challis et al., 2005). Ultrasound has enormous potential for addressing all these needs. Table 2.2 shows typical powers and particle displacement, among other parameters, associated with the properties of ultrasound. In the food industry, ultrasonic techniques employ one of two types of ultrasound powers, high-intensity (>10 kW m^{-2}) and low-intensity (<10 kW m^{-2}) ultrasound (McClements, 1997, Povey, 1997). The ultrasound powers that will be used in this thesis correspond to those of low-intensity ultrasound, which is unlikely to disturb the properties of the material through which it is propagated. Most notably, low-intensity ultrasonic techniques have favourable characteristics for being non-destructive, rapid, precise, relatively inexpensive, and for lending themselves to be used on-line and in optically opaque foods (McClements, 1997). Ultrasonic techniques have been widely employed for many decades in food processing, with the first application dating as far back as 1927 when high power ultrasound was found very efficient for the production of oil-in-water emulsions (Povey, 1998) and have since found diverse applications in food processing applications. The reader is referred to Javanaud (1988) and McClements (1995, 1997) and the references therein for a good

Table 2.2. Typical power levels and other propagation parameters for ultrasound propagation in water at 1 MHz and 30 °C

f (MHz)	T_0 (K)	p_0 (MPa)	I (kW m^{-2})	Δp (MPa)	s (x 10^{-6})	ξ (nm)	ξ' (mm s^{-1})	ξ'' (km s^{-2})	Z (MPa s m^{-1})	ΔT (mK)	ξ'/v (x10^{-6})
1	303	0.1	0.1	0.017	7.6	1.8	11.5	72	1.47	0.38	7.6
1	303	0.1	10	0.17	76	18	115	720	1.47	3.8	76
1	303	0.1	1000	1.7	760	180	1150	7200	1.47	38	760

Legend: f is the frequency, T_0, absolute temperature (K); p_0, absolute pressure (MPa); I, intensity (kW m^{-2}); Δp, pressure change from p_0 owing to the passage of ultrasound (MPa); s, the condensation (=[ρ_0 - ρ]/ρ_0); ρ_0, the static density (kg m^{-3}); ρ, the instantaneous density (kg m^{-3}); ξ, the particle displacement (nm); ξ', the particle velocity (mm s^{-1}); ξ'', the particle acceleration (km s^{-2}); ΔT, the temperature change owing to the passage of the ultrasound (K); Z (= $\Delta P/\xi' = \rho\, v$); the specific acoustical impedance (Pa s m^{-1}); and v the velocity of a compression ultrasound wave (1509.11 m s^{-1}). Taken from Povey (1997).

account of the multiple applications of ultrasound in food research and in food processing. The use of ultrasound to measure the properties of dough is very recent, with the first work reported by Lee et al. (1992), although preliminary work in this area started much earlier, as far back as the early 1980's by Dr. Malcolm Povey at the University of Leeds (Rubena Moorjani, M.Sc. thesis – Martin Scanlon, personal communications, 2007). Although other early reports also employed ultrasound to characterize the mechanical properties of dough (Kidmose, 2001; Lee et al., 2004; Létang et al., 1996, 2001; Ross et al., 2004), the first work that used ultrasound to systematically examine the physical properties of dough (in both unleavened and leavened dough) is attributed to Elmehdi (2001).

Elmehdi's (2001) work, as well as further interpretative refinements of his data in subsequent peer-reviewed publications, have corroborated the view that low intensity ultrasound is sensitive to the presence of gas bubbles and to the properties of the matrix of dough *in situ* (Elmehdi, 2001; Elmehdi et al., 2003a, 2004; Scanlon et al., 2002). The ultrasonic technique has also been proven to be useful for measuring the physical (e.g.,

rheological) and structural properties of the dough and the resulting baked product (Elmehdi et al., 2003b, 2004). Elmehdi (2001) obtained fundamental rheological information on dough that had been mixed with no yeast, and in yeasted dough as it underwent expansion due to fermentation. Elmehdi's (2001) work on the un-yeasted dough (mixed at different headspace mixing pressures to vary the gas content of the dough) found that the velocity of ultrasound decreased with increasing gas content, particularly when the gas content increased from 1 to 4 %, where the velocity changed dramatically (about one order of magnitude: 1,400 to 170 m/s). Attenuation of the ultrasonic signal increased in a linear manner as gas content was increased, up to a void fraction of ~ 8.5% (ambient pressure mixed dough). Attempts to model the velocity changes using theoretical fittings from Wood's approximation (Wood, 1941) to the velocity data suggested that the dramatic drop in velocity could not be explained in terms of the physical effects of a higher gas phase fraction alone.

To interpret the ultrasonic data, Elmehdi (2001) used an effective medium model (Sheng, 1988) that made use of both the velocity and attenuation data to measure the individual contributions of the gas phase and the non-gas phase (dough matrix) to the overall mechanical properties of the dough. The model indicated that the high ultrasonic velocities in the least aerated doughs were brought about by the stiffening effects of partial vacuum mixing on the dough matrix (i.e., an increased shear modulus of the matrix). Elmehdi et al. (2004) surmised that oxygen deprivation in the partially vacuum mixed dough decreased the degree of protein polymerization but increased the formation of non-covalent bonding in the dough matrix. Increasing the oxygen content during mixing by lessening the vacuum level caused an increase in the number of covalent bonds

and the disruption of non-covalent bonds. Consequently, the effective medium theory proved to be a useful tool to probe the rheology of (non-fermented) dough. Using the ultrasonic technique he developed for unyeasted dough, Elmehdi (2001) also studied the mechanical properties of fermenting dough. Although it was observed that velocity decreased with increasing void fraction, Elmehdi's (2001) experimental technique did not enable him to measure both the absolute attenuation coefficient and the gas void fraction of the fermenting dough. These two pieces of information are crucial to employ the effective medium model to interpret the ultrasonic velocity and attenuation data and so Elmehdi (2001) was unable to distinguish the effects of the gas fraction on the overall rheological properties of the dough.

Part of the practical difficulty encountered by Elmehdi (2001) in determining the absolute attenuation coefficient and the void fraction in yeasted dough was that the biological activity of yeast on fermentable sugar not only generates CO_2 but also a myriad of metabolic by-products whose influence on dough rheology are very difficult to predict (Hoseney, 1998; Matsumoto, 1988; Hoseney et al., 1981; Matsumoto et al., 1975). In breadmaking, yeast contributes to the texture, taste, flavour, aroma and nutritional value of the bread (El-Dash & Johnson, 1970; Johnson & Sanchez, 1973; Wiseblatt & Kohn, 1960; Hoseney et al., 1981, 1988).

2.3. Gas production in fermenting dough

It is well established that measurements of gas production and gas retention during leavening of the dough are of great importance to breadmaking, since it has long been known that dough of good gas-production and good gas-retention capacities is a pre-requisite to make good bread (Elion, 1940). While measurements of a dough's gas-

retention properties have received a great deal of attention, particularly over the past few years (Campbell, 1991; Martin, 2004; van Vliet, 1999; Shimiya & Nakamura, 1997; Campbell et al., 1993, 2001; Mitchell et al., 1999; Shah et al., 1999; Martin et al., 2004a, 2004b), actual gas production properties are typically not measured, even though this information is required to model such important breadmaking phenomena as bubble growth during proving of the dough (Chiotellis & Campbell, 2003b). In a recent study, Chiotellis and Campbell (2003b) noted that a technique capable of providing accurate information on the rates of carbon dioxide production in fermenting dough is still needed.

2.3.1. Yeast

Yeast, *Saccharomyces cerevisae*, is added to dough to produce carbon dioxide gas to leaven the dough. The fermentative action of yeast on sugars in the flour (i.e., glucose, fructose, sucrose, and maltose) is responsible for the production of carbon dioxide as well as for ethanol and energy. Yeast fermentation, or more precisely, yeast respiration in dough is predominantly anaerobic as oxygen reserves in the gas bubbles are quickly depleted by the rising number of yeast cells soon after the end of mixing (Scanlon et al., 2002). The chemical reaction can be summarized as follows:

$$\underset{\text{Glucose}}{C_6H_{12}O_6} + \text{yeast} \text{ -----> } \underset{\text{Ethanol}}{2C_2H_5OH} + \underset{\text{carbon dioxide}}{2CO_2} + \text{energy} \qquad (2.9)$$

The rate and the total consumption of the sugar substrate by yeast during fermentation are not known with certainty (Chiotellis and Campbell, 2003b). Part of the problem arises from the fact that carbon dioxide in the dough is present in the dough as either carbon dioxide inside gas bubbles, or dissolved in the dough aqueous phase. Predicting gas production rates in dough is very important as it allows predicting the rates

of aeration in dough. It also facilitates determination of the correct dosage of leaveners (yeast or chemical) needed to produce a characteristic bread or bakery product when the number, quality and/or quantity of the other formula ingredients is varied. But predicting the aeration of yeasted dough during leavening has proven to be an extremely difficult task (Campbell, 1991; Shimiya & Nakamura, 1997; Campbell et al., 1993, 2001; Martin et al., 2004a, 2004b; Mitchell et al., 1999; Shah et al., 1999; van Vliet, 1999). The fact is that the fermentative action of yeast cells depends on glycolysis, a metabolic pathway for which is impossible to develop a precise analytical description (Bier et al., 2000). Nevertheless, the need to predict the gas production characteristics of yeasted dough has led to a better knowledge on the importance of gas production rates on the aeration of dough.

Generally, the rate of carbon dioxide accumulation in fermenting dough is thought to adopt a constant value once the dough liquid phase becomes saturated with carbon dioxide (Bloksma, 1990a). Bloksma (1990a) also argued that once the dough liquid phase is saturated with carbon dioxide, the rate of expansion of the gas bubbles keeps pace with gas production. Using Henry's law, Bloksma (1990a) calculated the amount of CO_2 required for saturating the dough liquid phase to be 4.3×10^{-2} kmoles per m^3 of dough liquid phase at 27 °C. Bloksma (1990a) estimated that under typical yeast fermentation conditions with 2% yeast and 27 °C, the rate of gas production adopts a constant value of 2.5×10^{-5} kmoles carbon dioxide per m^3 liquid dough phase per second. Using these figures, Bloksma (1990a) calculated that dough takes about 1,700 s before it becomes saturated with carbon dioxide. Though saturation of the dough liquid phase can take longer than that (e.g., yeast does not become fully active at the end of mixing; Ponte et

al., 1960), the analysis of Bloksma (1990a) exemplifies the influence of the rate of carbon dioxide production on the rate of growth of the dough gas phase. In reality, gas production in yeasted dough is far from constant (Akdogan & Ozilgen, 1992; Chiotellis & Campbell, 2003a, 2003b; Sahlstrom et al., 2004; Shah et al., 1998). If yeast cells are not fully active at the end of mixing (e.g., when yeast cells are still dormant), then there is an initial lag period (where the rate of gas production does not keep pace with the rate of expansion of the dough gas phase). After the initial lag period the rate of carbon dioxide production with time follows to some extent the trace left by an exponential growth function: it is constant and positive for a period of time (~100 min; Chiotellis & Campbell, 2003b), and then it slows down exponentially until it becomes zero (Akdogan & Ozilgen, 1992; Chiotellis & Campbell, 2003a, 2003b; Sahlstrom et al., 2004; Shah et al., 1998).

As fermentation proceeds, carbon dioxide produced by the yeast reacts with water to form carbonic acid, so that carbon dioxide dissolved in water is in equilibrium with carbonic acid (Hoseney, 1998):

$$CO_2 + H_2O \longleftrightarrow H_2CO_3 \qquad (2.10)$$

Depending on the pH, carbonic dioxide can exist in dough as the free CO_2 or as one of two salts of carbonic acids (also called bicarbonates and carbonates, respectively):

$$H_2CO_3 \longleftrightarrow HCO_3^{1-} + H^+$$

$$HCO_3^{1-} \longleftrightarrow CO_3^{2-} + H^+$$

Fermentation with 2% yeast lowers the pH of dough by about 0.5 units or less in fermentation times as short as 90 min (Miller et al., 1994) or as long as 3 h (Bloksma & Bushuk, 1988), so that typically the pH of dough at long fermentation times is lower than

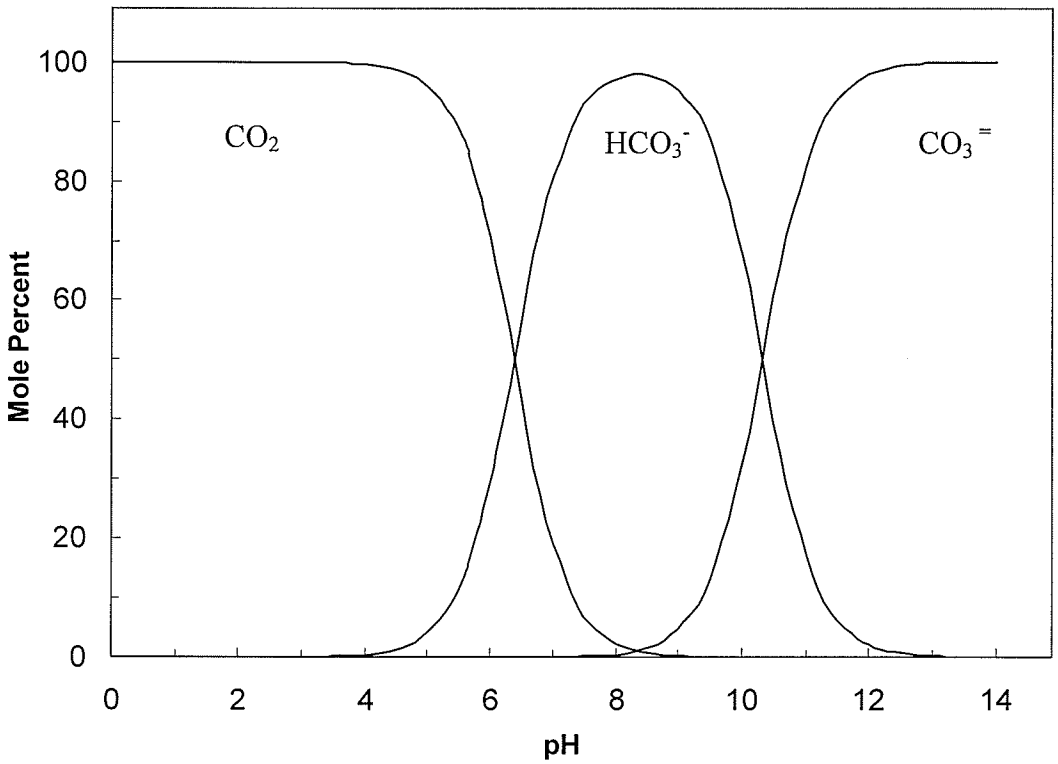

Figure 2.1. The relationship between pH and the chemical species under which CO_2 is present in the dough is shown. Constructed based on information from Hoseney (1988).

5.7 (Miller et al., 1994). The relationship between pH and the chemical species under which CO_2 is present in the dough is shown in Figure 2.1. At the normal pH of doughs (~ pH = 6; Holmes & Hoseney, 1987a), the carbon dioxide is mostly present as free CO_2 and a very small fraction is present as the chemical species HCO_3^- and CO_3^{2-}.

2.3.2. Chemical leavening agents

While fermentation of bread dough is traditionally carried out by the action of yeast cells on fermentable sugars, bread dough can also be leavened using chemical agents alone or in combination with the yeast (Heidolph, 1996; Holmes and Hoseney, 1987b). These chemical leavening agents have become particularly useful in leavening

bread dough during unconventional processing, such as extrusion processing (Geng & Hayes-Jacobson, 2001, 2003), or for doughs subject to refrigeration or frozen storage (Atwell, 1985; Laughlin & DeMars, 1999; Narayanaswamy & Daravingas, 2001; Perry & Colman, 2001, 2003; Hansen et al., 2003; Laughlin et al., 1999, 2000; Yong et al., 1983a, 1983b), or to microwave 'baking' (Corbin & Corbin, 1992, 1993; Geng & Hayes-Jacobson, 2003; Cochran et al., 1990). Chemical leavening offers several advantages over conventional (yeast) leavening. Chemically leavened dough is not sensitive to prolonged refrigeration or frozen storage conditions, having working temperatures that span from ambient to baking temperatures (Heidolph, 1996). Also, chemically leavened dough does not require long proofing times to start releasing carbon dioxide gas, thereby decreasing preparation times at the bakery facility (Huang & Panda, 2004).

Chemical leavening systems produce carbon dioxide by one of two methods, chemical decomposition or the chemical reaction of an acid with a base. The former method uses ammonium bicarbonate (NH_4HCO_3) to produce ammonia (NH_3), carbon dioxide and water once the dough or batter exceeds temperatures of about 59 °C (i.e., during baking). To prevent the retention of ammonia in the product and thus the formation of off-flavours, ammonium bicarbonate is only used in bakery products with a low moisture content (<5%), such as cookies and crackers (Conn, 1981; Heidolph, 1996; Hoseney, 1998). Most chemical leavening systems use the reaction of an acid with a base, or chemical neutralization, to produce carbon dioxide (Conn, 1981). Hence, typically, a chemical leavening system is comprised of a base and a source of acidity. Theoretically, any substance capable of releasing hydrogen ions could be used as the source of acidity in chemical leavening system. The *Food and Drugs Act* regulates the

acceptable sources of acidity in baking powder (which is a chemical leavening system) in Canada. The *Food and Drugs Act* stipulates that "the acid-reacting material" (leavening acid) can be one or any combination of lactic acid or its salts, tartaric acid or its salts, acid salts of phosphoric acid, and acid compounds of aluminum (Section 3 of the *Foods and Drugs Act*; Health Canada, 2007). Commercially, the North American baking industry employs a wider range of sources of acidity or *acidulants*, including adipic acid, ascorbic acid, citric acid, fumaric acid, glucono-δ-lactone, propionic acid and sorbic acid (Heidolph, 1996; Conn, 1981). The *Food and Drugs Act* stipulates, too, that "Baking Powder shall be a combination of sodium or potassium bicarbonate, an acid-reacting material, starch or other neutral material, [it] may contain an anticaking agent and shall yield not less than 10 percent of its weight of carbon dioxide, as determined by official method FO-3, Determination of Carbon Dioxide in Baking Powder, October 15, 1981."

The typical source of carbon dioxide used in chemically leavened products is sodium bicarbonate (Heidolph, 1996, Conn, 1981), which is used along with the leavening acid to evolve carbon dioxide at a specified rate. Hence, sodium bicarbonate and the leavening acid can be seen as the reactants in a chemical neutralization reaction. The type and quantities of reactants required to ensure complete neutralization is governed by stoichiometry, whereas the rates at which carbon dioxide is produced are governed by chemical kinetics. Hence, measurements of gas production in chemical leavening systems should provide valuable insights into the fundamental properties of chemical leavening systems, and so facilitate prediction of leavening performance in baked products (Hoseney, 1998).

The reaction between sodium bicarbonate and an acidulant can be characterized by the following chemical equation:

$$XH + NaHCO_3 \rightarrow NaX + CO_2\,(g) + H_2O \qquad (2.11)$$

The reaction shown in Eq. (2.11), however, only occurs after the acidulant and the sodium bicarbonate dissociate, according to the following general equations:

$$XH \rightarrow X^- + H^+ \;\; or \;\; XH + H_2O \rightarrow X^- + H_3O^+ \qquad (2.12)$$

$$NaHCO_3 \rightarrow Na^+ + HCO_3^- \qquad (2.13)$$

If the reaction shown in Eq. (2.12) proceeds at a much slower rate than the reaction in Eq. (2.13), then the overall rate of reaction (Eq. 2.11) will be determined by the rate of the slow reaction (Moore, 1962; Szabo, 1969). Because the sodium bicarbonate dissociates almost immediately upon contact with the formula water, the leavening acid's rate of dissociation, in fact, determines the rate of carbon dioxide production (Conn, 1981, Heidolph, 1996). Gas production with time in chemical leavened dough follows the trace of an exponential growth function (Parks et al., 1960). A measurement of the rate of reactivity of a chemical leavening system can be given by the dough rate of reaction (DRR) test. The rates of gas production and the methods to quantify them in leavening dough will be discussed in subsequent sections.

Determining the level of acidulant required to neutralize a given amount of sodium bicarbonate can be difficult. To address this problem, the chemical industry has developed the concept of neutralization value (NV). NV enables one to easily determine the level of leavening acid required to neutralize a given amount of sodium bicarbonate and compare the available acidity of leavening acids. NV is defined as the parts by

weight of sodium bicarbonate required to neutralize 100 parts by weight of the leavening acid (Heidolph, 1996):

$$Weight\ of\ leavening\ acid\ (g) = \frac{Weight\ of\ sodium\ bicarbonate\ (g)}{NV} x100 \qquad (2.14)$$

The neutralizing value of a leavening acidulant is determined by an official titration-based method, AACC Method 2-32A (AACC, 2000). Table 2.3 shows the neutralizing values of leavening acids available to the baking industry. The NV of a leavening acid increases with its acidity. The usefulness of the NV concept can be illustrated as follows. Let's say we need to determine the amount of potassium acid tartrate (NV=45) required to formulate refrigerated dough that has the following composition: 100 g of flour, water, salt, of which 2.5% by weight is sodium bicarbonate (Heidolph, 1996). The amount of potassium acid tartrate required to neutralize 2.5% sodium bicarbonate is 5.6 g $(= \frac{2.5\% x 100g}{45} x100)$. Figure 2.2 shows the chemical structures of the leavening acids that will be used in this thesis.

2.3.3. Other leavening agents

Besides carbon dioxide, steam, air and ethanol are the other leavening gases contributing to formation of the aerated structure of bread. Yet, the contribution of these 'secondary' leavening gases to dough aeration essentially only becomes important during baking, particularly the first stage of baking. Ethanol, another substance produced in dough with yeast during fermentation, is thought to contribute to dough leavening marginally, even though ethanol and carbon dioxide are produced in equivalent quantities (Bloksma, 1990a). Bloksma (1990a) claims that the ethanol produced during fermentation is completely dissolved in the dough liquid matrix and effectively does not

diffuse to the gas cells' interior. During baking, ethanol is thought to start to evaporate as the temperature of the dough increases during baking, a vapor that could theoretically work as a leavening gas; however, it is believed that ethanol mostly evaporates when the dough has reached a temperature (~ 50 °C) in which most of its gas retention capacity has already been lost (Bloksma, 1990a). Indeed, mathematical models describing the growth of gas bubbles during the baking stage neglect the contributions of ethanol to leavening while considering carbon dioxide and steam the major driving forces behind dough expansion during baking (Mitchell et al., 1999; Shah et al., 1998).

Table 2.3. Neutralizing value for acid sources that can be used in chemically leavened baked products

Acid source	Abbreviation[1]	NV[2]
Adipic acid	Adipic	115
Ascorbic acid	Ascorbic	52
Citric acid	Citric	159
Dicalcium phosphate dehydrate	DCPD	33
Dimagnesium phosphate	DMP	40
Fumaric acid	Fumaric	145
Glucono delta lactone	GDL	45
Lactic acid	Lactic	93
Monocalcium phosphate monohydrate	MCP.H_2O	80
Monocalcium phosphate anhydrous stabilized	AMCP	80
Monocalcium phosphate anhydrous	AMCP	83
Phosphoric acid	Phos Acid	172
Potassium acid tartrate	Cream Tartar	45
Propionic acid	Propionic	115
Sodium acid pyrophosphate	SAPP	72
Sodium aluminum phosphate anhydrous	SALPA	100
Sodium aluminum phosphate 4 hydrate	SALPH	100
Sodium aluminum sulfate	SAS	104
Sorbic acid	Sorbic	70

([1]) Common commercial abbreviation
([2]) Neutralizing value defined as parts (by weight) of sodium bicarbonate that 100 parts (by weight) of leavening acid will neutralized
Taken from Heidolph (1996)

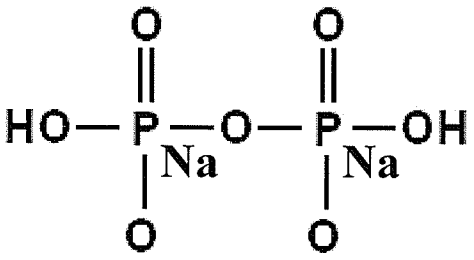

SODIUM ACID PYROPHOSPHATE

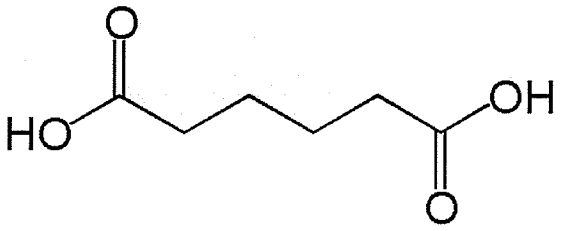

ADIPIC ACID

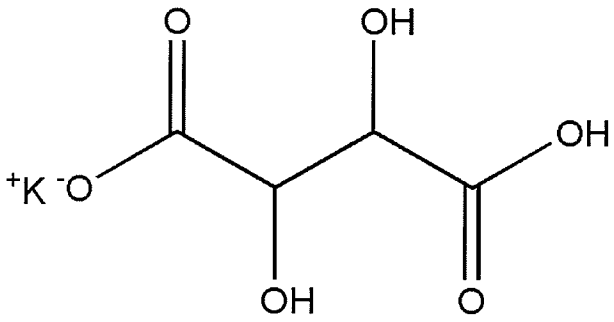

POTASSIUM ACID TARTRATE

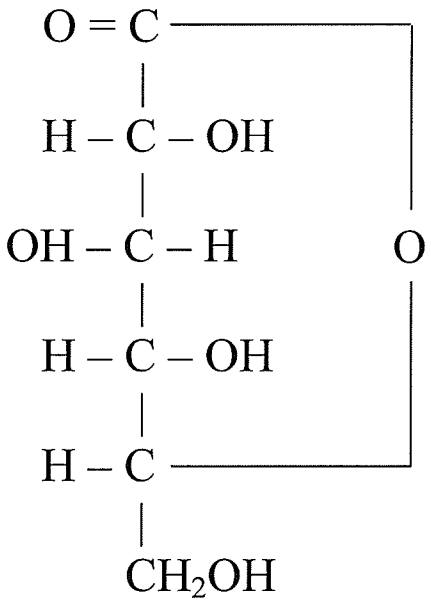

GLUCONO-DELTA-LACTONE

Figure 2.2. Chemical structures of four leavening acids that can be used in chemical leavening systems for bakery products.

It is worth noting that as the dough is heated during baking, the evaporation of water into steam and thermal expansion of air contribute to the expansion of the dough along with carbon dioxide. This is so because during baking carbon dioxide production from the yeast and carbon dioxide diffusion from the dough matrix are increased with respect to fermentation. In terms of the gas participating in thermal expansion, nitrogen is probably the only one left from the air initially entrapped in the dough during mixing, since the oxygen, the only other major gas in air, is thought to be quickly consumed by the yeast's metabolic activity early during respiration (Scanlon et al., 2002). Hence, nitrogen and carbon dioxide gases are responsible for thermal expansion, which occurs due to the increase in temperature according to the law of Gay-Lussac. For example, provided that the pressure in the gas phase of dough remains constant, nitrogen and carbon dioxide gases would expand by a factor of 343/300 = 1.14 if the temperature of the dough was increased from 27 to 70 °C (Bloksma, 1986); however, thermal expansion of the gas phase in the dough is likely not isobaric during baking due to changes in dough viscosity (Bloskma, 1990a; Fan et al., 1999). Bloksma (1990a) estimates that the contribution of all leavening gases to the expansion of dough during baking (i.e., oven rise) is as follows for a temperature increase from 27 to 70 °C (a reasonable change in temperature): 15% thermal expansion, 27% evaporation of carbon dioxide, 58% evaporation of water. During oven rise the void fraction (ϕ) of the dough has been estimated to increase from between 0.80 and 0.83 to between 0.83 and 0.88 (Bloksma, 1990a).

2.3.4. Chemical kinetics of carbon dioxide production in chemically leavened dough

Chemical kinetics theory is a valuable tool of physical chemistry that "is concerned with the dynamics of chemical reactions" (Hammes, 1978), allowing one to study "the rate of attainment of equilibrium" (Moore, 1962). Simply said, chemical kinetics is concerned with measuring the rate at which the reactants in a chemical reaction are transformed into the products of the reaction. Since gas production from a chemical leavening system or yeast is defined by a chemical reaction it seems logical to attempt to characterize carbon dioxide production in fermenting dough using chemical kinetics theory. However, a search in the literature indicates that chemical kinetics theory has not yet been used to characterize the properties of chemical leavening systems, nor has it been applied to study gas evolution in yeasted dough either.

Chemical kinetics was first investigated in 1850 by Wilhelmy (Moore, 1962) who followed with a polarimeter the dissociation of cane sugar (sucrose) into glucose and fructose in an acidic solution:

$$H_2O + \underset{\text{SUCROSE}}{C_{12}H_{22}O_{11}} \rightarrow \underset{\text{GLUCOSE}}{C_6H_{12}O_6} + \underset{\text{FRUCTOSE}}{C_6H_{12}O_6} \qquad (2.15)$$

Wilhelmy's experiments showed that the rate at which the concentration of sugar c decomposed with time t was proportional to the concentration of sugar remaining unconverted. He described the reaction velocity as:

$$-dc/dt = k_1 c \qquad (2.16)$$

The constant k_1 was defined as the rate constant or the specific rate of the reaction. Integration of this differential equation leads to the equivalence:

$$\ln c = -k_1 t + const.$$

At $t = 0$, the concentration has its initial value a, so that the constant is $ln\ a$. Therefore, $\ln c = -k_1 t + \ln a$, or

$$c = ae^{-k_1 t} \tag{2.17}$$

Wilhelmy's experiments did indeed show that the rate of sucrose hydrolysis closely followed this exponential decrease with time. Though the chemical equation noted above describes stoichiometrically the inversion of sucrose, it does not describe the reaction mechanism — a process which involves the sequence of individual chemical reactions that are needed to effect the overall chemical transformation. For chemical reactions requiring more than one step to produce a desired product (e.g., consecutive reactions with an intermediate state) the overall rate of the reaction is determined by the rate for the slowest step (Moore, 1962).

The principle behind chemical kinetics is that molecules (reactants) must collide with each other to react, with collisions involving two chemical species being more likely to occur than collisions involving three or more species. The reaction rate of a chemical reaction varies with the concentration(s) of the reactant(s), and this can be described mathematically in terms of their order of reaction (Boudart, 1968; Szabó, 1969; Lawrence et al., 1996). For instance, the decomposition of sucrose noted above is a first-order reaction because the rate of reaction depends on the concentration of the remaining sucrose raised to the power of one (i.e., rate = k_1 $[a]^1$). In a second-order reaction, the rate of reaction depends on the concentration of the remaining reactant raised to the power of two (i.e., rate = k_1 $[a]^2$). The order of a reaction provides information on macroscopic changes associated with the chemical reaction (Moore, 1962). The order of a reaction is determined by monitoring the appearance of products of a reaction or the disappearance

of reactants and can only be unequivocally determined experimentally (Boudart, 1968; Szabó, 1969; Lawrence et al., 1996). The difficulty in applying chemical kinetics principles to the study of chemical reactions relies on finding a suitable method to monitor the transformation of reactants into products, since maintaining the experimental system at constant temperature or timing the chemical reaction -the other two requirements- is usually straightforward (Moore, 1962).

Empirical work in chemical leavening systems shows that carbon dioxide production rates –thus the rate of the chemical reaction, closely follows exponential growth kinetics (Parks et al., 1960) as yeast gas production does (Akdogan & Ozilgen, 1992; Sahlstrom et al., 2004). Gas production in dough with yeast appears to be dependent on the rate at which yeast cells multiply during fermentation (de Cindio & Correra, 1995). The rate of yeast cell replication was described using a first-order reaction kinetics (exponential growth) by de Cindio and Correra (1995), with a time constant depending on various factors, those of which are at least temperature, pH, and water activity. However, unlike yeast-driven fermentation, CO_2 production starts immediately after the leavening acid hydrolyzes and comes into contact with the sodium bicarbonate. An exponential rate of decrease in the concentration of the leavening reactant, be it glucose in yeast fermentation or an acidulant in chemical leavening, suggests that the decomposition reaction is possibly first-order with respect to the reactant. Conventionally, an indirect measurement of the rate of reactivity of a chemical leavening system is given by the dough rate of reaction (DRR) test (Parks et al., 1960). This test is widely used by manufacturers of chemical leaveners to specify the leavening properties of their products (Heidolph, 1996; Innophos, no date). In the DRR test, the

percentage of available carbon dioxide in the dough that is evolved is measured over time (Conn, 1981; Heidolph, 1996; Parks et al., 1960).

For any stoichiometrically defined chemical process, reaction rates are typically obtained from measurements of changes in the concentration of reactants or products over time. Desirable analytical methods to study chemical kinetics include those that give a continuous and rapid measurement of the concentration of a specific compound. Therefore, it is only necessary to measure some property of the system which indicates the extent of the chemical reaction that is taking place (Hammes, 1978). Any property that can be linearly correlated with concentration can be conveniently used, including total pressure, volume and conductance (Hammes, 1978). Hence, a suitable technique to study kinetics of reaction in a gas-evolving chemical system would include devices that are capable of measuring pressure. The existence of computerized gas measuring devices amenable to measuring carbon dioxide production in dough (e.g., the Gassmart apparatus) suggests that characterization of the reaction kinetics of carbon dioxide production in fermenting dough is achievable.

2.3.5. Measurement of gas production

Interestingly, precise measurements of gas production in fermenting doughs became an important subject matter more than 70 years ago (Elion, 1933). At this time, many gas-measuring devices were proposed (Bailey, 1939, 1955; Elion, 1939, 1940; Mallock, 1939; Redfern, 1950; Landis & Frey, 1943; Working & Swanson, 1946; Sherwood et al., 1940). These devices differed essentially in their gas detection system, specifically the type of pressuremeter. The pressure manometers that were proposed ranged from rate meters (Landis & Frey, 1943), gas-collecting burettes (Bailey, 1955;

Elion, 1933; Sherwood et al., 1940), Bourdon tube gauges (Mallock, 1939), automatic recording gasometers (Working & Swanson, 1946) to electric pressure transducers (Redfern, 1950).

Today, gas production in yeasted dough is typically measured using apparatuses such as the Risofermentometer and Risograph, where carbon dioxide is measured indirectly by monitoring expansion in volume of a given amount of dough as a function of time. In either test, however, gas retention is not necessarily constant, and this may bias information inferred on gas production. Gelinas (1997) noted that the true values for gas production in fermenting dough could be obtained only if the volume of the evolving gas, or the pressure it exerts, is measured directly, not indirectly, as happens in the Risofermentometer and Risograph. One potential source of error in measuring the true CO_2 evolution in dough via a pressuremeter is the error arising from the amount of carbon dioxide dissolved in the liquid phase of the dough. This unaccounted carbon dioxide becomes a source of error in such instruments as the Risofermentometer and Risograph (Chiotellis & Campbell, 2003b).

In a study where several cereal research laboratories participated in the measurement of gas production in check samples, Gelinas (1997) found that the AACC Method (89-01) on total gassing power in yeasted dough (using the Risograph) gave good intra-laboratory repeatability but poor inter-laboratory reproducibility. Gelinas (1997) noted common sources of error included errors resulting from the analyst, systematic errors associated with the method, accidental errors, gas leaks during measurements, variation of barometric pressure, variation of temperature, lack of calibration, lack of measuring initial fermentation, and lack of standardization of ingredients. In addition, the

type of mixer and the weight of prepared dough were not standardized among the participating laboratories in Gelinas' (1997) study. These two variables can affect the degree of aeration of the dough (Campbell, 1991; Campbell et al., 1998), which in turn can affect the amount of CO_2 remaining dissolved in the dough liquid phase (Chiotellis and Campbell, 2003b).

One gas-measuring instrument that the AACC official methods specifically endorses is the Chittick gasometric apparatus to measure sodium bicarbonate available in a baking powder, AACC Method 12-20 (AACC, 2000), or in a prepared mix or self-rising dough, AACC Method 12-21 (AACC, 2000). However, the Chittick apparatus is only used to measure total carbon dioxide and not carbon dioxide evolution over time. Typically, this apparatus uses a graduated burette as a pressuremeter, which means that pressure readings need to be taken manually, increasing the likelihood of error arising from the analyst.

To monitor evolution of carbon dioxide over time, Parks et al. (1960) described a standardized method for measuring reactivity of chemical leavening systems in biscuit dough using a manometer. The Park et al. method was inspired by the work of Barackman (1954) who was the first to report the use of a metal bomb fitted with an airtight stirring device to measure pressure using a manometer burette. Parks et al. (1960) replaced the burette manometer and used an electronic pressure transducer to quantify gas evolution in a chemical leavening system (the pressure transducer was sensitive to slight changes in pressures on the dough – i.e., sensitive to pressure changes as small as 12 in. of water, or 3 kPa). In their paper, Parks et al. (1960) reported the dough rate of reaction (DRR) on two chemical leavening systems, sodium acid pyrophosphate (SAPP) and

anhydrous monocalcium phosphate (AMCP). The DRR plot of a chemical leavening system reports the percent of total leavening reacted as a function of fermentation time. Parks et al. (1960) found that ingredients (flour type, flour age, milk, and shortening) and differences in the gas bomb's geometry, stirring rate, and test temperature, could all influence test results (Figure 2.3).

The DRR test is widely used to quantify leavening power in chemical leavening systems, though the procedures to carry out the test have never been standardized. For example, Heidolph (1996) and Conn (1981) indicated that acidulants should be mixed for 3 min with the formula ingredients (including the water) prior to the DRR test, whereas Parks et al. (1960) mixed them for 3 and 8 min, depending on the type of acidulant used. Some discrepancies in the absolute values for the DRR values also exist. Parks et al. (1960) reported a DRR (8 min) of more than 70 % for AMCP while Heidolph (1996) and Conn (1981) reported values of about 60 % for the same acidulant. Nevertheless, the DRR test is an easy way of comparing the gas production properties of various chemical leavening systems. Today, there is no standard equipment commercially available to perform the DRR test.

A gas-measuring test apparatus with characteristics and capabilities similar to that of Parks et al. is the Gassmart (TMCO Inc.) apparatus. As is the case for the test apparatus of Parks et al. (1960), the Gassmart measures carbon dioxide evolution with time by placing the tested system in an airtight metal gas bomb of well-defined geometry and fitted with a pressure transducer. The Gassmart though is capable of monitoring manometric pressures of up to 100 kPa. Furthermore, the characteristics of the pressure transducer and the electronic converter are such that the computerized Gassmart

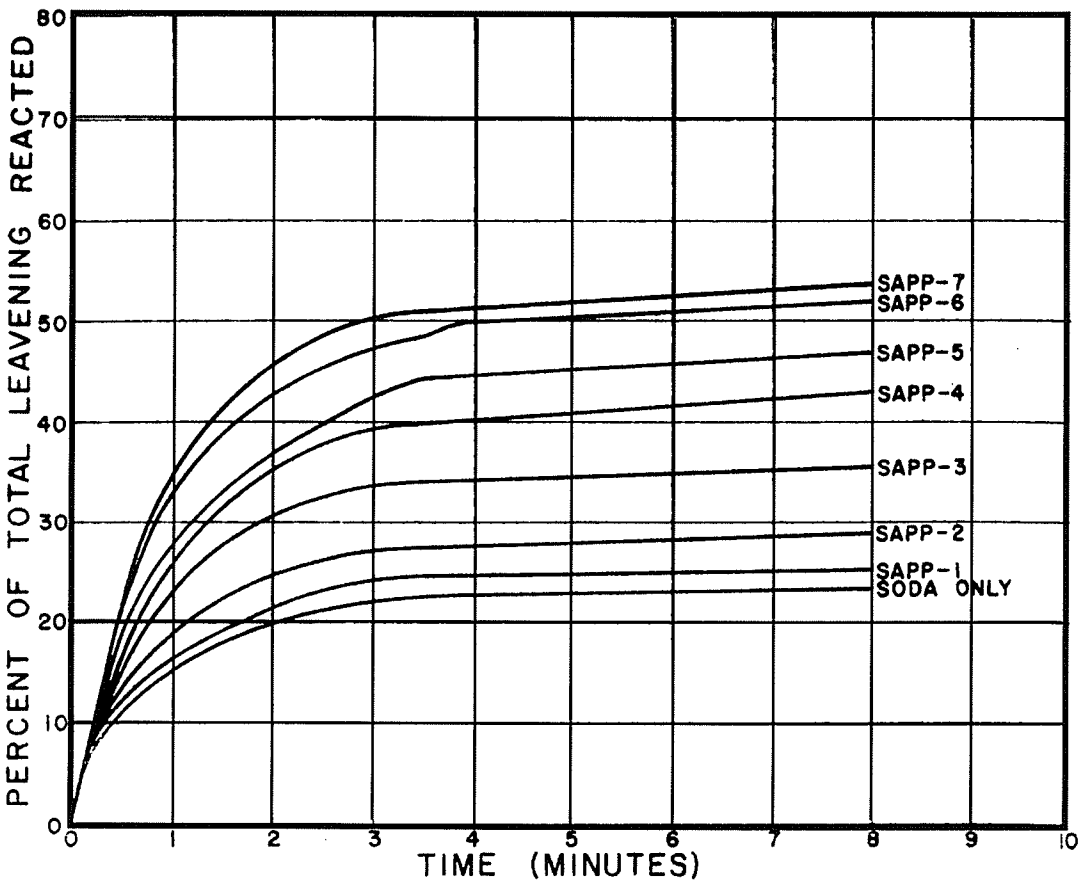

Figure 2.3. Dough rate of reaction (DRR) curves obtained with sodium bicarbonate (SODA ONLY) or a complete chemical leavening system containing sodium bicarbonate and sodium acid pyrophosphate of varying reactivity (SAPP-1, SAPP-2, SAPP-3, SAPP-4, SAPP-5, SAPP-6, and SAPP-7). Dough (3-min mixing time at 27 °C) contains 57g flour, 40g distilled water, 5g non-fat dry milk, 6g shortening, 1g sodium chloride, 0.755g sodium bicarbonate, and 1.057g sodium acid pyrophosphate. Taken from Parks et al. (1960).

apparatus is amenable for precise real-time measurements of carbon dioxide evolution. Although AACC Method 22-11 (AACC, 2000) and AACC Method 89-01 (AACC, 2000) specified the use of a pressuremeter (e.g., Gassmart) to measure total carbon dioxide production in dough, these two methods were not developed to measure gas evolution in chemical leavening systems nor were they developed to conduct the DRR test. For example, the Gassmart apparatus has been used to measure gas production in yeasted dough (Sahlstrom et al., 2004) and in chemically leavened dough (Jantzi et al., 1999), with test results typically shown as a pressure versus time plot. Such a plot, however, provides information that is not useful to users of chemical leaveners as it is incompatible with commercial specifications based on the DRR test.

2.4. Gas retention in dough

2.4.1. Aeration of dough during mixing

2.4.1.1. Dough mixing and gas occlusion

Attainment of a homogeneous dispersion of formula ingredients during mixing requires mechanical work input to the dough, a certain degree of chemical modification of the gluten proteins in the flour and the occlusion of gas cell nuclei (MacRitchie, 1986). Typically, this is achieved by mixing (or kneading) while allowing time for chemical and biochemical modification of gluten proteins. In modern breadmaking processes such as the Chorleywood Bread Process, mixing and chemical and biochemical modification of the gluten occur simultaneously with the aid of high speed mixers. Regardless of how the mixing and fermentation are performed, mixing serves three main objectives: (1) hydration and interaction of flour components, (2) development of gluten, and (3) occlusion of air. Information on the first two objectives can be found in the basic cereal

science literature, for example, Bloksma and Bushuk (1988). Occlusion of air during mixing is the first aeration process in breadmaking and is an essential step because the occluded gas will form the gas cell nuclei that will act as collection sites for CO_2 diffusion during fermentation and the initial stages of baking. Much of what it is known today about gas occlusion during mixing is owed to the work of Baker and Mize who published three superb papers in 1937, 1941 and 1946. These papers introduced important concepts and scientific methodology to interrogate the mechanisms responsible for the creation of the aerated structure of bread; these concepts and methods remain valid even today.

Baker and Mize (1937) investigated the effects of oxygen on the aeration of doughs by mixing them under vacuum and atmospheric pressure and in the presence of various atmospheric gases (air, nitrogen, hydrogen, oxygen, carbon dioxide). The effects of mixing headspace pressures on dough aeration were evaluated using various techniques, including dough density, dough rheology and baking performance. Dough density was measured using a method based on Archimedes principle where the displacement fluid was mineral oil. Dough rheology was measured using visual and manual inspections of the dough, while baking performance was evaluated visually by inspecting the texture and appearance of the loaves of bread and by measuring loaf volume (via seed displacement). Their studies demonstrated that mixing headspace atmosphere had a strong influence on dough rheology, baking performance, and the texture and appearance of bread; further demonstrating the importance of oxygen in dough development and on the handling properties of the dough and the quality of the

baked loaf. For example, doughs mixed under hydrogen or nitrogen could not be developed, even though they were mixed for extended periods of time.

The paper published in 1941 (Baker & Mize, 1941) is regarded as a "classic" as it gives indisputable evidence that the origin of gas cells in bread is the mixing stage. Baker and Mize (1941) concluded that no gas cells are formed after mixing in subsequent breadmaking operations, though such operations as moulding and punching can increase the number of gas cells by subdividing the number of gas cells already entrained in the dough. Further, Baker and Mize's work proved that the contributions of yeast cells or air trapped between flour particles to dough aeration were negligible.

In their 1946 paper, Baker and Mize studied gas occlusion during mixing and its relationship to dough development. They did so by comparing the amount of gas occluded during mixing (which was interrupted at various times) to the shape of the mixogram. The gas occluded in the dough was measured via density measurements using a series of calcium chloride solutions of known density. Dough samples were dropped in the solutions and the sample density was taken as being that of the solution in which the sample floated. Baker and Mize observed that the rate of gas occlusion increased slowly with increasing dough consistency, and a peak in the mixing curve was observed close to the point in which the gas occlusion rate was greatest. After the peak was reached, the rate of gas occlusion was very low. Similar results were observed when the oxidizing agent sodium chlorite (40 ppm) was used. Though it was apparent that the peak in the mixing curve was associated with gas occlusion, dough mixing experiments under vacuum proved otherwise. Mixing under normal pressure and then drawing a high vacuum before the peak in the mixogram caused the "removal" or "elimination" of gas

bubbles initially entrained, as dough was observed to have returned to its initial density. Drawing the vacuum after the peak in the mixogram was reached did not change the shape of the mixogram either. It was concluded that "the rise in the mixogram is not due to occlusion of gas". Gas occlusion was deemed "an accompanying phenomenon of mixing".

Additionally, Baker and Mize (1946) postulated that subdivision of gas cells, which was fastest following the rapid rate of gas occlusion, was an essential aspect of mixing. Bread with a large volume and a fine cell structure (optimum bread) was made when its dough was mixed just before it reached the peak in the mixing curve; otherwise, the rapid rate of gas occlusion in this region caused the dough to occlude too much gas. The amount of gas occluded (e.g., void fraction) was not the key factor in producing bread of good quality but it was the subdivision of the occluded gas. It was intimated that gas occlusion and gas subdivision occur concurrently during mixing, though gas subdivision is more preponderant past optimum mixing because the rate of gas occlusion is very slow in this region (or likely the rates of gas "disentrainment" becomes very high in this region – see subsequent paragraph). Baker and Mize (1946) implied that a balance between dough aeration and subdivision was essential during mixing to make good bread, and this was particularly true of 'no-time doughs" which relied on high speed mixers for optimum dough development (i.e., to cut bulk fermentation times of conventional breadmaking process).

Nearly fifty years later, Campbell (1991) re-interpreted Baker and Mize's (1946) views by proposing that aeration of dough during mixing is governed by gas entrainment and gas disentrainment processes (e.g., as mixing proceeds gas is coming in and out –

thus a balance is key for making good bread). Gas disentrainment was the missing aeration mechanism during mixing that was not accounted for by Baker and Mize (1946). Campbell and Shah (1999) proposed the first model describing bread dough aeration in terms of these two processes. This model was later tested by Chin et al. (2004) who found that it unsatisfactorily described the dough aeration process during mixing. Martin et al. (2004a) were able to satisfactorily describe the data on the number density of bubbles entrained during mixing by using a population balance model however. This model incorporated a third mechanism, bubble breakup, in addition to bubble entrainment and bubble disentrainment, to explain the aeration of dough during mixing. Interestingly, Baker and Mize (1946) were the first ones to introduce the concept of bubble breakup as it helped them to explain the effect of continuous mixing on the cellular structure of bread. Nonetheless, it was Campbell (1991) and Campbell et al. (1998) who employed the bubble breakup notion to explain the influence of mixing pressure on the number density of gas bubbles they measured in dough by light microscopy. They formulated the theory that that bubbles sizes do not change as mixing pressure is changed but rather that bubble numbers do, meaning that bubbles have the same size distribution in doughs mixed at various headspace pressures regardless of the mixing pressure. Subsequent refinement of the pressure mixing studies (Martin et al., 2004b) led to a modification of the conclusion that bubble size was invariant with pressure, since bubble size increased somewhat as mixer headspace pressure increased.

The research of Baker and Mize (1937, 1941, and 1946) and the work of Campbell and coworkers (Campbell, 1991; Campbell & Shah, 1999; Chin et al., 2004; Martin et al., 2004a) have a commonality: that the method for determining gas aeration in

dough is by following the gas void fraction in the dough via density measurements. Indeed, the degree of aeration of the dough during breadmaking is generally expressed in terms of its gas void fraction, which can be found as follows:

$$\phi(t) = 1 - \frac{\rho(t)}{\rho_{gf}} \tag{2.18}$$

where $\phi(t)$ is the dough gas void fraction as a function of fermentation time, $\rho(t)$ is the dough density as a function of time [kg m^{-3}], and ρ_{gf} is the gas-free dough density [kg m^{-3}]. One important shortcoming of void fraction calculations via density measurements is that the bubble size distribution cannot be estimated, which gives only an incomplete view of the aerated structure of dough following mixing. Bubble size distribution is a fundamental piece of information that is required to make meaningful interpretations of aeration data (Chiotellis & Campbell, 2003a).

2.4.1.2. Measurement of bubble size distribution

The importance of measuring the bubble size distribution in dough has been recognized for a long time, with the work of Baker and Mize (1946) being arguably the first to report it. While studying gas occlusion in dough, Baker and Mize (1946) stated that one important consequence of overmixing was that it "rapidly incorporates gas to yield irregular-sized bubbles and [leads to creation of] non-uniform grain". Baker and Mize's (1946) report intimates that the quality of bread is correlated with the size distribution of bubbles entrained during the mixing process, though they did not measure bubble sizes in their experimental doughs.

The first work attempting to measure bubble size distributions in dough is attributed to Carlson and Bohlin (1978). Carlson and Bohlin (1978) found that there were

no reports in the literature on the size distribution of bubbles in dough while attempting to determine the contribution of gas bubbles (i.e., free surface energy) to the mechanical properties of the dough. To measure bubble sizes in the dough, Carlson and Bohlin (1978) used transmission light microscopy to view gas bubbles in thin slices of frozen dough (30 μm thick) cut with a microtome. The dough specimens were imaged using photography. The bubble size (circle diameter) data (which started with bubble diameters larger than the effective resolution of the technique, 90 μm) was fitted using a one-parameter distribution:

$$\frac{f(D)}{N} = \frac{64}{\pi^2}\frac{D^2}{\overline{D}^3} exp\left(-\frac{4}{\pi}\frac{D^2}{\overline{D}^2}\right) \tag{2.19}$$

where $f(D)$ = the probability density function; $\overline{D}$ =mean bubble diameter (μm); and D is the bubble diameter (the midpoint of each class in the histogram of circle sizes) (μm).

The bubble size distribution proposed by Carlson and Bohlin (1978) is shown in Figure 2.4. From this distribution, it is possible to determine the mean bubble diameter to be 112 μm, which was close to the effective resolution of their technique (90 μm). With this mean bubble diameter, the void fraction of their dough (0.1) and their size distribution, it is also possible to determine the number of bubbles per unit volume in the dough to be 86,700 bubbles cm^{-3}.

Campbell et al. (1991) used stereological techniques to reconstruct the bubble diameters (i.e., diameter of spheres) based on information on bubble cross-sections (i.e., circles). As with Carlson and Bohlin (1978), they used light microscopy to image frozen specimens of dough (30 μm thick). The diameter of the circles was obtained using an image analyzer (Optomax V). Circles of diameter in the range 25-500 μm were measured,

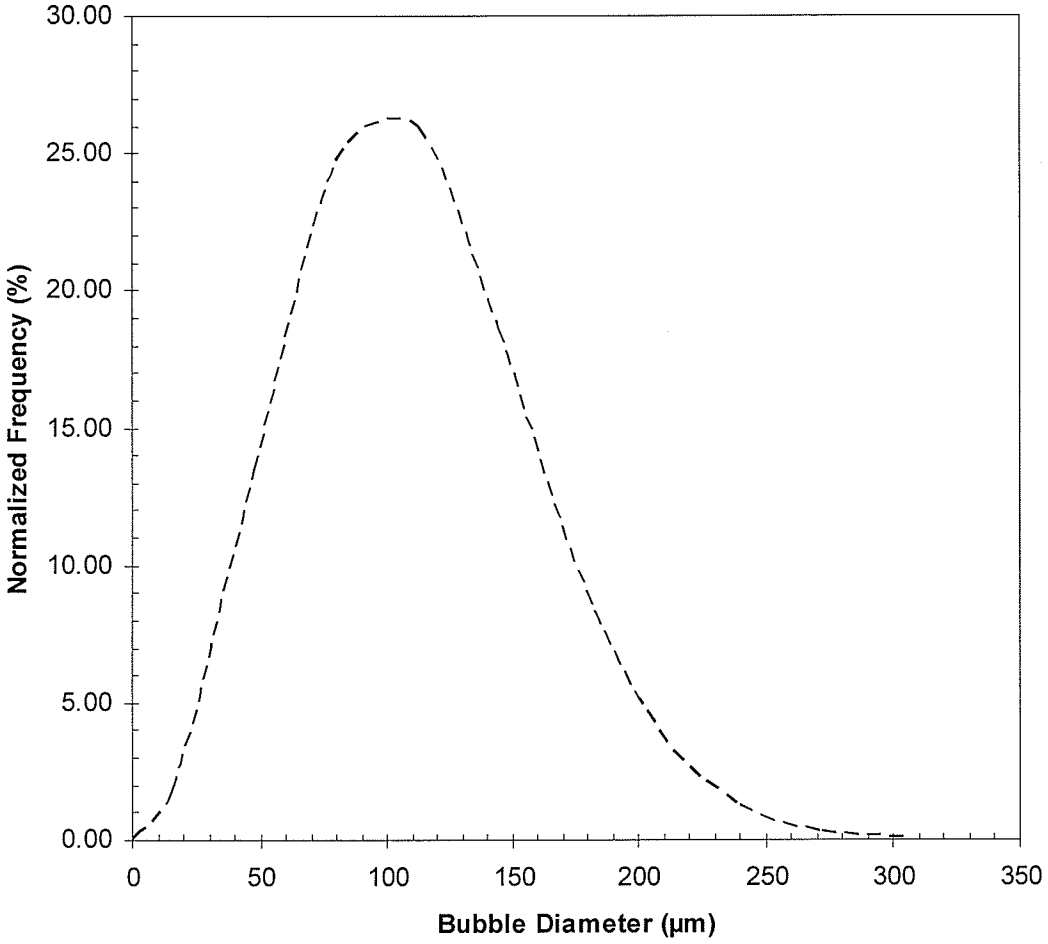

Figure 2.4. Bubble size (two-dimensional) analysis distribution in dough reported by Carlson and Bohlin (1978). Mean diameter is 112 µm. See text for details.

giving an effective resolution of 40 μm. Campbell et al. (1991) did not fit a statistical distribution to their bubble (sphere) diameter data but rather they characterized the shape of the bubble size distribution using two empirical parameters, the mean bubble size ($\overline{D}$) and the standard deviation (SD) of the distribution. Depending on the type of mixer used to prepare the dough, $\overline{D}$ was found to be 71 μm and 89 μm and SD 24.1 μm and 46.9 μm, for a Food Processor and a Tweedy 10 mixer, respectively.

More recently, Shimiya and Nakamura (1997) also used light microscopy to measure the bubble size distribution in dough. Their experimental data (discretized circle size) was characterized by a log-normal distribution:

$$f(\log D) = \frac{1}{\sigma\sqrt{2\pi}} exp\left(\frac{-(\log D - \log D_{50})^2}{2\sigma^2}\right) \qquad (2.20)$$

where f (log D) is the probability density function of a log-normal distribution, D is the bubble diameter in a log-normal distribution (the midpoint of each class in the histogram of bubble sizes in a logarithmic scale) (μm), D_{50} is the median diameter in a log-normal distribution (μm), and σ is the standard deviation in a log-normal distribution. Shimiya and Nakamura (1997) found D_{50} and σ to be 35 μm and 1.8, respectively, for dough mixed in a breadmaking machine. Recently, Campbell et al. (1999) introduced a sophisticated algorithm to the reconstruction technique they had developed earlier (Campbell et al., 1991) for calculating bubble diameters based on information on circle diameters. With this improvement, Campbell et al. (1999) estimated that the bubble size (diameter) distribution in dough could be characterized as log-normal.

Despite the usefulness of the studies discussed hitherto for examining the bubble size distribution in dough, the validity of these bubble data is questionable since freezing

and serial sectioning, or squashing of the dough, invariably affect the integrity of the sample. In addition, reconstruction of bubble size distributions from two-dimensional sections is not a statistically exact exercise (Campbell et al., 1999; Martin et al. 2004a, Underwood, 1970). Therefore, to unambiguously evaluate the bubble size distributions in the dough, it is desirable if techniques that eliminate additional treatment steps and non-invasively probe the bubble sizes in situ are performed.

One technique that has been used to non-invasively interrogate the structure of a number of materials including cereal-based snack foods (Lim & Barigou, 2004; Trater et al., 2005) and bread crumb (Falcone et al., 2005) is computerized x-ray microtomography. Typically, a sample is rotated as it is illuminated with x-rays from a sealed microfocus x-ray tube source and the three-dimensional reconstruction of the interior structure of the sample is achieved by software run on powerful computers (Cooper et al., 2003, 2004). A less common technique is to use x-rays from a synchrotron source; monitoring of the expansion of gas bubbles during fermentation has very recently been reported (Babin et al., 2005, 2006), although a description of the initial gas bubble size distribution was not communicated.

2.4.2. Aeration of dough during proving

2.4.2.1. Measurement of dough density

Density measurements have long proven themselves to be an invaluable tool to follow aeration of dough during mixing and proving. For example, the discovery more than 60 years ago that the gas cell structure of bread originates at mixing was supported by evidence from density measurements of dough mixed at various headspace pressures (Baker & Mize, 1941) The same authors (Baker & Mize, 1946) used density measurements to determine that strong flours produce bread with better loaf volume and

finer bread crumb than weak flours because the strong flour dough entrained less gas during mixing than weak flour dough did. They concluded that excessive aeration of dough during mixing is undesirable as it results in bread with poor loaf structure. Baker and Mize's (1946) conclusion has remained unchallenged by subsequent studies despite the refinement of experimental techniques (He & Hoseney, 1991; Campbell et al., 1993, 2001; Chin et al., 2004; Hayman et al., 1998b).

The reason why dough density evidence is rarely questioned is because density is a fundamental property of matter that can be measured relatively easily in dough with no yeast (Baker & Mize, 1937, 1941, 1946; Campbell et al., 1993; Elmehdi et al., 2004). In contrast, measuring the density of leavening dough has proven to be challenging. Until recently, quantification of dough density changes during fermentation typically required a new dough specimen for each measurement (single-point measurements), with density measurements of an expanding dough specimen being based on the displacement of oil (Baker & Mize, 1937; Dus & Kokini, 1990) or on the change in weight due to buoyancy forces (Archimedes principle) when the specimen was immersed in a fluid such as calcium chloride solutions (Baker & Mize, 1946, Junge et al., 1981; Campbell et al., 1993), or simply water (Elmehdi et al., 2004). Intuitively, taking multiple dough specimens from a fermenting dough piece over time is not only inconvenient but also prone to introducing sizeable experimental error. However, the introduction of an ingenious new method for density measurements based on Archimedes principle was made recently by Campbell et al. (2001). The method follows the changes in density of a single dough specimen as a function of fermentation time. Campbell et al.'s system measures dynamic dough density (DDD) by immersing a dough specimen of known

weight in xylene and following its change in volume by measuring the change in dough weight via Archimedes principle. Over the past few years, the technique has been used in multiple studies to investigate the effects of yeast, mixing speed, flour type, fermentation temperature and mixing headspace pressure on CO_2 gas production and retention (Campbell et al., 2001; Campbell & Herrero-Sanchez, 2001; Chiotellis & Campbell, 2003b). These studies have provided a new insight into the role of dough aeration and breadmaking, highlighting consistently the importance of gas bubbles to the rheological and physical properties of dough and to the quality of bread.

More recently, an alternative technique for measuring dynamic dough density changes in fermenting dough was introduced by Elmehdi et al. (2003a). Elmehdi et al. measured dough density by measuring the weight of a dough specimen in air and monitoring its volume change as a function of time using digital photography. Volume is calculated from the dough thickness (constant) and from the change in dough area by measuring the radial expansion of the dough specimen after it had been compressed between two acrylic plates to a preset thickness. Taking continuous digital images of the expanding specimen enables measurement in real-time density changes as a function of fermentation time (Chapter 5). Interestingly, on independent works using their own density measurement system, Elmehdi et al. (2003a) and Chiotellis and Campbell (2003b) found similar patterns for the curve of dough density versus time for dough prepared with yeast, with dough density starting to decrease after a lag period (up to 10 min) with respect to the onset of fermentation. The lag period was associated with the time required for yeast to multiply and metabolize fermentable sugars and for the CO_2 evolved to diffuse into the gas cell nuclei to effectively inflate the dough specimen

(Elmehdi et al., 2003a). One source of error associated with measuring the area of expanding dough based on digital photography by Elmehdi's (2001) technique is that the calibrant and sample are located at different focal planes from the camera lens. For example, since the calibrant is located closer to the camera lens relative to the sample, the area of the calibrant would appear larger than it actually is relative to the area of the dough sample. Furthermore, Elmehdi (2001) failed to communicate the digital image analysis protocol that is required to measure the area of the expanding dough or of the calibrant.

2.4.2.2. Carbon dioxide transportation in fermenting dough

Theoretically, leavening of dough is a carbon dioxide transportation problem. This is so because dough is viewed as a dispersion of gas bubbles in a continuous phase (Bloksma, 1981) where the gas bubbles constitute a dispersed gas phase that expands due to carbon dioxide diffusion from the continuous phase. From a chemical engineering viewpoint, such a transport problem entails mass and momentum transport processes (Chiotellis & Campbell, 2003a). Momentum transport suggests that the growth of bubbles should account for forces opposing the expansion of the phase boundary around the bubble, meaning that the dough viscoelastic properties must not be disregarded. Mass transport, on the other hand, deems bubble growth to arise solely due to the carbon dioxide concentration (or partial pressure) gradient across the gas-dough interface and disregards those forces opposing bubble growth, such as surface tension and the viscoelastic nature of the dough (Chiotellis & Campbell, 2003a). Hybrid models of momentum and mass transport models also exist which most notably include diffusion-controlled and diffusion-induced models that are good for describing the growth of a

single gas bubble (Venerus et al., 1998) or a population of bubbles (Chiotellis & Campbell, 2003a). Despite the well-developed theoretical framework for transport models of carbon dioxide in gas-saturated viscoelastic materials, experimental data on this subject is still scarce. This is particularly true in dough systems since monitoring the growth of individual or a population of gas bubbles is an experimentally difficult task because of the opacity of the dough.

Shah et al. (1998) described a simple, and yet very useful, model to predict the rate of expansion of individual gas bubbles:

$$\frac{dD}{dt} = \frac{12RTD_L(C_\infty - C^*)}{3P_\infty D + 8\gamma} \tag{2.21}$$

where D is the bubble diameter, R is the universal gas constant, T is the temperature, D_L is the coefficient of diffusivity, γ is the surface tension of the bubble interface, and C_∞ and C^* are the solute (CO_2) concentrations in the dough and at the interface, respectively. The pressure difference between the inside and the outside of the bubble, ΔP, is related to the bubble diameter and its surface tension by the Laplace pressure:

$$\Delta P = \frac{4\gamma}{D} \tag{2.22}$$

The Laplace pressure may give rise to disproportionation, which can be described as the mass transport of CO_2 gas from small to large bubbles (van Vliet et al., 1992). Disproportionation can occur because larger bubbles with their smaller internal pressures have lower solubility of CO_2 (due to Henry's law) in the region neighboring their interface. This causes a concentration gradient to be formed between the regions surrounding large and small bubbles. Hence, it is not surprising to find experimental data in the literature supporting the view that disproportionation is an important mechanism of

bubble growth and shrinkage in *non-fermenting dough* (Shimiya & Yano, 1988; Shimiya & Nakamura, 1997). However, disproportionation seems improbable in *fermenting dough* because yeast produces CO_2 that moves from the dough liquid matrix into the gas bubbles and not in the opposite direction. For carbon dioxide to travel from smaller to larger bubbles it would need to diffuse against a higher carbon dioxide concentration gradient, which is not possible (Campbell & Mougeot, 1999).

Shah et al.'s (1998) model implies that surface tension is an important aspect of gas bubble growth (i.e., it is a force that opposes bubble growth) and that the contribution of dough rheology to bubble growth is too small to be considered important. Though dough rheology may arguably not play a role during early fermentation (where gas expansion is thought to be diffusion controlled), it would likely become more significant at the later stages of fermentation where strain hardening is thought to take place (Dobraszczyk & Roberts, 1994). During the baking stage, dough rheology would certainly be critical.

Based on the mathematical model developed by Shah et al. (1998) and on the analysis of Venerus et al., (1998), Chiotellis and Campbell (2003a) developed a diffusion-controlled transport model for a population of bubbles. The model proved to be useful in providing relatively good predictions of bubble growth in fermenting dough. Chiotellis and Campbell (2003a) measured the volume changes during fermentation of the dough samples by using a dynamic dough density (DDD) technique capable of monitoring dough density changes over fermentation time. Information on the bubble size distribution was determined on frozen samples using light microscopy information from two-dimensional cross-sections of frozen dough samples and a 3D reconstruction

algorithm based on statistics (Campbell, 1991). In their subsequent publication, however, Chiotellis & Campbell (2003b) admitted that, because the DDD measurements required keeping the dough samples immersed in xylene (Campbell et al., 1993), not all the carbon dioxide evolved by the dough samples was accounted for in the calculations. Another possible source of error is that the DDD technique worked on the assumption that xylene was not absorbed by the dough during the course of fermentation. Nonetheless, the authors claim that the use of the DDD technique proved useful in gaining an insight into the mechanisms of bubble growth in wheat flour dough.

2.4.3. Dough aeration during baking

During the later stages of fermentation and the initial stages of baking, the bubbles undergo an additional, albeit more rapid, growth because yeast produce CO_2 at a higher rate, gas is expanded due to the law of Gay-Lussac, and water is transformed into steam (Bloksma, 1990a). Yeast cells become inactivated once the dough reaches about 50°C (Bloksma, 1990a). Because carbon dioxide solubility in the dough liquid matrix is inversely proportional to the fermentation temperature (Chiotellis & Campbell, 2003b), the rising temperatures during baking are expected to drive a portion of CO_2 out of solution which becomes an additional source of leavening gas for bubble growth. These events increase the tendency of gas cell walls to collapse and hence the likelihood of gas bubble coalescence.

Dobraszczyk (1977a, 1997b, 2004), Dobraszczyk and Morgenstern (2003), Dobraszczyk and Roberts (1994), and Dobraszczyk et al. (2003) argue that the resistance of gas cell walls to collapse under the influence of large strains is related to the strain hardening properties of the dough. Strain hardening can be defined as the ability of the

glutenin proteins to re-orient and form entanglements upon considerable strains of the gas cell walls. Other researchers have postulated that bubbles are lined by a thin aqueous film that enables them to preserve their gas retention properties even after discontinuities form in the starch-gluten matrix (McRitchie, 1976; Sahi, 1994, 2003; Gan et al., 1990; 1995). Surface active components, for example, are thought to stabilize gas bubbles against coalescence by strengthening the liquid film at the bubble interface (Mills et al., 2003; Ornebro et al., 2000; Salt et al., 2006). However, the existence of such a thin aqueous film is still speculative, and even if present, its role in bubble growth stability will require further research to be conducted in this area.

As the dough is baked during the later stages of fermentation and its temperature rises to about 60 °C, starch granules begin to gelatinize (Hoseney, 1998). Though these high temperatures are also going to cause denaturation of protein molecules, it is the gelatinization of the starch that rigidifies the structure of dough. At this point bubble growth ceases and the bubbles coalesce and become interconnected (Babin et al., 2006, 2007). Extensive bubble coalescence leads to the escape of gas cell contents and effectively transforms the foam structure of dough into a sponge. Also, "the predominantly liquid dough is transformed into a predominantly elastic bread or crust", Bloksma (1990a). Figure 2.5 summarizes the breadmaking process from the perspective of aeration stages, where "the foam" is created during mixing, it expands during fermentation, and finally it is transformed into "a sponge" during baking. It is important to highlight that the most important breadmaking step in terms of dough aeration is fermentation, as in white bread, for example, the density drops from 1,100 kg m^{-3} after mixing to 300 kg m^{-3} at the end of fermentation (before baking) to about 200 kg m^{-3} after

baking (Bloksma, 1986), which in terms of gas void fraction changes, for illustration purposes only, can be equated to about 8% to 75% to 83%, respectively, assuming that the gas-free dough density is 1,200 kg m^{-3} (Baker & Mize, 1941).

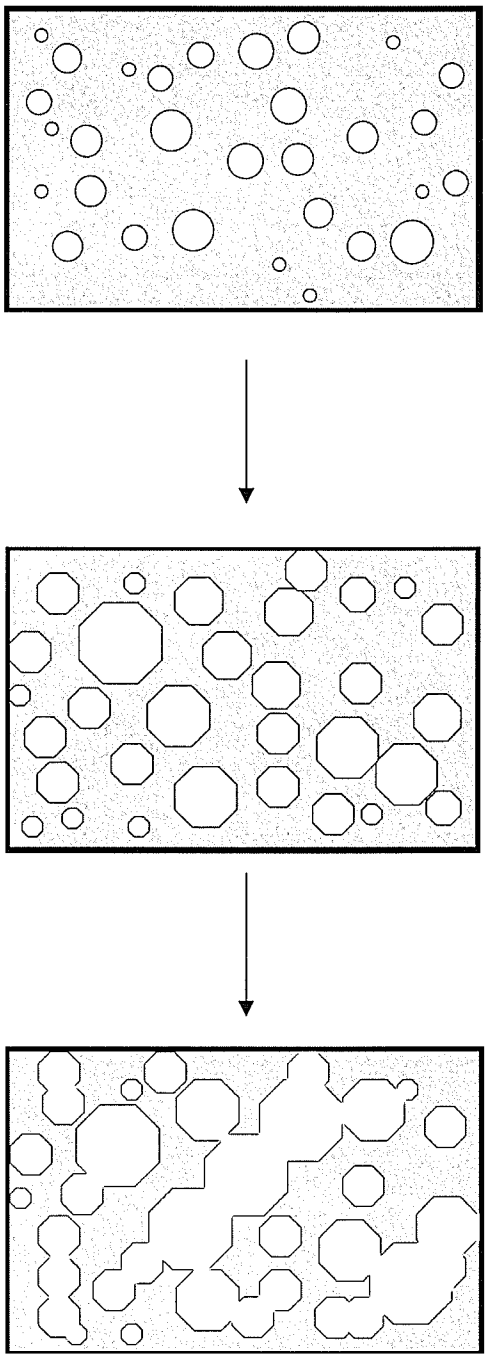

Foam Creation

Small gas cells nuclei are entrained during mixing

Foam Expansion

Gas cell nuclei expand due to CO_2 produced by yeast during fermentation, and steam during early baking

Foam Setting: Conversion to Sponge

Rigidification of gas cells walls due to starch gelatinization, loss of CO_2 and steam from bubbles due to extensive coalescence, and formation of sponge structure

Figure 2.5. Schematic representation of foam formation in dough systems. Adapted from Bloksma (1990a,b), Campbell (1991) and Mills *et al.* (2003).

CHAPTER THREE

The Bubble Size Distribution in Wheat Flour Dough

Abstract

This paper reports the use of non-invasive microcomputed tomography (μCT) to unambiguously determine the bubble size distribution in doughs made from strong breadmaking flour. The doughs studied were comprised of two types of dough made of two different formulae in order to yield distinct consistencies, one being a stiff dough and the other one being a slack dough. Reconstruction and three-dimensional visualization of the internal structure of the dough was accomplished at a resolution of 10^3 μm^3 per voxel, making possible to resolve gas bubbles as small as 10 μm in diameter. Morphological characterization of the stiff and slack doughs indicated that they entrained bubbles whose size distributions were well defined by a two-parameter lognormal distribution, with geometric mean x_g and geometric standard deviation σ_g. The bubble size distributions in the stiff and slack doughs were found to have similar geometric means, 100 and 109.3 μm, but quite distinct geometric standard deviation, 1.79 and 1.62, respectively. An analysis of anisotropy of bubble cross-sections (circles 10-μm thick) suggested that the small bubbles entrained in the slack dough were deformed during sample preparation to a greater degree than in the stiff dough, up to a size of 180 μm. Also, the stiff dough entrained a smaller void fraction and fewer bubbles per unit volume than did the slack dough. Furthermore, the distance between adjacent bubbles was obtained, indicating that the bubble separation distribution was normally distributed, with the stiff and slack doughs having a mean separation of 338 and 460 μm and standard deviation of 88 and

156 μm, respectively. Overall, this paper shows how the bubble size distribution in dough can be determined using x-ray microcomputed tomography, opening the possibility to gaining a more comprehensive insight into the aeration phenomenon in wheat flour dough.

3.1. Introduction

If breadmaking *can* be characterized as a series of aeration stages (Campbell et al., 1998), then the mechanisms by which gas cells in the dough create the cellular structure of the bread crumb need to be studied (Scanlon & Zghal, 2001). Understanding how air bubbles nucleate in the bread dough during mixing is a fundamental first step because it was shown conclusively over 60 years ago that these air bubbles are the only nuclei available for subsequent gas cell growth (Baker & Mize, 1941). A further reason for studying bubbles in dough is that dough exhibits extremely complex rheological properties (Bagley et al., 1998), and bubble numbers and sizes will affect dough rheology (Bloksma, 1981, 1990b; Carlson & Bohlin, 1978). For example, the rate of disproportionation of air bubbles in the dough is influenced by bubble sizes and by the separation between them (van Vliet, 1999), while the number density of bubbles has a remarkable effect on the rheological properties of the dough (Chin et al., 2005; Elmehdi et al., 2004). Despite the technological and scientific importance of acquiring quantitative data on the bubble size distribution in dough, dough's opacity and fragility have contributed to difficulty in acquiring these data. Consequently, very few researchers have investigated bubble size distributions in dough.

In a thorough evaluation of the effect of headspace mixing pressure on gas cell nuclei, Campbell (1991) and Campbell et al. (1998) used light microscopy to examine

sections of frozen dough. They showed that bubble sizes did not change as headspace pressure was varied (Campbell et al., 1998), and that for two types of mixers, mean bubble diameters of 71 and 89 um were nucleated, values close to those of the earliest study reported by Carlson and Bohlin (1978). Subsequent refinement of the pressure mixing studies (Martin et al., 2004b) led to a modification of the conclusion that bubble size was invariant with pressure, since bubble size increased somewhat as mixer headspace pressure increased. Whitworth and Alava (1999) also used light microscopy of frozen sections to show that different mixers altered the void fraction and bubble size cell distributions in doughs prepared with identical ingredients. Optical and stereo microscopy has also been used to examine gas bubble sizes in squashed fresh dough samples made without yeast (Shimiya & Nakamura, 1997). In this case, dough was prepared with a breadmaking machine, and a median bubble diameter of 15 μm was nucleated, but disproportionation increased the median diameter to 35 μm following 100 minutes of resting of the dough.

Despite the usefulness of these studies for examining how mixing conditions potentially affect crumb cell structure (Carlson & Bohlin, 1978; Campbell, 1991), and for modelling the rheological behaviour of dough (Elmehdi et al., 2004), the validity of these bubble data is questionable since freezing and serial sectioning, or squashing of the dough, invariably affect the integrity of the sample. In addition, reconstruction of bubble size distributions from two-dimensional sections is methodologically difficult (Underwood, 1970; Campbell et al., 1999; Martin et al., 2004b). Therefore, to unambiguously evaluate the bubble size distributions in the dough, it is desirable if

techniques that eliminate additional treatment steps and non-invasively probe the bubble sizes in situ are performed.

One technique that has been used to non-invasively interrogate the structure of a number of materials, including cereal-based snack foods (Lim & Barigou, 2004; Trater et al., 2005) and bread crumb (Falcone et al., 2005), is computerized x-ray microtomography. In this method, a sample is either rotated between a fixed x-ray source and detector or the x-ray source and detector rotate around the specimen. The backprojection data captured at each rotation step is then used to obtain cross-sectional images which can then be used to generate a 3D representation of the scanned object (Cooper et al., 2004). A less common technique is to use x-rays from a synchrotron source; monitoring of the expansion of gas bubbles during fermentation has very recently been reported (Babin et al., 2005, 2006), although a description of the initial gas bubble size distribution in the dough was not communicated. The objective of this paper is to use x-ray microtomography to non-invasively evaluate the bubble size distributions in two doughs made from strong breadmaking flour that did not contain yeast. The ingredients for the two doughs were selected in order to create doughs that would be classified as "stiff" and "slack", with a view to understanding how bubble distributions influence the rheology of breadmaking doughs.

3.2. Materials and Methods

A straight grade flour milled from a number 1 grade Canadian Western Red Spring wheat of the 2003 crop year was obtained from the pilot mill of the Canadian International Grains Institute, Winnipeg, MB. Characteristics of the flour are summarized in Table 3.1.

Table 3.1. Characteristics of the hard red spring wheat flour

Analysis	CWRS Grade 1	Method
Analytical		
Moisture (w.b.), %	14.3	AACC 44-15A
Protein content, %	14.0	AACC 46-30
Wet Gluten, %	37.8	AACC 38-12A
Dry Gluten, %	13.3	AACC 38-12A
Ash Content, %	0.45	AACC 08-01
Agtron colour, %	63	AACC 14-30
Falling number, s	428	AACC 56-81B
Minolta Colour		Manufacturer's instructions[a]
*L**	91.77	
*a**	-0.21	
*b**	11.20	
Farinogram		AACC 54-21A
Absorption	69.0	
Dough Development Time, min	9.0	
Mixing Tolerance Index (MTI), BU	20	
Stability, min	17.9	

(a) To assess colour in the flour sample, a slurry of flour and water was made according to AACC 14-30 with respect to flour weight, volume of water, mixing time and waiting time. Flour samples were tested seven days after milling using a Minolta CR-310 colorimeter equipped with a D65 illuminant according to manufacturer's instructions.

Doughs were prepared from this flour using one of the following two formulas. Formula A encompassed 100 g flour (14% m.b.), 63.0 g deionised water and 2.40 g NaCl,while Formula B comprised 100 g flour (14% m.b.), 67.4 g deionised water and 0.75 g NaCl. All ingredients were mixed together for 4 min using a GRL 200 mixer (Hlynka & Anderson, 1955) at a constant pin speed of 165 rpm and at room temperature. All dough ingredients were equilibrated overnight to room temperature (22 ± 1 °C) prior to experimentation.

To minimize imaging artefacts arising from relaxation of polymeric constituents in the dough, the doughs were gently placed on a clean plastic surface immediately after mixing and covered with cellophane film (to minimize dehydration) and allowed to rest for approximately 90 min. Four spherical sub-samples were then carefully excised from the experimental doughs using a pair of sharp scissors. Three sub-samples were used for density measurements, which were carried out using a specific gravity method based on Archimedes principle of water displacement. The fourth sub-sample was used for the x-ray microtomography scans.

Density measurements based on water displacement were accomplished by excising a dough sub-sample weighing about 2.5 g, which was accurately weighed using a scale precise to +/- 0.0001 g. The sub-sample was placed in a 25 mL specific gravity bottle previously filled with deionised water, and density calculated from the weight of water displaced. Density was reported as the average of three sub-samples obtained from the same dough batch.

For tomography measurements, a sub-sample (~ 0.50 g) of the batch of dough was gently squashed between two cellophane layers –aided by two blocks of Plexiglas- to

a fixed height (2.17 ± 0.01 mm), and then mounted altogether as a sub-sample-cellophane arrangement into a standard hollow T-shaped sample holder (20.00 mm in diameter) made by SCANCO Medical (Bassersdorf, Switzerland). The cellophane served as an effective moisture loss barrier as well as preventing stickiness-related issues. Squashing was done in every sample prior to its mounting into the sample holder.

Morphological characterization of the dough samples was accomplished at the University of Calgary 3D Morphometrics Laboratory, using the SCANCO Medical VIVACT 40 (Bassersdorf, Switzerland) x-ray microtomograph (μCT) scanner. In this scanner, designed for *in vivo* animal studies, the x-ray source and CCD array detector rotate around a stationary specimen. Image reconstruction was *via* a cone-beam algorithm (Kuhn et al., 1990). Preliminary experiments were carried out to optimize the scanning protocol. Accordingly, we used a peak energy level of 70 kV and a constant current of 109 μA. Analogous characterization techniques to those used in cortical bone analysis, including analogous structural parameters for bone histomorphometry (Parfitt et al., 1987) (Table 3.2), were implemented to determine the bubble size distribution and void fractions in wheat flour dough.

Sub-samples of the dough were scanned at a spatial resolution of 10 μm. For image acquisition, the scan protocol included rotation through 180 degrees at a rotation step of 0.35 degrees, and an exposure time of 0.205 s per frame. Four-frame averaging was used to improve the signal to noise ratio. Scan times were approximately 420 s. Each μCT scan produced 200 serial cross-sectional 1024 x 1024 pixel images –representing 2 mm along the sample- which collectively resulted in a volume of isotropic 10 μm^3 voxels.

Table 3.2. Analogous morphological parameters for trabecular bone and bubbles in dough.

Trabecular bone	Bubbles in dough
Tissue Volume (TV)	Dough Volume (DV)
Bone Volume (BV)	Bubble Volume (BV)
Bone Surface (BS)	Bubble Surface (BS)
Bone Volume Fraction (BV/TV)	Bubble Volume Fraction (BV/DV)
Bone Surface to Tissue Volume (BS/TV)	Bubble Surface to Dough Volume (BS/DV)
Trabecular Thickness (Tb.Th)	Bubble Diameter (Bu.Dm)
Trabecular Separation (Tb.Sp)	Bubble Separation (Bu.Sp)

*Trabecular bone abbreviations follow standard nomenclature (Parfitt et al., 1987)

For image processing, the eight-bit grayscale slices were inverted in colour (white to black and vice versa) and median filtered (3 x 3 quadratic kernel) to improve the signal to noise ratio using ImageJ 1.35f (http://rsb.info.nih.gov/ij/) (National Institutes of Health, Bethesda, MD, USA). To facilitate 3D morphometric analysis and 3D visualisation of the bubbles, these slices were cropped using a volume of interest (VOI) function, for which the regions of interest (ROI) were interpolated across slices, and then segmented into white and black regions, which represented the bubbles and the dough matrix, using Skyscan® software (CT-Analyser, version 1.4.0.0, Aartselaar, Belgium). The criterion for segmentation of a stack of images was to fix the grayscale threshold value to the minimum value lying in the plateau region that connected the white and black areas of its composite histogram.

For image analysis, the parameters bubble diameter (Bu. Dm), bubble size distribution (Bu.Sd), bubble spacing (Bu.Sp), and bubble number (Bu.N) were measured

directly by means of their analogues in trabecular bone analysis (Table 3.2) using SkyScan software (CT-Analyser, version 1.4.0.0). 3D renderings of the bubbles were created from the segmented binary images using Skyscan® ANT Visualisation Software (version 2.2.6.0). Anisotropy analysis, where anisotropy was calculated in each slice from the ratio of the major to the minor axis of ellipses fitted to each individual bubble, was carried out using matching rectangular regions of 732 x 120 pixels cropped from the center region of the sample, across 200 serial images, using the particle size function of ImageJ 1.35f. An ellipticity of one denoted a perfectly spherical object.

To construct the frequency distributions, the discrete bubble sizes were tabulated in ascending order of diameter then grouped into size classes (20-μm wide) over the range of bubble sizes observed. The number of observations in each class was then expressed as a percentage of the total and plotted against the midpoint of the class. For the sake of clarity, bubble sizes greater than 320 μm were not plotted but were accounted for in the statistical analysis.

3.3. Results and Discussion

3.3.1. Bubble size distributions

The bubble diameter distribution as seen in the 3D analysis of both doughs is shown in Figure 3.1. Bubbles were reconstructed as spheres from the 10-μm thick μCT serial cross-sections (i.e., *slices*) by using a 3D volume reconstruction algorithm (built-in marching cubes algorithm of SkyScan CT-Analyser, version 1.4.0.0). Bubble size distributions were asymmetrical and skewed to the left, suggesting that bubble size distributions were log-normal. Table 3.3 shows the results of the 3D morphometric

analyses performed using a combination of μCT scans and powerful software. The scans examined a population of more than 3000 bubbles in each dough.

The two-parameter log-normal distribution used to characterize the bubble distribution was based on equations of Cohen (Cohen, 1988) for the case in which the threshold parameter γ (i.e., the lower limit) was equal to zero. The positive random variable bubble diameter D_i of both doughs was characterized with two parameters, the mean μ and the variance σ^2. This characterization assumes that the random variable, $\ln D_i$, is normally distributed, so that the lines in Figure 3.1 are given by the probability density function of D_i and the μ and σ of Table 3.3:

$$f(D_i) = \frac{1}{\sigma \cdot D_i \sqrt{2\pi}} \exp\left(\frac{-(\ln D_i - \mu)^2}{2\sigma^2} \right) \tag{3.1}$$

where

$f(D_i)$ = probability density function of D_i

D_i = midpoint of the i-th class in the histogram of bubble sizes

μ = mean of the log-normal distribution

σ = standard deviation of the log-normal distribution

It is worth noting how μ and σ^2 have been derived from the raw data, as this information is not readily available in the literature. For bubble size data grouped into frequency classes the most efficient (maximum likelihood) estimators of μ and σ^2 are as follows:

$$\hat{\mu} = \frac{1}{n} \sum_{i=1}^{k} \left[\ln D_i * f_i \right] \tag{3.2}$$

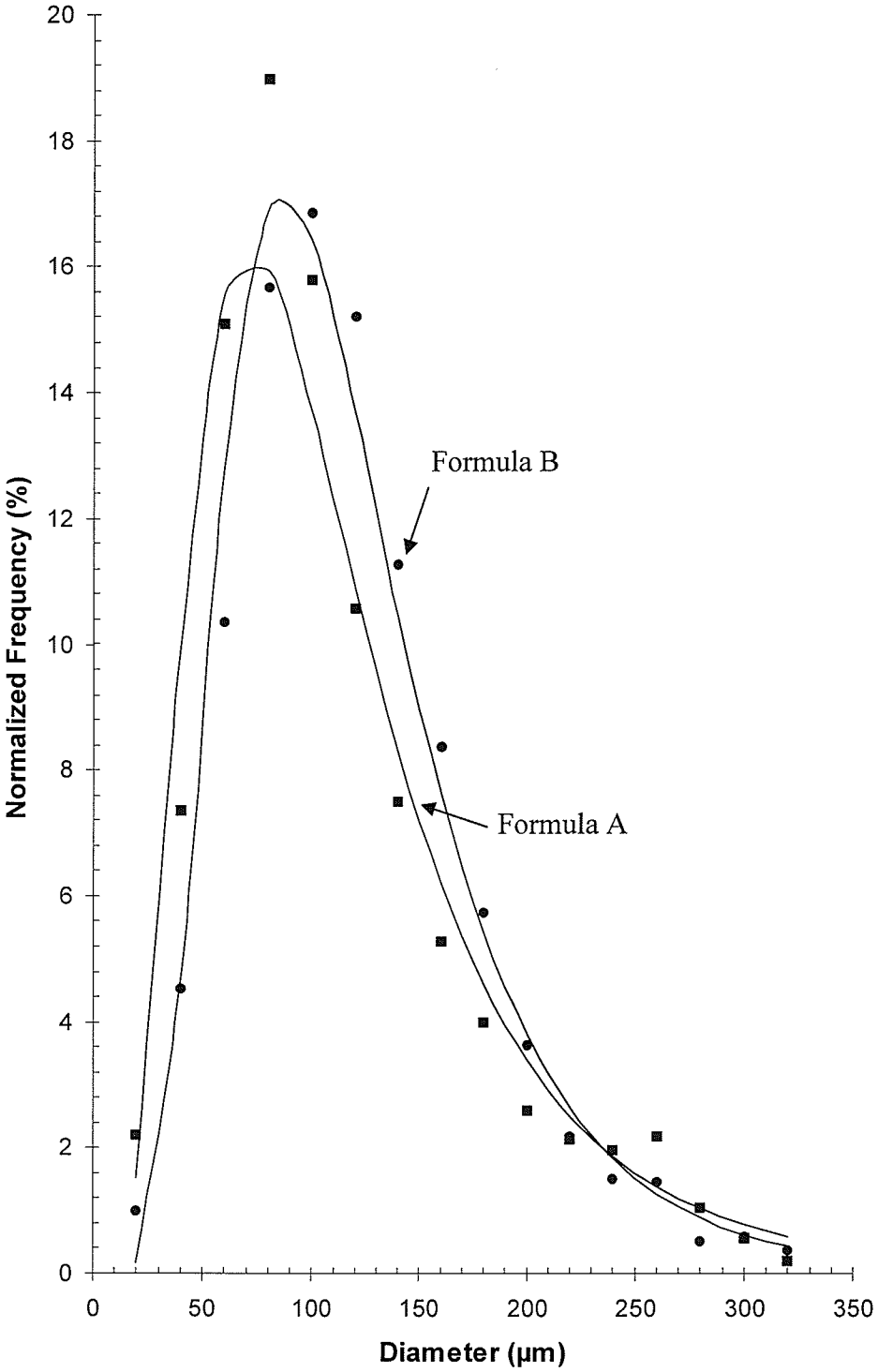

Figure 3.1. Bubble size (3D analysis) distribution in doughs prepared with one of two lean bread formulas as determined by x-ray microtomography.

$$\hat{\sigma}^2 = \frac{1}{n}\sum_{i=1}^{k}\left[(\ln D_i)^2 * f_i\right] - \left[\frac{1}{n}\sum_{i=1}^{k}\ln D_i * f_i\right]^2 \quad (3.3)$$

Here k is the number of classes, n the size of the sphere population, and f_i the number of spheres falling into class i. Interpretation of data in the log scale, however, is not as transparent and so μ and σ^2 are customarily transformed back into their original scale as follows:

$$x_g = \exp(\mu) \quad (3.4)$$

$$\sigma_g = \exp(\sigma) \quad (3.5)$$

Here x_g and σ_g represent the geometric mean and the geometric standard deviation, respectively, of $f(D_i)$.

As with many variables in real life (Johannesson & Mitson, 1983; Crow, 1988; Shimizu & Crow, 1988; Limpert et al., 2001), gas bubble break-up in dough can be viewed as a log-normal phenomenon (Campbell, 1991). The tomographic analysis on bubble sizes from our experimental slack and stiff doughs (Figure 1 and Table 3) agrees with this view, suggesting that subdivision of gas bubbles during mixing creates bubbles whose sizes are geometrically proportional. This mechanism operates in keeping with the log normality of the gas bubble size distribution measured, since log normality has been qualitatively defined by Kolmogoroff (1941) as 'the asymptotic result of an iterative process of successive breakage of a particle into two randomly sized particles' (Shimizu & Crow, 1988).

One important feature of a log normal distribution as compared to a normal distribution is that it has a multiplicative rather than an additive standard deviation. This means, for example, that instead of 95.5% of the random variables being found around a

Table 3.3. Statistical parameters[1] of the best-fit log-normal probability density functions describing experimental bubble size distribution data and void fraction determinations derived from analysis of spheres (3D) by μCT.

	Geometric Mean (x_g/μm)	Geometric SD (σ_g/μm)	95.5% CL [x_g/σ_g^2 - $x_g*\sigma_g^2$] (μm)	$\phi_{\mu CT}$ (%)	$\phi_{gravimetric}$ (%)	N (spheres per cm^3)
Formula A	100.0	1.79	31-321	7.64	7.58	30410
Formula B	109.3	1.62	42-286	9.52	10.41	56540

(1) $x_g = \exp(\mu)$ and $\sigma_g = \exp(\sigma)$; where μ and σ are respectively the mean and standard deviation of the log-normal distribution fitted to the random variable D_o, the mid-point in the class range (Cohen, 1988; Shimizu and Crow, 1988).

mean value plus or minus 2 standard deviations, the same interval of confidence is found for the log normal distribution within the mean multiplied or divided by $(\sigma_g)^2$. This distinction is a key property of the log-normal distribution and leads to the confidence intervals for bubbles in the two doughs shown in Table 3.3.

The two doughs were made from different formulae in order to produce two distinct consistencies. Based on Bloksma and Bushuk (1988), a water content increase of 1% (flour basis) in a dough formula reduces the stiffness of the dough by 5 to 15%, so that for these experiments the stiff dough (Formula A) would be about 20 to 50% stiffer than the slack dough (Formula B). This contrast in consistency was further accentuated by the use of a higher concentration of NaCl in Formula A relative to Formula B, as NaCl stiffens the wheat flour doughs when used at higher concentrations (Bloksma & Bushuk, 1988; Eliasson & Larsson, 1993). It can be observed that using these two different lean formulae to produce a stiff dough and a slack dough, different bubble size distributions were obtained in the doughs (Figure 3.1, Table 3.3). Although the geometric mean has not altered substantially, the distribution of bubble size in stiffer dough is statistically broader, even though substantially less air was entrained in the dough, as measured by the void fraction (ϕ). The latter result is consistent with dough density measurements of doughs made from flours of different strength (Campbell et al., 1993), where stronger (and presumably stiffer) doughs entrained less air.

The void fraction (ϕ) of the doughs was calculated in two ways (Table 3.3). Firstly, from the ratio (expressed as a percentage) of the total volume of bubble spheres in the scanned dough to that of the total volume of the scanned dough. Secondly, from the

density of the dough and its gas-free extrapolation ($\rho_{\text{gas-free dough}}$) determined from gravimetric measurements of the mass and volume of the dough, as follows:

$$\phi_A = 1 - (\rho_A/\rho_{\text{gas-free dough A}})$$

$$\phi_B = 1 - (\rho_B/\rho_{\text{gas-free dough B}})$$

where ρ_A = 1,190 kg/m^3 (experimentally determined, CV=2%) and $\rho_{\text{gas-free dough A}}$ = 1,285 kg/m^3 (taken from Elmehdi et al., 2004), as they used the same mixer and formula to prepare their experimental dough). As well, ρ_B= 1,075 kg/m^3, which was experimentally determined (CV=1%), whereas $\rho_{\text{gas-free dough B}}$ was estimated to be 1,200 kg/m^3 by using the gas-free density of Formula A dough but accounting for differences in the masses and volumes of NaCl and water between Formulae A and B.

The 3D analysis of the bubbles indicated that the dough made from Formula A (i.e., the stiff dough) had a void fraction of 7.64%, while the gravimetric technique indicated a void fraction of 7.58%. The disparity in void fraction between the two techniques was less than 1%, which translates to an uncertainty of less than 0.1% for the density of the gas-free dough, if it were to be derived from these void fractions. The gas-free dough density of Formula A (the stiff dough), based on a gravimetric-based technique first developed by Campbell (1991), was taken from the work of Elmehdi et al. (2004) using an extrapolation step. The tomography results confirm the validity of this extrapolation.

Although the preparation method for the stiff dough was identical to that of the dough of Elmehdi et al. (2004), their dough had a larger void fraction (8.46%). The smaller amount of gas entrained in our dough may be attributed to a substantial difference in the headspace pressure used during mixing, as our experimental dough was mixed in a

city situated at an altitude about 810 m higher than the city in which Elmehdi et al. (2004) mixed their sample – atmospheric pressure drops to 1/e of its ground level value at a height of about 8650 m at ambient temperature (Wolfson & Pasachoff, 1987). Accounting for the differences in altitude, and using the empirical relationship between headspace pressure and void fraction determined by Elmehdi et al. (2004), the void fraction of the stiff dough is predicted to drop from 8.46% to 7.70%, a value only slightly greater than what we measured by tomography (7.64%). Other contributing factors also include differences in resting times (i.e., gas losses to the atmosphere) of the dough ex-mixer and variability in the quality of the flour used due to differences in crop years even though both studies used CWRS flour.

For the slack dough, the void fractions measured by μCT compared to those measured by a gravimetric-based technique differed by nearly 9% (Table 3.3). The 3D analysis determined the density of the gas-free dough to be 1,188 kg/m^3 whereas the rule of mixtures estimated it to be 1,200 kg/m^3. Here the difference is just under 1%, which does not seem unduly large, but the difference led to an error of about 9% when void fractions were compared. The rule of mixtures should be used with caution as it does not take into account interactions between NaCl and water (e.g., solubility effects) and their interactions with polymers in the dough. For instance, chloride anions have been found to promote the aggregation of gluten proteins (Preston, 1981), suggesting that lowering their concentration in the slack dough (relative to the stiff dough) would result in a dough matrix less dense than that estimated by the rule of mixtures. The matrix (i.e., gas-free dough density) of the slack dough as measured by μCT was indeed less dense than that estimated from the rule of mixtures.

Bubble concentrations, as shown in Table 3.3, were also determined from these experiments. The stiff dough entrained nearly half the number of bubbles of that of the slack dough, and had nearly a 20% lower gas content, suggesting that the rheology of breadmaking dough was indeed influenced by the characteristics of the gas phase (and vice versa). Martin et al. (2004b) observed that aeration of a dough increased when the dough mixer was scaled up, chiefly, due to an increase in the Reynolds number. In the same way, the fewer bubble numbers and lower void fraction of the stiffer dough in the present study may be explained in terms of the Reynolds numbers, as this number decreases when the viscosity (e.g., consistency index) increases.

3.3.2. Comparison with other research on bubble size distributions in dough

A summary of research where the bubble size distribution in wheat flour doughs was measured is shown in Table 3.4. Shimiya and Nakamura (1997) found that the bubble size distribution (using circles) in dough changed quickly after mixing due to disproportionation; thus Table 4 includes only their data for 100 min after the end of mixing, which corresponds with the resting time of our doughs (90 min). However, Shimiya and Nakamura (1997) measured bubble (circle) sizes following a simple procedure that likely sacrificed precision, as evidenced by the large disparities between their reported bubble numbers and other previously published data (Table 3.4). In their technique, a sample was excised immediately after mixing of the dough, squashed between a slide and a cover glass and then directly observed under a microscope or stereoscope (depending on the level of magnification required). The thickness of their slices of dough, however, was fairly large, either 150 or 1000 μm, which in turn limited detection of all bubble circles smaller than the slice thickness, for these circles were not

necessarily sectioned and thus analysed. Other bubble size distributions reported in the studies included in Table 3.4 were obtained by physical sectioning of frozen/unfrozen dough using microtomy. Carlson and Bohlin (1978) found a median bubble size, $\overline{D}$, of 112 μm in dough for which the formula and preparation procedure were not reported. Their one-parameter probability density distribution provided only a location parameter $\overline{D}$ and recognized that the bubble size distribution did not conform to a normal distribution. In addition to a location parameter, a more sophisticated fitting function such as a log-normal density function (Equation 1.1) is also defined by a dispersion parameter (i.e., the standard deviation) which in turn facilitates an adequate characterization of the bubble size population. For instance, the number of bubbles having a particular size could be predicted from these fitting functions using such derived statistics as the intervals of confidence (Table 3.3).

3.3.3. Anisotropy analysis

Anisotropy was calculated in each slice from the 3D volumetric data by using the ratio of the major to the minor axis in ellipses fitted to the bubbles. Tomographic slicing occurred in the *xz*-plane of Figure 3.2, whereas the dough samples were compressed parallel to the z-direction to the fixed height of 2.17 mm. An anisotropy value greater than 1 represented a bubble that had undergone deformation during dough preparation and in which the anisotropy persisted for 90 min after sample preparation (Figure 3.2 inset, lower right). The anisotropy analysis indicated that bubble cross-sections were elliptical (Figure 3.3). Because anisotropy in small bubbles was prone to large errors due to the inability of pixels (square elements) to adequately follow the contours of a circular geometry, results for bubbles smaller than 80 μm are not included. Figure 3.3 shows that

Table 3.4. Literature reports of morphometric analyses of gas bubbles in dough

Reference	Mixer	Maximum Resolution (μm)	Slice thickness (μm)	Number of bubbles	ϕ (%)	$\overline{D}$ (μm)	SD (μm)
Carlson and Bohlin (1978)[a]	Not Communicated	90	30	86700 cm^{-3}	10	112	47.3
Bloksma (1990b)	Not Communicated	-	-	10^5–10^8 cm^{-3}	10	35	-
Campbell et al. (1991)	Food processor	39	30	78500 cm^{-3}	2.90	70.9	24.1
Campbell et al. (1991)	Tweedy 10	39	30	33100 cm^{-3}	2.80	89.4	46.9
Shimiya and Nakamura (1997)[b]	Bread-making machine	3	150	2500 cm^{-2}	3.5	35	1.8[c]

([a]) Number of bubbles and mean diameter derived from their proposed probability density function; SD derived using empirical formula proposed by Campbell et al. (1991)

([b]) Slice thickness increased to 1 mm when circle diameters > 40 μm; ϕ was the total sectional area covered by the circles (m^2/m^2); mean diameter following 100 min resting of dough; $\overline{D}$ was the median diameter in a log-normal distribution (see reference for more details)

([c]) It represents a geometric SD (SD = exp (1.8))

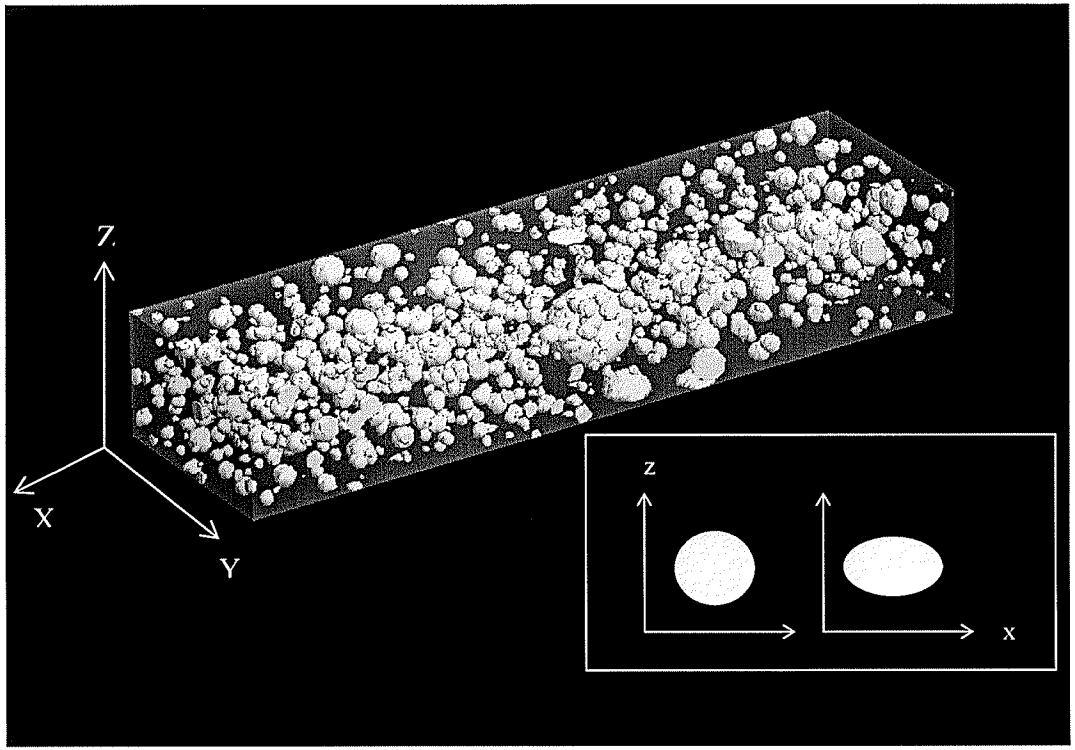

Figure 3.2. Spatial rendering of the 3D bubble size distribution in a dough specimen with dimensions (X,Y,Z) = 732 x 200 x 120 voxels (equivalent to 7.32 x 2.00 x 1.20 mm^3). 200 μCT slices were assembled to produce this rendering using Skyscan® ANT Visualization Software (version 2.2.6.0). Inset at the bottom depicts an isotropic (left) and anisotropic (right) deformation of a bubble as seen in the tomographic slices.

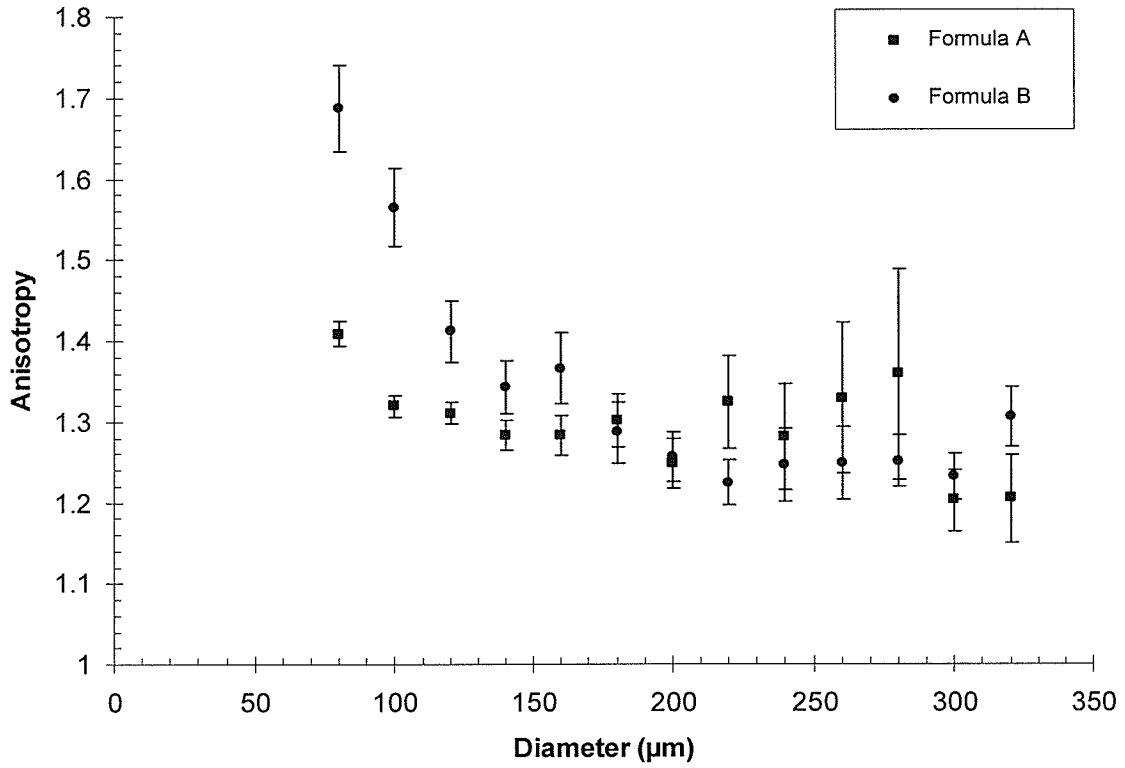

Figure 3.3. Anisotropy as a function of bubble sizes in a dough specimen with dimensions 7.32 x 1.20 x 2.00 mm^3. Anisotropy was the ratio of the minor to major axis of best-fitted ellipses to the circle data across 200 serial μCT *slices* (*slice* thickness=10 μm). Error bars represent 95% confidence limits.

bubble cross-sections in the *xz* plane were more elliptical (more anisotropic) in the slack(Formula B) dough up to bubble sizes of 180 μm, at which point they became essentially similar.

3.3.4. Bubble separation

Bubble separation is the distance between bubbles within a volume of interest, and is of relevance in calculations of rates of disproportionation of gas bubbles in doughs (van Vliet, 1999). The distributions of distances between bubbles in both doughs were well defined by the normal distribution (Figure 4.4). Bubbles were separated by a mean distance of 338 μm in the stiff dough (Formula A) and by 460 μm in the slack dough (Formula B) (Table 3.5). Relative to the mean bubble sizes, the bubble separation analysis suggests that bubbles were discretely separated in both experimental doughs, as the distance between bubbles was on average 3 to 5 times the size of an average bubble. Bubble separations were more dispersed in the slack dough compared to the stiff dough. This is shown graphically in Figure 3.4 and in tabulated form in Table 3.5.

According to the model of Bloksma (1981) where spherical air bubbles of uniform diameter are arranged cubically (i.e. hexagonal array) in dough, the distance between bubbles (e.g., bubble separation distance) is proportional to both the bubble diameter and a constant $\left(\pi/\sqrt{18}\right)^{1/3}$ and is inversely proportional to the cubic root of the void fraction. Consequently, Bloskma's model would predict that the stiff and slack doughs had approximately the same separations between bubbles (213 and 217 μm), a prediction that is significantly far from the bubble separation distances measured in here by μCT scans (338 and 460 μm). This disparity highlights the importance of integrating

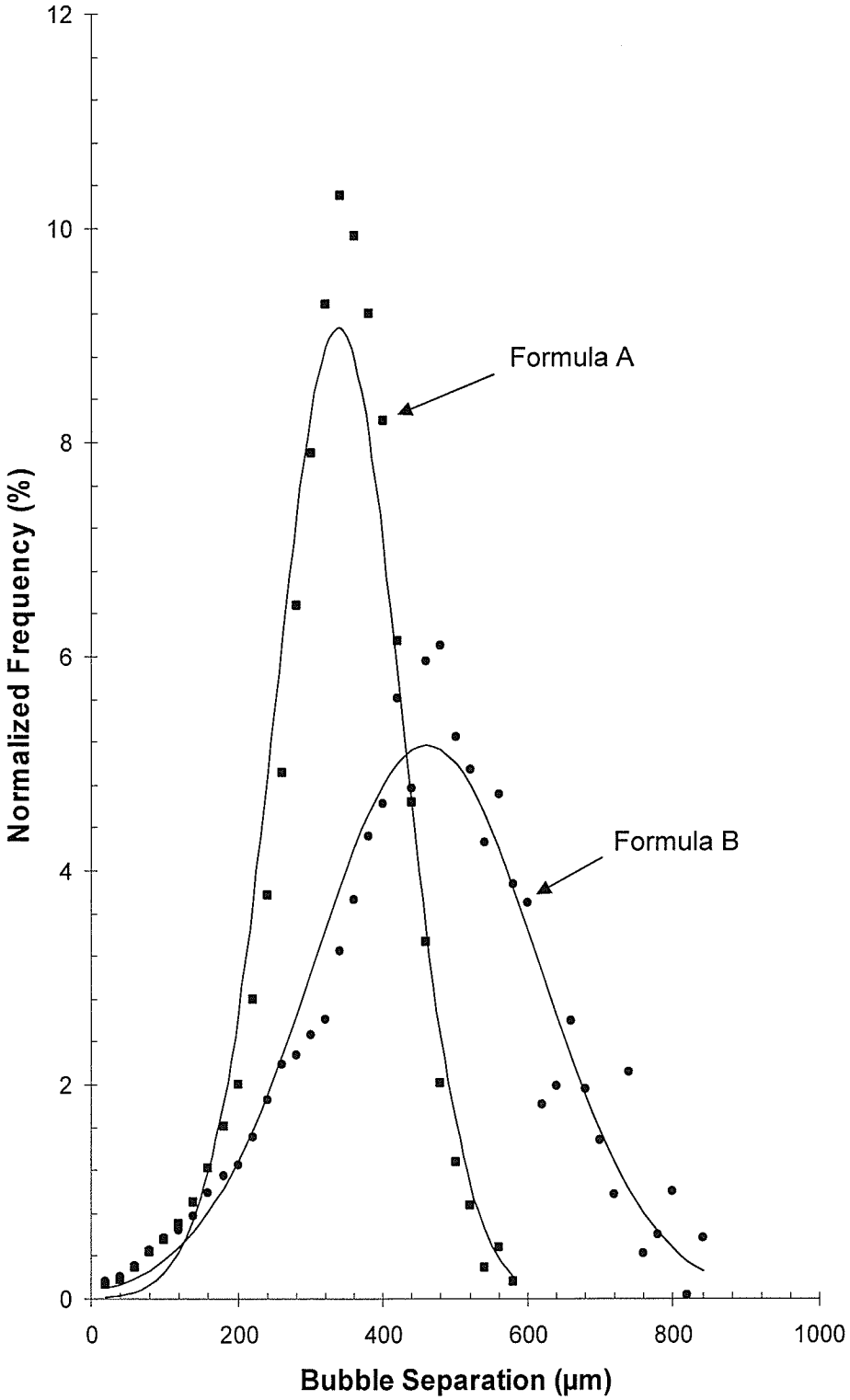

Figure 3.4. Bubble separation (3D analysis) distribution in doughs prepared with one of two lean bread formulas. Solid lines represent fits to normal distributions with means μ and standard deviations σ (Table 3.5).

Table 3.5. Statistical parameters from the best-fit normal probability density functions used to describe the distribution of separation distances between gas bubbles in dough as detected by 3D analyses on μCT radiographs.

	μ (μm)	σ (μm)	95.5% Confidence Level (μm)
Formula A	338	88.1	74-602
Formula B	460	155.6	0-936

information on bubble size distributions in order to develop good mathematical models for predicting the properties of wheat flour dough.

3.4. Conclusions

These experiments showed how the bubble size distribution in wheat flour dough can be characterized based on information from μCT scans and the use of powerful software. Bubble sizes were reconstructed in three dimensions from circles (i.e., bubble cross-sections) found in 200 μCT slices 10-μm thick of both experimental doughs, without the need to resort to their physical sectioning. The bubble size distribution in the doughs was well described by a two-parameter log-normal density function, with smaller bubble sizes and a wider size distribution in doughs of a stiff consistency. Anisotropy analysis showed that bubbles were deformed in the direction perpendicular to the compressional force (because of sample preparation procedures). Overall results support the view that dough consistency (i.e., viscoelastic properties of the dough) affects the number and size distribution of bubbles that are entrained during mixing. Dough consistency was also found to affect the packing of bubbles as determined by the distribution of distances between bubbles. Bubbles entrained in the stiff dough were

dispersed over a narrower range of distances than those in the slack dough. The stiff dough occluded a smaller concentration of bubbles than the slack dough, which is in agreement with reports showing that doughs made from strong breadmaking flours had smaller void fractions than doughs made from weak flours. Establishing a clearer relationship between the degree of dough aeration, the dough formula, and the processing conditions during mixing is a sought-after goal in the baking industry, as it could provide, for example, clues as to how to design more energy efficient dough mixers. The present work suggests that using x-ray microtomography to study bubble size distributions warrants a clearer elucidation of such a relationship.

CHAPTER FOUR

The Use of a Pressuremeter to Measure the Kinetics of Carbon Dioxide Evolution in Chemically Leavened Wheat Flour Dough

Abstract

The production of carbon dioxide (CO_2) in fermenting dough is rarely measured in breadmaking studies, yet CO_2 is the driving force for the creation of the highly aerated structure of bread. While yeast is the primary source of CO_2 for breadmaking, an alternative and viable source of the gas is provided by chemical leavening systems. One major impediment to a wider use of chemical leavening agents is the lack of standardized instrumentation capable of providing information on the rates of CO_2 production from chemical leaveners in a format that is meaningful to both the technologist (i.e., the dough rate of reaction or DRR) and the researcher (e.g., in terms of reaction rate constants for the kinetics of carbon dioxide evolution, or in terms of fundamental units - kmol CO_2 per kg of dough per second). This paper presents an original methodology to carry out the dough rate of reaction (DRR) test using a commercial pressuremeter, the Gassmart apparatus, and to model the kinetics of CO_2 evolution of chemically leavened dough. Lean formula doughs were leavened at 27 °C and 39 °C with four chemical leavening systems containing sodium bicarbonate and one of four leavening acids, sodium acid pyrophosphate 40 (SAPP), adipic acid (ADA), potassium acid tartrate (KAT), and glucono-delta-lactone (GDL). Results for SAPP and KAT doughs show that the DRR curves based on the Gassmart had equivalent trends and the same percentages of evolved CO_2 as those reported in the literature. No reports were found in the literature for the

DRR curves of ADA doughs, so new data is being presented. The DRR curves associated with GDL exhibited the same trends as those for SAPP, KAT and ADA, though differing from the DRR results included in a previously published report. Possible factors affecting the said discrepancies are discussed. Chemical kinetics theory was used to gain an insight into the reaction mechanisms responsible for the evolution of carbon dioxide from the leaveners. A first-order reaction kinetics model was found to be suitable for describing the neutralizing properties of glucono-delta-lactone and adipic acid as leavening systems, whereas a first-order reaction kinetics model for irreversible parallel reactions better described the leavening properties of the acidic salts potassium acid tartrate (cream of tartar) and sodium acid pyrophosphate 40.

4.1. Introduction

It is well established that measurements of gas production and gas retention during leavening of the dough are of great importance to breadmaking, since it has long been known that dough of good gas-production and good gas-retention capacities is a pre-requisite to make good bread (Elion, 1940). While measurements of a dough's gas-retention properties have received a great deal of attention, particularly over the past few years (Campbell, 1991; Campbell et al., 1993; Shimiya & Nakamura, 1997; Mitchell et al., 1999; Shah et al., 1999; van Vliet, 1999; Campbell et al., 2001; Martin, 2004; Martin et al., 2004a, 2004b), actual gas production properties are typically not measured, even though this information is required to model such important breadmaking phenomena as bubble growth during proving of the dough (Chiotellis & Campbell, 2003b). In a recent study, Chiotellis and Campbell (2003b) noted that a technique capable of providing

accurate information on the rates of carbon dioxide production in fermenting dough is still needed.

While fermentation of bread dough is traditionally carried out by the action of yeast cells on fermentable sugars, bread dough can also be leavened using chemical agents alone or in combination with the yeast (Heidolph, 1996; Holmes & Hoseney, 1987b). These chemical leavening agents have become particularly useful in leavening bread dough during unconventional processing, such as extrusion processing (Geng & Hayes-Jacobson, 2001, 2003), or for doughs subject to refrigeration or frozen storage (Atwell, 1985; Laughlin & DeMars, 1999; Narayanaswamy & Daravingas, 2001; Perry & Colman, 2001, 2003; Hansen et al., 2003; Laughlin et al., 1999, 2000; Yong et al., 1983a, 1983b), or to microwave 'baking' (Corbin & Corbin, 1992, 1993; Geng & Hayes-Jacobson, 2003; Cochran et al., 1990). Chemical leavening offers several advantages over biological (yeast) leavening. Carbon dioxide production capabilities are not affected by prolonged refrigerated or frozen storage in dough prepared with chemical leaveners. Also, judicious selection of chemical leaveners enables the production of dough capable of producing carbon dioxide at working temperatures that span from ambient to baking temperatures (Heidolph, 1996), which could aid in shortening the proofing time and hence the preparation time at the bakery facility (Huang & Panda, 2004).

Gas production in chemically leavened products is defined by a chemical neutralization reaction whereby sodium bicarbonate, the preferred source of carbon dioxide (Heidolph, 1996; Conn, 1981), reacts with a leavening acid to evolve carbon dioxide at a specified rate. Conveniently, the chemistry of the reaction is straightforward as the type and quantities of reactants required to ensure complete neutralization is

governed by stoichiometry (Conn, 1981; Heidolph, 1996), whereas the rates at which carbon dioxide is produced are governed by chemical kinetics. Although the stoichiometry of the chemical leavening reaction has been recognized in various reports (Heidolph, 1996; Hoseney, 1998; Miller et al., 1994), the use of chemical kinetics theory to describe the chemical leavening reactions has not yet been reported.

In a chemically reacting system, many simultaneous chemical processes take place via consecutive or parallel chemical reaction paths, with the overall goal of chemical kinetics being to measure and interpret the evolution in time of these paths, so that the rate of reaction of the chemical process can be described analytically (Boudart, 1968). In biochemical reactions, the number of parallel and consecutive paths can comprise dozens of chemical reactions or *pathways* (Boudart, 1968), so that, for example, an analytical description of carbon dioxide production by yeast fermentation of sugars can become extremely complex (Bier et al., 2000). The simplicity of the chemical leavening reactions suggests that it may lend itself to be analytically described in terms of chemical kinetics principles. Such description will permit the identification of not only reactant and by-product species, but also of intermediate species which often vanish during the course of the reaction (Moore, 1962). Recognition of intermediate species should provide a more complete description and understanding of the chemical leavening reaction. Hence, the study of chemical leavening systems from a perspective of chemical kinetics should aid in identifying the factors controlling the rates at which chemical leavening system convert acids and bases into carbon dioxide, salts and water. The rate of reaction of a leavening acid is the single most important consideration when choosing the leavening acid component of a chemical leavening system (Hoseney et al., 1988).

In the chemical industry, the rate of reaction of leavening acids is typically measured in terms of the dough rate of reaction (DRR) (Parks et al., 1960). The DRR test is an empirical test that measures the evolution in time of the percentage of carbon dioxide evolved from the chemical leavening system. A gas-measuring test apparatus with characteristics and capabilities similar to that described by Parks et al. is the computerized Gassmart apparatus, and this instrument has been used to measure gas production in yeasted dough (David, 2003; Sahlstrom et al., 2004; Sapirstein et al., 2007) and in chemically leavened dough (Jantzi et al., 1999), with test results typically shown as a pressure versus time plot. However, such a plot does not directly characterize the chemical leavening systems in terms of the DRR test nor can it be easily interpreted using chemical kinetics theory.

Gas production rates in chemical leavening systems depends on the type and concentration of reactants and products, availability of water, and the reaction temperature and pressure via the laws of chemical kinetics for a chemical neutralization reaction. Therefore, it is theoretically possible to express the properties of chemical leaveners in terms of chemical kinetics parameters (e.g., order of the chemical reaction and reaction–rate constant at a given temperature or pressure). The objective of this paper is to use the Gassmart apparatus, a pressuremeter, to characterize the gas production properties of selected chemical leavening systems in wheat flour dough based on the test results of the dough rate of reaction (DRR) test. Gas production rates are discussed in light of chemical kinetics theory underlying chemical neutralization reactions.

4.2. Materials and Methods

4.2.1. Wheat sample

The flour employed in this study was obtained from a number 1 grade sample of Canadian Western Red Spring wheat milled as a straight-grade flour in the pilot mill of the Canadian International Grains Institute, Winnipeg, MB. Flour protein and ash contents in the flour were 14.0 % and 0.45 %, respectively (14% moisture basis).

4.2.2. Chemical leavening systems

Six chemical leavening systems containing sodium bicarbonate and one of four leavening acids (sodium acid pyrophosphate 40 (SAPP), adipic acid (ADA), potassium acid tartrate (KAT), and glucono-δ-lactone (GDL)) were used. Dough formulations are described in Table 4.1. The amount of water added to the formula was equivalent to Farinograph water absorption minus 2%. Formula ingredients (except the flour) were accurately weighed to the nearest 0.0001 g. The ingredient suppliers were Sigma Aldrich Co., St. Louis, MO, for sodium chloride and sodium bicarbonate; Aldrich Chemical Company Inc., Milwaukee, WI, for SAPP 40 and potassium acid tartrate; and Acatris, Oakville, ON, for GDL.

4.2.3. Measurements of gas evolution

Gas production of each chemical leavening system was measured using the Gassmart apparatus (TMCO Inc., Lincoln, NE). The latter comprised six 250-ml aluminum pressure vessels connected to a PC running proprietary Gassmart data acquisition and analysis software (Version 2.0). Data analysis was accomplished in Excel compatible software (Origin 7.5. Scientific software; Originlab®, Northampton, MA)

after converting the Gassmart data files (.MXG) into comma delimited files using CSV Builder (RAR Software Systems Inc., Winnipeg, MB). A circulating water bath was used to maintain the pressure vessels at constant temperatures (27 or 39 °C) for all experiments. The pressure vessels were fitted with a temperature gauge whose readings were displayed in real time on the PC. Prior to the start of the experiments, the water bath was run for a sufficiently long time to ensure that the vessels were equilibrated to the experimental temperature.

The experimental samples were prepared as follows. The dry ingredients were poured inside a randomly assigned pressure vessel and blended using a glass rod. The formula water, pre-heated to the experimental temperature, was added to the dry ingredients and quickly but gently mixed (less than 40 s) into a homogenous mixture using the glass rod. Thirdly, the gas vessel was sealed, immersed in the water bath, and its pressure (manometric) brought to 0 kPa using the gas release valve fitted on the vessel lid, at which time, the experiments began. The time interval between the addition of water and the first pressure reading was carefully controlled and kept constant at 55 ± 5 s. All experiments were carried out in duplicate. Gas pressure, in kPa, exerted by the evolved CO_2 was measured over a period of 150 min at a rate of 5 readings per second. The pressure transducer sensitivity was better than 10 Pa which corresponded to the maximum detection limit for variation in gas pressure. To determine the pressure exerted by the CO_2 evolved by the chemical leavening system only, a baseline pressure was determined to correct the pressure contributions of non- CO_2 gases, such as water vapour. The baseline pressure was measured using the same ingredients used to prepare the

TABLE 4.1. Formulation [a,b] employed to prepare experimental dough samples

Ingredients	SAPP 40 (HL)	ADIPIC (LL)	ADIPIC (HL)	K-TART (ML)	GDL (LL)	GDL (HL)
Wheat flour	10 g	10 g	10 g	10 g	10 g	10 g
Water	67.4%	67.4%	67.4%	67.4%	67.4%	67.4%
Sodium chloride	0.75%	0.75%	0.75%	0.75%	0.75%	0.75%
Sodium bicarbonate	4.20%	1.40%	4.20%	2.80%	1.40%	4.20%
Sodium acid pyrophosphate 40	5.83%	-	-	-	-	-
Adipic acid	-	1.22%	3.65%	-	-	-
Potassium acid tartrate	-	-	-	6.22%	-	-
Glucono-delta-lactone	-	-	-	-	3.11%	9.33%

[a] Ingredient amounts expressed on percent flour basis (14% m.b.)

[b] Labels in the columns reflect leavening acid in formula. Letters in parentheses denote the concentration of sodium bicarbonate (fwb): LL = low level (1.40%); ML = medium level (2.80%); and HL = high level (4.20%).

formula, except for the sodium bicarbonate, which was excluded to eliminate the source of CO_2. This baseline pressure was subtracted from the appropriate leavening system's total gauge pressure in every experimental sample.

4.3. Results and Discussion

4.3.1. Gauge pressure

A typical CO_2 production curve using GDL as the chemical leavener is shown in Figure 4.1. The result shows that gauge (manometric) pressure of the system initially and rapidly increased in a linear manner before quickly slowing down until a maximum value was reached at long fermentation times. A similar pattern of pressure evolution with time was observed for the baseline pressure. Depending on the type of leavening system, the level of sodium bicarbonate, and the fermentation temperature (Table 4.2), the baseline pressure represented as low as 4 % to as high as 50% of the maximum gauge pressure. A pressure-meter to measure gas production in yeasted flour is described in the AACC Approved Method 22-11 (AACC, 2000) that indirectly determines diastatic activity in flours. This approved method recommends that the manometer be adjusted to zero pressure 5 min after the start of an experiment to allow the gas contents of the system to attain thermal equilibrium. Similarly, AACC Approved Method 89-01 (AACC, 2000), used for measuring total gas production in yeasted dough by a pressure-meter, recommends that a 5 min waiting time before data acquisition. In contrast, for a chemical leavening system, timing is critical to accurately determine the amount of CO_2 evolved from a system, and so data acquisition should start as soon as the formula water is added

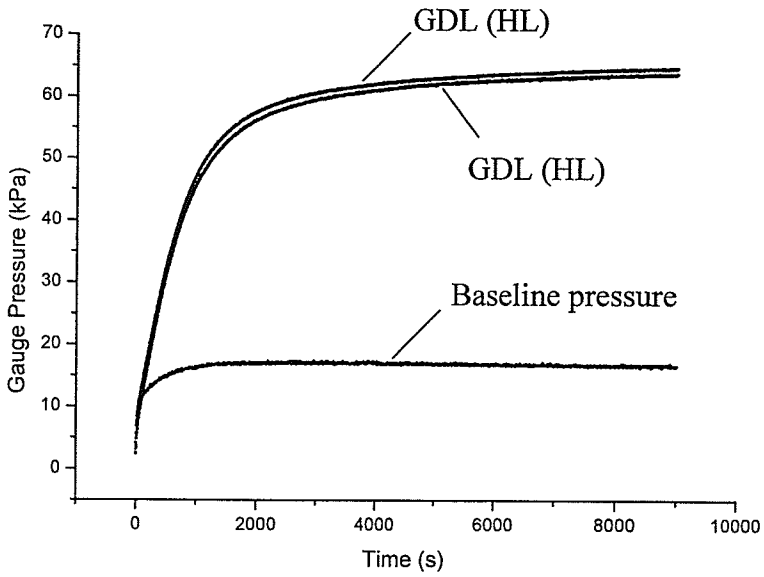

Figure 4.1. Typical pressure-time plot and baseline pressure generated by the Gassmart apparatus for duplicates of GDL (HL) dough, as specified in Table 4.1. Leavening temperature was 39 °C. Baseline pressure (two virtually superimposed lower lines) prepared without 0.42 g sodium bicarbonate.

TABLE 4.2. Contribution of baseline pressure to the total final gauge pressure registered in the Gassmart apparatus from various chemical leavening systems at two fermentation temperatures

Chemical leavening system	Baseline pressure (percent of total gauge pressure)	
	27 ° C	39 ° C
SAPP 40 (HL)	16 ± 1.2	34 ± 2.5
ADIPIC (LL)	42 ± 2.1	42 ± 0.5
ADIPIC (HL)	6 ± 0.1	20 ± 0.3
K-TART (ML)	10 ± 0.6	30 ± 2.1
GDL (LL)	40 ± 0.4	50 ± 0.6
GDL (HL)	9 ± 0.3	17 ± 0.3

to the system. The importance of timing can be seen in Figure 4.1 (an extreme case), where nearly 27 % of the total leavening capacity was given off within 5 min of the start of the experiment. Also, in the same time period, as much as 73% of the total baseline pressure was reached. Measurement of baseline pressure ensured that initial thermal expansion of gases, in addition to the pressure contribution of water vapour, was accounted for and cancelled out when subtracted from the gauge pressure readings, thus negating the need for a 5 min waiting time, as for yeasted dough.

4.3.2. Dough rate of reaction

The dough rate of reaction (DRR) test is commonly used to measure or predict the rate of carbon dioxide evolution during mixing and holding of the dough. In this test, the percentage of evolved carbon dioxide from the dough is measured over time (Conn, 1981; Heidolph, 1996; Parks et al., 1960). Given that the sodium bicarbonate dissolves almost immediately in the aqueous phase of dough (Conn, 1981), the rate of carbon dioxide production actually reflects the rate of reaction of the leavening acid (i.e., the rate of hydrogen ion production by the leavening acid assuming instant reactivity between

bicarbonate and the hydrogen ions). Mathematically, a chemical leavening system's dough rate of reaction with time, *DRR (t)*, is defined by the following relationship:

$$DRR\ (t) = n\ (t) / n_{total} * 100\ \% \tag{4.1}$$

where *n (t)* is the moles of evolved carbon dioxide as a function of time [mol s^{-1}] and n_{total} is the moles of carbon dioxide included in the formula [mol]. Because the number of moles of carbon dioxide evolved from the chemical leavening system is equivalent to the number of moles of sodium bicarbonate therein, the following equation applies:

$$n_{total} = n_{NaHCO_3} = \frac{m_{NaHCO_3}}{MW_{NaHCO_3}} \tag{4.2}$$

where n_{NaHCO_3} is the number of moles of sodium bicarbonate, m_{NaHCO_3} is the mass of sodium bicarbonate, and MW_{NaHCO_3} is the molecular weight of sodium bicarbonate (84 g mol^{-1}).

However, a chemical leavening system evolves carbon dioxide that either escapes the dough in the gaseous state or remains dissolved in the liquid state in the dough. To evaluate the amount of gaseous carbon dioxide evolved from the chemical leavening reaction, $n_1(t)$, the pressure exerted by the gaseous carbon dioxide was converted into suitable units of mass of carbon dioxide by using the ideal gas law:

$$P(t)\ V = n_1(t)\ R\ T$$

$$n_1(t) = P(t)\ V\ R^{-1}\ T^{-1} \tag{4.3}$$

Here *P(t)* stands for the pressure exerted by the gaseous CO_2 as a function of time (Pa), *V* is the volume of the gas vessel (2.5 x 10^{-4} m^3), $n_1(t)$ is the number of moles of gaseous CO_2 evolved as a function of time (mol), and *R* is the universal gas constant (8.315 J mol^{-1} K^{-1}). To determine the concentration of CO_2 in the liquid state in the

dough, C_M, it was assumed that the dough achieved saturation immediately (Bloksma, 1990a; Shah et al., 1998). Hence, the number of moles of CO_2 in the liquid state in the dough did not vary as a function of time but was rather a constant, n_2. To calculate n_2, C_M was calculated based on the fact that its magnitude is proportional to the final partial pressure of CO_2 in the gas bomb, P, as dictated by Henry's law:

$$C_M = P * H^{-1}$$

But, $C_M = n_2$ / (volume of non-aerated part of the dough) = n_2 / ($m_{dough} * \rho_{dough}^{-1}$)

Therefore,

$$n_2 = P * H^{-1} * m_{dough} * \rho_{dough}^{-1} * 1000 \quad (4.4)$$

where C_M stands for the CO_2 concentration in the dough (mol per m^3), P is the final partial pressure of CO_2 in the gas bomb at long fermentation times (since the [gauge] pressure in the Gassmart increased over time only due to CO_2 evolution, $P = P(t)$ for $t \sim$ 9000 s), H is Henry's law constant (J mol^{-1}), m_{dough} is the mass of dough (kg), and ρ_{dough} is the density of the gas-free dough (assumed to be 1,285 kg m^{-3} for all doughs; Elmehdi et al., 2004). For any given leavening system, the pressure measured at 9,000 s was very close (>98%) to the pressure estimated by the fits at time 10^{34} s. Henry's law constant (J mol^{-1}) was taken to be equal to 60 * (T – 273) + 900 (Chiotellis & Campbell, 2003b), where T is temperature (K).

Therefore, the total number of moles, $n(t)$, evolved by a chemical leavening system at any given time t was given by:

$$n(t) = n_1(t) + n_2 \quad (4.5)$$

From the 12 sets of experimental values and equations (4.3) and (4.4), 12 sets of values for Eq. (4.5) as a function of time could be obtained for the leavening treatments shown

in Table 4.1. Then, substituting equations (4.2) and (4.5) into equation (4.1) created 12 DRR curves representing six leavening treatments and two fermentation temperatures. Figures 4.2 and 4.3 show the dough rate of reaction for various chemical leavening systems (i.e., DRR curves) for 27 and 39 °C, respectively.

Figure 4.2 shows that at 27 °C SAPP 40 was able to evolve about 40 % of the available carbon dioxide. This percentage of carbon dioxide is in agreement with values reported by Conn (1981), Heidolph (1996), Parks et al. (1960) and Innophos (Undated) for SAPP 40. In fact, SAPP 40 derives its industrial name *40* because it evolves 40% of the available carbon dioxide in the DRR test (Heidolph, 1996). However, these reports indicated that the time required for SAPP 40 to evolve 40% of the available carbon dioxide was about 8 min. In constrast, SAPP 40 required at least 1 h to evolve the same percentage of available carbon dioxide in the Gassmart apparatus (Figure 4.2). Despite the disparities in the absolute values of evolution times, the Gassmart apparatus produced a DRR curve for SAPP 40-leavened dough that was highly correlated in shape with previously published results.

Similarly, Figure 4.2 shows that potassium acid tartrate (KAT) evolved about 70% of the available carbon dioxide, which was in agreement with the reports of Conn (1981) and Heidolph (1996). However, in this study the time was about 20 min instead of the 8 min reported by the same authors. Similar to the results for SAPP, the shape of the DRR curve for KAT (Figure 4.2) was highly correlated with those of Conn (1981) and Heidolph (1996). Differences in time scales between the DRR curves obtained from the Gassmart and those reported in the literature will be discussed below.

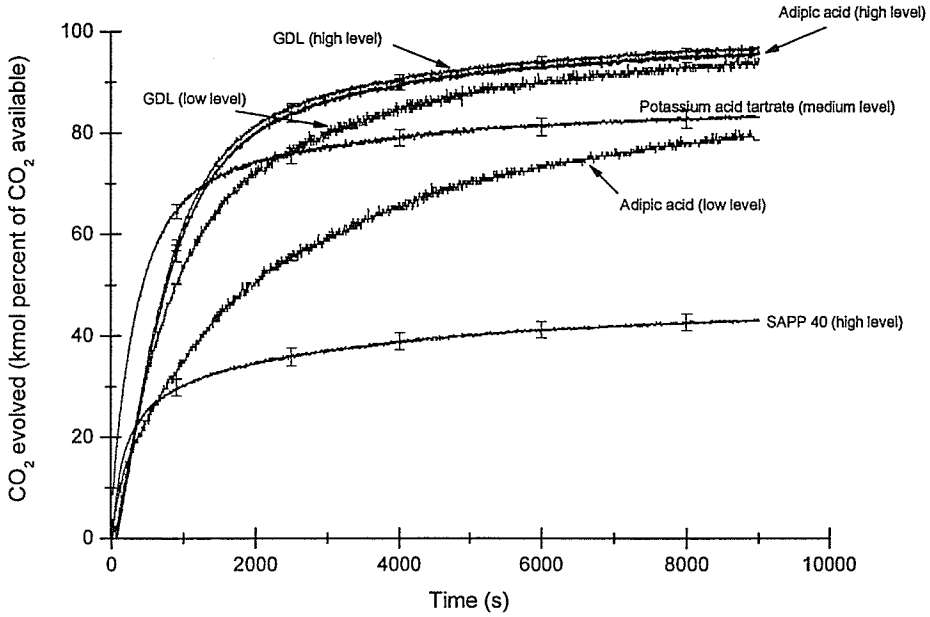

Figure 4.2. Evolution of carbon dioxide at 27 °C in undeveloped wheat flour doughs that had been prepared with various chemical leavening systems as detected by the Gassmart apparatus. Chemical leavening systems consisted of one leavening acid (SAPP 40, GDL, potassium acid tartrate or adipic acid) and one of the following levels of sodium bicarbonate (100 g flour basis, 14% w.b.): high level = 4.2 %; medium level = 2.8 %; and low level = 1.4 %. Error bars denote ± 1 SD.

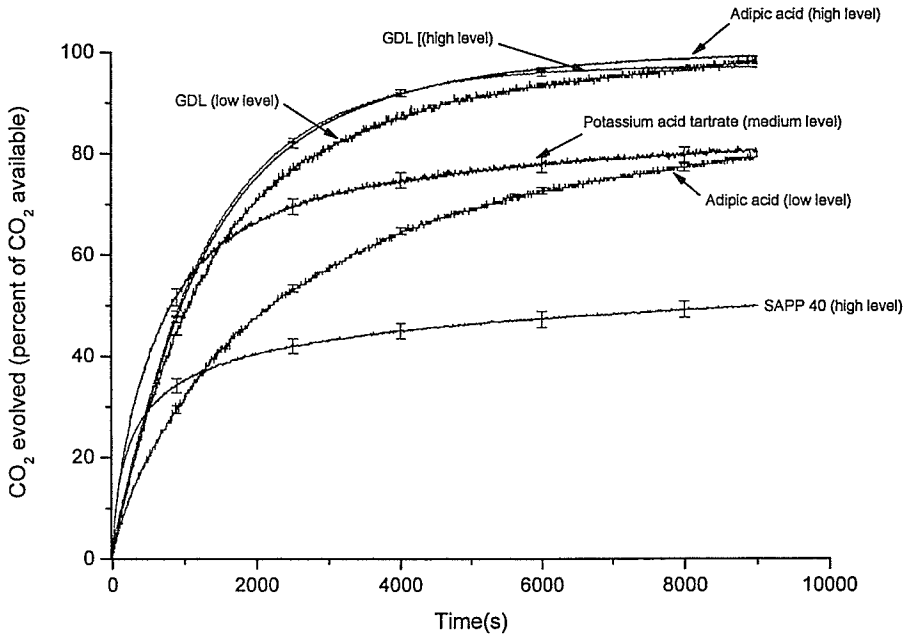

Figure 4.3. Evolution of carbon dioxide at 39 °C in undeveloped wheat flour doughs that had been prepared with various chemical leavening systems as detected by the Gassmart apparatus. Chemical leavening systems consisted of one leavening acid (SAPP 40, GDL, potassium acid tartrate or adipic acid) and one of the following levels of sodium bicarbonate (100 g flour basis, 14% w.b.): high level = 4.2 %; medium level = 2.8 %; and low level = 1.4 %. Error bars denote ± 1 SD.

For GDL-leavened dough, Figure 4.2 shows that the percentage of evolved carbon dioxide followed the same pattern as that for adipic acid, though the DRR pattern of GDL could not be directly compared against that reported by Conn (1981). This was because the reported DRR curve for GDL included data only up to 10 min, even though the positive slope of their DRR curve was a clear indication that the percentage of evolved carbon dioxide would continue to rise after 10 min. Figure 4.2 shows that the percentage of evolved carbon dioxide from GDL reached a maximum value of about 90% after nearly 1 h fermentation. For the sake of comparing time scales, Conn (1981) reported that for GDL to evolve 40% of the available carbon dioxide it required 10 min of fermentation, whereas, by contrast, Figure 4.2 shows that evolving the same percentage of carbon dioxide required at least 30 min. No DRR curves for adipic acid have been found in the literature. In terms of temperature effects, a comparison between Figures 4.2 and 4.3 indicated that increasing the fermentation temperature from 27 to 39 °C increased carbon dioxide production rates of the chemical leaveners studied only slightly.

Among the sources of variability contributing to the differences observed in time scales between DRR curves generated by using the Gassmart apparatus and the apparatus described by Parks et al. (1960), temperature, geometry and dimensions of the gas bomb, geometry and dimensions of the agitator, level of chemical leaveners in the formula, and dough formulation can be regarded as the most significant (Parks et al., 1960; Conn, 1981). Sample size can also impact the repeatability of gas production measurements made by a gas detection system (Gelinas, 1997). A comparison of the technique and testing apparatus between the present experiment and that described by Parks et al. (1960) shows that the sample size, the dimensions of the gas bomb, and dough

formulation were all relevant factors that accounted for the deviations in time scales between the observed and Parks et al. (1960) results. The fact that the Gassmart apparatus lacks an agitator (stirring mechanism) can also explain at least in part the longer than expected reaction times that have been observed (Figures 4.2 and 4.3). It is worth noting that temperature was also comparable in both experiments (27 °C). The present experiment as well as that reported by Parks et al. (1960) employed gas bombs of similar geometry (both used cylinder-shaped vessels) and tested experimental dough samples formulated with comparable leavening power (i.e., 1.4 g $NaHCO_3$ per 100 g flour in the Gassmart *versus* 1.3 g per 100 g flour in Parks et al., 1960). No sample preparation procedure was described in the work of Conn (1981) or Heidolph (1996).

Though relevant sources of variability have been identified above, the type and total number of experiments conducted in this study was not suitable to determine the individual contributions of every source of variability to the observed disparities in reaction times (i.e., time required to reach a maximum value in the DRR test curve). An attempt will be made, though, to explain the observed differences by taking into account the physics behind the time evolution of gaseous CO_2 in the headspace of the gas measuring device. The following discussion on the time evolution of CO_2 from the surface of the dough is supported by the mathematical framework developed for mass diffusion of CO_2 in fermenting doughs (Shah et al., 1998, 1999; Chiotellis & Campbell, 2003b).

Mass diffusion of CO_2 from the dough to the headspace of a gas measuring device such as the Gassmart (or of the apparatus described by Parks et al., 1960) is governed by the following relationship (Shah et al., 1998):

$$Q = K_L A (C_M - C_A) \quad (4.6)$$

where Q = the rate of diffusion of carbon dioxide to the headspace atmosphere (kmol s^{-1})

K_L = the overall mass transfer coefficient (m s^{-1})

A = surface area for mass transfer (m^2)

C_M = CO_2 concentration in the dough (kmol m^{-3})

C_A = CO_2 concentration in the headspace atmosphere (kmol m^{-3})

Equation (4.6) suggests that there would be a Q associated with the Gassmart (Q_g) and another one associated with the apparatus described by Parks et al. (1960) (Q_p). Because K_L, C_M and C_A were the same, or almost the same, for both Q_g and Q_p, the only parameter that could explain differences in time scales between the experimental (Figure 4.2) and the DRR test results reported in the literature (Conn, 1981; Parks et al., 1960) is A, the surface area for mass transfer associated with the experimental samples. Interestingly, the sources of variability identified in preceding paragraphs as relevant (sample size, the dimensions of the gas bomb, dough formulation and the lack of an agitator in the Gassmart apparatus) all have an influence on dough surface area. Most notably, the sample size used in the present experiment was substantially smaller (~ 18 g) than that used in the work of Parks et al. (1960) (~ 111 g). Assuming identical shapes of dough (i.e., spheres) were formed in the apparatus of Parks et al. (1960) and in the Gassmart, the surface area of the sample in the former one would have been at least 3 times as large as that found in the present experiment (ratio of masses is proportional to the ratio of surface areas to the power of 2/3). Equation 6 suggests that such a difference in surface area would mean that the diffusion of CO_2 from the experimental dough was significantly smaller than the one associated with Parks et al.'s experiment ($Q_p > 3\ Q_g$). A comparison

of the observed (Figure 4.2) and the literature (Parks et al., 1960) DRR test results for SAPP 40 indicates that a sample in the Gassmart took about 13 times as long to reach a peak value in these DRR curves as that registered in the apparatus of Parks et al. (1960). This leads to the suggestion that the differences in sample size could have been only partly responsible for difference in the experimental DRR test results.

Another important factor that may contribute to the timescale differences for the DRR detected by the Gassmart and Park's instrument is the ratio of dough surface area (*A*) to the volume of the headspace above the dough in the gas bombs (*VH*). If *A*/*VH* is very large (e.g., placing a very large sample in the Gassmart), it is possible that the chemical leavening system ceases to evolve CO_2 at the experimental temperature not because the reactants became exhausted during chemical leavening (which is what we desire to measure) but because an equilibrium was established between the partial pressure of CO_2 gas in the Gassmart bomb and the concentration of CO_2 dissolved in the dough (Le Chatelier's principle). To determine which of these hypotheses was true an experiment was run whereby the gas bomb containing the leavening system with the greatest CO_2 production capacity (i.e., HL GDL at 39 °C) was bled at the end of the fermentation (2.5 h) and its gas pressure monitored for one more hour at the same controlled temperature (i.e., 39 °C). No pressure increase was detected (results not shown) after bleeding of the gas bomb, which indicated that the evolution of CO_2 by the chemical leavening system was not governed by the partial pressure of CO_2 gas in the Gassmart bomb but by the equilibrium of reaction established in the dough at the experimental temperature (i.e., an increase in temperature will shift the equilibrium towards the evolution of the remaining CO_2).

If *A/VH* is very small, then it is possible that a time delay before the CO_2 evolved by the dough inside the gas bomb can be detected as a change in pressure by the pressuremeter, be it the Park's system or the Gassmart instrument. Because the Gassmart detected pressure changes immediately after the start of the experiments, it is reasonable to assume that the ratio *A/VH* was sufficiently large in our experiments (Figure 4.1). Similarly, the DRR reported by Parks et al. (1960) indicates that *A/VH* was also large enough in their systems because CO_2 was also detected immediately after the start of the experiments.

Another contributing factor for the delayed reaction times observed for the SAPP 40 systems may have been the fact that the apparatus of Parks et al. (1960) possessed a built-in stirring mechanism (the Gassmart did not). This stirrer might have facilitated the escape of CO_2 into the overhead space in the pressure vessels by rapidly removing zones of the dough that had already discharged its high gradient of CO_2 and exposing fresh, CO_2-saturated areas of the dough. Regardless of which source of variability or another was mainly responsible for the observed reaction times, it is important to note that various factors can affect the reaction times detectable by a given CO_2 detection system. It is therefore necessary to be mindful of all these sources of variability if one is to make meaningful comparisons of leavening characteristics for a single or a mix of leavening acids that are found in the literature. The present discussion suggests, for example, that reaction times, though not extent of the reaction, associated with the DRR test was limited by the small sample size and the lack of a stirring mechanism in the Gassmart. Unfortunately, no sample size effects or even experimental methods have been communicated previously in other works citing DRR test results for the acids studied in

the present study (Conn, 1981; Heidolph, 1996). Yet the present discussion points out that the Gassmart is able to accurately and consistently measure the CO_2 production characteristics of chemical leaveners in terms of the DRR test, provided that known sources of variability –as noted above, are adequately controlled.

4.3.3. Reaction kinetics

The use of two levels of adipic acid and of GDL, and the use of two fermentation temperatures for all the chemical leaveners studied permitted us to gain an insight into the effects of concentration of reactants and reaction temperature on reaction kinetics. Increasing the temperature during fermentation generally increased the initial rate at which carbon dioxide was evolved by a chemical leavener (Figures 4.2 and 4.3). However, the shape of the DRR curves in Figures 4.2 and 4.3 for any given chemical leavener remained unchanged. This suggested that the mechanism by which carbon dioxide was released from the chemical leavening system was similar, and possibly the same regardless of the system. To understand the kinetics of reaction in chemical leavening one first must understand how carbon dioxide is generated.

The reaction between sodium bicarbonate and an acidulant is characterized by the following chemical equation:

$$XH + NaHCO_3 \rightarrow NaX + CO_2\,(g) + H_2O \qquad (4.7)$$

The reaction shown in Eq. (4.7), however, only occurs after the acidulant and the sodium bicarbonate dissociate, according to the following general equations:

$$XH \rightarrow X^- + H^+ \;\; or \;\; XH + H_2O \rightarrow X^- + H_3O^+ \qquad (4.8)$$

$$NaHCO_3 \rightarrow Na^+ + HCO_3^- \qquad (4.9)$$

If the reaction shown in Eq. (4.8) proceeds at a much slower rate than the reaction in Eq. (4.9), then the overall rate of reaction (Eq. 4.7) will be determined by the rate of the slow reaction (Moore, 1962; Szabó, 1969). Because the sodium bicarbonate dissociates almost immediately upon contact with the formula water, the leavening acid's rate of dissociation, in fact, determines the rate of carbon dioxide production (Conn, 1981, Heidolph, 1996).

Let the initial concentration of XH be *a* kmol per m^3. If after a time *t*, *c* kmol per m^3 of XH have decomposed, the residual concentration of XH will be *a-c*, and *c* kmol per m^3 of X^- or H^+ will have been formed. The rate of formation of X^- or H^+ is thus *dc/dt*, and if a first-order reaction rate is followed, this rate is proportional to the instantaneous concentration of XH, so that:

$$\frac{dc}{dt} = k(a - c) \tag{4.9}$$

Eq. (4.9) could then be separated and integrated into the following equation:

$$- \ln (a - c) = kt + \text{constant}$$

When $t = 0$, none of the chemical leaveners has dissociated, so that c = zero; then the constant in the above equation will be = - ln a. The integrated rate of reaction is therefore:

$$\ln\left(\frac{a - c}{a}\right) = -kt$$

or

$$c = a * [1 - e^{-kt}] \tag{4.10}$$

The rate of reaction of chemical leavening cannot be unambiguously derived from its chemical neutralization equation but rather it must be determined from mathematical functions fitted (best-fit analysis) to empirical data (Moore, 1962). An example for GDL showing a comparison of experimental data and the model is shown in Figure 4.4,

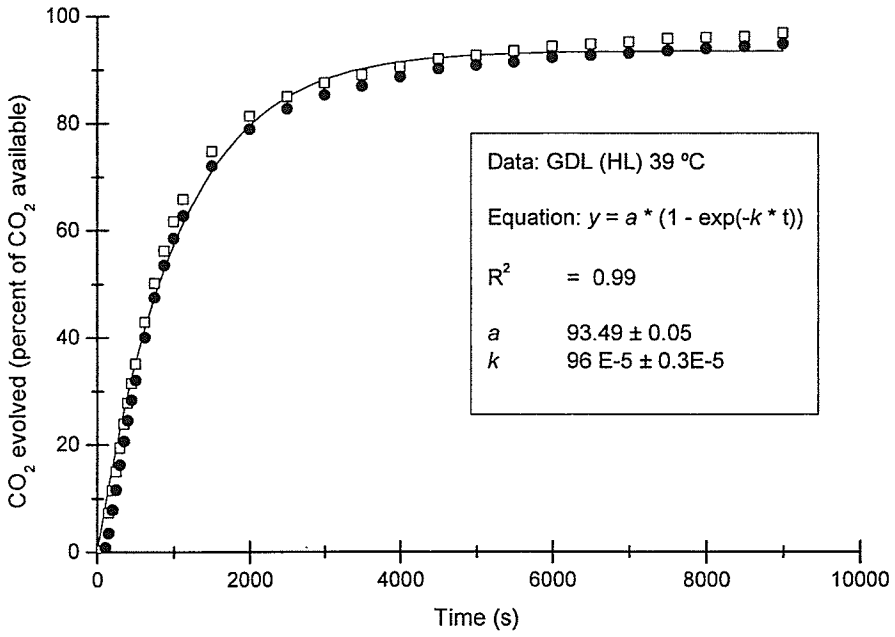

Figure 4.4. A comparison of experimental data (circles and squares showing duplicates) with a first-order reaction kinetics model (solid line) for the decomposition of glucono-δ-lactone (present as D-gluconic acid) into gluconate and hydrogen ions: $C_6H_{12}O_7$ ----> $C_6H_{10}O_7^- + H^+$. The products of this reaction became the reactants of a much faster reaction: $C_6H_{10}O_7^- + H^+ + NaHCO_3 \rightarrow C_6H_{10}O_7Na + H_2O + CO_2$.

including the associated determination coefficient using the chi-square test to minimise the sum of squares of deviations from the mean. A determination coefficient of unity indicated a perfect fitting.

The fitting analysis was performed by plotting for each leavening treatment the data for the two replicates against time in a single plot and fitting a single exponential fit to the plot using Equation 4.10. Fitting analysis was done on the duplicate raw data to reduce bias. The results of this fitting analysis are summarized in Table 4.3. The first-order reaction rate model described the observed reaction rates for the GDL and adipic acid treatments remarkably well but was found not suitable for describing the observed reaction rates for the systems containing the acidic salts (i.e., potassium acid tartrate and SAPP 40, see below). For GDL and adipic acid, the high determination coefficients (R^2), 99 and 97 %, respectively, and the relatively small uncertainty (error) associated with estimating the parameters a and k further indicated that the proposed models explained a large percentage of the variation observed for these leavening systems. The fact that the values of the fitting parameters for a given dough system varied with fermentation temperature or concentration of chemical leaveners reflected the sensitivity of the model to these experimental parameters. Regardless of the leavening system, faster reaction kinetics (i.e., higher k) were observed when the fermentation temperature was increased from 27 to 39 °C or when the concentration of sodium bicarbonate was increased from 1.4 to 4.2 g/100 flour. A faster reaction kinetics is expected to occur when the concentrations of sodium bicarbonate was increased because this would increase the frequency at which reactant species collided (Moore, 1962).

Because the rates of carbon dioxide evolution for the experimental samples

TABLE 4.3. Parameters and coefficients of determination for curves fitted to data on CO_2 evolved (percent of total CO_2 in dough formula) *versus* time ($n = 2$) using Eq. (4.10), as detected by the Gassmart in doughs prepared with one of two levels of sodium bicarbonate[1] and fermented at 27 and 39 °C.

Chemical Leavening System[2]	*Equation*[3]: $c = a * (1 - \exp(-k t))$		
	$a \pm$ error	$k \pm$ error ($\times 10^{-4}$ s^{-1})	R^2
27 °C			
ADIPIC (LL)	79.77 ± 0.12	5.10 ± 0.03	0.961
ADIPIC (HL)	76.64 ± 0.07	6.50 ± 0.02	0.978
GDL (LL)	94.45 ± 0.04	6.70 ± 0.01	0.995
GDL (HL)	98.30 ± 0.03	7.20 ± 0.01	0.996
39 °C			
ADIPIC (LL)	79.78 ± 0.12	5.10 ± 0.03	0.961
ADIPIC (HL)	84.06 ± 0.08	7.60 ± 0.03	0.969
GDL (LL)	89.80 ± 0.05	8.20 ± 0.02	0.991
GDL (HL)	93.49 ± 0.05	9.50 ± 0.03	0.988

(1) Sodium bicarbonate concentrations: LL = 1.40 g and HL = 4.20 g
(2) See Table 1 for key on chemical leavening systems
(3) c = percentage of CO_2 evolved (percent of original); t = fermentation time (s)

containing acidic salts (sodium acid pyrophosphate and potassium acid tartrate) did not conform to a first-order reaction rate, the overall reaction rate for the dissociation of the acidic salts was surmised to be attributable to more than one elementary reaction. Szabó (1969) specified that parallel reactions may be present in a chemical reaction when a substance forms in more than one way. In such a case, the dissociation of the acidic salt is underlined by two parallel reactions occurring at comparable rates so that the overall chemical neutralization reaction (i.e., the one producing the CO_2 molecule) could not be attributed exclusively to either of the parallel chemical reactions. In such a case, the dissociation of SAPP 40 and potassium acid tartrate involved two elementary steps, one of which may have occurred at a slower rate than the other.

A simple model for parallel reactions involving two steps in which three species, *A*, *B* and *C*, participated was discussed by Szabó (1969). His analysis was applicable to parallel reactions where the steps followed first-order kinetics and were irreversible:

$$\underset{x}{A} \xrightarrow[k_1]{} \underset{z}{C} \xleftarrow[k_2]{} \underset{y}{B} \qquad (4.11)$$

where

k_1 = rate constant for $A \rightarrow C$ reaction

k_2 = rate constant for $B \rightarrow C$ reaction

x, y, and z = concentrations of initial reactants, and of the final product, respectively.

The simultaneous differential equations are:

$$-\frac{dx}{dt} = k_1 x \qquad (4.12)$$

$$-\frac{dy}{dt} = k_2 y \tag{4.13}$$

$$\frac{dz}{dt} = k_1 x + k_2 y \tag{4.14}$$

Eq. (4.12) can be integrated directly, resulting in $-\ln x = k_1 t + constant$. When $t = 0$, let $x = a$, with the intention that a be the initial concentration of A, then the constant = - ln a, and $x = ae^{-k_1 t}$. This last equation reiterates what is known for a first-order reaction: the concentration of species A drops exponentially with time (Szabó, 1969). Similarly, it can be found that $y = be^{-k_2 t}$, if one lets $y = b$ at $t = 0$, with b being the initial concentration of B.

Replacing the value found for x and y into Eq. (4.14) and integrating gives:

$$z = a - ae^{-k_1 t} + b - be^{-k_2 t}$$

In this model every time a molecule of A or B reacts, a molecule of C is formed so:

$$a + b = c$$

where c, the concentration of species C, will be equivalent to the maximum percentage of dissociation of the acidic salt or the maximum percentage of CO_2 that will be evolved provided that the reaction goes to completion. Therefore, the concentration of the final product, z, is calculated to have the form of a second-grade exponential function:

$$z = c - ae^{-k_1 t} - be^{-k_2 t} \tag{4.15}$$

Equation (4.15) shows that the formation of the hydrogen anion is brought about by a chemical reaction involving two steps that denote the parallel reactions associated with the dissociation of the acid salt to liberate the hydrogen ions. It is worth noting that the model described in Eq. (4.15) assumes that when a molecule of C is formed a subsequent

(albeit fast) reaction between C and the bicarbonate ion (i.e., a rapid neutralization reaction) leads to the formation of CO_2.

To investigate the hypothesis that the dissociation of potassium acid tartrate and SAPP 40 involved parallel reactions, mathematical functions were fitted to the experimental data. The exponential function was fitted to the experimental data (duplicates -non-averaged data), associated with each experimental treatment. Figure 4.5 illustrates for SAPP 40 that a second-grade exponential function provided a good fit to the experimental data associated with this acidic salt. A summary of the fitting analysis is shown in Table 4.4. Coefficients of determination were high (> 88%), although R^2 is known to increase when additional factors are added to fitting functions. Interestingly, the DRR values shown in Table 4.4 can be converted into fundamental units (e.g., kmol CO_2 per kg of dough per second) using a straightforward calculation (see Appendix I for details). The fact that the experimental data for the decomposition of the acidic salts was well described by the reaction kinetics for parallel reactions suggested that parallel reactions were indeed important in determining the overall rate of reaction in SAPP 40 and potassium acid tartrate.

Figure 4.6 shows the influence of pH on the relative proportions of each of the pyrophosphate species that are present in a solution of sodium pyrophosphate (McGilvery & Crowther, 1953). Figure 4.6 shows that at any given pH, no more than three pyrophosphate species can be present in solution. As well, the literature suggests that the pH of dough chemically leavened with SAPP should not be more than 8.0, which would correspond to the pH of a dough containing only the sodium bicarbonate at a level of2.5% (flour basis) (Chokri Zghal, personal communications, 2006), and not less than

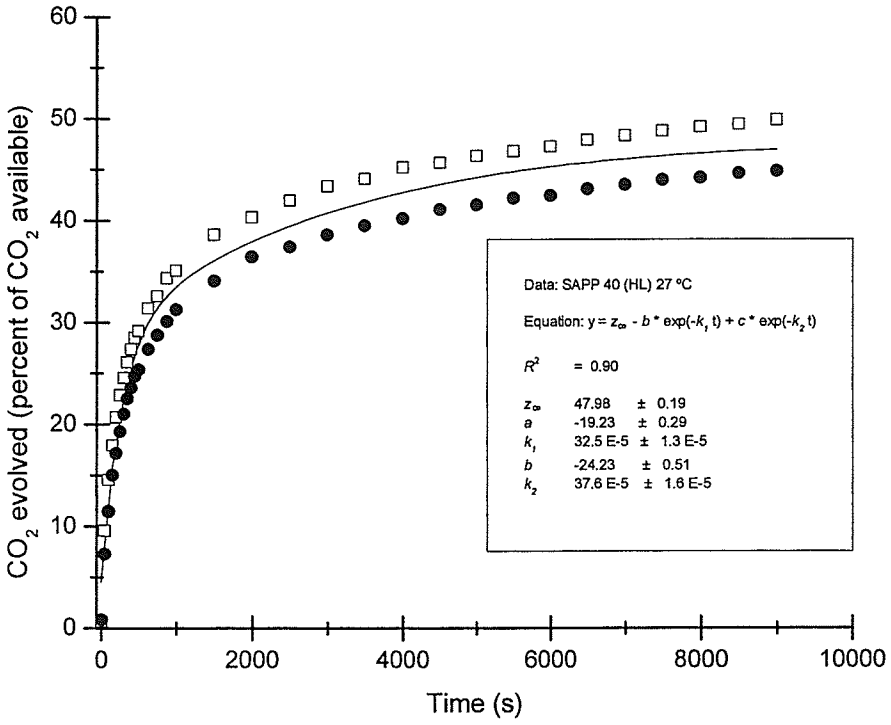

Figure 4.5. A comparison of experimental data with a two-step parallel first-order reaction model (solid line) for the decomposition of sodium acid pyrophosphate into sodium pyrophosphate and hydrogen ions: $Na_2H_2P_2O_7 \rightarrow Na_2P_2O_7^{-2} + 2H^+$ and $Na_2H_2P_2O_7 \rightarrow Na_2HP_2O_7^{-1} + H^+$. The products of these reactions became the reactants of a much faster reaction: $Na_2P_2O_7^{-2} + Na_2HP_2O_7^{-1} + 3H^+ + 3\ NaHCO_3 \rightarrow Na_4P_2O_7 + Na_3HP_2O_7 + 3\ H_2O + 3\ CO_2$.

TABLE 4.4. Parameters and coefficients of determination of curves fitted to data on CO_2 evolved (percent of initial CO_2) *versus* time (n = 2) using Eq. (15), as detected by the Gassmart in doughs prepared with one of two levels of sodium bicarbonate[1] and fermented at 27 and 39 °C.

Chemical Leavening System[2]	*Equation*[3]: $z = c - ae^{-k_1 t} - be^{-k_2 t}$					
	$k_1 \pm$ error ($\times 10^{-4}$ s^{-1})	$k_2 \pm$ error ($\times 10^{-3}$ s^{-1})	$c \pm$ error	a	b	R^2
27 °C						
SAPP 40 (HL)	3.25 ± 0.13	3.76 ± 0.16	47.98 ± 0.19	19.23 ± 0.29	24.23 ± 0.51	0.904
K-TART (ML)	4.01 ± 0.22	2.22 ± 0.09	84.24 ± 0.26	30.53 ± 1.25	47.68 ± 1.33	0.942
39 °C						
SAPP 40 (HL)	3.39 ± 0.14	4.69 ± 0.21	45.89 ± 0.18	17.85 ± 0.27	24.83 ± 0.56	0.875
K-TART (ML)	4.04 ± 0.26	3.04 ± 0.10	79.57 ± 0.22	19.79 ± 0.78	54.83 ± 0.93	0.912

(1) Sodium bicarbonate concentrations: ML = 2.80 g and HL =4.20 g
(2) See Table 1 for key on chemical leavening systems
(3) z = CO_2 evolved (percent of original); t = fermentation time (s)
(4) k_1 and k_2 are rate constants (s^{-1}); c correspond to the maximum CO_2 that could be evolved from the sample; a and b are constants defined in the text.

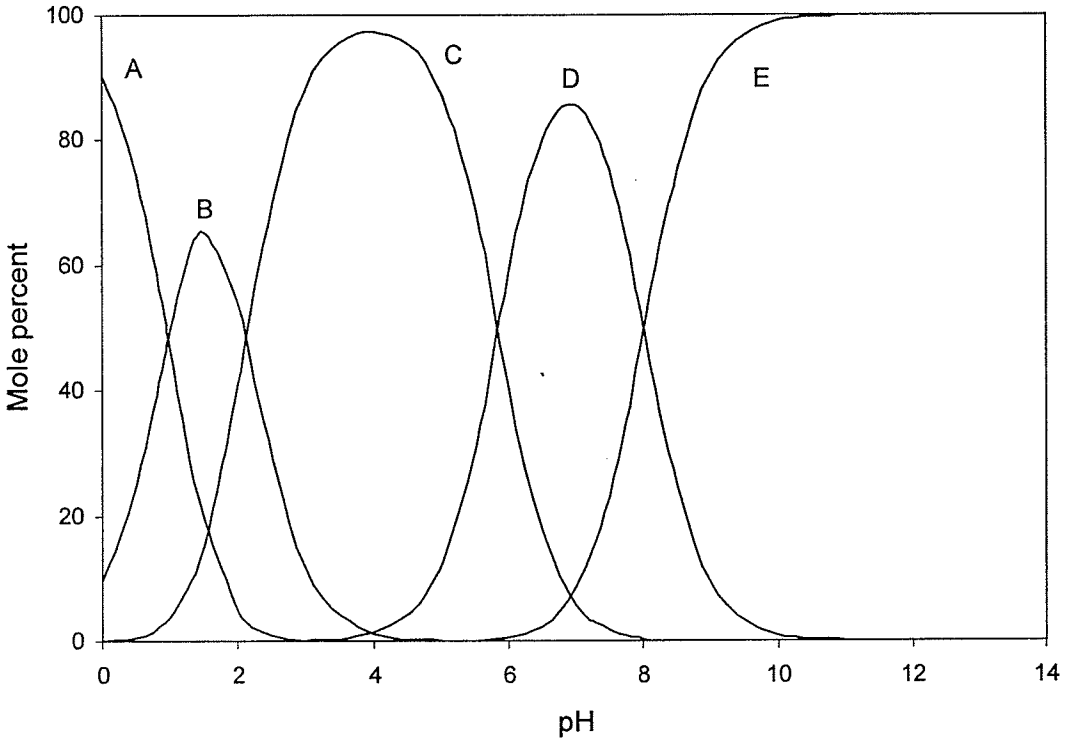

Figure 4.6. The percent of each of the species of pyrophosphate present in solution as a function of pH. A, $H_4P_2O_7$; B, $H_3P^2O_7^{1-}$; C, $H_2P_2O_7^{2-}$; D, $HP_2O_7^{3-}$; E, $P_2O_7^{4-}$. Constructed based on equations 5-13 and the dissociation rate constants of a pyrophosphoric acid solution at 65.5 °C published by McGilvery and Crowther (1953).

7.2, which would be the lower end of the pH range for bakery products that had been chemically leavened with SAPP (Heidolph, 1996). At a pH range between 7.3 and 8.0 for SAPP dough, Figure 4.6 suggests that the following pyrophosphate anionic species can be present in solution: $H_2P_2O_7^{2-}$, $HP_2O_7^{3-}$ and $P_2O_7^{4-}$, with the former two species predominating over this pH range. Hence, it is reasonable to propose that the reaction mechanism of SAPP 40 involved two elementary steps, one of which occurred at a slower rate than the other. The slower rate step would therefore be regarded as the rate-limiting step. These elementary two steps are shown in the following stoichiometric equations:

$$Na_2H_2P_2O_7 \xleftrightarrow{k_1} Na_2HP_2O_7^{-} + H^+$$

$$Na_2H_2P_2O_7 \xleftrightarrow{k_2} Na_2P_2O_7^{-2} + 2H^+$$

Given the order of magnitude difference between the rate constants k_1 and k_2 (Table 4.4) the reaction liberating the two hydrogen ions has been assigned the rapid rate of reaction (k_2). The two-step reactions noted above are followed by the rapid neutralization reaction of sodium bicarbonate as follows:

$$Na_2HP_2O_7^{-} + Na_2P_2O_7^{-2} + 3H^+ + 3NaHCO_3 \longrightarrow Na_4P_2O_7 + Na_3HP_2O_7 + 3CO_2 + 3H_2O$$

It is further intimated that the CO_2 formed during chemical leavening will cause a drop in pH in the dough (Miller et al., 1994).

It must be recognized that although the data shown in Table 4.4 shows that the mechanism of reaction of KAT involved two parallel irreversible first-order reactions, there was less certainty in identifying the actual elementary steps responsible for the parallel reactions in KAT. Nonetheless, it is important to note that the reaction mechanism cannot necessarily be predicted from the stoichiometry of the reaction but it

is customarily determined experimentally based on the observed kinetics of reaction (Moore, 1962; Hammes, 1978). Further, the experimental results indicated that the rate of carbon dioxide production for these two chemical leavening systems increased with fermentation temperature (from 27 to 39 °C), a relationship that was also captured by the rate constants k_1 and k_2 as they also increased with temperature (Table 4.4). This is agreement with Arrhenius' law, which indicates that the rate of a reaction increases with the temperature, because at higher temperatures the molecules of the reactants move faster and collide more frequently due to their greater kinetic energy. Although the proposed models characterized the reaction rates for SAPP 40 and KAT well, more comprehensive experiments are required to prove the validity of the models in a wider range of experimental conditions as well as to determine the suitability of using kinetic theory to the study of a wider group of chemical leavening systems.

4.3.4. Mechanisms of acid-base chemistry in chemical leavening systems

In order to improve our knowledge of chemical leavening agents, the underlying mechanisms of acid-base chemistry associated with the chemical neutralization reaction need to be understood. A mechanism of reaction that requires clarification is how the reaction substrates and products affect the pH in the dough. For example, no clear mechanistic understanding was provided by Miller et al (1994) to explain the influence of reaction salts (containing anions and cations) on the pH of refrigerated canned doughs during chemical leavening. Similarly, the addition of bakery ingredients containing cations (e.g., calcium from milk or added calcium salts) has been observed to "suppress" (slow down) the rate of reaction of chemical leaveners, supposedly, "by interacting with the acid salts and preventing them from undergoing hydration or dissolution" (Heidolph,

1996). Elucidating the role played by anions and cations in acid-base chemistry is not a trivial subject. In fact, there is ongoing debate in the physiological sciences literature over the validity of classical descriptions of acid-based chemistry as it relates to the role played by anions in regulating physiological pH (Kemp, 2005; Lindinger et al., 2005; Robergs et al., 2004). Though the interests of these debates have focused in clarifying the role of lactic acid in skeletal muscle fatigue and in elucidating the mechanisms lying behind exercised-induced metabolic acidosis, they do provide a more comprehensive conceptual and analytical basis to understand acid-base chemistry. One important development made in physical chemistry by physiologists is to recognize that in aqueous solutions all ions in solution govern the dissociation of water. The formation/disappearance of ions in the dough aqueous phase can be expected to bring about changes in the pH of the dough. In particular, according to Lindinger et al. (2005), three independent variables have been identified as responsible for determining the concentrations of $[H^+]$ in aqueous solutions: "1) conservation of mass, 2) the equilibrium state between water and weak electrolytes, as defined by their equilibrium constants, and 3) maintenance of electrical neutrality". This discussion is concerned with the latter principle.

The electrical neutrality principle dictates that the electrical charges in an aqueous solution are always neutralized, so that the sum of all strong and weak anions equals the sum of all strong and weak cations (Lindinger et al., 2005):

$$\Sigma\,[\text{strong base cations}] - \Sigma\,[\text{strong acid anions}] + \Sigma\,[\text{weak base cations}] - \Sigma\,[\text{weak acid anions}] + [H^+] - [HO^-] = 0 \qquad (4.16)$$

We can further simplify our discussion by grouping the changes brought about by the ionic species in the aqueous phase of dough during chemical leavening:

$$[TAD] = \Sigma\,[\text{strong base cations}] + \Sigma\,[\text{weak base cations}] - (\Sigma\,[\text{strong acid anions}] + \Sigma\,[\text{weak acid anions}]) \quad (4.17)$$

The total anion difference (TAD) include the strong anions resulting from the dissociation of leavening acids (e.g., $P_2O_7^{4-}$ [pyrophosphate anion], $C_4H_4O_6^{2-}$ [tartrate anion], $C_6H_8O_4^{2-}$ [adipate anion], $C_6H_9O_6^{1-}$ [gluconate anion]) and the weak anions consumed during chemical leavening (those that are only partially dissociated) (e.g., $H_2P_2O_7^{2-}$, $HP_2O_7^{3-}$, $HC_4H_4O_6^{1-}$, HCO_3^{1-}). From Eq. 4.17 it should be clear that the concentration of cations (weak or strong) remains the same during chemical leavening because they appear in the acid and in the salt.

Using an approach similar to that used by Lindinger et al. (2005), one can find the following relations based on Eqs. 4.16 and 4.17:

$$[TAD] + [H^+] - [OH^-] = 0 \quad (4.18)$$

Since the dissociation of water into H^+ and OH^- is dictated by the following relation:

$$K_W\,[H_2O] = [H^+][HO^-] \quad (4.19)$$

where the dissociation of constant (K_W) is very small [~ 4.4×10^{-14} (Equivalents $dm^{-3})^2$; 1 equivalent weight [=MW/(number of equivalent weights)] of $[H^+]$ and $[OH^-]$ is 1.008 and 17.007, respectively], and hence the concentration of H^+ and OH^- [~10^{-7} Eq. dm^{-3}] is also very small. Equation 4.19 can be re-written as:

$$[H^+] = K_W\,[H_2O]/[HO^-]$$

or

$$[H^+] = K'_W/[HO^-] \quad (4.20)$$

where $K'_W = K_W\,[H_2O]$. Hence Eq. 4.18 can be expressed as:

$$[H^+]^2 + [TAD] \,.\, [H^+] - K'_W = 0 \tag{4.21}$$

Since $[H^+] > 0$, this last quadratic equation is equivalent to:

$$[H^+] = \left(K'_W + \frac{[TAD]^2}{4} \right)^{1/2} - \frac{[TAD]}{2} \tag{4.22}$$

Eq. 4.22 explains that decreasing the concentration of weak anions such as HCO_3^- would directly cause an increase in $[H^+]$ in the solution. As shown in Eq. 4.7, the carbon dioxide gas diffusing out of solution is responsible for a reduction in the concentration of HCO_3^- ions that are dissolved in the dough aqueous phase. Thus, Eq. 4..22 dictates that a change in the concentration of ions in the dough arising from the chemical leavening reactions (or yeast fermentation reactions) is indeed an important mechanism by which pH is regulated in dough during leavening, irrespective of whether CO_2 is being dissolved in the dough liquid matrix or not.

Equation 4.22 also explains the observation made by Heidolph (1996) with regards to the effect of cations in chemically leavened dough. Adding cations to the dough would cause a decrease in $[H^+]$ in the aqueous phase of dough (i.e., increase pH) which could explain a retardation of the rate of reaction of the chemical leavening system. Eq. 4.22 also provides an explanation to the data reported by Miller et al. (1994). Miller et al. (1994) investigated the effect of measuring the pH of leavened dough using a 10% aqueous slurry (a common and yet unofficial method to measure pH in dough; Collatz, 1943; Holmes and Hoseney, 1987a) and using a surface pH electrode. Miller et al. (1994) found that the surface electrode method detected a lower pH (0.5 pH units) over that measured by the slurry method, and explained the differences in terms of dilution effects. The dilution of carbonic acid and of reaction salts found in the dough in

an excess of water (to prepare the slurry) would cause the slurry to exhibit a lower pH over the pH measured in the undiluted doughs. To demonstrate the effect of salts on the pH of dough, Miller et al. (1994) measured the pH of 0.5M and 0.05M phosphate solutions with varying concentrations of sodium chloride (0-10% in increasing steps of 2.5%). In both solutions, the pH dropped as the sodium chloride solution increased, with the largest drop in pH (from 6.73 to 6.08) observed in the 0.5M phosphate solution when the NaCl concentration was increased from 0 to 10%. For the same salt concentration increase, a more moderate decrease in pH (6.79 to 6.69) was observed in the more diluted (0.05M) phosphate solution. While it is reasonable to believe that dissolving the CO_2 that is in the gas bubbles of the dough in an excess of water (to make the slurry) can explain the lower pH detected in a slurry (i.e., a slurry possessed more carbonic acid than the dough liquid phase did), the dilution hypothesis of Miller et al. (1994) fails to establish a mechanistic connection between the effect of diluting doughs into slurries and of diluting and changing the salt concentrations in phosphate solutions on the pH of either milieu. Notwithstanding the buffer capacity of gluten proteins, consideration of the principle of electrical neutrality in solutions indicates that reducing the concentration of TAD by diluting the dough in water, or by diluting and changing the salt concentrations in the phosphate solutions, would lead to an increase in the concentration of $[H^+]$, as dictated by Eq. 4.22; such interpretation of Miller et al.'s (1994) experimental data in light of fundamental acid-base chemistry provides a mechanistic explanation of the changes in pH brought about by changes in the concentration of ionic species. This mechanism needs to be recognized to gain a better understanding on the acid-base chemistry underlying chemical leavening reactions.

4.4. Conclusions

A new method to carry out the dough rate of reaction (DRR) test using the Gassmart apparatus is presented. For SAPP 40 and potassium acid tartrate, the DRR curves based on the Gassmart had equivalent trends and the same percentages of evolved carbon dioxide as those reported in the literature for the same fermentation temperature (Heidolph, 1996). The DRR curves associated with GDL exhibited the same trends as those for SAPP 40 or potassium acid tartrate, differing from the DRR results included in the report of Conn (1981). The differences in the absolute values for the DRR time scales were attributed to various experimental parameters, most importantly to the sample size and the presence/absence of an agitator in the gas bomb. It was proposed that sample size and an internal agitator via their effects on the size of the dough surface area may affect the reaction times detected by the CO_2 measuring device, but not the total percentage of evolved carbon dioxide from the dough A first-order reaction kinetics model was found to be suitable for describing the properties of GDL and adipic acid as leavening systems, whereas a first-order reaction kinetics for irreversible parallel reactions better described the leavening properties of the acidic salts potassium acid tartrate (cream of tartar) and sodium acid pyrophosphate. A fundamental acid-base mechanism based on the principle of maintenance of electrical neutrality was put forward to explain changes in pH during chemical leavening of bread dough.

CHAPTER FIVE

The Measurement of Dough Specific Volume and Carbon Dioxide Transport in Chemically Leavened Dough Systems

Abstract

The gas production and gas retention properties of doughs are central to make bread of good quality; however, these properties are rarely measured directly in fermenting dough due to the lack of adequate instrumentation. This investigation provides a description on how to conduct measurements of the dynamic specific volume (DSV) of chemically leavened dough using a technique based on digital image analysis. Experimental results indicated that chemical leavening systems consisting of sodium bicarbonate and glucono-delta-lactone (GDL), potassium acid tartrate (KAT), adipic acid (ADA) or sodium acid pyrophosphate 40 (SAPP), were useful bakery ingredients for leavening dough at ordinary fermentation temperatures. Sodium bicarbonate at a level of 1.4 to 2.8 g per 100 g of flour in combination with equivalent neutralizing amounts of the said leavening acidulants was able to consistently raise the specific volume of bread dough so that their gas void fractions spanned between 5 and 67 %. The relationship between the specific volume of dough at the end of fermentation and the actual gas evolved (measured independently) was fairly linear and was characterized by a slope that provided a good index of the actual gas-trapping properties of dough. The linear relationship between the biaxial expansion of dough and square-root of fermentation time, in the early region of the chemical leavening expansion curve, suggested that initially the growth of the gas phase with time was diffusion limited. To interpret this diffusion-controlled region, the

analysis for diffusion-controlled bubble growth for a viscoelastic liquid proposed by Venerus et al. (1998) was invoked. The results of the mathematical analysis yielded empirical values for the mass diffusion coefficient of carbon dioxide in the fermenting dough samples (D_L). The empirical D_L values were $4.5 \pm 3 \times 10^{-9}$ m^2 s^{-1} (GDL), $4.2 \pm 1.6 \times 10^{-9}$ m^2 s^{-1} (KAT), $1.8 \pm 0.5 \times 10^{-9}$ m^2 s^{-1} (ADA), and $2.1 \pm 1.5 \times 10^{-10}$ m^2 s^{-1} (SAPP). These values were in relatively good agreement with other predictions made in the literature. Overall, the experimental results indicated that the predictability of the chemical leavening reaction can make chemical leavening systems amenable to controlled-release of carbon dioxide and a useful tool to study the gas retention properties of chemically leavened dough.

5.1. Introduction

Chemical leavening systems are bakery ingredients added to batter or dough to raise or *leaven* the volume by evolving leavening gas, most typically carbon dioxide. In breadmaking, the leavening step is fundamental in creating a bread loaf that conforms to the textural requirements of its class (Bloksma, 1981). Leavening brings changes in the cellular structure of dough and hence in the textural properties of bread by expanding the sizes of the distribution of gas cells in the dough with carbon dioxide (Bloksma, 1990a; Baker & Mize, 1941; Scanlon & Zghal, 2001). Despite the strong relationship between dough structure and bread texture, much more attention has been focused on how proteins, carbohydrates, lipids, and water interact to form the continuous gas-trapping network of dough with less emphasis on the dough gas phase (Bloksma, 1990a, 1990b; Scanlon & Zghal, 2001). More recently, however, it has become clearer that such fundamental dough properties as dough rheology cannot be unambiguously established

without knowledge on bubble numbers and sizes (Bloksma, 1981; Bloksma, 1990a; Carlson & Bohlin, 1978; Chin et al., 2005; Elmehdi et al., 2004). In fact, there is a wealth of evidence supporting the thesis that the basis of breadmaking is aeration of the dough (Campbell, 1991; van Vliet, 1999; Chiotellis & Campbell, 2003a, 2003b; Shimiya & Nakamura, 1997; Campbell et al., 1991, 1993, 1998, 1999, 2001; Chin et al., 2005; Martin et al., 2004a, 2004b; Mitchell et al., 1999; Shah et al., 1998). Typically, mixed dough has a gas void fraction no greater than 20%, whereas void fractions can be as high as 74% in fermented dough and about 50-80% in bread (Bloksma 1990a, 1990b; Scanlon & Zghal, 2001). Clearly, the most significant aeration step in breadmaking is the leavening step.

Though yeast is the typical source of carbon dioxide in breadmaking, it is by no means the only source. A viable source of carbon dioxide is a chemical leavening system which is traditionally used only for leavening batters, but that more recently have started to be incorporated in breadmaking applications. Chemical leavening systems, in fact, can leaven bread dough faster, more consistently and often times more conveniently than yeast because they do not require lengthy activation periods or stringent environmental conditions for evolving carbon dioxide (Heidolph, 1996). The chemical nature of chemical leavening systems makes them capable, once incorporated in the dough, of producing carbon dioxide even if they have undergone harsh processing or storage conditions such as high extrusion temperatures, microwave fields, and prolonged refrigeration or frozen storage (Atwell, 1985; Heidolph, 1996; Laughlin & DeMars, 1999; Narayanaswamy & Daravingas, 2001; Perry & Colman, 2001, 2003; Hansen et al., 2003; Laughlin et al., 1999, 2000; Yong et al., 1983a, 1983b). One major disadvantage of

chemical leaveners, though, is that they are unable to duplicate the distinctive flavour that yeast imparts to bread, and rather can impart undesirable flavour and taste on bread products (Heidolph, 1996). This undesirable effect can be mitigated with the use of adequate formulation and/or other flavoured bakery ingredients. Also, yeast may be used in conjunction with chemical leavening systems to improve sensory properties (Holmes & Hoseney, 1987b).

Heidolph (1996) suggested that judicious selection of chemical leavening systems can afford good control over the production of carbon dioxide during dough leavening. Better control over gas production should then translate into better control over the quality of bread. Gas production in chemically leavened dough very closely obeys the laws of stoichiometry and reaction kinetics for a chemical neutralization reaction (Hoseney, 1998). This means that controlling the type of leavening acid in the formula and the fermentation temperature can afford good theoretical control over the leavening step. In chemical leavening, the leavening acid neutralizes a bicarbonate salt in the presence of heat and water, to produce carbonic acid that quickly dissociates into carbon dioxide and water. Sodium bicarbonate, also known as baking soda or simply soda, is almost ubiquitously used as the carbon dioxide carrier because of its low cost, high purity, lack of toxicity, ease of handle, and high carbon dioxide content (Heidolph, 1996). Alternative carbon dioxide sources include potassium bicarbonate, sodium carbonate, ammonium carbonate, and ammonium bicarbonate. One important property of sodium bicarbonate is that it dissolves quickly in water so that the rate of reaction in a chemical leavening is essentially given by the speed at which hydrogen is dissociated from the acidulant.

Heidolph (1996) divided acidulants into groups on the basis of their time-release characteristics. Fast-acting or nucleating acidulants are those that react with sodium bicarbonate during mixing; slow-acting or time-released acidulants react during holding or shortly after mixing; and heat-activated acidulants react upon reaching high temperature such those found during baking. This categorization, though somewhat imprecise, is widely used in the baking industry (Heidolph, 1996). More specifically, fast-acting acidulants include such organic acids as tartaric acid or cream of tartar, glucono-δ-lactone, adipic, fumaric, lactic, and malic acids or such acidic salts as calcium phosphates, monocalcium phosphate, anhydrous monocalcium phosphate. Time-released acidulants include sodium acid pyrophosphate (SAPP) of various reactivities (for example, SAPP 40 releases 40% of the available carbon dioxide under standard conditions), and potassium hydrogen tartrate, among others. Those that react mainly at baking are called slow-acting acidulants (e.g., sodium aluminum phosphate), while double-acting acidulants react both during mixing and baking (Heidolph, 1996). Encapsulation of either the acidulant or sodium bicarbonate provides a means for controlling the release of carbon dioxide (Holmes & Hoseney, 1987a). Typical coating materials include cornstarch, hydrogenated vegetable oil, monoglyceride, maltodextrin, or gum (Heidolph, 1996).

Theoretically, leavening of dough is a carbon dioxide transportation problem. This is so because dough is viewed as a dispersion of gas bubbles in a continuous phase (Bloksma, 1981) where the gas bubbles form a gas phase that expands due to carbon dioxide diffusion from the continuous phase. From a chemical engineering viewpoint, such a transport problem entails mass and momentum transport processes (Chiotellis &

Campbell, 2003a). Momentum transport suggests that the growth of bubbles are affected by forces opposing the expansion of the phase boundary around the bubble, i.e., surface tension and the dough viscoelastic properties. Mass transport, on the other hand, deems bubble growth to arise solely due to the carbon dioxide concentration (or partial pressure) gradient across the gas-dough interface and disregards those forces opposing bubble growth, such as surface tension and the viscoelastic nature of the dough (Chiotellis & Campbell, 2003a). Hybrid models of momentum and mass transport models also exist which most notably include diffusion-controlled and diffusion-induced models that are good for describing the growth of a single gas bubble (Venerus et al., 1998) or a population of bubbles (Chiotellis & Campbell, 2003a). Despite the well-developed theoretical framework for transport models of carbon dioxide in gas-saturated viscoelastic materials, experimental data on this subject is still scarce. This is particularly true in dough systems since monitoring the growth of individual or a population of gas bubbles is an experimentally difficult task because of the opacity of the dough

The diffusion-controlled transport model for a population of bubbles reported by Chiotellis and Campbell (2003a), and which was based on the analysis of Venerus et al. (1998), provided relatively good predictions of bubble growth. The volume changes during fermentation of the dough samples were measured using a dynamic dough density (DDD) technique capable of monitoring dough density changes over fermentation time. Information on the bubble size distribution was determined on frozen samples using light microscopy information from two-dimensional cross-sections of frozen dough samples and a 3D reconstruction algorithm based on statistics (Campbell, 1991). In their subsequent publication, however, Chiotellis and Campbell (2003b) admitted that, because

the DDD measurements required keeping the dough samples immersed in xylene (Campbell et al., 1993), not all the carbon dioxide evolved by the dough samples was accounted for in the calculations. Another possible source of error is that the DDD technique worked on the assumption that xylene was not absorbed by the dough during the course of fermentation. Nonetheless, the use of the DDD technique proved useful in gaining an insight into the mechanisms of bubble growth in wheat flour dough.

Recently, Elmehdi et al. (2003a) have introduced a dynamic dough density apparatus that is based on digital image analysis and which has also proven to be useful in studying the state of aeration in fermenting dough. As with the technique used by Chiotellis and Campbell (2003a, 2003b), the DDD method of Elmehdi et al. can be useful for studying the fermentation process in dough. Because the specific volume of dough is preferred over density information in the baking industry, with one being the reciprocal of the other, a technique capable of monitoring dynamic specific volume (DSV) is therefore highly desirable.

The objective of this study was to determine the effects of four types and three levels of chemical leavening systems and three fermentation temperatures on the dynamic specific volume of dough made from bread wheat flour. Experimental results were interpreted in light of the theoretical model developed by Venerus et al. (1998) for describing diffusion-controlled bubble growth in a viscoelastic medium.

5.2. Materials and Methods

The flour employed in this study was a straight grade flour milled from number 2 grade Canada Western Red Spring wheat in the pilot mill of the Canadian International Grains Institute, Winnipeg, MB. Flour was stored in sealed double bags placed in plastic

pails at 5 °C until a bulk sample was equilibrated overnight (as a minimum) to room temperature prior to experimentation. The effect of storage on the mixing characteristics of the flour was monitored during the course of experimentation (about four months) and was found to be negligible. This conclusion was based on the overall shape of GRL 200 mixing curves and work energy inputs associated with mixing a lean formula dough to optimum development at various times during the course of the experiments (results not shown). Table 5.1 shows the chemical composition and technological characteristics of the flour. The dough formula included 100 g of flour (14% m.b.), 69.6 g deionised water (Farinograph absorption - 2%), and 0.75 g NaCl. In preliminary experiments using potassium tartrate, it was found that the levels of water and NaCl used produced doughs with relatively good handling properties even at the highest sodium bicarbonate level.

The chemical leavening systems employed included sodium bicarbonate, as the source of carbon dioxide, plus one of four chemical leavening acids (also called acidulants), which acted as the source of acidity (Table 5.2). In the experiments, three levels of sodium bicarbonate were used: 1.40, 2.80 and 4.20 g per 100 g flour. These levels covered the working range (1.68-2.10g/100g) suggested by Heidolph (1996) for chemically-leavened refrigerated dough systems. The amount of acidulant added ensured the stoichiometric neutralization of the chosen level of sodium bicarbonate, according to the following relationship:

$$\text{Acidulant (g)} = (\text{sodium bicarbonate (g)} / \text{NV}) \times 100 \qquad (5.1)$$

Where NV is the neutralization value and is defined as the amount of sodium bicarbonate (g) that 100 g of acidulant will completely neutralise. (Heidolph, 1996). The supplier provided the neutralization values for each acidulant (Table 5.2).

Table 5.1. Characteristics of the experimental flour

Analysis	CWRS Grade 2	Method
Analytical		
Moisture (w.b.), %	14.1	AACC 44-15A
Protein content (CNA[a]), %	13.1	AACC 46-30
Wet Gluten, %	37.8	AACC 38-12A
Dry Gluten, %	13.4	AACC 38-12A
Ash Content, %	0.46	AACC 08-01
Agtron colour, %	58	AACC 14-30
Falling number, s	379	AACC 56-81B
Minolta Colour		Manufacturer's instructions[b]
*L**	93.25	
*a**	-0.63	
*b**	9.70	
Farinogram		AACC 54-21A
Absorption	71.6	
Dough Development Time, min	6.7	
Mixing Tolerance Index (MTI), BU	35	
Stability, min	10.2	

(a) Combustion nitrogen analysis

(b) To assess colour in the flour sample, a slurry of flour and water was made according to AACC 14-30 with respect to flour weight, volume of water, mixing time and waiting time. Flour samples were tested seven days after milling using a Minolta CR-310 colorimeter equipped with a D65 illuminant according to manufacturer's instructions.

Table 5.2. Chemical leavening reagents used in preparing the doughs

Chemical reagent	Key	Chemical formula	MW[a]	NV[b]	Supplier
Sodium bicarbonate	Na Bicarbonate	$NaHCO_3$	84.01	-	Sigma Aldrich Co., St. Louis, MO
Sodium acid pyrophosphate 40	SAPP 40	$Na_2H_2P_2O_7$	221.95	72	Aldrich Chemical Company Inc. Milwaukee, WI
Glucono delta lactone	GDL	$C_6H_{10}O_6$	178.14	45	Acatris, Oaville, ON
Adipic acid	Adipic acid	$HOOC(CH_2)_4COOH$	146.14	115	Solutia Inc. Gonzales, FL
Potassium tartrate	K Tartrate	$KHC_4H_40_6$	188.18	45	Aldrich Chemical Company Inc. Milwaukee, WI

a) Molecular weight
b) Neutralization value

Doughs were mixed at room temperature (23 ± 1 °C) using a GRL 200 mixer (Hlynka & Anderson, 1955) at a constant speed of 165 rpm. Preliminary experimentation suggested that the chemical leavening systems worked best when they were added after the formula water was fully absorbed by the flour. Otherwise, the chemical leavening systems reacted too quickly while the dough was being mixed and thus hindered dough development, resulting in doughs with reduced gas power and poor handling properties (e.g., sticky dough). A mixing time of 1 min was found to be long enough to ensure flour hydration and yet was short enough to ensure that the remaining mixing time (3 min) permitted homogeneous dispersion of chemical leaveners when they were added to the dough. Later addition of the chemical leaveners to the dough was a strategy that was also employed by Holmes and Hoseney (1987a). Figure 5.1 shows the sequence of steps followed to prepare the experimental doughs.

Immediately after mixing, the dough was removed from the mixing bowl and a sub-sample of about 4 g was excised from the dough using sharp scissors. The weight of dough was measured accurately to 0.01 g. The dough sub-sample was then placed in the apparatus (see below) used to measure specific volume of the dough as a function of fermentation time. Fermentation was carried out in a pre-heated proving cabinet set at the experimental temperature (± 1 °C) and at a relative humidity of 80%.

To determine the specific volume ($cm^3\ g^{-1}$) of the dough as a function of fermentation time, a modified version of the digital imaging technique described by Elmehdi et al. (2003a) was used. A couple of 2.54-cm thick acrylic plates, whose temperature had been previously equilibrated to that of the experimental run in the

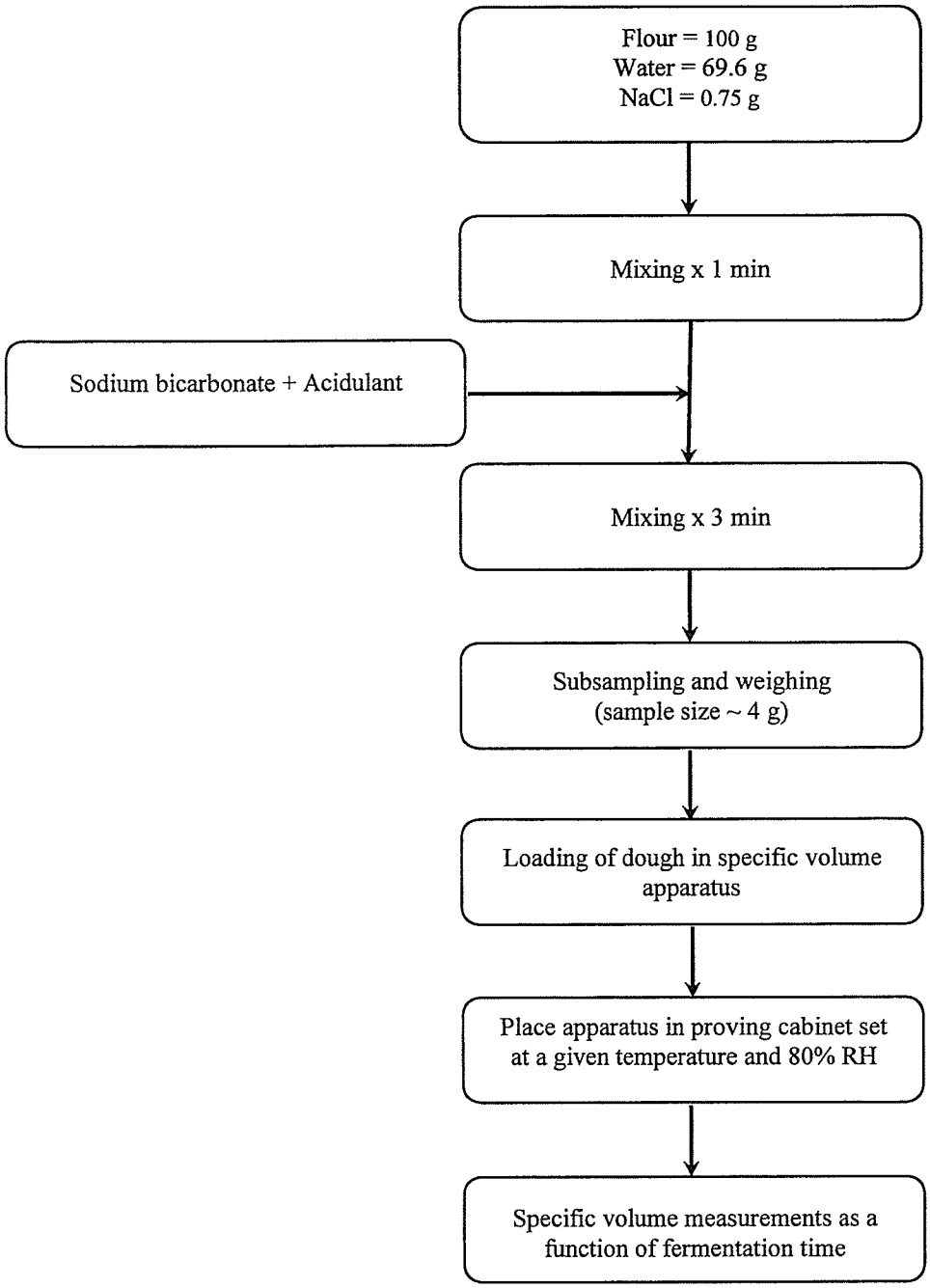

Figure 5.1. Flow diagram showing the procedure followed for preparing a dough sample to measure its specific volume during fermentation. Temperature in ultimate stage varied (see text).

proving cabinet, was used to gently squash the excised sub-sample of dough to a preset thickness (2.11 ± 0.01 mm). Sample thickness was maintained constant throughout the experiment by clamping the plates together (Elmehdi et al., 2003a). Clamping of plates ensured dough expansion was restricted to the radial direction. The apparatus was then placed in the proving cabinet against a black background directly below a digital camera affixed to a tripod (Figure 5.2). Calibration of pixel measurements in mm^2 was accomplished by digitizing a circular Maxwell CR 2016 battery (Hitachi Maxwell, Ltd., Japan) which had a precise diameter of 19.90 mm. The calibrant used was placed on top of the upper plate directly above the centre of the dough.

Digital images of the radial expansion of the dough were taken at 3 min intervals for about 1 h, with the stopwatch zeroed immediately at the end of mixing. Measurements of the area of the dough were acquired using a digital camera (Nikon Coolpix 4500) that possessed a 4-megapixel charged-coupled device (CCD) sensor. The field of view was approximately 103 x 77 mm, so that with a captured image size of 640 x 480 pixels, the spatial resolution was approximately $(160\ \mu m)^2$/pixel or ~ 39 pixels per mm^2 of the dough surface. The image analysis software employed to measure the area of the expanding dough piece with time (and of the calibrant) was APS ASSESS® (Image Analysis Software for Plant Disease Quantification, The American Phytopathological Society, 2002).

The area of the dough in pixels was measured in three steps after loading a captured image (640 column x 480 row pixels) of the dough into APS ASSESS®. Firstly, the area of interest (AOI) function was used to manually define the object (i.e., the dough) so that as little as possible of the background was selected. Secondly, to

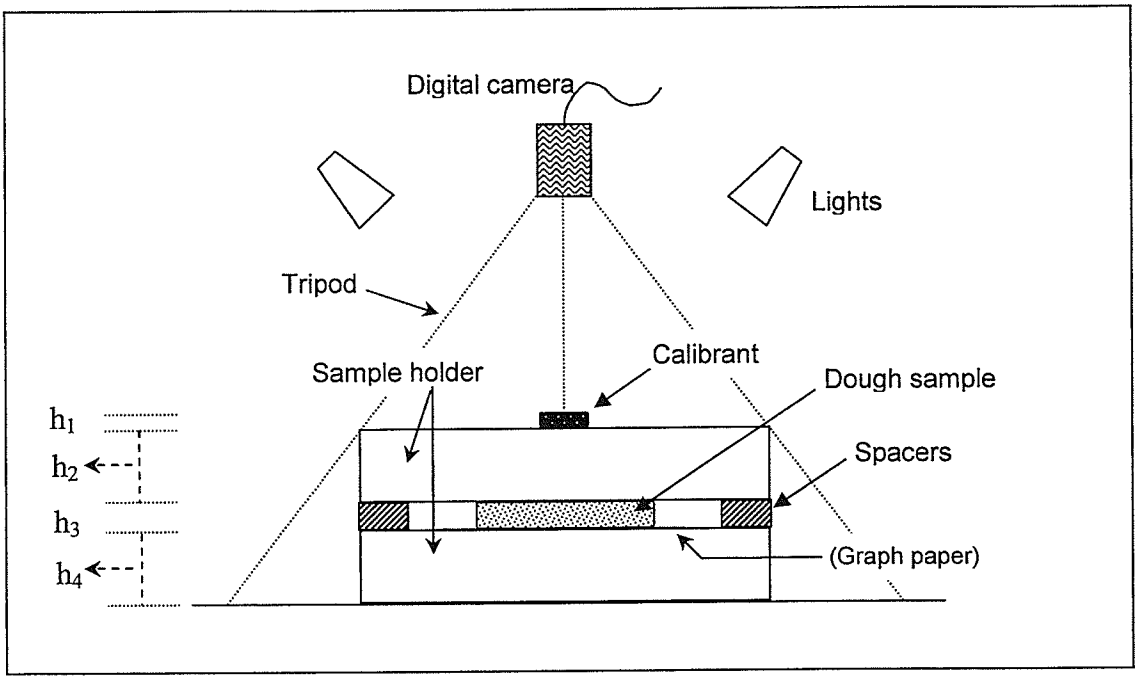

Figure 5.2 Schematic diagram of the apparatus used for specific volume measurements. Actual widths are shown on the left-hand side: h_1 = 1.60 mm; h_2 = 25.0 mm; h_3 = 2.11 mm; h_3 = 25.0 mm. Distance between camera and top of sample holder = 260 mm. Graph paper only used during calibration steps (see text).

unambiguously separate the pixels associated with the dough from those associated with the background, the delimited area was converted into a binary image by setting low and high threshold levels in the green/saturation colour plane of the RGB (Red/Intensity, Green/Saturation, Blue/Hue) colour space. The green colour plane was suitable for discriminating dough from the background and also permitted a robust determination of the area of the dough. For example, if in a typical 8-bit binary image (256-green levels) of fermenting dough the threshold range was lowered by 10 levels (substantially exaggerating the operator's day-to-day variability), it resulted in an increase in the number of pixels for the object by only about 0.50%. Lastly, the number of pixels associated with the area of the dough was calculated using the area measurement function of APS ASSESS®. The specific volume (ψ) of the dough as a function of time was calculated from: $\psi(t) = L\, A(t) / m$, where L is the sample thickness (maintained at 2.11 mm), $A(t)$ is the area of the dough as a function of time (from image analysis), and m is the dough mass. The area of the expanding dough was measured relative to that of the calibrant using APS ASSESS® image analysis.

The image analysis technique for precise quantification of the area of the dough included a calibration procedure that has not been described before. The calibration procedure was carried out in exactly the same way as the fermentation experiments, but, instead of using a fermenting dough, a 60x60-mm piece of graph paper was placed on top of the bottom acrylic plate (plates maintained at their preset thickness of 2.11 mm) (Figure 5.2). The number of pixels corresponding to the imaged area of the battery ($I_{battery}$) and those of the image of the graph paper ($I_{graph\text{-}paper}$) were extracted from the

acquired images at 7 increasingly higher magnification steps (using the zoom-in button in the digital camera). These results are plotted in Figure 5.3.

By geometrical comparison, the slope of the plot $I_{battery}$ *versus* $I_{graph\text{-}paper}$ (Fig. 5.3) must be proportional to the ratio of the actual area of the battery ($A_{battery} = \pi D^2/4 = 311.0$ mm^2) to that of the graph paper ($A_{graph\text{-}paper} = L^2 = 3600$ mm^2), as follows:

$$\frac{I_{battery}}{I_{graph-paper}} = \frac{A_{battery}}{A_{graph-paper}} \times f = \frac{\pi \cdot D^2}{4 \cdot L^2} \times f \qquad (5.2)$$

where f is a correction factor (dimensionless) associated with using image analysis to calculate the area of the graph paper using a calibrant located on a slightly different focal plane. Replacing values in Eq. (5.2), including the slope value for $I_{battery}$ *versus* $I_{graph\text{-}paper}$, f was found to be 1.083. Therefore, the area of the expanding dough on fermentation was calculated from:

$$A_{dough} = \frac{I_{dough(t)}}{I_{battery}} \times A_{battery} \times f \qquad (5.3)$$

The density of the gas-free doughs was also determined. The methodology employed made use of a combination of X-ray microtomography and density measurements using a gravimetric bottle, according to the methods described in Chapter 3. To eliminate the effects of carbon dioxide evolution from interfering with acquisitions of the X-ray microtomograph, chemical leavening systems were reacted separately with a portion of the formula water. This solution was then added to the dough formula along with the remaining formula water, and followed by standard mixing. Sample preparation and image reconstruction techniques, as well as the methodology for void fraction determination were all described in Chapter 3.

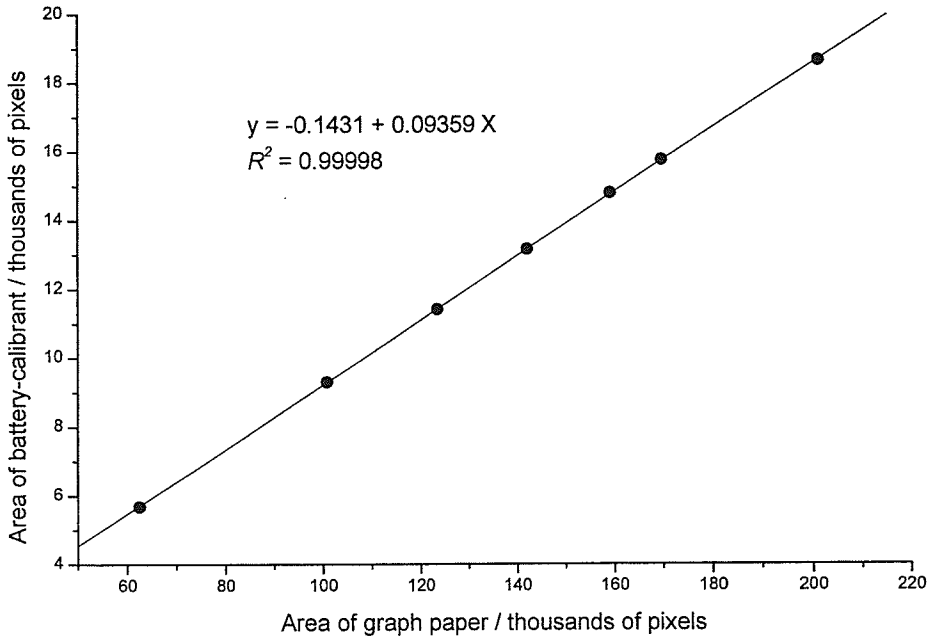

Figure 5.3. Calibration curve for correcting measured areas by an image analysis technique. The graph shows the relationship between number of pixels (x1,000), of a 60x60-mm piece of graph paper and a circular battery (diameter = 19.90 mm, lying at different focal planes) obtained when zooming in seven steps with the zoom-in function of a digital photographic camera. The solid line is a linear fit to the data.

To examine the effect of chemical leavening systems on the specific volume of wheat flour doughs, a full factorial design, with triplicates of each treatment, was used. Four leavening acids (adipic acid, glucono-delta-lactone, potassium acid tartrate and sodium acid pyrophosphate 40), three concentrations of sodium bicarbonate (based on 1.4, 2.8 and 4.2 g per 100 g of flour), and three fermentation temperatures (27, 33 and 39 °C) were the experimental treatments (4 leavening acids x 3 levels of sodium bicarbonate x 3 temperatures x 3 replicates = 108 experiments). Experimental treatments were assigned according to a randomized complete block design where the blocks represented fermentation temperature (i.e., experimental running order within a block was completely randomized by associating each treatment with a computer generated random number and then sorting them out in numerical order).

5.3. Results and Discussion

5.3.1. Effect of the type of chemical leavening system on dough specific volume

Typical curves of dough specific volume (DSV) as a function of fermentation time for various chemical leavening systems are shown in Figure 5.4. These results indicated that the ability of a chemical leavening system to evolve carbon dioxide depends strongly on the leavening acid component. For the chemical leavening systems studied, regardless of the fermentation temperature, the proposed DSV technique was found to yield specific volume values whose CV was better than 5% for triplicate determinations, except for the leavening system containing GDL where the repeatability was up to 7%. For instance, at 27 °C the final specific volume of dough containing GDL was 2.18 $cm^3\ g^{-1} \pm 6\%$ whereas that of KAT, ADA and SAPP was 1.68 $cm^3\ g^{-1} \pm 2\%$, 1.43 $cm^3\ g^{-1} \pm 4\%$, and 0.84 $cm^3\ g^{-1} \pm 2\%$. The precision of the DSV technique was

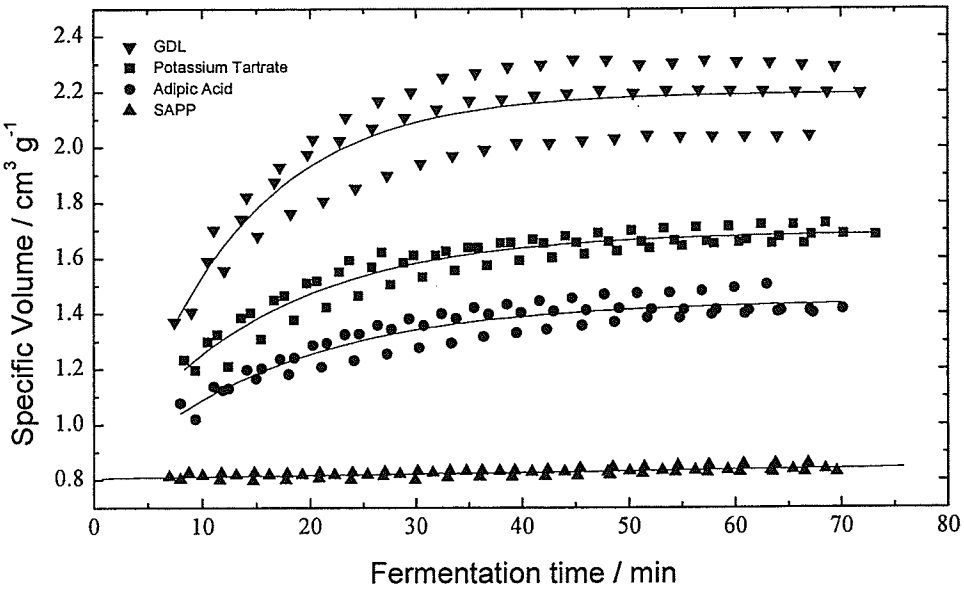

Figure 5.4. Specific volume changes during fermentation at 27 °C for dough prepared with 2.80 g sodium bicarbonate and 6.22 g GDL, 2.43 g adipic acid, 6.22 g potassium tartrate or 3.89 g SAPP 40.

indicative of its potential for being used as an effective test to discriminate the leavening power of chemical leavening systems.

The DSV technique, however, was only able to provide information on the carbon dioxide that had been retained in dough but gave no indication of the carbon dioxide that escaped the dough. During mixing, sample preparation, and even during fermentation a certain amount of gas is lost to the atmosphere and thus not accounted for by the dough specific volume measurements. Carbon dioxide loss to the atmosphere is critical to ascertain the total amount of carbon dioxide that was actually evolved by the chemical leavening systems when in the product. Knowing the actual carbon dioxide production in the dough enables one to determine the relative proportion of carbon dioxide retained versus that evolved in the dough, providing a good index of gas retention properties in dough (Chiotellis & Campbell, 2003b). Interestingly, the total amount of carbon dioxide produced by the four chemical leavening system studied has already been determined using the dough rate of reaction (DRR) technique as described in Chapter 4. Accordingly, results from the DSV technique and the DRR technique were consolidated to determine actual values for total carbon dioxide production and total carbon dioxide retention properties in chemically leavened dough as discussed later in this chapter.

5.3.2. Fermentation temperature

Increasing fermentation temperature in yeasted dough has been found to increase the evolution of carbon dioxide for leavening (Chiotellis & Campbell, 2003a, 2003b). This effect has also been observed in chemically leavened dough in Chapter 4. This is so because as temperature increases the solubility of carbon dioxide in the liquid (continuous) phase of dough decreases whereas the rate of carbon dioxide production

increases (Campbell & Mougeot, 1999; Chiotellis & Campbell, 2003a, 2003b). However, experimental results showed that increasing fermentation temperature did not necessarily cause an increase in specific volume (Figure 5.5). In fact, results suggested that the level of sodium bicarbonate in the dough was much more influential than fermentation temperature in bringing about changes in the volume of dough. In the temperature range between 25-40 °C, Dobraszczyk et al. (2003) found that strain hardening, a means of assessing gas retention properties in wheat flour dough, decreased consistently with increasing temperature, regardless of the quality of wheat flour used in making the dough. Their results therefore provided evidence that gas retention properties in dough should decrease with increasing temperature, though the extent to which this should be manifest in the actual specific volume of dough cannot be directly predicted. A possible explanation for the subtle specific volume changes brought about by temperature is that while an increase in fermentation temperature is expected to increase gas production, it also decreases gas retention. In fact, Bloskma (1990a) found that increasing the fermentation temperature in the range 25-40 °C reduced the apparent viscosity of dough, thereby causing a decrease in gas retention. So, the net effect of increasing temperature on the actual gas retention properties of dough is difficult to establish.

5.3.3. Amount of sodium bicarbonate

The influence of the level of sodium bicarbonate on the specific volume of dough was more pronounced than that of fermentation temperature. Increasing the amount of sodium bicarbonate in the formula led to higher specific volumes in dough as illustrated in Figure 5.5, which corresponded to dough chemically leavened with ADA. However, there was not a one-to-one correspondence between sodium bicarbonate level and

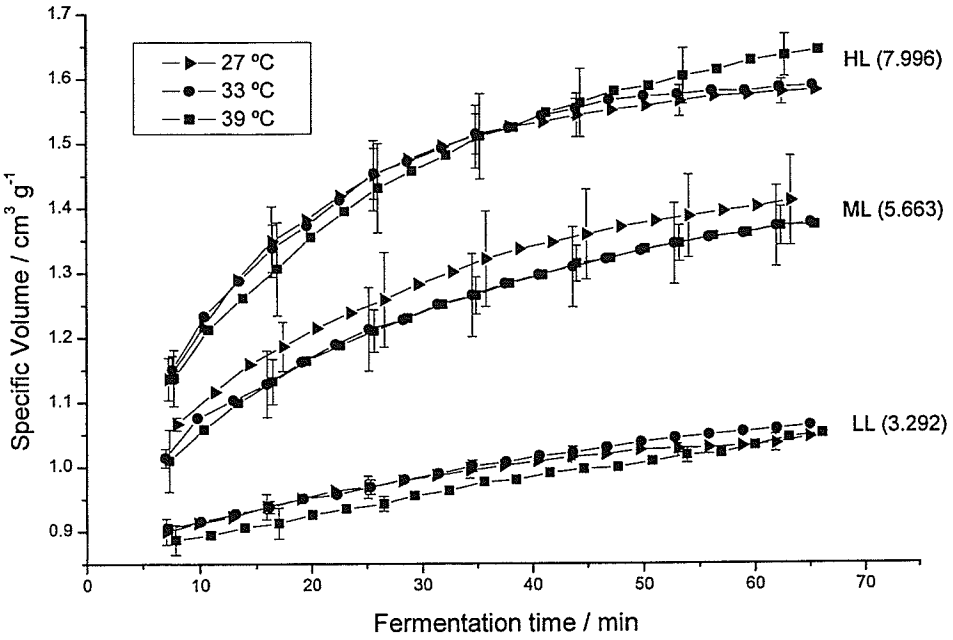

Figure 5.5. Effect of fermentation temperature and level of the chemical leavener adipic acid on the specific volume of fermenting dough. LL, ML, and HL denote addition of adipic acid in sufficient amounts so as to completely neutralize 1.40 (low level), 2.80 (medium level), and 4.20 (high level) g of sodium bicarbonate, respectively, in a base dough formula. Values in parentheses represent theoretical maximum specific volumes ($cm^3\ g^{-1}$) assuming 100% evolution and 100% retention of CO_2.

specific volumes achievable during fermentation. For example, at 27 °C doubling and then tripling the initial level (1.40 g/100 g) of sodium bicarbonate in dough leavened with adipic acid increased its specific volume from a basal value of 1.1 cm^3 g^{-1} to only 1.4 cm^3 g^{-1} and 1.6 cm^3 g^{-1}, respectively. A less-than-proportional increase in dough specific volume with sodium bicarbonate level was true for other fermentation temperatures as well.

5.3.4. Dynamics of dough specific volume

Figure 5.6 shows how the specific volume of doughs depended upon fermentation time. In the temperature range from 27 to 39 °C the time-dependent behaviour of the specific volume of dough could be described (Figure 5.6) by a first-grade exponential growth fit of the form:

$$Y = Y_0 - A_1 * e^{-t/\tau} \tag{5.4}$$

Where Y is the specific volume of dough, Y_o the maximum specific volume attained by the dough for a given leavening system and at a given temperature (cm^3 g^{-1}), A_1 a scaling parameter, and τ a time constant. Goodness of fit, estimated using the coefficient of determination was calculated using the chi-square test. Error terms in the fitted functions represented the amount by which observed values differed from those predicted by the model (Tables 5.3, 5.4 and 5.5). Data on dough that had been chemically leavened with SAPP did not exhibit exponential growth behaviour but linear (Figure 5.4) and so the fitting function reflected this relationship (Table 5.6).

The statistically significant coefficients of determination in Table 5.3, 5.4 and 5.5 supported the thesis that specific volume in chemically leavened dough was well described by exponential functions. In addition, as illustrated in Figure 5.6, changes in

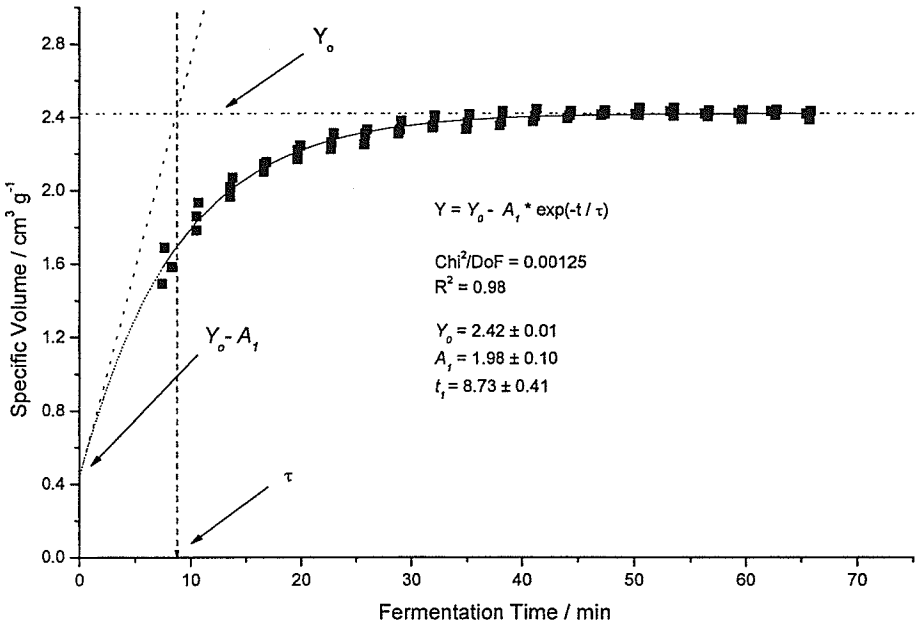

Figure 5.6. Mathematical characterization of the exponential growth function used for describing changes in specific volume with fermentation time for three replicates of a selected dough sample. Sample corresponds to dough prepared with GDL and sodium bicarbonate at a level of 9.33 g and 4.2 g, respectively, per 100 g flour, and fermented at 33 °C.

Table 5.3. Parameters for exponential growth fits of specific volume ($cm^3\ g^{-1}$) *versus* fermentation time (min) data (n=3; 20 data points per replicate) for doughs prepared with one of three levels of GDL[a] and fermented at 27, 33 or 39 °C.

	Equation[b]: $Y = Y_o - A_1 * \exp(-t/\tau)$			
GDL[a]	$Y_o \pm$ error	$A_1 \pm$ error	$\tau \pm$ error	R^2
27 °C				
LL	1.55 ± 0.01	0.785 ± 0.003	15.83 ± 0.82	0.978**
ML	2.14 ± 0.02	1.516 ± 0.159	11.39 ± 1.21	0.884*
HL	2.11 ± 0.01	1.31 ± 0.06	12.49 ± 0.85	0.953*
33 °C				
LL	1.62 ± 0.00	0.929 ± 0.021	13.53 ± 0.39	0.993**
ML	2.16 ± 0.03	1.502 ± 0.210	11.59 ± 1.85	0.965**
HL	2.42 ± 0.01	1.981 ± 0.105	8.73 ± 0.41	0.976*
39 °C				
LL	1.57 ± 0.02	0.784 ± 0.091	13.55 ± 2.13	0.808*
ML	2.00 ± 0.01	1.237 ± 0.175	10.33 ± 1.37	0.836*
HL	2.22 ± 0.01	1.275 ± 0.129	9.43 ± 0.98	0.890*

(a) LL = 3.11g GDL + 1.40 g sodium bicarbonate; ML = 6.22 g GDL + 2.80 g sodium bicarbonate; HL = 9.33 g GDL + 4.20 g sodium bicarbonate.
(b) Y = specific volume ($cm^3\ g^{-1}$); t = fermentation time (min)
(*) $p < 0.01$; (**) $p < 0.001$

Table 5.4. Parameters for exponential growth fits of specific volume ($cm^3\ g^{-1}$) *versus* fermentation time (min) data (n=3; 20 data points per replicate) for doughs prepared with one of three levels of potassium tartrate[a] and fermented at 27, 33 or 39 °C.

	Equation[b]: $Y = Y_o - A_1 * \exp(-t/\tau)$			
K tartrate[a]	$Y_o \pm$ error	$A_1 \pm$ error	$\tau \pm$ error	R^2
27 °C				
LL	1.08 ± 0.01	0.233 ± 0.035	18.65 ± 5.52	0.614*
ML	1.69 ± 0.01	0.874 ± 0.069	14.58 ± 1.47	0.914*
HL	2.11 ± 0.01	1.31 ± 0.06	12.49 ± 0.85	0.953*
33 °C				
LL	1.16 ± 0.01	0.263 ± 0.023	15.38 ± 2.38	0.843**
ML	1.85 ± 0.01	0.850 ± 0.034	14.72 ± 0.97	0.965**
HL	2.10 ± 0.01	1.59 ± 0.11	7.80 ± 0.47	0.954*
39 °C				
LL	1.17 ± 0.03	0.268 ± 0.028	23.36 ± 7.84	0.648*
ML	1.85 ± 0.03	0.852 ± 0.090	15.20 ± 2.70	0.794*
HL	1.99 ± 0.00	1.09 ± 0.71	4.48 ± 1.12	0.618*

(a) LL = 3.11g potassium tartrate + 1.40 g sodium bicarbonate; ML = 6.22 g potassium tartrate + 2.80 g sodium bicarbonate; HL = 9.33 g potassium tartrate + 4.20 g sodium bicarbonate.
(b) Y = specific volume ($cm^3\ g^{-1}$); t = fermentation time (min)
(*) $p < 0.01$; (**) $p < 0.001$

Table 5.5. Parameters for exponential growth fits of specific volume ($cm^3\ g^{-1}$) *versus* fermentation time (min) data (n=3; 20 data points per replicate) for doughs prepared with one of three levels of adipic acid[a] and fermented at 27, 33 or 39 °C.

	Equation[b]: $Y = Y_o - A_1 * \exp(-t/\tau)$			
Adipic acid[a]	$y_o \pm$ error	$A_1 \pm$ error	$\tau \pm$ error	R^2
27 °C				
LL	1.08 ± 0.02	0.217 ± 0.013	39.58 ± 7.83	0.926**
ML	1.44 ± 0.05	0.515 ± 0.055	24.89 ± 8.40	0.665*
HL	1.65 ± 0.03	0.735 ± 0.054	19.58 ± 3.31	0.897*
33 °C				
LL	1.16 ± 0.03	0.295 ± 0.022	60.20 ± 9.36	0.978**
ML	1.43 ± 0.05	0.501 ± 0.037	31.09 ± 9.20	0.788*
HL	1.61 ± 0.01	0.681 ± 0.022	17.86 ± 1.19	0.971**
39 °C				
LL	1.49 ± 0.67	0.637 ± 0.662	196.46 ± 250	0.871**
ML	1.43 ± 0.02	0.534 ± 0.015	28.32 ± 3.12	0.959**
HL	1.70 ± 0.04	0.726 ± 0.037	26.32 ± 4.87	0.876*

(a) LL = 1.22 g adipic acid + 1.40 g sodium bicarbonate; ML = 2.43 g adipic acid + 2.80 g sodium bicarbonate; HL = 3.65 g adipic acid + 4.20 g sodium bicarbonate.
(b) Y = specific volume ($cm^3\ g^{-1}$); t = fermentation time (min)
(*) $p < 0.01$; (**) $p < 0.001$

Table 5.6. Parameters for linear fits of specific volume ($cm^3\ g^{-1}$) *versus* fermentation time (min) data (n=3; 20 data points per replicate) for doughs prepared with one of three levels of SAPP[a] and fermented at 27, 33 or 39 °C.

	Equation[b]: $Y = A + B*t$		
SAPP[a]	$A \pm$ error	$B \pm$ error	R^2
27 °C			
LL	0.825 ± 0.002	$5.83 \times 10^{-5} \pm 3.14 \times 10^{-5}$	0.153
ML	0.807 ± 0.003	$50.9 \times 10^{-5} \pm 7.6 \times 10^{-5}$	0.653*
HL	0.813 ± 0.008	$89.2 \times 10^{-5} \pm 18.5 \times 10^{-5}$	0.532**
33 °C			
LL	0.815 ± 0.003	$20.0 \times 10^{-5} \pm 7.9 \times 10^{-5}$	0.317*
ML	0.798 ± 0.005	$110 \times 10^{-5} \pm 14 \times 10^{-5}$	0.709**
HL	0.787 ± 0.004	$195 \times 10^{-5} \pm 11 \times 10^{-5}$	0.919**
39 °C			
LL	0.801 ± 0.002	$51.6 \times 10^{-5} \pm 5.2 \times 10^{-5}$	0.795**
ML	0.789 ± 0.003	$126 \times 10^{-5} \pm 7 \times 10^{-5}$	0.914**
HL	0.811 ± 0.013	$316 \times 10^{-5} \pm 31 \times 10^{-5}$	0.876*

(a) LL = 1.94 g SAPP + 1.40 g sodium bicarbonate; ML = 3.89 g SAPP + 2.80 g sodium bicarbonate; HL = 5.81 g SAPPP + 4.20 g sodium bicarbonate.
(b) Y = specific volume ($cm^3\ g^{-1}$); t = fermentation time (min)
(*) $p < 0.01$; (**) $p < 0.001$

specific volume with fermentation time (except for leavening systems containing SAPP 40 where only one region was present) was characterized by three regions: (1) a linear region, where leavening systems brought about the most rapid change in dough specific volume with time; (2) a transitional region where reactant availability began limiting the evolution of carbon dioxide; and (3) a plateau region in which the amount of carbon dioxide entering in solution and into the gas bubbles was offset by that lost to the atmosphere.

Furthermore, the mathematical models provided information on the rates and extent of carbon dioxide retention in dough. The time constant (τ) in Tables 5.3, 5.4, and 5.5 gave a measure of the rate of change in dough specific volume for dough prepared with GDL, potassium tartrate and ADA, respectively. The time constant – the time required to reach 1/e (~37%) of the maximum specific volume Y_0 – increased with both sodium bicarbonate concentration and also, though slightly, with fermentation temperature. Overall, the time constants were the smallest for doughs prepared with GDL and the largest for those prepared with ADA. Interestingly, for SAPP, modelled using linear functions, the rate of change in dough specific volume also increased with both sodium bicarbonate level and fermentation temperature (Table 5.6).

The maximum specific volume, Y_0, gave an indication of the final degree of aeration achievable in the dough at the end of fermentation. As discussed previously, Y_0 increased, though not proportionally, with the amount of sodium bicarbonate in the formula (Tables 5.3, 5.4 and 5.5). Part of the basis for this less-than-proportional effect of sodium bicarbonate on specific volume was due to the use of fixed mixing times and

fixed water levels during sample preparations. No clear relationship could be established between fermentation temperature and Y_0.

The difference $Y_0 - A_1$ was expected to theoretically yield the specific volume of dough at the end of mixing because it was equivalent to extrapolating the specific volume of dough to zero fermentation time (immediately after mixing). However, the uncertainty associated with the specific volume of dough immediately after mixing, $Y_0 - A_1$, was relatively high so an alternative means or measuring it was required.

Based on the experimental techniques and the methodology described in Chapter 3, the gas void fraction of dough at the end of mixing (also initial void fraction) was measured using X-ray microtomography (refer to Chapter 3). Imaging of the internal structure of the experimental dough samples by X-ray microtomography required that no carbon dioxide gas be evolved during data acquisition, as the scanning times were relatively long (7 min) compared to the time scales associated with gas evolution (seconds). To achieve this, chemical leavening agents were first reacted on the side before mixing by combining them with a portion of the formula water until the bubbling ceased. In this way, no carbon dioxide was produced in the samples used in X-ray microtomography scans. The reacted (neutralized) salts were then added to the dough ingredients as per the standard mixing protocol described in Figure 5.1.

5.3.5. Gas void fraction

Figure 5.7 shows the relationship between the final gas void fractions in chemically leavened dough and the sodium bicarbonate level in the formula. The gas void fractions were derived from the specific volume of the dough (i.e., final specific volume data on Table 5.3 thru Table 5.6) and the specific volume of the gas-free dough, which

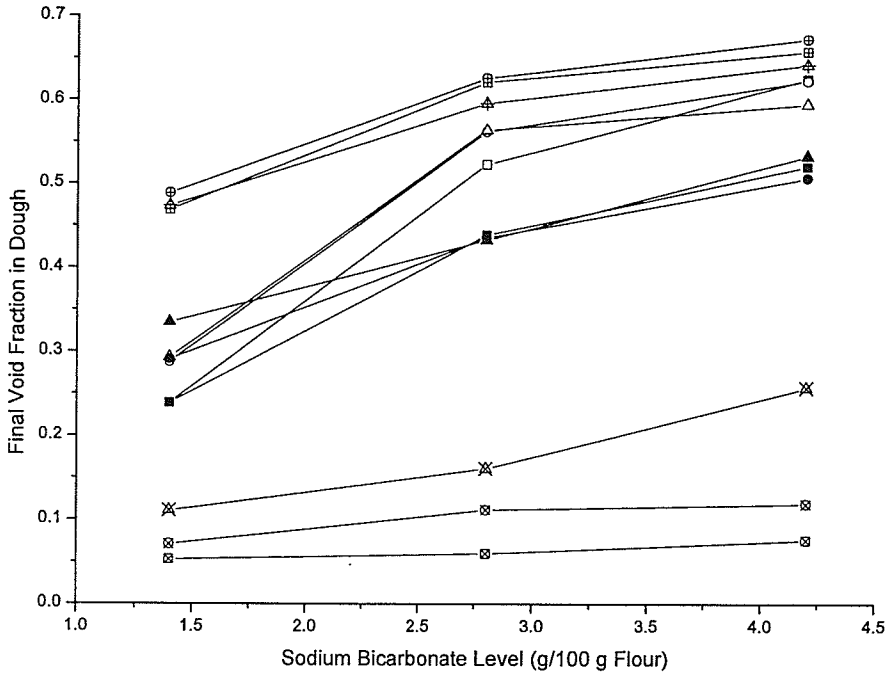

Figure 5.7. The final void fraction of doughs that had been proved at 27 (triangles), 33 (squares) and 39 °C (circles) for 1h and formulated with 1.40 g, 2.80 g, or 4.20 g of sodium bicarbonate per 100 g flour (14% m.b.) and one of four acidulants, GDL (vertically crossed (+) symbols), K tartrate (open symbols), adipic acid (closed symbols) and SAPP 40 (crossed (x) symbols), each at a level determined by their neutralisation value. See text for details on void fraction calculations.

was obtained from experiments using X-ray microtomography and density measurements as per the descriptions outlined in Appendix II. Figure 5.7 indicates that for the same level of sodium bicarbonate in the formula, which theoretically should lead to equivalent levels of gas production, the final gas void fraction in the dough samples depended strongly on the type of acidulant employed. Although the different gas production capacities of the different chemical leavening systems under study in this work may have played a role in determining the final gas void fraction in the dough (as will be discussed in the following section), attention should be focused on an alternate hypothesis: that acidulants affected the development of the gas-trapping network of dough (i.e., gluten development), during mixing and/or fermentation, so that gas retention properties in the dough were the basis for differences in final void fractions.

Figure 5.7 supports the view of gas retention properties being a function of chemical leavener levels in that doubling the initial level of sodium bicarbonate brought about a considerable increase in the dough's void fraction, while tripling it caused only a modest increase. The overall trend in Figure 5.7 is that final void fractions achievable in the dough would level off at sodium bicarbonate levels greater than 2.8 g per 100 g flour. This may explain why Heidolph (1996) recommended that bread be leavened using sodium bicarbonate at a level between 1.68 to 2.10 g per 100 g flour. Increasing the level of sodium bicarbonate beyond 2.8 g per 100 g flour does not have a major impact on dough specific volume as the dough becomes more permeable to carbon dioxide. Changes in gas retention properties at high levels of chemical leavening systems may have arisen due to the fact that water in the formula was not adjusted. Competition between chemical leaveners and gluten proteins for the available water can affect dough

development. However, delayed addition of chemical leaveners to the formula was a strategy that was intended to provide a means for proteins to hydrate preferentially over the leavening agents' need to dissolve in the available water, and thus this thesis was not supported (Figure 5.1).

Dough rheology can also be affected by the presence of salts due to their effects on gluten protein aggregation (Kinsella & Hale, 1984; Holmes & Hoseney, 1987a; He et al., 1992; Wellner et al., 2003). Sodium chloride, for instance, improves the cohesiveness of dough and increases its mixing strength due to the influence of the chloride anion on shielding charges on the gluten proteins, which overall contributes to greater protein aggregation (Guy et al., 1967). In the present experiment, anions were added directly to the dough as either acidic salts (e.g.., tartrate anion from potassium tartrate and phosphate from SAPP 40), or acids (e.g., anions from adipic acid or glucono-delta-lactone). Theoretically, the stability effect of the anion on native configuration of the protein (i.e., protein aggregation effect) is given by the position of the anion in the lyotropic series: citrate > phosphate > tartrate > sulfate > acetate > chloride > nitrate > bromide > iodide > thiocyanate (Preston, 1981, 1984, 1989; Eliasson & Larsson, 1993; Holmes & Hoseney, 1987a; Kinsella & Hale, 1984; Wellner et al., 2003). Holmes and Hoseney (1987a) provided experimental evidence that addition of non-chaotropic anions, such as those of phosphate from sodium aluminum phosphate, to bread flour reduced the ability of the dough to retain gas, causing a decrease in loaf volume. Similarly, Figure 5.7 shows that dough leavened with the tartrate salt had a greater final void fraction than that leavened with the salt of pyrophosphate (SAPP 40). However, the fact that the different gas production capacities of the leavening systems studied was not factored out represents a

source of uncertainty in ascribing a chemical mechanism to the results of Figure 5.7. In addition, the position of the anions of adipic acid and GDL in the anionic lyotropic series has not been reported, so no theoretical framework is available for understanding the effects of their chemistry on gas retention.

That the rheological properties of dough depend only on how proteins, carbohydrates, lipids, and water interact is nonetheless debatable (Bloksma 1990a, 1990b; Scanlon & Zghal, 2001). Recently, Babin et al. (2005) demonstrated that the physical properties (e.g., gas retention) of fermenting doughs made of different compositions depended little on the composition but strongly on the relative density of the dough (relative density = 1 - void fraction). This dependence of mechanical behaviour on cellular structure is supported by the model of Gibson and Ashby for open cell foams (Gibson & Ashby, 1997). Using X-ray microtomography measurements of relative density of dough as a function of fermentation time, Babin et al. (2005) found that increasing the concentration of yeast in dough can lead to a premature onset of coalescence. Bubble coalescence is a recognized mechanism of dough development responsible for gas losses which can negatively affect the formation of the foam like structure of dough. (Shah et al., 1998; van Vliet, 1999; van Vliet et al., 1992). Similarly, in the present experiments higher rates of carbon dioxide production arising from higher levels of sodium bicarbonate in the dough may have precipitated the early onset of coalescence, thereby increasing the extent to which gas was lost during fermentation (Figure 5.7). Coalescence can lead to gas losses because it causes bubble to become first interconnected with each other and then with the exterior where the gas is discharged, as it occurs at advance stages of fermentation (Weegels et al., 2003). However,

mathematical predictions estimate that coalescence only becomes extensive when the void fraction of dough is nearly 0.7 (Bloskma, 1990b). This prediction has been corroborated in the work of Babin et al. (2005). Figure 4.7 shows that no experimental dough system was able to reach a void fraction greater than 0.65, which suggest that coalescence could have been only partly responsible for the decreased ability of dough to retain gas at the high concentration of sodium bicarbonate.

5.3.6. Gas retention versus gas evolution

Knowledge on the final void fraction of fermented dough provided quantitative data on the state of aeration, but gave no information on the levels of carbon dioxide that had been lost during mixing, sample preparation and fermentation. During mixing and sample preparation, gas loss differences among chemical leavening systems could not be measured though gas loss differences may be considered negligible since these two preparation steps followed standard protocol and their duration was relatively short compare to fermentation. Accordingly, the fermentation stage was suitable to measure gas retention properties on chemically leavened dough while taking into account the actual levels of carbon dioxide produced by the leavening system (i.e., mass of gas retained per unit mass of gas produced).

In fact, one way of eliminating bias from carbon dioxide production it is to determine the amount of gas retained per unit of gas produced. Figure 5.8 shows the relationship between CO_2 evolved and CO_2 retained in the dough samples after 60 min of fermentation. Gas production data was pooled from data obtained using the Gassmart apparatus (DRR technique; Chapter 4) whereas gas retention in the dough was based on the final specific volume of the dough. Gas production data corresponding to

fermentation temperatures of 33 °C were interpolated from the measured data at 27 and 39 °C (see Appendix III for further details).

Figure 5.8 shows that the volume of carbon dioxide retained per unit of carbon dioxide evolved was still a strong function of the acidulant in the leavening system. Figure 5.8 also shows lines that represent linear fits to the experimental data. The data was pooled for various fermentation temperatures since data on CO_2 evolved against CO_2 retained showed no clear relationship with the fermentation temperature. The slopes of these lines could be interpreted as the effectiveness of the chemical leavening system to leaven the dough. Accordingly, the efficacy of the leavening system to leaven dough was ranked (in decreasing order) as follows: KAT (0.306 cm^3 of CO_2 retained per cubic centimetre of CO_2 evolved), GDL (0.143), ADA (0.110) and SAPP (0.039). As well, the linear fits to the data shown on Figure 4.8 were found to be associated with reasonably good coefficients of determination (R^2): 0.96, 0.81, 0.96 and 0.47 for KAT, GDL, ADA and SAPP, respectively. Statistically, the R^2 for all these systems, except for SAPP, were highly significant (based on the chi-squared test). Though it shall be stated that the efficacy of the leavening systems changes with fermentation temperature, it is opportune to reiterate that the present experiments were meant to provide an insight into chemical leavening of dough at ordinary fermentation temperatures. Furthermore, despite the use of identical ranges of sodium bicarbonate in the formula, different leavening systems released different levels of carbon dioxide, with SAPP covering the narrowest range (179-538 cm^3 CO_2 per 100 g dough), and GDL the widest (390-1196 cm^3 CO_2 per 100 g dough).

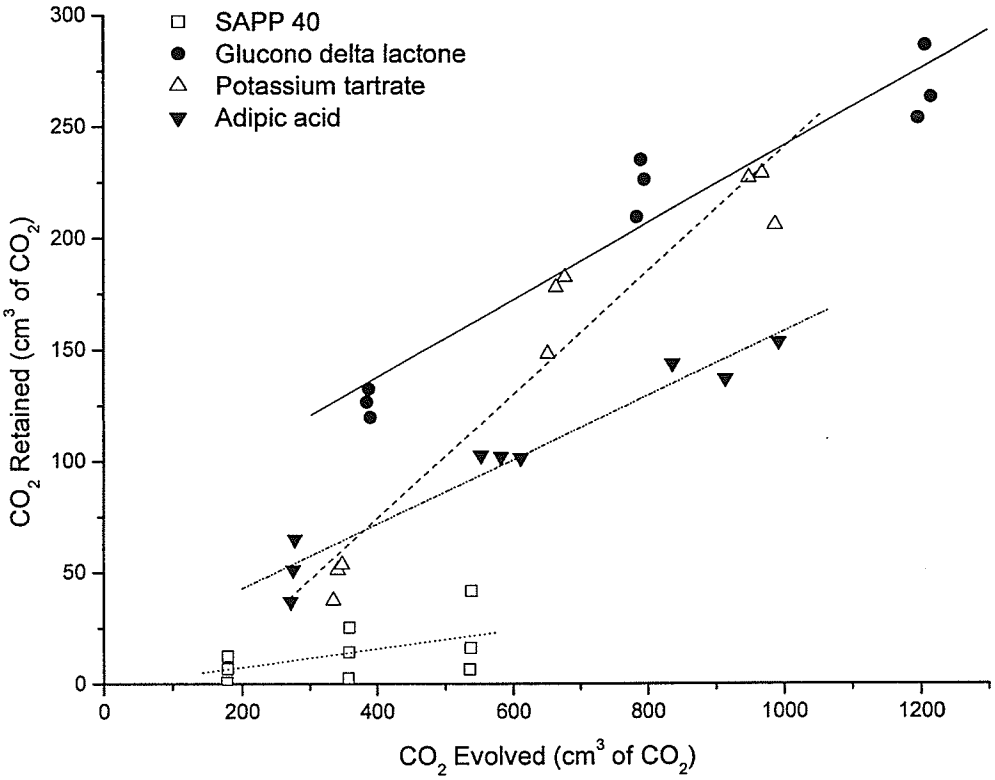

Figure 5.8. Relationship between the amount of carbon dioxide retained to that evolved during fermentation of dough prepared with various chemical leavening systems. Data pooled for various fermentation temperatures. Lines represent the fit given by a linear regression (see text). Chemical leavening systems were composed of sodium bicarbonate (1.40 g, 2.80 g, or 4.20 g) and leavening acid at a level given by its neutralisation value.

Despite the fact that a true index of effectiveness in chemical leavening systems required knowledge on gas production to eliminate bias from the gas lost during fermentation, the underlying reasons for gas losses were uncertain. Gas losses, as discussed earlier, may have occurred due to coalescence of the gas bubbles in the dough or due to the permeability of the dough to carbon dioxide gas. From a food engineering point of view, gas transport is associated with the coefficient of mass diffusion of carbon dioxide across the gas-dough interface. A higher carbon dioxide diffusivity coefficient, for instance, would be associated with a more permeable, albeit more leaky, dough.

5.3.7. Apparent coefficient of mass diffusion

Diffusion of gas into bubbles is a classical chemical engineering problem (Shah et al., 1998). The theoretical view is that bubble growth is a transport phenomenon where a molecule of carbon dioxide diffuses or is transported from the aqueous phase in the dough, across the gas-dough interface, and into the gas cell interior, and this phenomenon continues indefinitely until a gas-concentration equilibrium is established across the interface. More unambiguously, this phenomenon is described in terms of two transport mechanisms, a momentum transport and a mass transport, the contributions of which are customarily analysed independently for simplifying the mathematics associated with this transport problem (Chiotellis & Campbell, 2003a). While momentum transport focuses on the viscoelastic properties of the liquid that surrounds the bubble, mass transport focuses on diffusion-controlled growth of the bubbles and neglects the contributions of the dough phase (e.g., viscoelastic and surface tension properties of dough). Resolution of the actual mass transport problem is quite complex since the governing equations

constitute a non-linear, moving boundary problem for which an exact analytical solution is not available as of yet (Venerus et al., 1998; Chiotellis & Campbell, 2003a).

Venerus et al. (1998) has recently proposed a comprehensive model for bubble growth in a viscoelastic liquid which accounts for both the mass transfer and the viscoelastic properties of the liquid surrounding the bubble by making some assumptions and simplification. This model is known as a diffusion-induced bubble growth model and is suitable to describe the growth of a bubble exhibiting a linear dependence between the growth of its radius (e.g., due to carbon dioxide evolution) and the square root of time (e.g., fermentation time). Because such temporal behaviour was observed in the growth of the fermenting doughs (Figure 5.5), the dynamic changes in the specific volume of chemically fermented dough was interpreted in light of the analysis of Venerus et al. (1998). The application of this mathematical analysis yielded experimental values for the mass diffusion coefficient of carbon dioxide in fermenting dough.

Carbon dioxide diffusivity in dough data, though of great importance to modelling the proving process (Campbell, 1991; Campbell et al., 1993, 1998, 1999, 2001; Chin et al., 2005; Chiotellis & Campbell, 2003a, 2003b; Martin et al., 2004a, 2004b; Mitchell et al., 1999; Shah et al., 1998; Shimiya & Nakamura, 1997; van Vliet, 1999), is scarce. Typically, carbon dioxide diffusivity in dough is estimated on the basis of the water fraction of dough (X_W) because carbon dioxide is thought to diffuse only in the water phase of dough as described in a relationship reported by de Cindio & Correra (1995):

$$D_L = 1.77 \times 10^{-9} X_W \left(\frac{T}{298} \right) \tag{5.5}$$

For the dough leavened at 33 °C with GDL and sodium bicarbonate at a level of 4.2 g per 100g flour, Equation (5.5), for example, estimates D_L = 7.14 x 10^{-10} m^2 s^{-1}, since the

dough's water fraction, X_w, was 0.393. Similarly, Equation (5.5) predicts, based on all combinations of dough water contents and fermentation temperatures (27-39 °C), that the chemically leavened doughs in this experiment had diffusivity coefficients spanning the range between 7.1-7.4 x 10^{-10} m^2 s^{-1}, a relatively narrow range if one were to consider the remarkably different states of dough development measured (0.039 to 0.306 cm^3 of CO_2 retained per cubic centimetre of CO_2 evolved in the samples studied; a nearly ten-fold difference in gas-trapping properties).

Venerus et al. (1998) proposed a mathematical model capable of describing the growth of a single, spherical gas bubble surrounded by a polymeric liquid of infinite extent comprised of a polymeric and a volatile species, which, by analogy with the present experiment, correspond to the dough phase and carbon dioxide species, respectively. Mass diffusion is assumed to be governed by Fick's law with a constant diffusivity, D_L. Also, the entire system is considered to be isothermal, which is in agreement with the fermentation conditions employed; the gas within the bubbles is assumed to be inviscid and to obey the ideal gas law; the pressure of the gas within the bubble is assumed to be uniform as inertial effects in the bubble are neglected; and the gas-liquid interface is governed by Henry's law with Henry's law constant, H.

Since the mathematical analysis of Venerus et al. (1998) was developed to describe the growth of a single gas bubble, the volume of this bubble needed to be determined. This was accomplished using the volume of the dough sample at time t, $V_{dough}(t)$; the volume of the gas-free dough in the dough, $V_{gas-free}$; and the volume of the single bubble in the dough sample, V_{bubble}, as follows:

$$V_{dough}(t) = V_{gas-free} + V_{bubble}(t) \tag{5.6}$$

$$m_{dough} \times \gamma_{dough}(t) \cong m_{dough} \times \gamma_{gas-free} + \frac{4\pi R^*(t)}{3}$$

$$R^*(t) = \sqrt[3]{\frac{3m_{dough}}{4\pi} \times \left(\gamma_{dough}(t) - \gamma_{gas-free}\right)} \qquad (5.7)$$

where, $R^*(t)$ is the radius of *the single* bubble in the dough, m the mass of the dough, and $\gamma_{gas-free}$ the specific volume of the gas-free dough, which was obtained from information based on X-ray microtomography scans made on selected chemical leavening systems using the methods described in Chapters 3 and 4 and Appendix II ($\gamma_{gas-free}$ = 0.785, 0.779 and 0.776 $cm^3\ g^{-1}$ for SAPP, or 0.825, 0.808 and 0.792 $cm^3\ g^{-1}$ for all other systems, for when high, medium and low levels of sodium bicarbonate were employed, respectively). A plot of $R^*(t)$ against the square root of fermentation time was then constructed, and the slopes of the plots used for further analysis, much in the same way as Venerus et al. (1988) analyzed the experimental data of Han and Yoo (1981), researchers who reported bubble radius versus time data obtained from isothermal, foam injection experiments for a polystyrene/CO_2 system. Figure 5.9 illustrates how a region of the chemically leavening expansion curve did indeed show a linear dependence with the square-root of fermentation time, suggesting that bubble growth in this region was diffusion controlled.

Venerus et al. (1998) postulated that the relationship between bubble radius and the square-root of time for diffusion-controlled bubble growth is given by:

$$R^*(t) = (2\beta\sqrt{D_L})\sqrt{t} \qquad (5.8)$$

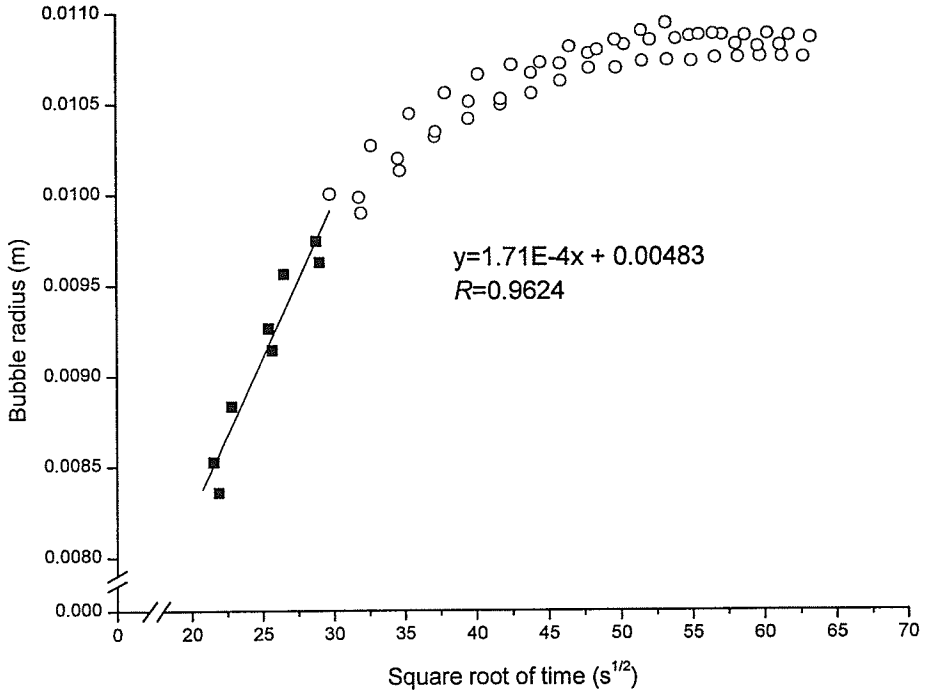

Figure 5.9. Experimental growth dynamics (n=3) of a gas bubble in chemically leavened dough, whose radius was calculated from Eq. (5.7). Chemical leavening system consisted of sodium bicarbonate and GDL used at a level of 4.2 g and 9.33 g, respectively, per 100 g of flour. Filled squares correspond to diffusion-controlled bubble growth case and empty circles to reactants-limited bubble growth case. Line is a best-linear fit corresponding to diffusion-controlled bubble growth as per the predictions of Eq. (5.8).

If the relationship between bubble radius and square-root of time is indeed linear, the transport analysis is valid and D_L can be determined from the slope of the $R^*(t)$ versus $\sqrt{t}$ plot. The dimensionless growth rate constant β is defined as follows:

$$\beta = \frac{N_A}{P_g} \tag{5.9}$$

where,

$$N_A = \frac{RT\rho}{MP_\infty}\left(\frac{C_\infty - C^*}{\rho - C^*}\right) \cong \frac{RT}{MP_\infty}\left(C_\infty - C^*\right) \tag{5.10}$$

$$P_g = \frac{P_g^*}{P_\infty} \tag{5.11}$$

Here, N_A is a dimensionless number, R is the universal gas constant (8315 J K^{-1} $kmol^{-1}$), T absolute temperature (K), ρ dough density (kg m^{-3}), M molecular weight of carbon dioxide (44 kg $kmol^{-1}$), P_∞ atmospheric pressure (101 kPa), C_∞ solute (CO_2) mass density (1.917 kg m^{-3} at saturation; Bloksma, 1990a), C^* initial CO_2 mass density, P_g^* bubble pressure (1.03 x P_∞; Bailey, 1955). All these parameters can be either measured directly from independent experiments or estimated from published data, except for C^*. Estimation of the initial solute concentration, C^*, is rather difficult because the onset of carbon dioxide evolution cannot be accurately determined as in most cases chemical leaveners react with the formula water as soon as they come into contact. When analyzing the experimental data of Han and Yoo (1981), Venerus et al. (1998) also admitted that estimating the initial solute concentration is in practice extremely difficult. Hence, it was decided to use an upper bound and a lower bound for this term instead. The lower bound for the initial concentration of carbon dioxide in the bubble was given as the

concentration of carbon dioxide entrained in the gas phase of the dough during mixing. This concentration, as per Henry's law, is given by both the partial pressure of carbon dioxide in air, $P_b^{CO_2}$, which is about 380 ppm or 39 Pa (Wrigley, 2006), and H, Henry's law constant (60,000 x (T-273) + 900,000 J kmol^{-1}; Chiotellis & Campbell, 2003a). The upper limit corresponded to the partial pressure of carbon dioxide in the bubble at the end of fermentation, assuming that the bubble grew due to carbon dioxide diffusion and that none of the original gas entrained (nitrogen and oxygen) diffused out of the bubble. Shah et al. (1998), using a mathematical model that predicted the growth of individual bubbles, found that the initial diameter of a bubble can grow up to five times when C_∞ is below saturation (C_∞ < 1.917 kg CO_2 per m^3 dough). The upper limit was estimated to be ~ 99,500 Pa, based on a five-fold growth in the diameter of the mean bubble (initial bubble diameter = 100 μm, Chapter 3) as per the predictions made by Shah et al. (1998). See Appendix IV for further details on calculations.

The transport analysis of diffusion-controlled bubble growth yielded experimental values for D_L that were weakly influenced by fermentation temperature, so the results were pooled for the range of temperatures studied. Using the lower bound for C^*, the empirical mass diffusivity coefficients of carbon dioxide in dough were, in decreasing order, 4.5 ± 3 x 10^{-9} m^2 s^{-1} (GDL), 4.2 ± 1.6 x 10^{-9} m^2 s^{-1} (KAT), 1.8 ± 0.5 x 10^{-9} m^2 s^{-1} (ADA), and 2.1 ± 1.5 x 10^{-10} m^2 s^{-1} (SAPP). When the upper limit of C^* was used, the empirical D_L values were, in decreasing order, 3.1 ± 3.6 x 10^{-7} m^2 s^{-1} (GDL), 2.6 ± 3 x 10^{-7} m^2 s^{-1} (KAT), 1.4 ± 1.8 x 10^{-7} m^2 s^{-1} (ADA), and 6 ± 2 x 10^{-9} m^2 s^{-1} (SAPP). Based on the water contents found in the experimental doughs, the equation of de Cindio and Correra (1995) estimated that D_L should span the range 7.1 x 10^{-10} to

7.4 x 10^{-10} m^2 s^{-1}. Because it is physically impossible that carbon dioxide diffusivity in dough be greater than that in pure water (carbon dioxide should only diffuse in the water fraction of the dough; de Cindio & Correra, 1995), the results yielded by the upper bound of C^* were neglected. The lower limit of C^* therefore yielded D_L values in agreement (within one order of magnitude) with the theoretical predictions made by de Cindio and Correra (1995).

The assumption that the bulk (macroscopic) growth rate of a bubble is given by the relation R vs. $t^{1/2}$ is regarded as a very good approximation for describing diffusion-controlled growth of bubbles in many other fluids (Lubetkin, 1995). In this regime the radial rate of growth of a bubble is limited by how much CO_2 can be transported across the bubble interface (Lubetkin, 1995; Venerus et al., 1998). Hence, it is safe to assume that D_L played an important role in determining the effectiveness of the chemical leavening systems to aerate dough (on a carbon dioxide evolved basis) (Figure 5.8). It is conceivable that a dough property such as D_L is not only a function of the water content and temperature (de Cindio & Correra, 1995), but also of the type of leavener in the formula (e.g., type of leavening acidulant). Accordingly, when a chemical leavening system affects the matrix of the dough in a way that causes a reduction in the diffusivity coefficient of CO_2 in the dough, the effectiveness of the chemical leavening system to aerate the dough is also reduced, likely because the dough becomes less permeable to CO_2. Conversely, this study suggests that the effectiveness of a chemical leavening system to leaven dough may be studied using the transport model of Venerus et al. (1998). The most effective chemical leavening system was, in decreasing order, GDL, KAT, ADA, and SAPP. These results coincided well with the results given by an

independent analysis (Figure 5.8), where the most effective leavening system was found to be, in decreasing order, KAT, GDL, ADA and SAPP. Because the error associated with estimating D_L for any one system was large (CV = 26-70%), a quantitative interpretation of the specific volume results in terms of D_L could not be adequate. Yet, given the number of theoretical assumptions and simplifications that have been made, and the difficulty in determining the initial solute concentration, the analysis just described gave reasonable estimates of D_L.

5.4. Conclusions

The present paper provided a description on how to conduct measurements of the dynamic specific volume (DSV) of chemically leavened dough using a technique based on digital image analysis. The accuracy of the DSV technique was improved with the use of a novel calibration step. Experimental results indicated that chemical leavening systems consisting of sodium bicarbonate and one of the following GDL, potassium tartrate, ADA or SAPP, were useful bakery ingredients for leavening dough at ordinary fermentation temperatures.

Sodium bicarbonate at a level of 1.4 to 2.8 g per 100 g of flour in combination with equivalent neutralizing amounts of the said leavening acidulants was able to consistently raise the specific volume of bread dough so that their final gas void fractions spanned between 5 and 67 %. The relationship between the specific volume of dough at the end of fermentation and the actual gas evolved (measured independently using the Gassmart) was fairly linear and characterized by a slope that provided a good index of the actual gas-trapping properties of dough. Doughs with better gas-trapping networks had

more positive slopes because they retained more units of carbon dioxide on a carbon dioxide evolved basis.

The linear relationship between the biaxial expansion of dough and square-root of fermentation time, in the early region of the chemical leavening expansion curve, suggested that initially the growth of the gas phase with time was diffusion limited. To interpret this diffusion-controlled region, the analysis for diffusion-controlled bubble growth for a viscoelastic liquid proposed by Venerus et al. (1998) was invoked. The results of the mathematical analysis yielded empirical values for the mass diffusion coefficient of carbon dioxide in the fermenting dough samples. The empirical mass diffusivity coefficients of carbon dioxide in the doughs were $4.5 \pm 3 \times 10^{-9}$ m^2 s^{-1} (GDL), $4.2 \pm 1.6 \times 10^{-9}$ m^2 s^{-1} (KAT), $1.8 \pm 0.5 \times 10^{-9}$ m^2 s^{-1} (ADA), and $2.1 \pm 1.5 \times 10^{-10}$ m^2 s^{-1} (SAPP). These values were in relatively good agreement with the predictions made by de Cindio and Correra (1995), based on water contents and fermentation temperatures.

Overall, the experimental results indicated that the predictability of the chemical leavening reaction can make chemical leavening systems amenable to controlled-release of carbon dioxide. Further, the DSV technique introduced in this paper was useful in mapping out some of the effects of level and type of chemical leavening systems on the specific volume of bread dough. The technique was less able to discern the effects of fermentation temperature on specific volume however. It is expected that the use of this simple yet effective technique for monitoring the specific volume of dough may serve as a valuable tool to further the knowledge on mechanisms of bubble growth and coalescence in wheat flour doughs.

CHAPTER SIX

Effects of Chemical Leavening Systems on Dough Development during Mixing and on Dough Aeration during Proving: A Comparison of the Canadian and British Techniques for Measuring Dynamic Dough Density in Fermenting Dough

Abstract

A far more practical approach to assess the cellular structure in dough than quantifying bubble size distributions is to measure the gas content of dough via density measurements. This study characterized the effects of chemical leavening systems on dough development in the Tweedy 1 mixer and monitored the subsequent growth of the dough during fermentation with the two best known dough density measurement systems. Results show that the addition of the chemical leavener to the dough decreased dough strength. The effects of chemical leaveners on dough rheology were associated with changes in dough gluten strength and with aeration of the dough during mixing. Dough consistency, as measured during dough development, showed that the strength of the experimental doughs varied with chemical leavener (in decreasing order): ADA > KAT ~ GDL > SAPP. A comparison of Campbell's DDD system and Bellido's DDD system was also made for the first time using chemical leaveners as the source of CO_2. The measured change in dough density during fermentation with respect to the initial density (ex-mixer) was compared to assess the two DDD systems. For small changes in dough density (<0.1 g cm^{-3}), both techniques were in very good agreement, and these small changes were found in dough fermented with SAPP and, at early times, in dough containing ADA and KAT. However, discrepancies for the density changes measured by Campbell's DDD

system and Bellido's DDD system began when doughs underwent larger density changes (> 0.1 g cm^{-3}), particularly when the dough densities changed by more than 0.2 g cm^{-3}. Very interestingly, density measurements detected in Campbell's DDD system were suitable to identify the point at which gas cell coalescence, an important mechanism for structure formation in dough, came to happen. The onset of bubble coalescence was observed to occur in GDL dough (the system with the highest CO_2 production power) when it reached a gas void fraction of 70%, much in agreement with the theory (Bloksma, 1990a, 1990b; Scanlon & Zghal, 2001). However, because signs of bubble coalescence were detected in KAT at a surprisingly lower void fraction (~50%), it was proposed that bubble coalescence cannot be ascribed as an event that takes place at a given void fraction, but rather takes place over a range of void fractions. Independent studies using x-ray microtomography (Babin et al., 2006) confirm that this view is physically sound.

6.1. Introduction

Fresh bread texture is largely determined by bread crumb (grain) as this has a direct effect on bread palatability, with fine bread crumb, for instance, being a highly desirable attribute in North American or English bread, while a coarse bread crumb being a more attractive attribute in a French baguette. Owing to the fact that bread crumb structure is defined by gas cell structure (Baker & Mize, 1937, 1941; Scanlon & Zghal, 2001; Shimiya & Nakamura, 1997), it is of interest to cereal science to understand the mechanisms underlying the creation, growth and stability of gas cells during breadmaking. Because the gas cell structure of bread is largely defined by the end of mixing (MacRitchie, 1986), research efforts have been focused on assessing and

monitoring either the gas bubble size distribution (Carlson & Bohlin, 1978; Chiotellis & Campbell, 2003a; Shimiya & Nakamura, 1997; Campbell et al., 1991; Chapter 3) or the gas bubble content of dough after mixing (Baker & Mize, 1937, 1941; Campbell et al., 1993, 2001; Martin et al., 2004a). X-ray microtomography has proven an excellent means to unequivocally measure both bubble size distributions and the gas content of dough (Chapter 3; Babin et al., 2005, 2006); however, routine measurement of dough microstructure with X-ray microtomography is not practical in a cereal research laboratory. Also, a conventional X-ray microtomography instrument scans objects with a time resolution of minutes, typically 7 min (Chapter 3), whereas gas bubble growth in fermenting dough occurs at much faster timeframes (Campbell et al., 2001). A more practical approach to assess gas cell structure than quantifying bubble size distributions is to measure the gas content of dough via density measurements (Campbell et al., 1993, 2001). In particular, density measurements have proven an invaluable tool to follow aeration of dough during mixing and proving (Baker & Mize, 1941, 1946; Campbell et al., 1993, 2001; Chin et al., 2005).

While measuring the density of dough with no yeast can be done relatively easy, measuring the density of a fermenting dough is not trivial, i.e., evaluating dough density changes with time. Conventional techniques to measure density in fermenting dough do so by calculating the volume of a pre-weighed dough specimen via Archimedes principles; that is, by measuring the volume of fluid displaced by the specimen after its immersion in the fluid. Immersion fluids range from oil (Baker & Mize, 1937; Dus & Kokini, 1990), calcium chloride solutions (Baker & Mize, 1946; Campbell et al., 1993; Junge et al., 1981), to simply water (Elmehdi et al., 2004, 2007). One problem with

conventional techniques for measuring dough density dynamically is that one specimen is required per density measurement. Following dough density changes in a fermenting dough piece by extracting multiple dough specimens over time is not only inconvenient, but it is also subject to introducing significant experimental error.

Recently, Campbell et al. (2001) introduced an ingenious new method for measuring changes in dough density in real time based on Archimedes principle. Unlike conventional density measurement techniques, Campbell et al.'s technique measures dynamic dough density (DDD) over the course of fermentation in a single dough specimen. It does so by immersing a dough specimen of known weight in xylene and following its change in volume by measuring the change in dough weight. Particulars on Campbell et al.'s DDD system, including Campbell et al.'s DDD experimental technique (henceforth simply "Campbell's DDD technique") can be found in Campbell et al. (2001). The novelty and wealth of quantitative evidence generated by Campbell's DDD technique has unofficially made it an international standard (Campbell & Herrero-Sanchez, 2001; Chiotellis & Campbell, 2003b; Campbell et al., 2001).

More recently, an alternative technique for measuring density changes in fermenting dough dynamically was introduced by Elmehdi et al. (2003a, 2007). Elmehdi et al.'s technique measured the changes in volume of a pre-weighed fermenting dough specimen using digital photography. In independent investigations using their own density measurement system, Elmehdi et al. (2003a) and Chiotellis and Campbell (2003b) found good correspondence for changes in density over time for yeasted doughs. More recently, Elmehdi et al. (2003a)'s density measurement system has been improved by including a novel calibration step that reduces the error in calculating the area of the

expanding dough (Chapter 5). Chapter 5 further describes, for the first time, the protocol for image analysis of the area of dough and discusses other common sources of error. The substantial improvements made to the density measurement system conceived by Elmehdi et al. (2003a) warrant the use of a new designation; hence, the present paper refers to the technique discussed in Chapter 5 as "Bellido's technique". Interestingly, Chapter 5 of this thesis expanded the applicability of Bellido's technique as it proved suitable for estimating the coefficient of diffusivity for carbon dioxide in chemically leavened dough. Moreover, Chapter 5 showed that chemical leavening systems could be used as a substitute to yeast for the purposes of generating carbon dioxide at controlled rates in dough over a wide range of temperatures.

In fact, the use of only four chemical leavening systems (containing sodium acid pyrophosphate, adipic acid, potassium acid tartrate or glucono-delta-lactone) at specified concentrations was sufficient to produce experimental doughs with a broad range of gas contents at room temperature (Chapter 5). Chapter 4 characterized the CO_2 production powers of these chemical leavening systems based on pressure measurements. Hence, the said four chemical leavening systems are well-characterized in terms of gas retention and gas production capacities in fermenting dough. However, little is known of the effects of chemical leavening systems on dough development during mixing.

Based on their chemistry, the mode of action of the organics acids, adipic acid and glucono-delta-lactone, on wheat glutens proteins is expected to be different than that of acidic salts such as potassium acid tartrate and sodium acid pyrophosphate. At a molecular level, ionic interactions between the chemical leavening agents and the dough gluten proteins should be the basis for explaining dough development in the mixer. Galal

et al. (1978) studied the combined effects of organic acids on dough rheological properties. They noted that the Farinograph dough stability (measured in minutes) for the dough dropped considerably (~ 9 min) after incorporating organic acids (a mix of lactic [80%] and acetic [19%] acids) to the formula. They hypothesized that at a low pH (< 4), dough strength becomes weaker because appreciable repulsions between ionisable side chains in the amino acids of the gluten proteins occurs. The increased intermolecular repulsions would change protein conformation by reducing inter- and intra-glutenin protein interactions and be the basis for the observed reduction in dough gluten strength (Galal et al., 1978). Conversely, anionic salts, such as phosphate and tartrate, are expected to interact with gluten proteins via their effect on water structure (i.e., based on salt lyotropicity). Kinsella and Hale (1984) explained that non-chaotropic anions such as phosphate and tartrate accentuate hydrophobic interactions between gluten protein molecules by increasing the ordering of water structure (i.e., by increasing the structure of water molecules). This would cause gluten proteins to remain more aggregated and more resistant to hydration during mixing which would impair the formation of subsequent protein-protein interactions or physical entanglements in the dough (Kinsella & Hale, 1984). Non-chaotropic anions would therefore be expected to reduce the mechanical strength of the dough to which they are added. Chaotropicity effects on dough development were also reported by Holmes and Hoseney (1987a). They observed that the amount of chemical leavener required to produce a standard mixogram pattern (for dough mixed for 8 min) increased with chaotropicity. Holmes and Hoseney (1987a) found that a chaotropic salt like sodium chloride required 339 mg to produce a specified Mixogram pattern, whereas non-chaotropic salts such as sodium tartrate required 194 mg,

and sodium phosphate only 142 mg. The report of Hlynka (1962) also illustrates the strengthening effect of chloride ions by stating that dough development time (time to reach 500 B.U.) in a Farinograph increases by about 0.5 min for each additional 1% of salt in the dough formula.

Regardless of their mechanism(s) of action, chemical leaveners, due to their effect on protein strength (Kinsella & Hale, 1984; Galal et al., 1978; He et al., 1992), are also expected to affect dough development by altering the amount of gas that is entrained during mixing (Chin et al., 2005). Bubbles in the dough can affect dough rheology (Elmehdi et al., 2003a, 2004; Chin et al., 2005), and hence the torque recorded by the Farinograph or Mixograph or other torque recording mixer. In a recent work, Chin et al. (2005) found that the work input rate (i.e., total work input required to mix a dough for a period of 130 s) increased as the dough contained higher concentration of gas bubbles, providing evidence that gas bubbles may indeed influence the rheological properties of the dough. However, most dough mixing studies disregard the effect of dough aeration on dough rheology, typically assuming that mixing patterns predominantly reflect the interaction of the dough gluten proteins with the mixing blade (Bushuk, 1985; Bloksma & Bushuk, 1988; Hoseney & Finney, 1974). Part of the problem is that conventional laboratory mixers are not equipped for mixing dough at various headspace pressures or to specific energy inputs, which are important considerations to elucidate the contribution of gas bubbles to dough development.

Chin and Campbell (2005a) used a laboratory scale Tweedy–type chemical dough development mixer to study the effects of dough aeration during mixing on the mechanical properties of dough. Total work input, mixing speed, mixing headspace

pressure were all varied to study strong and weak doughs in terms of peak torque, end torque, total mixing time to peak torque and to end torque, total number of revolutions to peak torque and to end torque, and energy input at peak torque. Though the sensitivity of these mixing parameters to discriminate between strong and weak doughs was not always suitable, the ability of the mixer to apply a constant energy input (40 kJ kg^{-1}) and to work at high and low headspace pressures enables one to precisely discern the effects of bakery ingredients on dough aeration from those on dough gluten strength.

The literature suggests that measurements of dough development during mixing along with measurements of dough gas content during fermentation would be an interesting approach to better understand the effect of chemical leaveners on dough rheology. Hence, the objectives of this paper were two-fold (1) to characterize the development of dough with or without the addition of chemical leavening systems and mixed under various headspace pressures using a Tweedy-type mechanical dough development mixer and (2) to monitor and compare the density changes of chemically leavened dough with both Campbell's and Bellido's DDD techniques. Chemical leaveners included sodium bicarbonate and one of four leavening acids (sodium acid pyrophosphate, adipic acid, potassium acid tartrate or glucono-delta-lactone).

6.2. Materials and Methods

6.2.1. Dough formulation

The dough samples were prepared using the formulae listed in Table 6.1. Strong English flour was obtained from Nelstrop & Co (Stockport, UK). Formula ingredients (except the flour) were accurately weighed to the nearest 0.1 mg. The ingredient suppliers were Sigma Aldrich Co., St. Louis, MO, for sodium chloride; Sigma Aldrich Co., St.

Louis, MO, for sodium bicarbonate; Aldrich Chemical Company Inc., Milwaukee, WI, for SAPP 40; Solutia Inc. Gonzales, FL, for adipic acid; Aldrich Chemical Company Inc. Milwaukee, WI, for potassium acid tartrate; and Acatris, Oakville, ON, for GDL. The four chemical leavening systems were expected, based on previous studies, to produce leavening dough with a wide range of gas contents (5-67%). The level of water and salt in the dough samples were held constant and had been chosen, based on preliminary experimentation, so that the mixed doughs would have adequate handling properties.

6.2.2. Mixing protocol

Doughs were mixed at room temperature (25 ± 1 °C) under various mixing headspace pressures, high vacuum (-0.9 bar *or* 7.5 cm Hg), ambient (1 bar *or* 75 cm Hg) and over-pressure (2 bar *or* 150 cm Hg), using a Tweedy 1 mixer (Chin and Campbell, 2005a). The mixer was set to work at a constant speed of 55 rad s^{-1} and mixed the doughs to a constant total work input of 40 kJ per kg [of dough]. Because chemical leavening systems work best when they are added to the dough once the formula water has been absorbed by the flour (Holmes & Hoseney, 1987a; Chapter 5), the mixing operation was accomplished in two steps: the first step consisted in mixing all the formula ingredients except for the chemical leavener, and the second one involved mixing the dough with the chemical leavener. For dough mixed at atmospheric pressure the chemical leavener was added to the dough after the mixer applied to the dough a work input of 10 kJ per kg of dough. For doughs prepared under vacuum or at over-pressure the chemical leavener was added only after the mixer had applied a work input of 20 kJ kg^{-1} so as to facilitate achieving vacuum or over-pressure conditions in the mixer prior to the addition of chemical leaveners. A complete randomized design was used to evaluate the effects of

TABLE 6.1. Formulation[a] employed to prepare experimental dough samples

Ingredients[b]	Control	SAPP	ADA	KAT	GDL
Wheat flour	300 g	300 g	300 g	300 g	300 g
Water	60%	60%	60%	60%	60%
Sodium chloride	0.75%	0.75%	0.75%	0.75%	0.75%
Sodium bicarbonate	-	4.20%	1.40%	2.80%	4.20%
Sodium acid pyrophosphate 40	-	5.83%	-	-	-
Adipic acid	-	-	1.22%	-	-
Potassium acid tartrate	-	-	-	6.22%	-
Glucono-delta-lactone	-	-	-	-	9.33%

[a] Ingredient amounts expressed on percent flour basis (14% m.b.)
[b] SAPP, ADA, KAT and GDL denote doughs containing sodium bicarbonate and one leavening acid, sodium acid pyrophosphate 40, adipic acid, potassium acid tartrate and sodium bicarbonate glucono-delta-lactone, respectively, at a level specified by their neutralization value (NV –see Chapter 4 for more details).

mixing headspace pressure on the specific volume of chemically leavened wheat doughs.

Various parameters can be measured from each mixing curve generated by the Tweedy 1 mixer, including the instantaneous specific power (ISP) and total specific energy (TSE):

$$ISP = \frac{\text{torque x rotational speed}}{\text{dough mass}} \tag{6.1}$$

$$TSE = \int_0^{t_m} \text{ISP} \,.\, \mathrm{d}t \approx \sum_{i=1}^{n} (ISP)_i \,.\, \Delta t \tag{6.2}$$

where t_m is the total mixing time (s), Δt is 1 s and n is $t_m/\Delta t$. Prior to the start of dough mixing, the dough formulation is entered into the computer program running the mixer so that ISP and TSE are calculated per unit kg of dough.

6.2.3. Analysis of mixing curves

Figure 6.1 shows a recorded torque versus mixing time curve and other mixing parameters for a representative dough sample mixed in the Tweedy 1 mixer at

atmospheric headspace pressure. Following the method described by Chin and Campbell (2005a), the originally recorded torque versus time data was used to calculate the average torque trace using the 20-point moving average data analysis function of Microsoft Excel. The total number of mix blade revolutions needed to reach a total work input of 40 kJ per kg of dough was calculated by multiplying the average blade speed by the time required to reach such total work input. Error bars for mixing parameters derived from the mixing curves were based on replicate runs. Unless stated otherwise, analysis of the mixing curves was based on at least two replicate runs.

6.2.4. Density measurements

To measure the density of the experimental doughs dynamically, three sub-samples (~ 4 g each) were taken from each batch of dough using the procedures described below; one sample was used in Bellido's DDD system and the other two in Campbell's. For density measurement(s) using Bellido's system, one sub-sample (~ 4 g) was excised from the dough batch using sharp scissors. As described in the following paragraph, the preparation procedure for measuring DDD in Campbell's system requires dough to be dusted with flour. Preliminary experiments (results not shown) indicated that flour dusting to some extent restricted the expansion of the fermenting dough in Bellido's system. Hence, the flour-dusting step was omitted for DDD using Bellido's system. Following sample excision from the dough, the sub-sample was gently squashed between two 3-cm think acrylic plates and placed underneath a digital camera that took photographs of the expanding dough piece as a function of fermentation time. Details on the methods and experimental techniques to measure DDD using Bellido's system can be found elsewhere (Chapter 5), bearing in mind that density is the reciprocal of specific

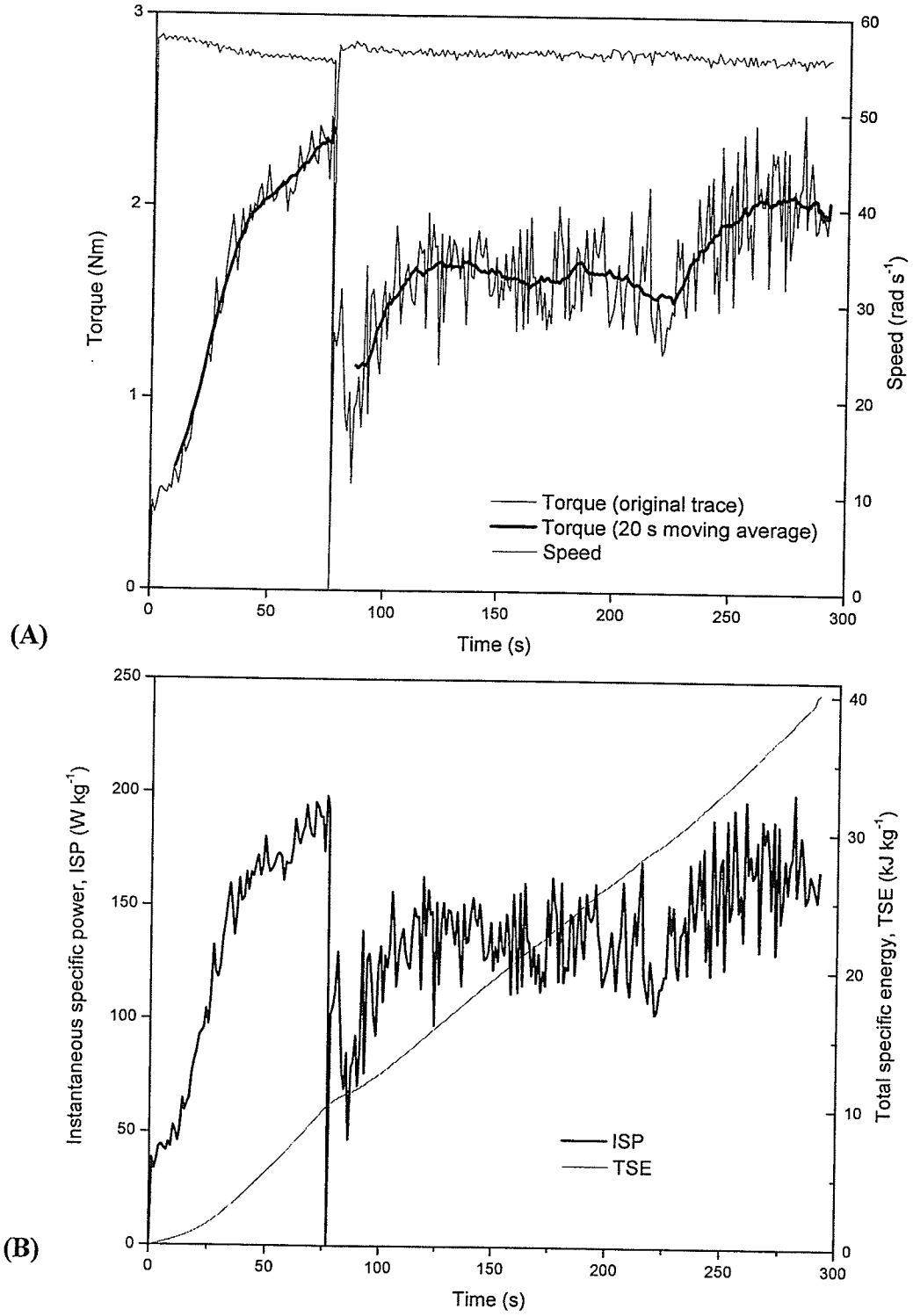

Figure 6.1. Representative Tweedy 1 mixing curves showing some commonly measured parameters: (A) torque and speed, and (B) ISP and TSE; illustrated here for strong (English) flour dough mixed at atmospheric pressure (1 bar) and formulated with SAPP.

volume. The first density measurement was taken about 4 min after the end of dough mixing. All density measurements were conducted at room temperature (25 ± 1 °C).

For density measurement using Campbell's DDD system, the dough batch sub-samples (2) were taken using the following procedure. Firstly, the dough was sparingly dusted with flour and placed on a flat, clean tabletop that was also dusted with flour. Secondly, the dough was gently flattened to a constant height of about 1.3 cm using a smooth acrylic roll (length ~ 20 cm; diameter ~ 4 cm) and two parallel guides (1.3 x 1.3 x 20.5 cm) that were set apart by about 10 cm from one another. Lastly, two sub-samples were cut out of the dough by pressing a metal die (~ 2 cm dia.) into the dough. Each sub-sample was then carefully placed in a lightly flour-dusted volumetric flask (500 ml). In the last sample preparation step, the shape of each sub-sample was transformed into a seamless sphere by swirling each sub-sample (~ 15 sec) around the inner wall of the volumetric flask, after which the sub-samples were loaded into Campbell's DDD system. In this system, a double cup metal structure affixed to an accurate (4 d.p.) balance is suspended in a water-jacketed beaker with xylene so that the upper cup is in the air and the bottom cup is immersed in xylene. The bottom cup has an antifloat cap (an inverted cup) that ensures that dough with density lower than that of the xylene remains immersed in the xylene. The temperature of the xylene is maintained constant by circulating water at controlled temperature through the jacketed beaker. The first step in measuring dough density dynamically is to weigh the dough sub-sample in the upper cup (i.e., weight in air) and then place the sub-sample in the bottom cup (i.e., weight in xylene). Because the weight of the dough is monitored by an accurate (4 d.p.) balance, changes in the weight of the dough immersed in xylene can be used to monitor the volumetric expansion of the

dough (thus dough density changes) via Archimedes principle. The weight of the sample is recorded every 10 seconds by a data acquisition system that is connected to Campbell's DDD system. Further details on Campbell's DDD system can be found in Campbell et al. (2001). The first density measurement occurred about 120 seconds after the end of mixing. As with density measurements using Bellido's DDD system, density changes were monitored in real time at a constant temperature of 25 ± 1 °C. However, once it was observed that the chemical leavening system stopped producing CO_2 leavening gas (i.e., once the dough density ceased to drop with fermentation time), Campbell's DDD system's temperature was raised to more than 60 °C to study the influence of fermentation temperature on the aeration of chemically leavened dough. All density measurements using Bellido's DDD technique were made at 25 ± 1 °C.

6.3. Results and Discussion

6.3.1. Problems in defining a mixing parameter to evaluate dough consistency

Figure 6.1 shows a typical recorded torque versus mixing time curve for dough formulated with a chemical leavening system. The mixing curve is comprised of two regions: the first region corresponds to the torque exerted by the dough with no added chemical leavening system; and the second one to the torque exerted by the dough after the dough had been combined with the chemical leavening agent (i.e., sodium bicarbonate and the leavening acid). The interruption in the mixing curve (i.e. the end of the first region) marks the moment at which the energy input was 10 kJ or 20 kJ per kg of dough (depending on the headspace pressure, see above). The end of the second region corresponds to a total energy input of 40 kJ per kg of dough. Since the height of the mixing curve reflects the resistance of dough to mixing, which is often regarded as an

index of dough consistency (Hlynka & Anderson, 1955, Bloksma & Bushuk, 1988), a drop in dough resistance upon resumption of dough mixing (i.e., after the chemical leavener was added) can be interpreted as the influence of chemical leaveners on dough consistency. However, the interruption in the mixing curve occurred after the dough was mixed to different energy inputs (10 and 20 kJ kg^{-1} for doughs mixed at atmospheric pressure and above/below atmospheric pressure, respectively; Figures 1-5 of Appendix V), which precluded unambiguous comparisons of changes in dough consistencies among the experimental doughs arising from the addition of the chemical leaveners or changes in mixing pressure.

Another difficulty was that a peak value in the Tweedy 1 mixing curves could not be clearly identified because of the interruption that had to be made during mixing to incorporate the chemical leavening ingredient. The peak value in the Tweedy 1 mixing curve was used by Chin and Campbell (2005a) to obtain information on the mixing properties of doughs made from flours of different strength, though these authors warned that a peak value in the Tweedy 1 mixing curve needed to be interpreted with care. As a caveat to the present discussion of the mixing curves generated by the Tweedy 1 mixer, it needs to be recognized that the peak resistance to mixing in the Tweedy 1 mixer does not necessarily correlate to the peak resistance to mixing measured in conventional mixing systems such as the Mixograph, where the peak resistance to mixing represents "the point to which a dough should be mixed for producing an [optimum] loaf of bread" (Hoseney, 1985). Instead, following mechanical dough development guidelines set by the Chorleywood Bread process (Chin & Campbell, 2005a), in England (and other Commonwealth countries) a dough is mixed in a high speed mixer (e.g., Tweedy 1) until

it has received a total energy input of 40 kJ per kg of dough. Achieving this optimum energy input would not necessarily occur at the peak torque value in the Tweedy 1 mixing curve (Chin & Campbell, 2005a). This is shown in Figure 1 of Appendix V for the control dough where the peak torque in the Tweedy 1 mixing curve (~ 60 s into mixing) did not correspond to the optimum total energy input of 40 kJ kg^{-1} which was reached at the end of mixing (~ 190 s).

An alternative means for making meaningful comparisons of the effects of chemical leaveners and mixing pressure on dough consistency was found in another mixing parameter obtainable from the Tweedy 1 mixer, the number of revolutions required to achieve a total energy input of 40 kJ kg^{-1} (11 Wh kg^{-1}).

6.3.2. Dough development during mixing: total number of revolutions to 40 kJ kg^{-1}

The total number of revolutions needed to reach a total energy input of 40 kJ per kg dough (TNR to 40 kJ kg^{-1}) is regarded as an unambiguous dough development parameter (Chin & Campbell, 2005a) that will be used to compare the strength of dough with or without added chemical leavening systems. Figure 6.2 summarizes graphically the total number of revolutions to 40 kJ kg^{-1} for dough mixed with one of the four experimental chemical leavening systems (SAPP, ADA, KAT or GDL) and under three mixing headspace pressures (7.5, 75 and 150 cm Hg). Because the error bars were of comparable size to the size of the symbols used to construct Figure 6.2, error bars have been omitted for the sake of clarity. Regardless of the mixing pressure, addition of a chemical leavener increased the TNR to 40 kJ kg^{-1} compared to the control dough. Because the mixing speed in this experiment was set constant at 55 rad s^{-1}, the total number of revolutions was directly proportional to the mixing time taken to achieve 40

kJ kg^{-1} (TNR = mixing time [s] x speed [rad s^{-1}] x $1/2\pi$). Weaker doughs are expected to offer less resistance to the mixing action and so they should take longer times to reach a given energy input than a stronger dough would. Hence, based on the total number of revolutions to end torque results summarized in Figure 6.2, the strength of the experimental doughs could be ranked as follows (in decreasing order): ADA > KAT ~ GDL > SAPP. This rank was applicable to doughs mixed under vacuum and under atmospheric pressure, but when they were mixed under a pressure of 2 bars (over-pressure), the rank changed, with ADA becoming weaker than KAT/GDL (i.e., dough strength ranking was as follows KAT ~ GDL > ADA > SAPP). Figure 6.2 shows that raising the headspace mixing pressure from a high vacuum to one atmosphere strengthened the consistency of the doughs (it decreased the number of revolutions to [and the mixing time taken to] reach 40 kJ kg^{-1}), which was anticipated since higher mixing pressures are expected to increase the concentration of bubbles in dough (Campbell et al., 1998), which, in turn, is expected to increase dough strength (Chin et al., 2005). Also, increasing headspace pressure during mixing should increase the availability of oxygen in the dough which is expected to increase dough strength by promoting oxidation processes (Bloksma, 1990b; Marston, 1986; Chin & Campbell, 2005a; Elmehdi et al., 2004). However, when the mixing pressure was raised from 1 to 2 atmospheres, the consistency of dough to which a chemical leavening system had been added decreased (increased number of revolutions to [or mixing time to] reach 40 kJ kg^{-1}), though dough strength for the control did increase. Clearly, the presence of chemical leavening systems in the dough affected dough development in ways that could not be predicted solely in terms of increased oxygen availability and increased bubble

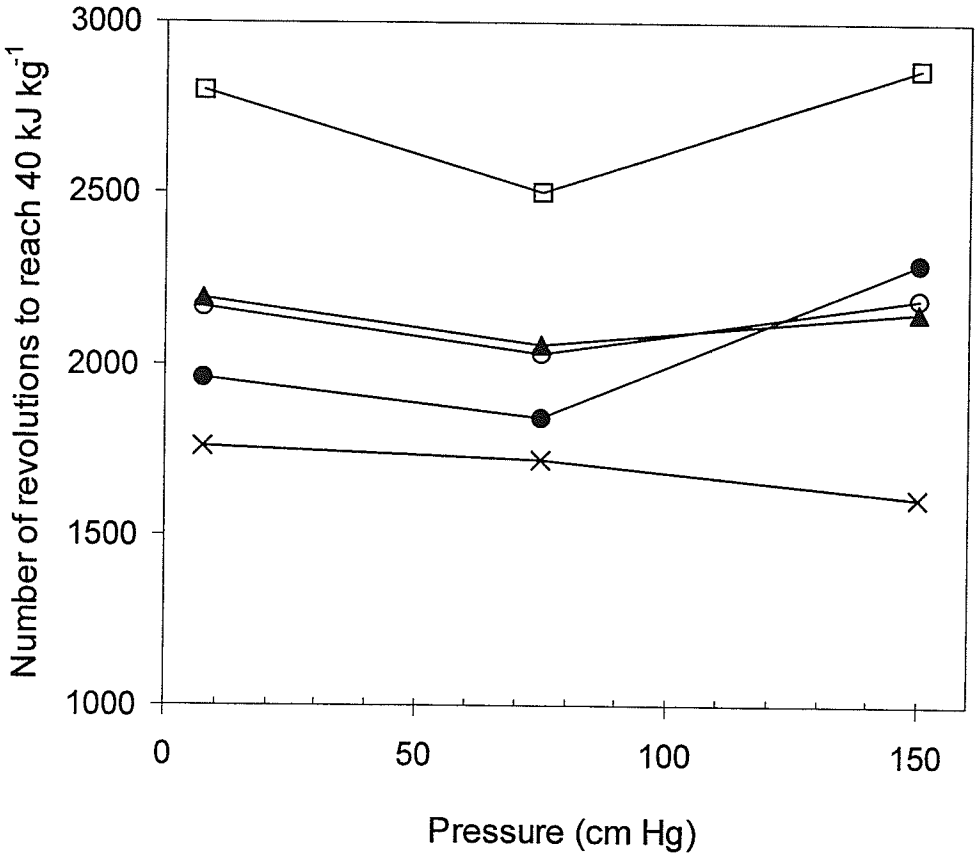

Figure 6.2. Total number of revolutions to reach a total work input of 40 kJ per kg dough for dough mixed under various mixing headspace pressures and formulated with SAPP (squares), ADA (closed circles), KAT (open circles), GDL (triangles), and with no leavener (Xs). Error bars (n=2) were of comparable size to the size of the symbols and so they were omitted for the sake of clarity.

numbers due to a rise in headspace pressure, as, for example, chemical leavening systems are capable of contributing to the nucleation of gas during mixing as they can evolve carbon dioxide virtually immediately after they come into contact with the water formula (Chapter 4; Heidolph, 1996). Development of dough during mixing has been explained in terms of achieving alignment of glutenin molecules, which would lead to a large number of noncovalent interactions (Bloksma, 1990b). This desirable parallel alignment of the glutenin molecules can be affected by the presence of the chemical leaveners, though the mode of action by which they do so still needs to be more clearly elucidated (Heidolph, 1996). Regardless of whether the effect of chemical leaveners on the dough protein matrix arises from the pH lowering effects of organic acidulants (GDL and ADA) (Heidolph, 1996; Cepeda et al., 2000; Galal et al., 1978) or the lyotropic properties of non-chaotropic anionic salts (KAT and SAPP) (Preston, 1981, 1984, 1989; Holmes & Hoseney 1987a; Kinsella & Hale, 1984; He et al., 1992; Wellner et al., 2003), it is evident that aeration of the dough during mixing also affected the development of dough (Figure 6.2). One way of determining the contribution of a chemical leavening system to the degree of aeration of the dough during mixing is *via* measurements of dough density immediately after the end of mixing (Chin et al., 2005). Measurements of the degree of aeration of unyeasted dough during and immediately after mixing *via* density measurements has long been used as a valuable means for gaining an insight into dough development (Baker & Mize, 1941, Chin & Campbell, 2005b; Chin et al, 2005); however, this is impractical when using dough that contains an evolving leavening gas. Therefore, the density of dough was measured dynamically (DDD) immediately after mixing using two DDD measuring systems, Campbell's and Bellido's, and the

experimental results compared and discussed in light of the mixing data obtained from the Tweedy 1 mixer.

6.3.3. Effect of chemical leaveners on dough density for doughs mixed at atmospheric pressure

Figure 6.3 shows the density changes captured by Campbell's technique for dough chemically leavened with SAPP, ADA, KAT and GDL. Density measurements were not averaged to illustrate the variability of the technique in the various experimental treatments (e.g., chemical leavener type). Each of the graphs shown in Figure 6.3 was constructed using four measurements, obtained from two replicate runs. The CV for density measurements using Campbell's technique varied depended on the type of chemical leavening system, SAPP (<1.6%), ADA (<1.4%), KAT (<4.7%) and GDL (2-13%). The CV for density measurements of doughs mixed from strong and weak flours (no yeast added) at various pressures using Campbell's DDD technique is typically better than 0.5% (Campbell et al., 2001). Figure 6.3 shows the temperature of the dough on the right-hand Y-axis because dough temperature was increased when isothermal dough expansion had finished. The influence of temperature on dough density is discussed later. Figure 6.4 shows the density changes measured using Bellido's DDD system for dough that was chemically leavened with SAPP, ADA, KAT, and GDL. Figure 6.4 shows single density measurements as well as representative standard deviations. As with Campbell's system, the CV for the density measurements made by Bellido's system varied depending on the type of chemical leavening system employed: SAPP < 2.0%; ADA < 4.5; KAT < 4.4%; and GDL < 8.2%. The precision error of Bellido's DDD technique was determined in a separate experiment by measuring densities of dough sub-samples (n=6) from the

same batch of dough without a leavener (100 g CWRS #1 flour + 67.4 g water + 0.75 g NaCl). The weight of dough samples was determined using a precise balance (4 d.p.). The standard deviation for a given dough density measurement (e.g., 1.070 g cm^{-3}) was found to be 0.002 g cm^{-3} and the standard error 0.001 g cm^{-3} ($SD/\sqrt{n}$). Because the instrumentation variability (error) associated with density measurements using either Bellido's or Campbell's DDD system is better that 0.5%, variability greater than 0.5% arises from the intrinsic variability of the dough sample (sample reproducibility). Hence, Figures 6.3 and 6.4 show that sample reproducibility was the greatest source of variability for density measurements, with SAPP being the most reproducible system and the highly aerated GDL the least reproducible.

Interestingly, Figures 6.3 and 6.4 show that during the first minutes of fermentation, the density of the experimental leavening systems dropped rapidly, a finding that is consistent with the view that carbon dioxide evolution starts as soon as the acidulant comes into contact with sodium bicarbonate (Heidolph, 1996, Chapter 4). Chemical leavening systems, unlike yeasted dough, do not require an adaptation period to start evolving CO_2 (Heidolph, 1996), highlighting an important difference between yeast and chemical leavening: that CO_2 evolution in dough containing chemical leaveners can occur as early as during mixing. Previous reports on ex-mixer density changes of yeast dough show that CO_2 evolution does not appear to start during mixing. For instance, Campbell et al. (2001) and Elmehdi et al. (2003a) reported that yeasted dough's density changes little, if at all, during the first few minutes of fermentation (post mixing). This lag period extended past 200 s after the end of mixing in yeasted dough fermented at 27°C, as detected by Campbell's DDD (Campbell et al., 2001), or past 300 s for yeasted

(A)

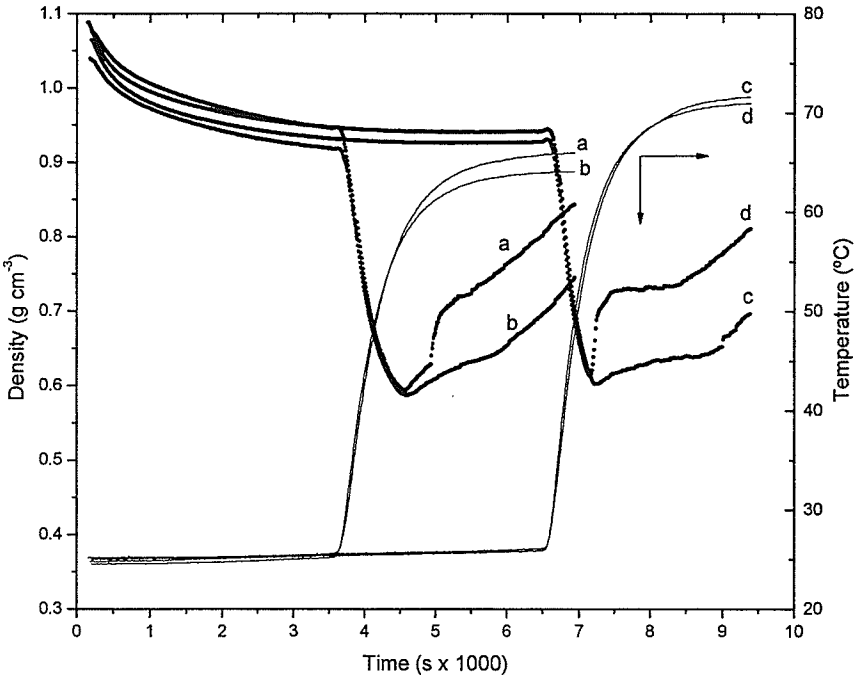
Density (g cm^{-3})
Temperature (°C)
Time (s x 1000)
a
b
c
d

(B)

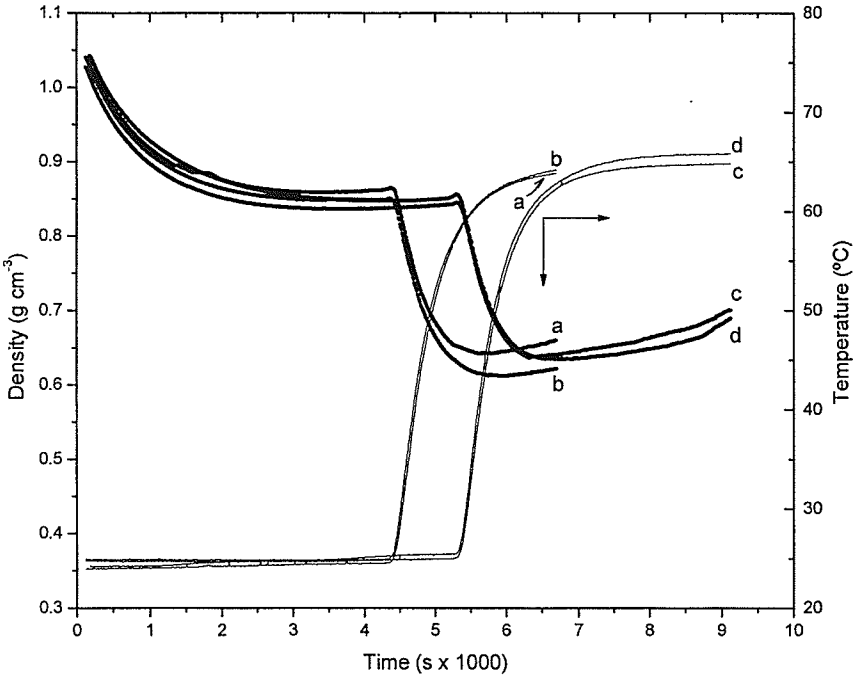
Density (g cm^{-3})
Temperature (°C)
Time (s x 1000)
a
b
c
d

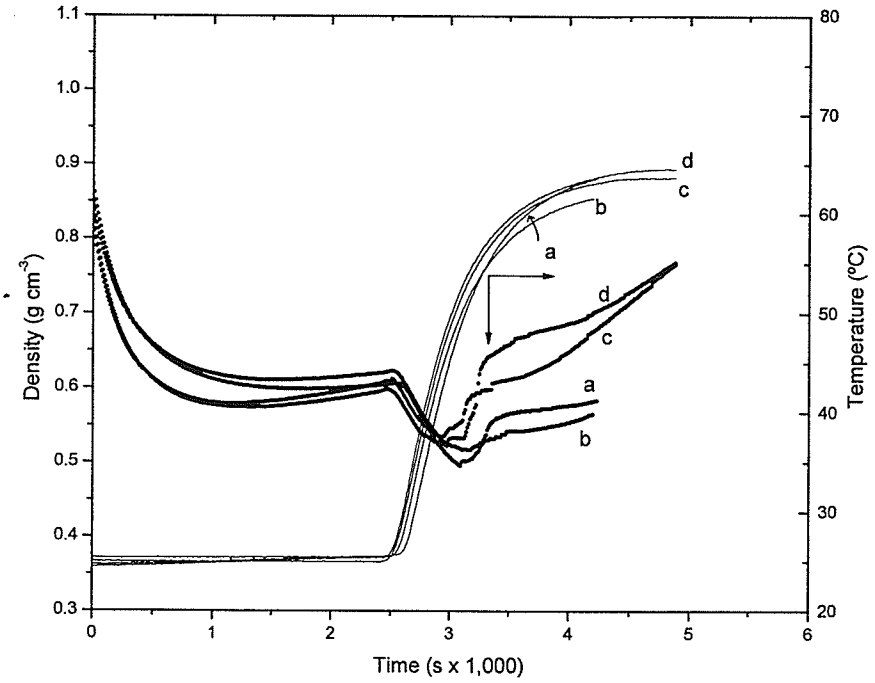

(C)

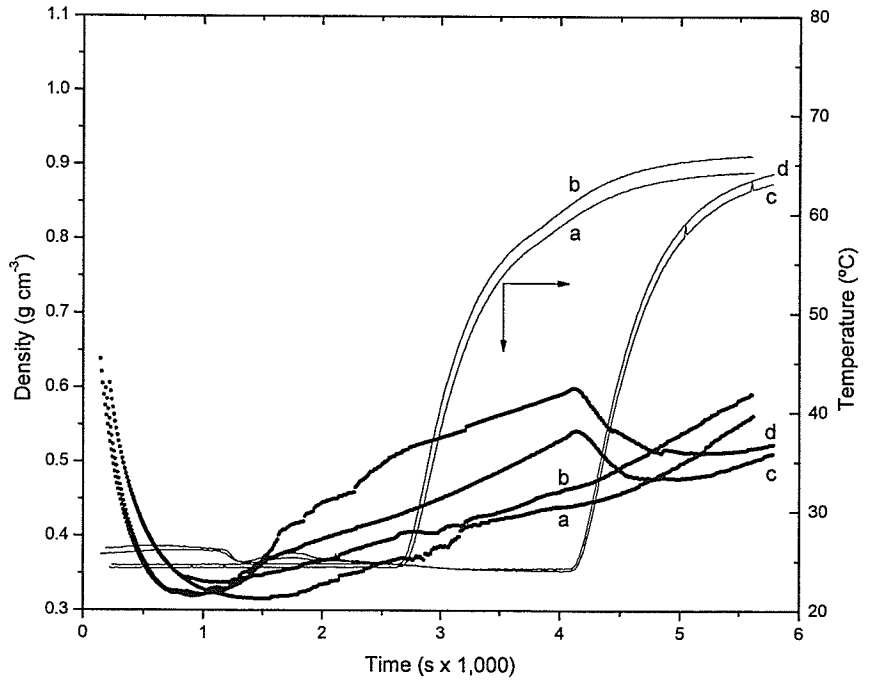

(D)

Figure 6.3. Density changes detected by Campbell's DDD for chemically leavening dough mixed at atmospheric pressure (1 bar) and formulated with (A) SAPP, (B) ADA, (C) KAT or (D) GDL, and whose temperature was initially kept constant (25±1 °C) and then rapidly ramped up to more than 60 °C. Matching curves have matching lower-case letters.

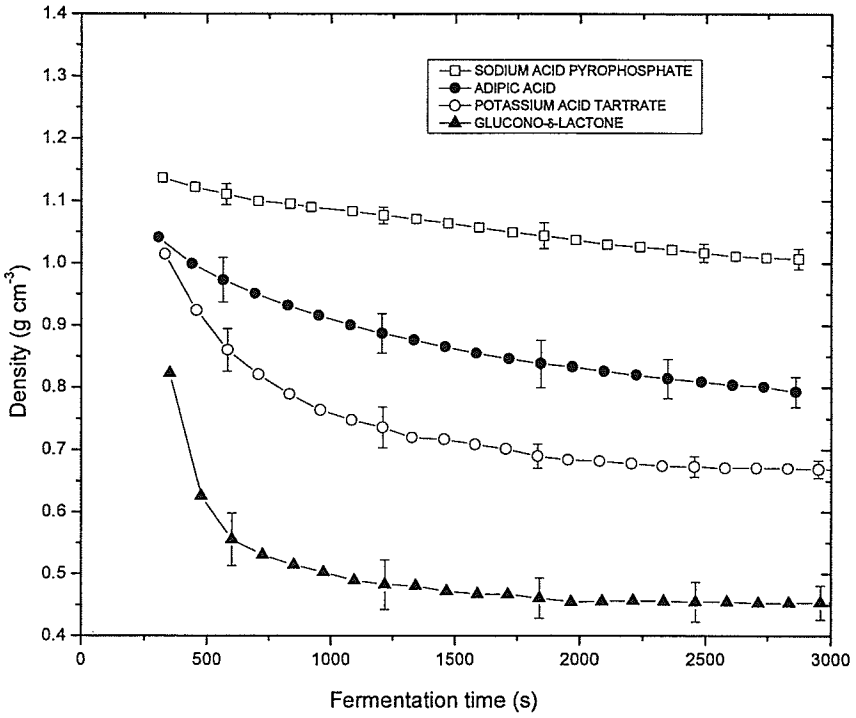

Figure 6.4. Density changes detected by Bellido's DDD system in chemically leavened dough that had been mixed at atmospheric pressure. Vertical bars represent typical SD.

dough fermented at 37 °C, based on Elmehdi's DDD technique (Elmehdi et al., 2003a). The initial lag period spanned even farther when dough is under a vacuum (Elmehdi et al., 2003a) or made with smaller amounts of yeast (Scanlon et al., 2002). Elmehdi et al. (2003a) explained that the lag in density variation following mixing of yeasted dough results from both the time taken by yeast to multiply and break down fermentable sugars (adaptation period) and the time taken by CO_2 to diffuse into the gas bubbles for expansion (length of the diffusion path).

Figures 6.3 and 6.4 show that the rate of growth of the dough piece (drop in density) over fermentation time depended on the type of chemical leavener used, with dough containing GDL experiencing the fastest growth with time, followed by KAT, ADA and, lastly, SAPP. Although Campbell's system generally detected a higher initial density than Bellido's system for the same experimental dough (1.14 and 1.06 g cm^{-3} (SAPP); 1.04 and 1.04 g cm^{-3} (ADA); 1.01 and 0.90 g cm^{-3} (KAT); 0.82 and 0.63 g cm^{-3} (GDL), respectively), the measurements did not start simultaneously. Density measurements using Campbell's and Bellido's DDD systems started about 2 min and 6 min, respectively, from the end of mixing. It is worth noting that the range of densities covered by Campbell's DDD system encompassed the range detected by Bellido's DDD system. Even though the first density measurement obtained from these two DDD systems could not be directly compared because of the differences in time in acquiring the data, density measurements at equivalent fermentation times were expected to provide a useful means of comparing the degree of aeration experienced by dough from the same mixing batch that was chemically leavened in the two different DDD systems.

6.3.4. Comparison of Bellido's and Campbell's DDD technique

Figure 6.5 shows a comparison of the two techniques wherein the change in dough density (relative to the gas-free dough density – see next section for ρ_{gf} calculations) captured by Campbell's DDD technique is plotted against the change in dough density that was registered by Bellido's DDD technique. Each data point was taken at exactly the same time after the end of mixing. Using this strategy, Figure 6.5 eliminated the effect of having taken the first density measurement at slightly different times, so it does provide an unequivocal means of comparing the performance of the two DDD techniques. The line $y = x$ in Figure 6.5 represents an ideal one-to-one correspondence for when the relative dough density change detected by one technique is identical to the other.

Figure 6.5 suggests that differences in density changes detected by the two DDD systems became larger at increasing dough gas contents. For instance, for ADA dough the ratio of density changes detected by the two techniques were comparable with one another and, hence, data points closely followed the line y = x (i.e., ratio ~ 1). For dough with GDL, the density changes detected by the two techniques towards the end of fermentation were so far off from each other that their ratio took a value that tended to infinity. Unlike Bellido's technique, Campbell's technique detected an inflexion point in density in GDL dough which can be interpreted as the onset of greater CO_2 losses than CO_2 generation. This inflexion point in dough density occurred at a later time in KAT dough relative to GDL dough and was not detected at all in ADA or SAPP doughs. Conversely, Bellido's technique did not register the inflexion point for any of the

leavening systems studied, as can be seen by the steady descent of the density versus time curves of Figure 6.4.

Results indicate that when a chemically leavened dough specimen, for example, containing GDL, is placed in Campbell's system the specimen holds the internal gas for only about 17 min but when placed in Bellido's technique it holds the internal gas for more than 50 min. Similarly, dough containing KAT held the internal gas for about 30 min and for more than 50 min when placed in Campbell's and Bellido's DDD systems, respectively. The discrepancies shown in Figure 6.5 have their basis in the fact that the growth of the dough specimen during DDD testing depends on both the sample preparation procedure and the physical environment in which the dough was allowed to

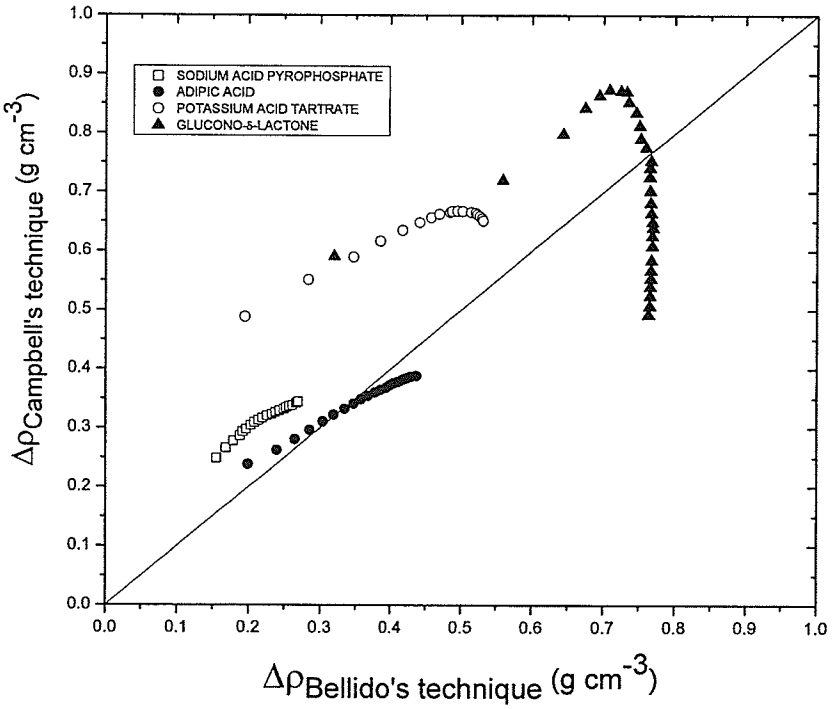

Figure 6.5. Comparison of density changes detected by a photography-based DDD technique and Campbell's DDD technique for dough that was formulated with one of four chemical leavening systems and mixed at atmospheric pressure.

expand (i.e., constraints of the sample holder in Bellido's technique and the presence of a liquid surrounding the dough specimen in Campbell's technique).

In Bellido's technique, because the sample is squashed between two acrylic plates, the growth of dough is biaxial and limited to the radial direction along the plane of the acrylic plates. It is possible that frictional forces between the dough sample and the acrylic plates are sufficiently large that the growth of the dough is curtailed relative to the expansion that occurs in an environment where frictional forces can be ignored (i.e., in Campbell's system). Another way in which frictional forces could influence dough density is by masking the onset of gas losses during the later stages of leavening. If frictional forces are large enough at this stage, then it is possible that gas escaping from the dough due to, for example, collapsed cell walls (e.g., coalescence) would end up being trapped between the acrylic plates and the dough which would prevent the shrinkage of the dough specimen when cells coalesce (Weegels et al., 2003). To determine the extent to which frictional forces between the dough and the acrylic plates affected dough expansion, an experiment was conducted whereby mineral oil was added to the surface of the acrylic plates in contact with the dough specimen (Figure 6.6).

Figure 6.6 shows that though the use of oil restricted dough expansion to some extent, the interaction between the dough and the acrylic plate did not influence either the initial or the final density measurements of Bellido's DDD system. As with chemically leavened dough (Figure 6.4), yeasted dough did not exhibit an increase in dough density (i.e., no CO_2 gas losses) during fermentation under either condition. Similarly, the use of dusting flour on the dough specimen, a requirement for testing samples in Campbell's DDD system, was not used when testing specimens in Bellido's systems as it was

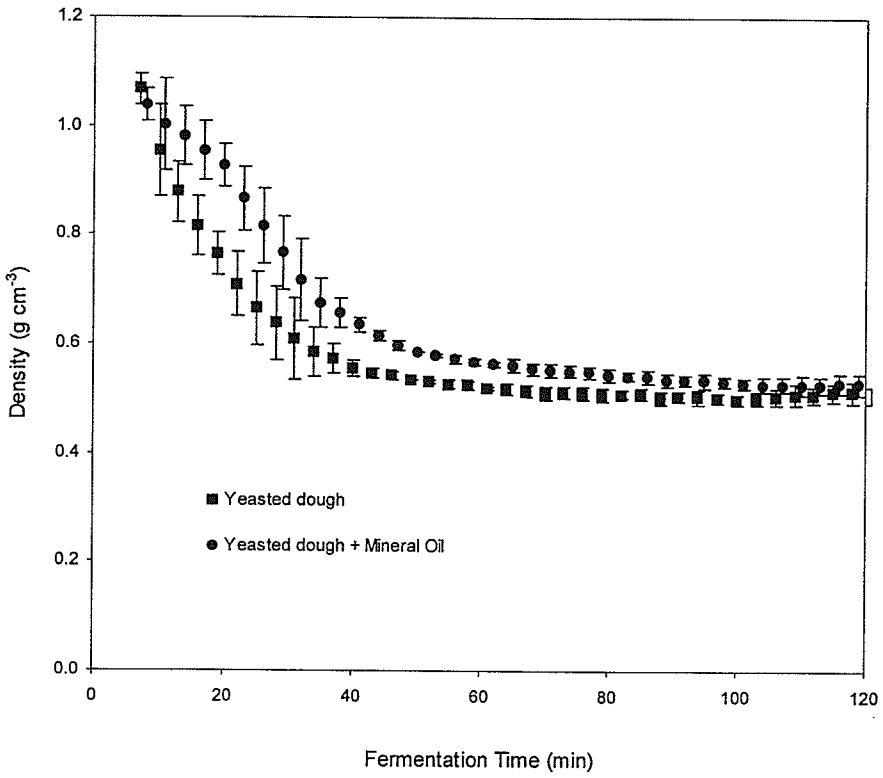

Figure 6.6. Effect of adding mineral oil to the surface of the acrylic blocks in contact with the dough specimen on the dough densities measured by Bellido's DDD technique. Dough [100 g CWRS #1 flour, 1.50 g NaCl, 3 g commercial dry yeast and 71.6 g water] was mixed in a GRL 200 mixer (Hlynka and Anderson, 1955) and fermented at 33 ± 1 °C. Error bars represent SD (*n =3*).

observed (results not shown) that the growth of the dough was also somewhat restricted (less than with the oil though). On the other hand, careful examination of the *modus operandi* of Campbell's DDD system indicates that a possible explanation for the increase in dough density (i.e., CO_2 losses) was that the xylene (immersion fluid) migrated into the internal dough structure. This would occur if the outer side of the dough becomes open to the exterior (xylene) due to the bursting of gas bubbles (Weegels et al., 2003) or due to the transformation of dough from a foam into a sponge (Bloksma, 1990a, 1990b; Zghal & Scanlon, 2001; Babin et al., 2005, 2006; 2007). Another mechanism which does not depend on opening of the dough structure is the movement of xylene into the dough by first dissolving into the dough matrix and then into internal bubbles. However, since a previous study has shown that the dissolution of dough constituents in xylene during fermentation is insignificant (Campbell et al., 2001), movement of xylene by dissolution into the dough matrix is improbable and therefore it will not be discussed further. To determine which of the other two mechanisms, if any, was responsible for the onset of early CO_2 loss, the gas void fraction of the dough was manipulated by mixer headspace pressure variation.

6.3.5. Effect of mixing headspace pressure and temperature on the void fraction of gas in dough

The void fraction, or volume fraction, of gas in a dough (ϕ) can be calculated from knowledge of the dough density (ρ), and the gas-free dough density (the matrix density) (ρ_m), as follows:

$$\phi = 1 - \frac{\rho}{\rho_m} \tag{6.3}$$

Plotting the density of the dough (measured from Campbell's DDD technique) as a function of the mixing headspace pressure (Figure 6.7) and extrapolating the density back to zero pressure (absolute vacuum) is a practical strategy to calculate ρ_m (Campbell et al., 1991, 1993, 1998, 2001; Elmehdi et al., 2003a; Mehta, 2007). These studies have proven the excellent linearity of the relationship between dough density and mixing pressure. Hence, measuring the density of dough mixed at two different pressures is sufficient to determine ρ_m, though the error is significantly reduced when the pressure includes a high vacuum and a large overpressure. Though the density of dough mixed at atmospheric pressure was also measured, the dough sample was prepared using a slightly different mixing protocol than dough mixed at vacuum or at overpressure (see materials and methods). Therefore, the data for dough mixed at atmospheric pressure was not used for the calculation of ρ_m. The density data for dough mixed at atmospheric pressure is shown for reference in Figure 6.7. Accordingly, using the densities corresponding to dough mixed under high vacuum (0.15 cm Hg) and at high overpressure (150 cm Hg) and a linear extrapolation of these data back to zero pressure, the gas-free dough densities (± 1 SD) were calculated to be: 1.295 ± 0.021, 1.240 ± 0.012, 1.231 ± 0.027 and 1.143 ± 0.012 g cm^{-3}, for SAPP, ADA, KAT and GDL, respectively.

Figure 6.8 shows the gas void fraction as a function of fermentation time for chemically leavened dough mixed under various headspace pressures. At the onset of fermentation (i.e., immediately after mixing) the void fraction of dough mixed under high vacuum was very low, 1.2%, 0.9%, 1.9%, 0.6% for SAPP, ADA, KAT and GDL, respectively, which is in agreement with the widely accepted view that the void fraction of dough decreases with the headspace pressure in the mixer (Baker and Mize, 1941),

despite the fact that some of these leavening systems are rapidly producing carbon dioxide. When the mixing headspace pressure was raised to 1 atmosphere (relative to vacuum mixing), the void fraction of the doughs was substantially increased to 18% (SAPP), 17% (ADA), 32% (KAT), and 52% (GDL) as shown in Figure 6.8B. When the headspace pressure was further increased to 2 atmospheres, the initial void fraction of dough also increased (19%, 24%, 38%, and 44%, respectively). Similarly, for a given dough, the final void fraction that was achieved at the end of fermentation increased with mixing pressure, though not in a linear fashion (Figure 6.8). The absence of a 1 to 1

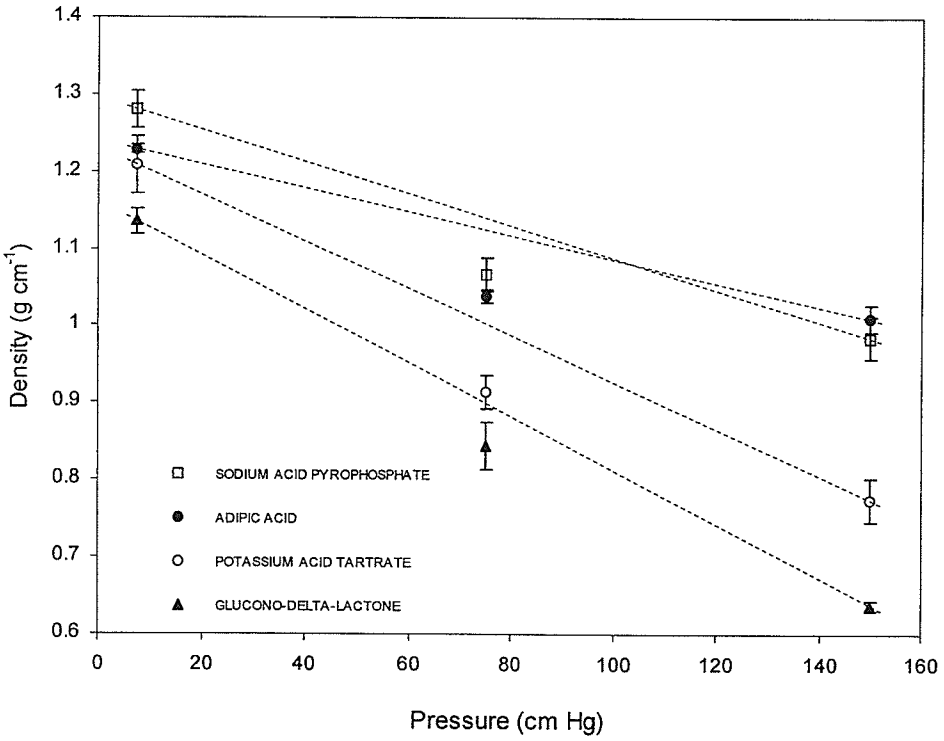

Figure 6.7. Density of chemically leavening dough as a function of mixer headspace pressure. Density measurements made immediately (~ 2 min) following the end of mixing using Campbell's DDD system. Error bars represent the standard deviation. Dashed lines represent best linear fits to the data corresponding to dough mixed under vacuum and at over-pressure. (i.e., not including density for dough mixed at atmospheric pressure).

relationship between the mixing headspace pressure and initial void fraction suggested that the influence of chemical leavening systems on the aeration of dough during mixing and during fermentation was not straightforward though it was evidently dependent on the mixing pressure. Identification of the mechanisms responsible for the observed effects of chemical leavening systems and mixing pressure on (1) the aeration of dough during mixing, and (2) the gas retention capacity of dough during fermentation, are expected to provide an insight into the effect of chemical leaveners on dough rheology during mixing.

With regard to the effect of chemical leavening systems and mixing pressure on dough aeration at mixing, one must note that the chemical industry regards chemical leavening systems such as ADA, KAT and GDL as "nucleating agents" (Heidolph, 1996). These nucleating agents "quickly give up protons that react with sodium bicarbonate and evolve CO_2 during mixing" and so they "play a key role in determining the crumb structure and appearance [of bread or other baked goods] by providing gas cell nuclei [during mixing]" (Heidolph, 1996). The so-called nucleating agents are therefore able to 'aid' in the creation of gas nuclei (i.e., gas number density) during the mixing step (Heidolph, 1996). If Heidolph's hypothesis is true then the density of the dough matrix, ρ_m, obtained from the extrapolation of the density data to zero pressure (Figure 6.7) should be higher for ADA, KAT and GDL. X-ray microtomography studies of doughs containing reacted chemical leavening systems showed that the density of the matrix of ADA, KAT and GDL was 1.21, 1.24, and 1.26 g cm^{-3} (Appendix 5.1), values that are in agreement (arguably except for GDL) with those found in the present study: 1.24, 1.23, and 1.14 g cm^{-3}, respectively. Therefore, the experimental data suggests that the 'nucleating agents' actually contribute to the aeration of dough during mixing not by

A

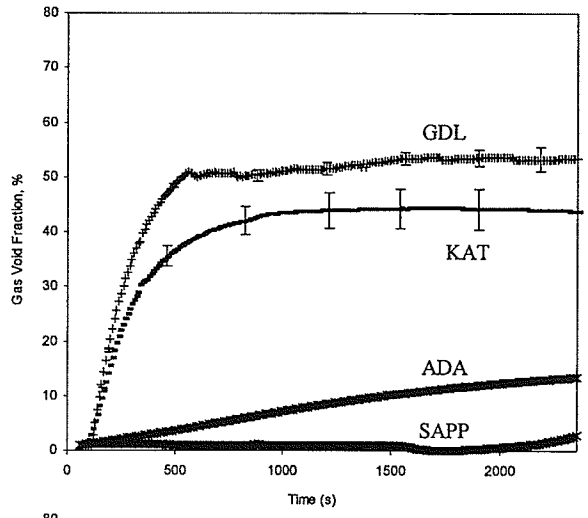

B

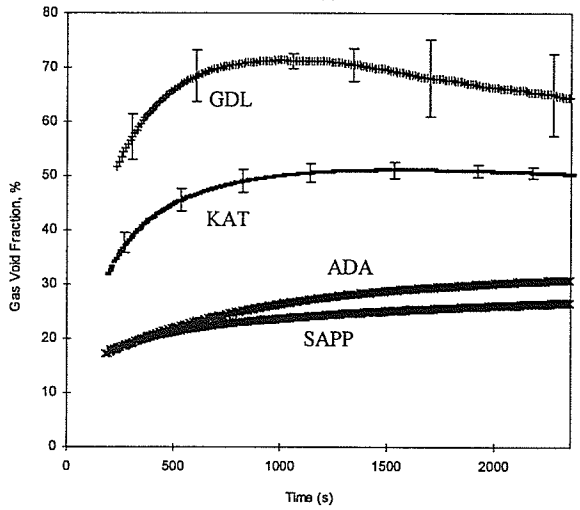

C

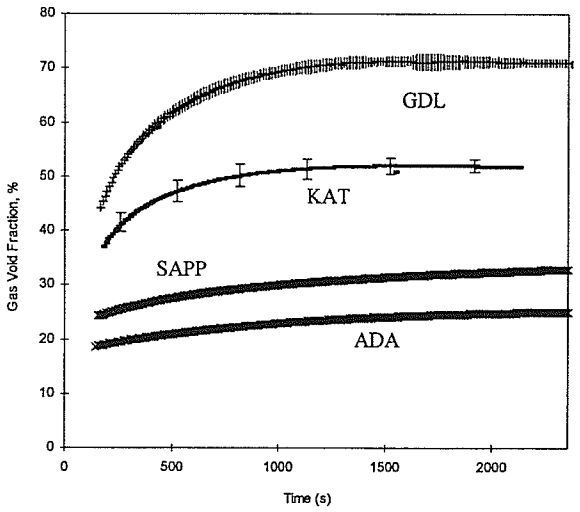

Figure 6.8. The gas void fraction of chemically leavened dough mixed under vacuum (A), at atmospheric pressure (B) and at 2 atmospheres (C). Based on dough density data obtained from Campbell's DDD system. Error bars represent SD.

nucleating gas bubbles but rather by expanding the gas bubble nuclei that had been entrained by the mechanical action of the mixer. It is important to note that the discrepancy found between the ρ_m of GDL dough obtained from density measurements (Figure 6.7) and that obtained from x-ray microtomography suggests that, surprisingly, the bubbles entrained in GDL doughs may have undergone expansion during the mixing stage, even when the doughs were mixed at the lowest headspace pressures (i.e., even when very few gas cell nuclei are expected to be present in the dough; Campbell et al., 1998). While the apparent growth of the gas cell nuclei during mixing of GDL could be simply explained in terms of the rate of CO_2 production associated with this leavener (i.e., a high rate of CO_2 production), independent measurements of gas production demonstrated that this hypothesis was not true. Data on gas production rates (Figure 4.2 in Chapter 4) showed that at 27 °C the rates of CO_2 production from GDL doughs were not higher than those of say KAT doughs. Hence, the growth of the gas cell nuclei during mixing of GDL doughs appears to be related to the superior ability of CO_2 to diffuse through the GDL dough matrix to the gas bubble nuclei compared to that in the other systems (e.g., KAT doughs). Support for this view is found in Chapter 5 of this thesis where the diffusivity coefficient of carbon dioxide in dough was estimated to be the highest in GDL dough compared to that in SAPP, ADA and KAT doughs. Hence, a possible mechanism explaining the mixing pressure dependence of chemical leavening systems in aerating dough is related to the time taken by the dissolved CO_2 species to diffuse through the dough matrix to the gas cell nuclei (Scanlon et al., 2002).

Scanlon et al. (2002) proposed that for CO_2 to increase the void fraction of yeasted dough after the end of mixing, CO_2 first needs to diffuse through the liquid

matrix of the dough prior to reaching the gas cell nuclei that had been entrained during mixing. Unlike yeast, chemical leavening agents quickly evolve CO_2 upon coming into contact with the aqueous phase of dough (Heidolph, 1996; Chapter 4), so it is expected that CO_2 from chemical leaveners starts to be evolved as early as during mixing. Accordingly, the few gas cell nuclei expected to be present in vacuum mixed doughs meant that the 'diffusion path' of CO_2 to the gas cell nuclei was long. Molecules of CO_2 traveling a longer diffusion path would require longer time to reach the gas cell nuclei, which explains the experimental data showing that the CO_2 evolved from the chemical leaveners in dough mixed under vacuum was unable to inflate the gas cell nuclei: it did not have enough time to reach the gas nuclei during the course of mixing. Conversely, the larger number of gas bubbles that are entrained in dough when mixed at higher pressures (Campbell et al., 1998) infers that the diffusion path was shorter so that CO_2 did not require as much time to reach the gas cell nuclei, and gas cell growth takes place during mixing. Interestingly, Figure 6.7 shows that dough mixed at atmospheric pressure was off the line connecting the density data for low and high pressures. This can be explained by the 'extra time' spent by chemical leavening systems in dough mixed at atmospheric pressure due to the slightly different mixing protocols used for sample preparation (see Materials and Methods). This 'extra time' allowed the leavener to produce more gaseous CO_2 so that the dough densities of atmospheric-mixed dough followed the gas production pattern of the leavening system (Chapter 4).

As said earlier, there is a need to identify possible mechanisms responsible for interactions between chemical leavening systems and mixing pressure that affect gas retention capacity of dough during fermentation. A comparison among Figures 6.8A,

6.8B and 6.8C indicates that doughs mixed at reduced pressure were only able to reach substantially lower final void fractions, 3% (SAPP), 13% (ADA), 44% (KAT) and 53% (GDL) compared to doughs mixed at atmospheric pressured, 26%, 31%, 50%, 64% (GDL), or doughs mixed at two atmospheres of pressure, 25%, 33%, 52% and 71%, respectively. Though increasing mixing headspace pressure is expected to lead to an increase in the void fraction of dough ex-mixer (Campbell et al., 1998), such an increase in void fraction is of the order of 6% and 11% for an increase in pressure of 1 and 2 atmospheres, respectively, for strong (British) flour doughs (with no added leavening system) mixed in the Tweedy-1 mixer (Chin et al., 2005). Clearly, increasing the mixing pressure improved the ability of the dough to retain the carbon dioxide gas evolved by the leaveners. These findings appear to be consistent with more bubble numbers in the dough and hence a greater surface area for CO_2 mass transfer to the bubbles and reduced gas losses during mixing and fermentation. For example, the high void fractions achieved by SAPP dough when mixing pressure was increased to 1 or to 2 atmospheres (Figure 6.8) could be explained in terms of higher bubble numbers, with bubble numbers being particularly important in SAPP dough because the initial rate of CO_2 production of SAPP has been shown to be the highest among the other leavening systems studied (Figure 4.2 of Chapter 4). The higher bubble number entrained during mixing will ensure that the CO_2 produced in SAPP doughs is not lost in large amounts to the atmosphere. However, entraining too many bubbles in the dough during mixing (i.e., increasing the mixing pressure from 1 to 2 atmospheres) was not additionally beneficial in terms of the subsequent growth of the dough piece during fermentation, as can be seen for ADA and KAT dough (Figures 6.8B and 6.8C).

Another aspect of the results shown in Fig. 6.8 worth discussing is associated with gas cell stability as KAT and GDL doughs exhibited signs of coalescence (i.e., no void fraction change followed by a drop in void fraction) during the fermentation experiments (Figure 6.8). For GDL dough mixed under atmospheric pressure (Figure 6.8B), the sample started losing CO_2 at the point (~17 min) in which the gas void fraction was 70% (the minimum in the density versus time curve), which is equivalent to the void fraction at which the dough is expected to be transformed from a foam to a sponge structure (70%) (Bloksma, 1990a, 1990b; Scanlon & Zghal, 2001). Interestingly, this finding supports the view that the xylene penetrated the dough interior once gas bubbles in the dough became interconnected due to the transformation of the dough into a sponge-like structure.

However, for KAT dough (Figure 6.8B), which was also mixed at atmospheric pressure, the point at which the dough began losing CO_2 (30 min into fermentation) corresponded to a gas void fraction of 50%, which was substantially lower than the void fraction at which bubble coalescence is expected to occur (70%). In fact, it is difficult to reconcile the fact that densities as low as 0.35 g cm^{-3} ($\phi \sim 73\%$) have been registered on yeasted dough by Campbell's technique before (Campbell et al., 2001), with no apparent increase in dough density 2 h into fermentation. An explanation for the gas losses detected by Campbell's system during fermentation of KAT dough was found in the work of Weegels et al. (2003).

Based on CLSM (Confocal Scanning Laser Microscopy) observations of bubbles in fermenting dough, Weegels et al. (2003) postulated that the burst or collapse of a single bubble at the outer side of the dough can cause the simultaneous collapse of a

group of interconnected bubbles. Hence, it can be speculated that a 'chimney effect' for a given group of bubbles can cause xylene to migrate into the newly formed open channels when KAT was being fermented in Campbell's system. This hypothesis would explain the decrease in dough density in the KAT dough at a void fraction (~ 50%) that did not correspond to the onset of coalescence (~ 70%) and supports the view that coalescence cannot be ascribed solely as an all or none event (it cannot be said that coalescence occurs once the dough reaches 70% void fraction, but rather gas percolation is so widespread at 70% void fraction that gas losses from the dough are indisputably apparent). That coalescence is not an all or none event can also be inferred from the experimental work reported in Chapter 3. In Chapter 3, it was found that the distance between bubbles could not be attributed to a single value but rather it was described by a normal distribution. Since the distance between bubbles is the parameter (Bloksma, 1981; Scanlon & Zghal, 2001; van Vliet et al., 1992), or at least the most important parameter (Mills et al., 2003; Ornebro et al., 2000; Salt et al., 2006), determining the onset of bubble coalescence, it is reasonable to believe that a distribution of distances among bubbles would lead to a distribution of void fractions at which bubble coalescence would occur (i.e., at a given void fraction, a group of larger bubbles may have already coalesced and their gas contents escaped the dough while a pocket of smaller bubbles would still remain discretely dispersed in the same dough). This view is supported by the μCT data recently published by Babin et al. (2006) in which bubble coalescence in a lean formula dough (100 g flour + 60g water + yeast) became evident when the void fraction was about 40% (3g yeast) or 50% (1.5g yeast), even though early signs of coalescence began when the void fraction was as small as 30% (3 g yeast) or 35% (1.5 g yeast). Therefore,

the conventional view that bubble coalescence starts at a void fraction of 70% is open to question (Bloksma, 1990a, Scanlon and Zghal, 2001).

It is important to note that even when bubble coalescence is extensively present in the dough, it does not necessarily mean that all the bubbles in the dough are interconnected. This is shown in Figure 6.3D, where GDL doughs, in spite of growing past a void fraction of 70% and even after undergoing extensive gas loss (due to the transformation of the dough into a sponge-like structure), still show signs of isolated pockets of gas as its density dropped when the temperature was raised. An increase in fermentation temperature is expected to lead to greater gas evolution from the leaveners (Chapter 4) and to the volumetric expansion of gases inside the gas cells. The fact that the 'the chimney effect' concept was more prevalent in KAT doughs than in GDL doughs supports the hypothesis made earlier whereby it was proposed that, at equivalent bubble numbers, KAT doughs were more sensitive to the presence of high number of gas bubbles than GDL doughs were. The independent finding that gas bubbles can reduce the strain hardening properties of doughs gives support to this view (Chin et al., 2005).

6.4. Conclusions

This study characterized the effects of chemical leavening systems on dough development in the mixer and monitored the subsequent growth of the dough during fermentation with the two best known dough density measurement systems. Results show that the addition of the chemical leavener to the dough decreased dough strength. The effects of chemical leaveners on dough rheology were associated with changes in dough gluten strength and with aeration of the dough during mixing. In addition to their effects on gas entrainment, the mode of action of chemical leavening agents on dough

consistency were associated with the ionic interactions between leavening agents and the gluten protein molecules, which theoretically could have arisen from the salt-induced effects of lyotropic agents (SAPP, KAT) and/or the disruptive effects of organic acids (GDL, ADA) on the intermolecular H bonding of the gluten proteins. Dough consistency, as measured during dough development, showed that the strength of the experimental doughs varied with chemical leavener (in decreasing order): ADA > KAT ~ GDL > SAPP.

A comparison of Campbell's DDD system and Bellido's DDD system was also made for the first time using chemical leaveners as the source of CO_2. The measured change in dough density during fermentation with respect to the initial density (ex-mixer) was compared to assess the two DDD systems. For small changes in dough density (<0.1 g cm^{-3}), both techniques were in very good agreement, and these small changes were found in dough fermented with SAPP and, at early times, in dough containing ADA and KAT. However, discrepancies for the density changes measured by Campbell's DDD system and Bellido's DDD system began when doughs underwent larger density changes (> 0.1 g cm^{-3}), particularly when the dough densities changed by more than 0.2 g cm^{-3}. Very interestingly, density measurements detected in Campbell's DDD system were suitable to identify the point at which gas cell coalescence, an important mechanism for structure formation in dough, came to happen. The onset of bubble coalescence was observed to occur in GDL dough (the system with the highest CO_2 production power) when it reached a gas void fraction of 70%, much in agreement with the literature (Bloksma, 1990a, 1990b; Scanlon & Zghal, 2001). However, because signs of bubble coalescence were detected in KAT at a surprisingly lower void fraction (~50%), it was

proposed that bubble coalescence cannot be ascribed as an event that takes place at a given void fraction, but rather takes place over a range of void fractions.

CHAPTER SEVEN

Low-intensity (40 kHz) Ultrasound Study on Gas Bubble Growth in Chemically Leavened Dough

Abstract

The transformation of wheat flour dough into bread relies on the ability of dough to successfully entrain gas bubbles during mixing and sustain CO_2-induced gas bubble growth during proving of the dough. Therefore, a technique capable of real-time monitoring of the growth and coalescence of gas bubbles is useful for elucidating the mechanisms of gas bubble retention and stabilization in fermenting dough systems. This study used a low-intensity ultrasound (40 kHz) transmission technique to measure changes in the ultrasonic velocity and attenuation in chemically fermenting dough systems, thereby monitoring gas bubble growth as it actually occurred. Four chemical leavening systems consisting of sodium bicarbonate and glucono-delta-lactone (GDL), potassium acid tartrate (KAT), adipic acid (ADA) or sodium acid pyrophosphate 40 (SAPP), were employed for leavening dough at ordinary fermentation temperatures. Image analysis was used to measure changes in the density of the fermenting dough under identical conditions to the ultrasonic measurements. The ultrasonic velocity and attenuation were strongly affected by changes in the void fraction but also by the nature of the leavening system employed. Ultrasonic velocity, depending on the leavening system, dropped by as much as 50% over 50 minutes of bubble growth for some systems while remaining relatively constant in others. The attenuation always increased with fermentation time. Changes in void fraction alone (i.e., bubble growth) could not account

for the observed changes in ultrasonic velocity and attenuation, suggesting that ultrasonic properties were also sensitive to the presence of fermentation by-products (e.g., salts) through the effect of these by-products on the mechanical properties of the dough matrix. Experimental velocities as a function of void fraction were compared with velocities predicted from Wood's approximation, and were found to be consistently higher. This implied that the contribution of the shear modulus of the dough matrix to the properties of the dough could not be neglected. An effective medium theory, which makes use of the velocity and attenuation data to account for the viscoelastic nature of the dough, was capable of describing the individual contributions of the bubbles and the dough matrix to the overall mechanical properties of SAPP doughs. The longitudinal elastic modulus of the dough, calculated from the density, attenuation coefficient and velocity data, was found to be sensitive to changes in the mechanical properties of the dough matrix of ADA, KAT and GDL doughs, all of which were found to increase in viscous-like behaviour as void fraction increased. Possible mechanisms of action of the chemical leavening systems on dough mechanical properties were discussed in light of literature and previous characterizations made in this thesis. Overall, this investigation showed that ultrasonic velocity and attenuation measurements of fermenting dough could determine non-invasively, non-destructively, and in real time, the mechanical properties of chemically fermenting dough, and thus to provide insight into gas cell structure in the proved dough.

7.1. Introduction

Since the objective of breadmaking is to produce a tasty loaf of bread with a soft texture and even crumb structure (Bloksma, 1972a), it is reasonable to say that one of the

most important characteristic of bread quality is its cellular structure (Scanlon & Zghal, 2001). The cellular structure of bread is made possible by the unique ability of gluten proteins to form a viscoelastic network capable of trapping and retaining gas cells when flour is mixed with water and developed into dough (Belton, 1999; Bloksma, 1972a; Orth & Bushuk, 1972). Hence, to fabricate bread of good quality or, more importantly, to control the quality of bread, one must have a good control over the formation and subsequent growth of gas cells in the dough. Although it was conclusively demonstrated more than 60 years ago that the cellular structure of bread originates at the mixing stage (Baker and Mize, 1941), the mechanisms by which gas cells are entrained and stabilized during breadmaking are still not well understood (MacRitchie, 1976; Sahi, 1994; Chin & Campbell, 2005a; Gan et al., 1990, 1995; Mills et al., 2003; Ornebro et al., 2000; Salt et al., 2006).

The stability of gas cells in the dough is dictated by the limit of expansion of the gas cell wall since its failure leads to bubble coalescence and the eventual loss of the leavening gas (van Vliet et al, 1992; van Vliet et al., 1999; Dobraszczyk, 1997a, 1997b, 2004; Dobraszczyk & Morgenstern, 2003; Dobraszczyk & Roberts, 1994; Dobraszczyk et al., 2003). Since the limit of expansion of the gas cell walls during breadmaking is strongly influenced by the rheological characteristics of the dough (Bloksma & Bushuk, 1988; Collado & De Leyn, 2000), it makes sense to study such phenomena as the nucleation, growth and stability of gas cells or gas bubbles in the dough using rheological principles and techniques (Bloksma, 1972a; Bushuk, 1985; Baker & Mize, 1941, 1946, Carlson & Bohlin, 1978; Chin & Campbell, 2005a, 2005b; Navickis & Nelsen, 1992;

Bagley et al., 1998; Charalambides et al., 2006; Galal et al., 1978; Navickis et al., 1982; van Vliet et al., 1992).

Despite the success of various empirical and fundamental rheological tests to predict the behaviour of dough in the bakery, a causal relationship between dough rheology and breadmaking performance has not yet been clearly established, particularly because dough rheological measurements are often made under conditions that do not reflect the critical stages of breadmaking, where surface phenomena also play a role (Bloksma, 1990b). In fact, very recently, Chin et al. (2005) reported that the gas bubble content of unfermented dough does affect its rheology and so the need to state gas bubble content (e.g., void fraction) when reporting dough rheological information is warranted. The study of gas bubbles and their importance to the rheological properties of dough is far from being a recent subject matter though. The pioneering work of Baker and Mize (1946) established a strong connection between dough aeration and dough rheology by showing that a balance between dough aeration and gas bubble subdivision was essential during mixing to make good bread. Optimally mixed doughs were found to be able to entrain the most favourable number and sizes of gas bubbles during mixing compared to under-mixed or over-mixed doughs. Their findings indicated that mixing was important not only for developing the dough gluten proteins but also for occluding the gas cell nuclei that will give rise to the cellular structure of bread.

A technique that has proven to be sensitive to the influence of gas bubbles on the mechanical properties of dough *in situ* is low intensity ultrasound (Elmehdi, 2001; Elmehdi et al., 2003a, 2004; Kidmose et al., 2001; Lee et al., 1992; Létang et al., 1996, 2001; Scanlon et al., 2002). Sensitivity to the physical and structural properties of the

resulting baked product is also another important capability of the ultrasonic technique (Elmehdi 2001; Elmehdi et al., 2003b; Lagrain et al., 2006). Relatively recently, Elmehdi (2001) measured ultrasonic velocity and the absolute attenuation coefficient of non-fermenting dough to model its rheological behaviour. To interpret the ultrasonic data, Elmehdi (2001) used an effective medium model (EMT) (Sheng, 1988) that made use of both the velocity and attenuation data to determine the individual contributions of the gas phase and the dough matrix to the overall mechanical properties of the dough. Using the EMT, Elmehdi (2001) was able determine that vacuum mixing caused stiffening of the dough matrix, presumably because oxygen deprivation would decrease the degree of protein polymerization but would increase the formation of non-covalent bonding in the dough matrix. Increasing the oxygen content during mixing by lessening the vacuum level would cause an increase in the number of covalent bonds and the disruption of non-covalent bonds. Therefore, the effective medium theory proved to be a useful tool to delineate the influence of gas bubbles and the dough matrix on the bulk mechanical properties of the dough. Using the ultrasonic technique he developed for unyeasted dough, Elmehdi (2001) also studied the mechanical properties of fermenting dough. Although it was observed that velocity decreased with decreasing density, Elmehdi's (2001) experiments did not measure both the absolute attenuation coefficient and the density of the dough matrix necessary to measure the gas void fraction of the fermenting dough. These two pieces of information are crucial to employ the effective medium model to interpret the ultrasonic velocity and attenuation data and so Elmehdi (2001) was unable to delineate the contribution of gas bubbles on the rheological properties of fermenting dough.

A difficulty associated with measuring the absolute attenuation coefficient and the void fraction of yeasted doughs is that yeast is an organism whose fermentative action on sugars produces not only carbon dioxide (the leavening gas), but also a large number of organic compounds whose effects on the mechanical behaviour of the dough are very difficult to predict with certainty (Hoseney, 1998; Matsumoto, 1986; Hoseney et al., 1981; Matsumoto et al., 1975). In fact, it is believed that yeast plays various roles in breadmaking as it affects the texture, taste, flavour, aroma and nutritional value of bread (El-Dash & Johnson, 1970; Johnson & Sanchez, 1973; Wiseblatt & Kohn, 1960; Hoseney et al., 1981, 1988). An alternative means of producing carbon dioxide in a "cleaner" manner than yeast is to use chemical leavening systems (Conn, 1981; Heidolph, 1996; Hoseney, 1998; Holmes & Hoseney, 1987a, 198b; Miller et al., 1994; Parks et al., 1960; Chapter 3 and 4). The simplicity of the chemistry defining the chemical leavening reaction may in fact be of interest to those experimenters seeking to acquire a better understanding of the chemistry and physics of bubble nucleation, growth and coalescence.

A chemical leavening system is comprised of sodium or potassium bicarbonate and a source of acidity. Theoretically, any substance capable of releasing hydrogen ions could be used in chemical leavening system. The *Food and Drugs Act* regulates the acceptable sources of acidity in baking powder (which is a chemical leavening system) in Canada. The *Food and Drugs Act* stipulates that baking powders can be made with one or any combination of the following sources of acidity or *acidulants*: lactic acid or its salts, tartaric acid or its salts, acid salts of phosphoric acid, and acid compounds of aluminum (Section 3 of the *Foods and Drugs Act*; Health Canada, 2007). Commercially, the North

American baking industry employs a wider range of sources of acidulants, including adipic acid, ascorbic acid, citric acid, fumaric acid, glucono-δ-lactone, propionic acid, and sorbic acid (Heidolph, 1996). Chapters 4 and 5 of this thesis indicated that chemical leavening systems containing the acidulants adipic acid, sodium acid pyrophosphate, potassium acid tartrate or glucono-δ-lactone are suitable to produce dough with a wide range of void fractions at typical fermentation temperatures.

The objective of this study was to use a low-intensity ultrasound (40 kHz) transmission technique to unambiguously assign and model the individual contributions of the gas phase and of the dough matrix to the overall rheological properties of dough during fermentation. Experimental doughs were chemically fermented using one of four chemical leavening systems, each of which contained sodium bicarbonate and sodium acid pyrophosphate, adipic acid, potassium acid tartrate or glucono-δ-lactone.

7.2. Materials and Methods

7.2.1. Dough sample

The dough samples were prepared from straight grade wheat flour milled from a number 1 grade Canadian Western Red Spring wheat in the pilot mill of the Canadian International Grains Institute, Winnipeg, MB. Table 3.1 (Chapter 3) shows the chemical composition and technological characteristics of the flour. The dough formula included 100 g of flour (14% m.b.), 69.6 g deionised water (Farinograph absorption - 2%), 0.75 g NaCl, and one of four chemical leavening systems: 5.83 g sodium acid pyrophosphate 40 + 4.20 g sodium bicarbonate (SAPP), 1.22 g adipic acid + 1.40 g sodium bicarbonate (ADA), 6.22 g potassium acid tartrate + 2.80 g sodium bicarbonate (KAT), or 9.33 g glucono-delta-lactone + 4.20 g sodium bicarbonate (GDL). These chemical leavening

systems were chosen because, based on previous experimental work (Chapter 4), they were able to produce doughs with a wide range of void fractions during fermentation (5-67%). The levels of water absorption and NaCl used in this work were adequate to produce dough with relatively good handling properties, as shown by preliminary experiments using potassium acid tartrate as a leavener.

Doughs were mixed at room temperature (23 ± 1 °C) using a GRL 200 mixer (Hlynka & Anderson, 1955) at a constant pin speed of 165 rpm for 4 min using two sequential mixing steps. In the first step, the flour, sodium chloride and water were mixed for 1 min. In the second, the experimental chemical leavening system was added to the rest of the formula ingredients and mixed for an additional 3 min. Later addition of the chemical leaveners to the dough was a strategy used to ensure preferential hydration of the flour, avoiding chemical leaveners reacting too quickly. Immediately after mixing, the dough was removed from the mixing bowl and two sub-samples of about 4 g each were excised from the dough using sharp scissors. The rest of the dough was discarded so that a new batch of dough was used in each experiment. The weight of each dough sub-sample was measured accurately to 0.01 g. One sub-sample was used for density measurements and the other for ultrasonic measurements. The experimental set-ups for density and ultrasonic measurements were synchronized to start at the same time (~ 6 min after the end of mixing). Subsequent density and ultrasonic measurements were conducted at exactly the same time intervals (~ 3 min) for at least 60 min after the end of mixing. Under this scheme, both the density and the ultrasonic properties were measured concurrently but separately using sub-samples of the same batch of dough. At least two dough batches were prepared for each experimental treatment.

7.2.2. Dough density

Density measurements of fermenting dough as a function of time were carried out using a digital image analysis (DIA) technique described elsewhere (Chapter 5) after converting specific volume units into density units (one is the reciprocal of the other). To measure density, the apparatus shown in Figure 1 of Appendix VI was employed. A sub-sample of dough (~ 4g), from each experimental treatment (i.e., chemical leavening system) was gently squashed between two acrylic plates (each one 2.54 cm thick) to a preset, constant thickness of 2.10 ± 0.01 mm. Maintaining a constant sample thickness ensured that the expansion of the dough was restricted to the radial direction. The density apparatus was then placed in a proving cabinet against a black background directly below a digital camera affixed to a tripod (see Figure 5.2 of Chapter 5). Digital photographs of the expanding dough piece were taken at 3-minute intervals for about one hour, with the stopwatch zeroed immediately at the end of mixing. The density of the dough as a function of time, $\rho(t)$, was calculated from: $\rho(t) = L\ S(t) / m$, where L is the sample thickness (maintained at 2.10 mm), $S(t)$ is the area of the dough as a function of time (from image analysis), and m is the dough mass. The calibration is discussed elsewhere (Chapter 5). All density measurements were carried out in a pre-heated proving cabinet set at the experimental temperature of 27 °C (± 1 °C) and at a relative humidity of 70%.

7.2.3. Measurements of pH

The hydrogen-ion activity (pH) of a suspension of dough at a temperature of 23 ± 0.5 °C was measured using a pH meter (Sentron pH meter type Titan, SENTRON Europe B.V., Roden, The Netherlands), according to a modified version of the method of Holmes

& Hoseney (1987a) for a dough slurry, in itself a modified version of the method described by Collatz (1943) and the official AACC Method 02-52 (2000) for non-dough cereal products (i.e., flour, bread, cracker, cake and pastry products). The electrode of the pH meter was calibrated using standard buffer solutions prior to pH measurements. To prepare a suspension of dough, 10 g of a dough sample was stirred for 10 min in 100 ml of distilled water using a glass rod. Immediately after stirring, the pH of the sample was measured when the pH reading became stable. The dough samples were either freshly made (*control* and *control* + $NaHCO_3$) or taken from the dough density experiments after the dough was fully fermented (*control + a chemical leavening system*). Doughs were deemed fully fermented after they had been leavened for about 65 min after the end of mixing.

7.2.4. Ultrasonic technique

The ultrasonic velocity and attenuation coefficient of fermenting dough was measured using a basic pulse transmission technique with the equipment shown in Figure 7.1. Two sample holders for ultrasonic measurements were used depending on the type of chemical leavening system employed in the dough sample, as discussed in the Sample Holder section.

To measure ultrasonic properties, the two ultrasonic transducers (Figure 7.1) were perpendicularly positioned on either side of the plane where the dough expanded radially. One transducer acted as the transmitter of the ultrasonic signal and the other as the receiver. The transmitting transducer was excited by an electric signal (a short positive voltage spike) from a short pulse generator, the Portable Ultrasonic Non-Destructive Digital Indicating Tester (Panametrics 6, CNS Farnell Ltd., Borehamwood, Hertfordshire,

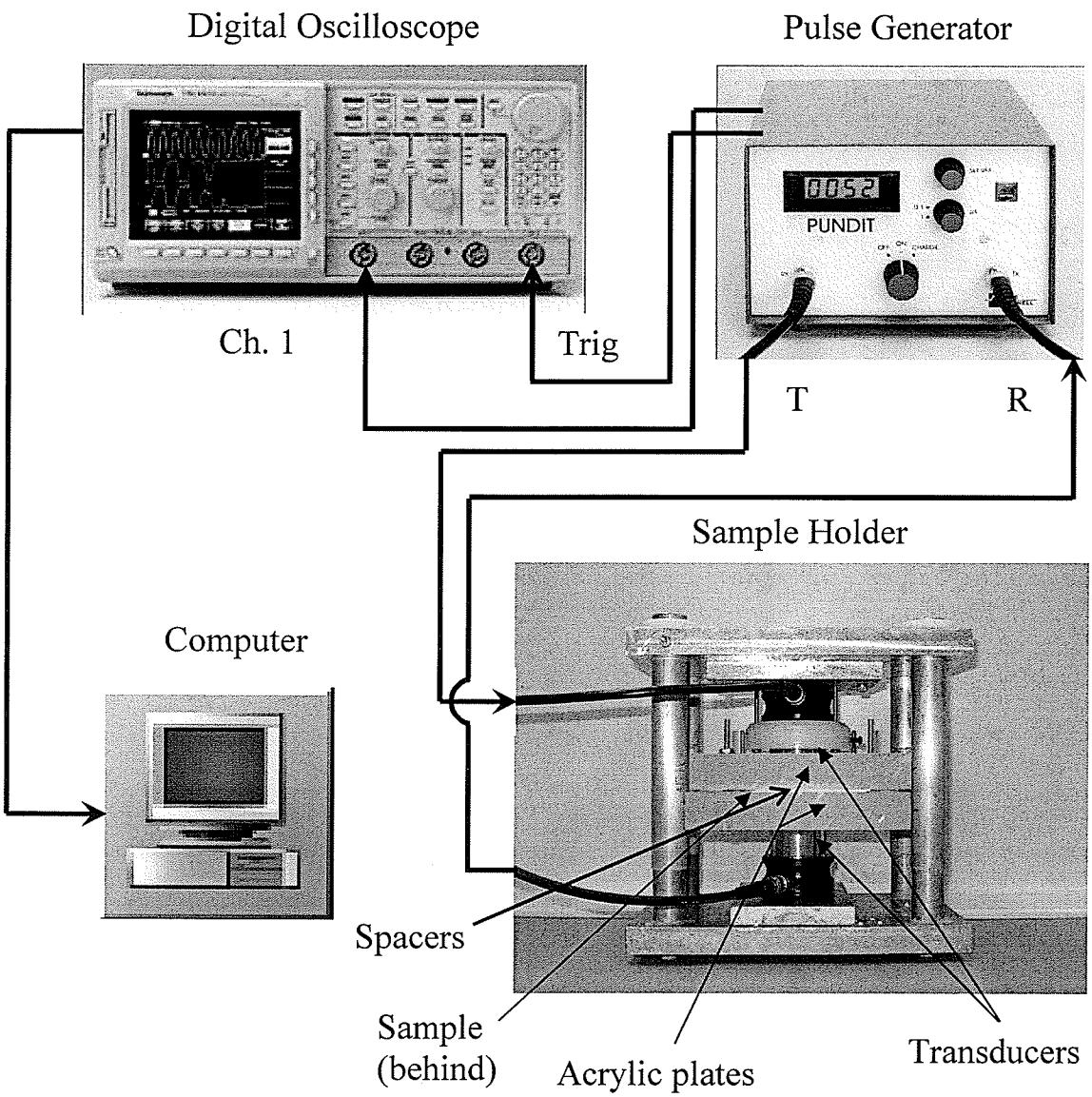

Figure 7.1. Block diagram illustrating the set-up for ultrasonic experiments. "Ch. 1" is the channel used to display the acquired signal on the digital oscilloscope, "Trig" is the trigger signal used to synchronize timing in the electronic detection system (the oscilloscope), T is the ultrasonic signal to be transmitted through the sample, and R is the signal received.

UK), to produce a pressure (ultrasonic) pulse that travelled through the dough sample. The pulse generator was set to output pulses at a pulse repetition rate of 10 pulses per second. The main output signal was synchronized with the pulse used to trigger the oscilloscope, a positive pulse with a rise time of 2 μs (Elmehdi, 2001). The transmitted pulse was amplified by a signal amplifier in the Panametrics unit and then averaged 120 times using the average function of the oscilloscope (Tektronix Digital Processing Oscilloscope model TDS 420A, Textronix Canada Inc., Toronto). Signal averaging reduced random noise (e.g., from the receiver amplifier) and increased the signal to noise ratio. The transducers, constructed with damped piezoelectric elements made of lead zirconate-titanate, had a nominal operating frequency of 54 kHz and an effective operating frequency of 40 kHz (Figure 7.2A and 7.2B). The transmitted ultrasonic signal or averaged waveform was downloaded into a PC for storage and for subsequent signal analysis.

7.2.5. Signal analysis

Each digitized "averaged" waveform was filtered using a multiplying Gaussian filter function set to a specified central frequency and a bandwidth of 10 kHz. The Gaussian filter function's central frequency was selected depending upon the characteristics of the sample in terms of absorption of the frequency components of the ultrasonic signal. The central frequencies chosen in the present experiments corresponded to the frequency of the peak of the amplitude *versus* frequency spectrum of the Fast Fourier Transform of the transmitted signal as determined by the Fourier analysis (FFT) function of Origin® software (Micrococal Origin® 7.5, Originlab Corporation, Northampton, MA). Figure 7.3, for example, shows the effect on the distribution of

frequency components of the two acrylic plates of the sample holder when positioned in the path of the transmitted pulse (no dough sample was placed in the sample holder). The central frequency of the reference pulse changed from 40 kHz for the transducer-transducer arrangement (Figure 7.2) to 35 kHz for the transducer-acrylic plate-acrylic plate-transducer arrangement (Figure 7.3). Similarly, the fermenting dough samples showed different degrees of absorption of the higher frequency components of the 40 kHz ultrasonic pulse. The central frequency of the Gaussian filter varied according to the dough samples as follows: 35 kHz, SAPP and ADA; 30 kHz, KAT; and 10 kHz, GDL. Figures 7.4 and 7.5 show typical results on the capabilities of the filtering technique for removing noise from the raw signal. From the leading edge (first dip) of each filtered waveform, the transit time (θ(t)) and amplitude (A(t)) as a function of fermentation time of the transmitted pulse were determined and used for measuring the velocity of ultrasound and the intensity attenuation coefficient according to the procedures described below.

7.2.6. Sample Holder

Measurements of ultrasonic velocity and intensity attenuation coefficient were carried out in the apparatus shown in Figure 7.1, but using one of the two sample holders shown in Figures 1 and 2 of Appendix VI. For SAPP and ADA dough, a sample holder identical to that used in the density experiments (Figure 1 of Appendix VI) was employed to measure ultrasonic properties (i.e., transit time and signal amplitude) across three dough thicknesses, 1.64 mm, 2.15 mm and 2.74 mm (± 0.01 mm), according to the procedure described by Elmehdi et al. (2004). Dough sample thickness was set using spacers of precise thickness.

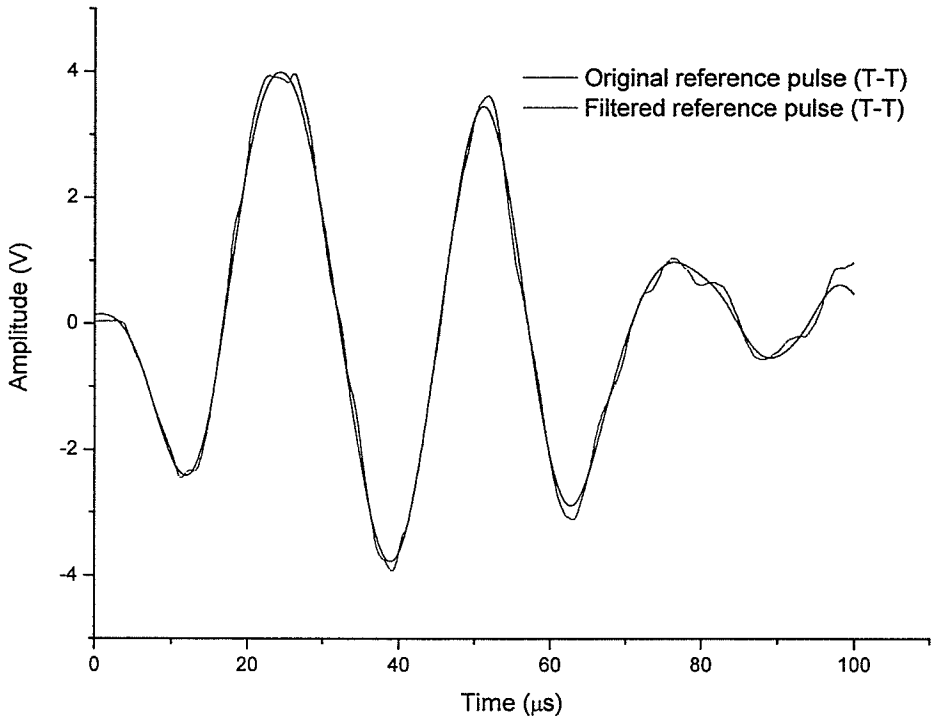

A

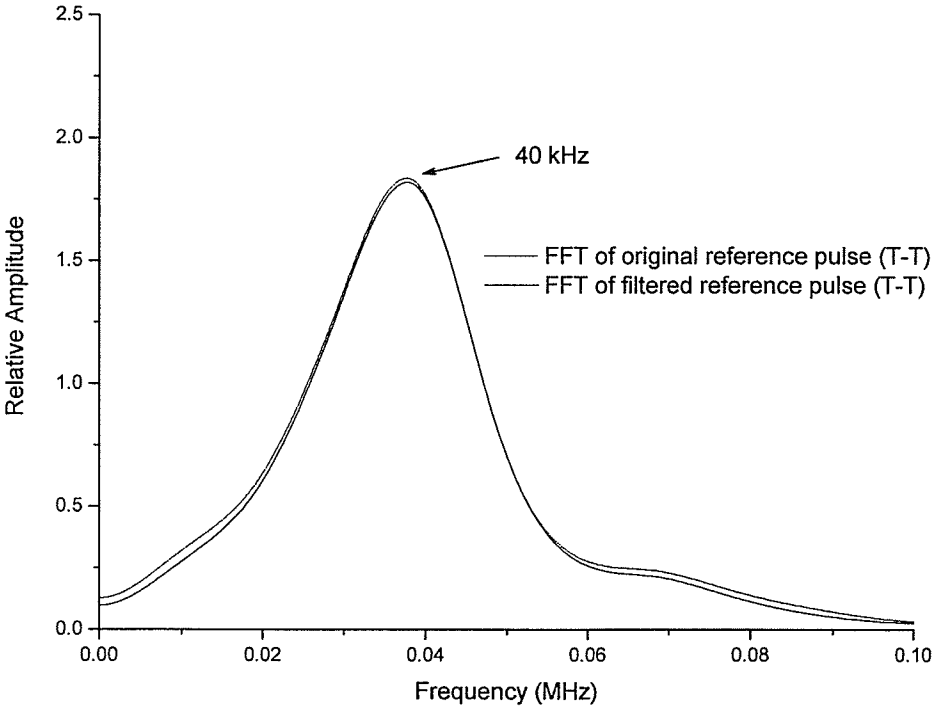

B

Figure 7.2. Characteristics of the reference pulse for when the faces of the Panametrics piezoelectric transducers were coupled (T-T) via a thin layer of ultrasound coupling gel (Ultrasonic Gel II, Diagnostic Sonar Ltd., West Lothian, Scotland). Amplitude of the reference pulse (A) as a function of time and (B) as a function of frequency after applying the Fast Fourier Transform. See text for details. The filtering step was accomplished by multiplying the reference pulse by a Gaussian filter function (central frequency = 40 kHz; and bandwidth = 10 kHz).

A

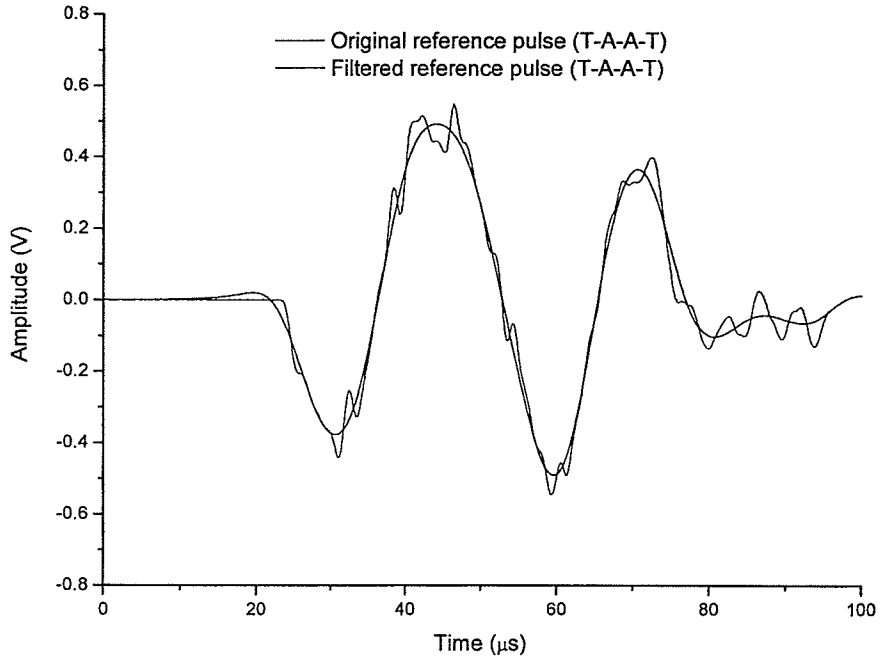

B

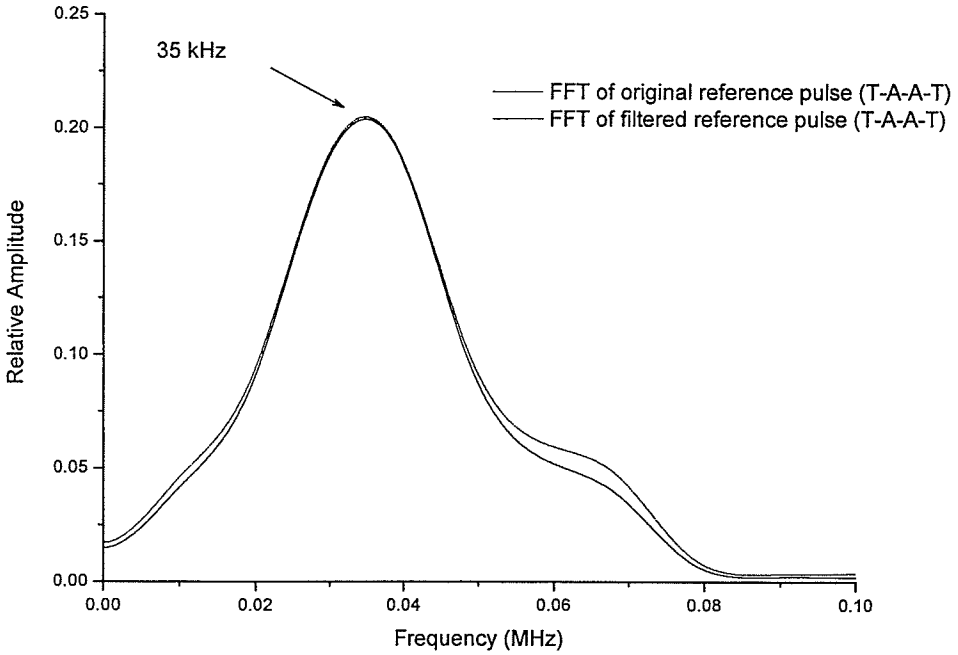

Figure 7.3. Characteristics of the reference pulse for when the faces of the Panametrics piezoelectric transducers were coupled via two blocks of acrylic plates (see Figure 7.1 of Chapter 7) and each interface coupled (T-A-A-T) via thin layers of ultrasound coupling gel (Ultrasonic Gel II, Diagnostic Sonar Ltd., West Lothian, Scotland). Amplitude of the reference pulse (A) as a function of time and (B) as a function of frequency after applying the Fourier analysis (FFT) function of Origin® software (Micrococal Origin® 7.5, Originlab Corporation, Northampton, MA). The filtering step was accomplished by multiplying the reference pulse by a Gaussian filter function (central frequency = 35 kHz and bandwidth = 10 kHz).

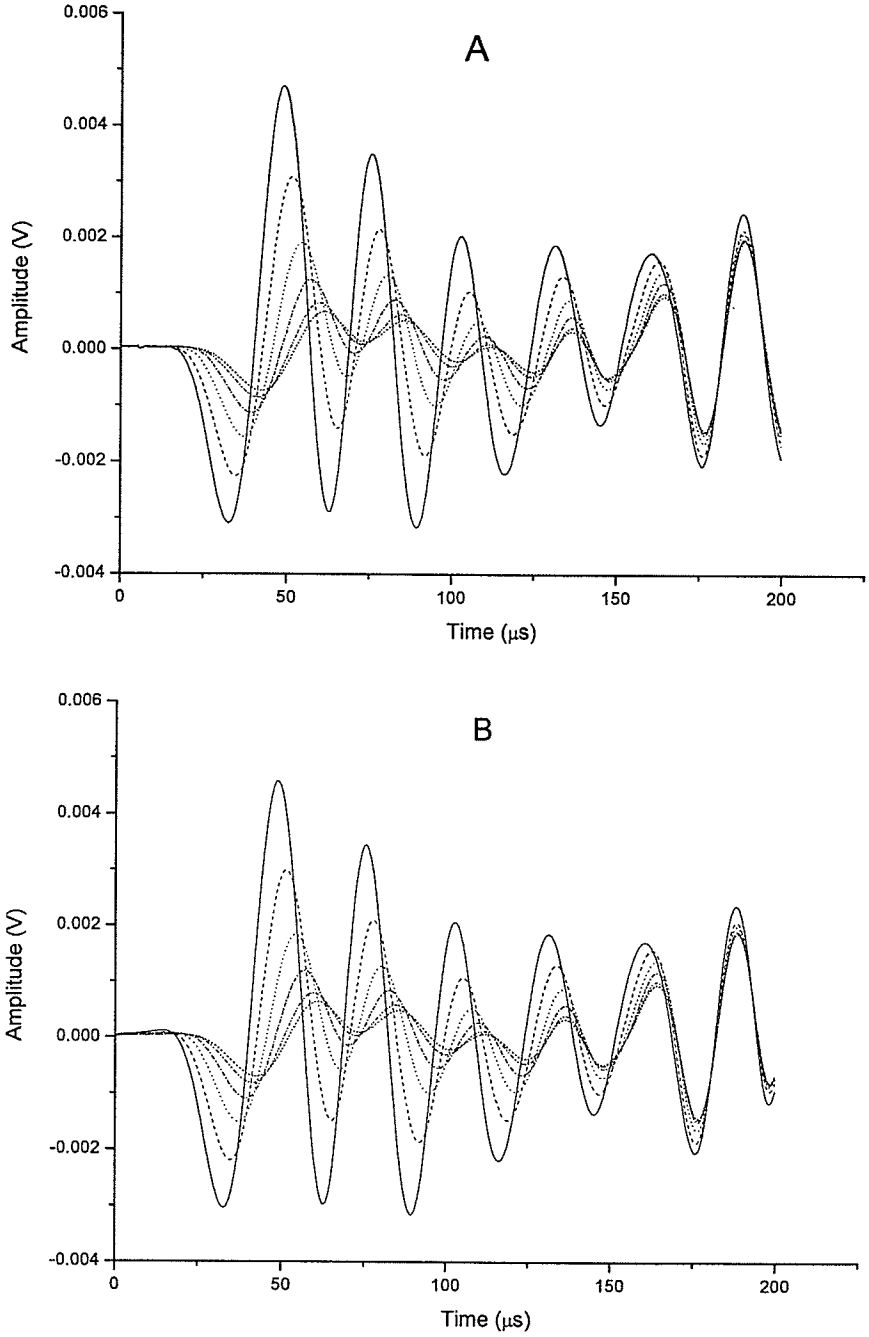

Figure 7.4. Typical results for the amplitude of original (A) and filtered (B) ultrasonic signals traveling through chemically leavened doughs containing SAPP or ADA, and illustrated here for dough (2.15 mm) containing SAPP. Waveforms represent different fermentation times: 7 min (solid), 22 min (dash), 37 min (dot), 52 min (dash dot), 67 min (dash dot dot), and 82 min (short dash). The filtered signal was obtained by multiplying the raw signal by a Gaussian filter function which was set to a bandwidth of 10 kHz and to a central frequency of 35 kHz (SAPP and ADA).

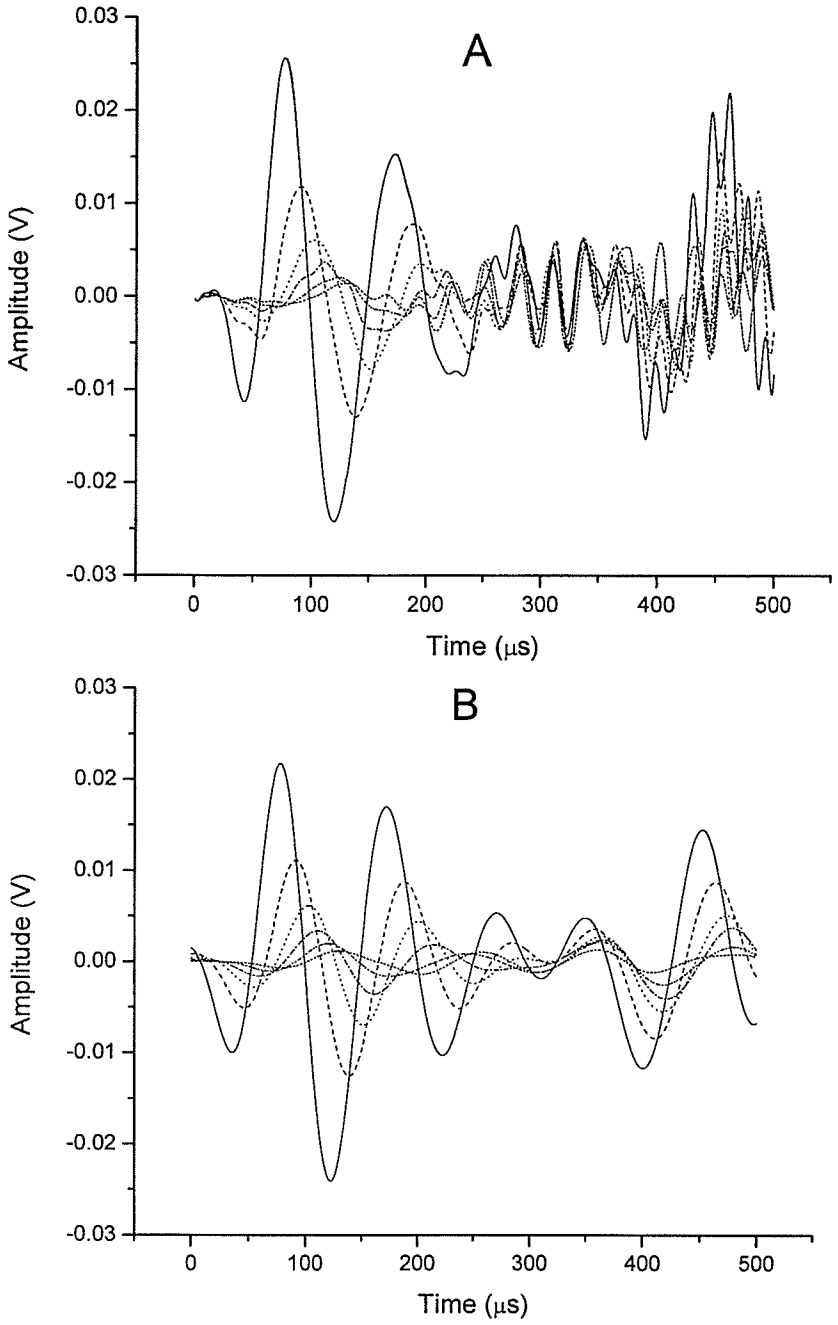

Figure 7.5. Typical results for the amplitude of original (A) and filtered (B) ultrasonic signals traveling through chemically leavened doughs containing KAT or GDL, after 60 min of fermentation, and illustrated here for dough containing GDL. Waveforms represent different sample thicknesses: 1.5 mm (solid), 2.0 mm (dash), 2.5 mm (dot), 3.0 mm (dash dot), 3.5 mm (dash dot dot), and 4.0 mm (short dash). The filtered signal was obtained by multiplying the raw signal by a Gaussian filter function which was set to a bandwidth of 10 kHz and to a central frequency of 30 kHz (KAT) or 10 kHz (GDL).

For KAT and GDL dough, the sample holder shown in Figure 2 of Appendix VI was employed because preliminary experiments using the original sample holder (Figure 1 of Appendix VI) showed that a spurious signal corrupted the signal travelling through the dough. The preliminary experiments demonstrated that the spurious signal was travelling through the frame of the original sample holder (Figure 1 of Appendix VI), specifically through the spacers and through the metal screws securing the acrylic plates together (i.e., through the contact areas connecting the acrylic plates). Corruption of the signal travelling through the dough only occurs when the pulse's arrival time was comparable to that of the spurious signal. This explained why the spurious signal did not affect the signal travelling through SAPP or ADA dough but it did contaminate the signal going through KAT or GDL dough. Signals travelling through higher void fraction doughs (KAT or GDL dough) take longer to get across the fermenting dough. The fact that signal attenuation also increases in high void fraction dough, made it easier for the spurious signal to predominate over the real signal travelling through the KAT and GDL doughs.

Some features of the original sample holder were modified and others introduced into the new sample holder to enable ultrasonic measurements to be made in the highly aerated KAT and GDL doughs (void fraction > 30%). The features of the new sample holder (Figure 2 of Appendix VI) included the following: (1) larger acrylic plates so as to delay the time taken by any spurious signal to travel through the contact points connecting the acrylic plates; (2) removal of the spacers to set the dough thickness and the introduction of three vertically positioned calipers (± 0.01 mm), reducing the contact surface between acrylic plates to the area of the tip (a ball bearing) of the calipers resting

on the lower sample acrylic plate; and (3) placing the transducers in direct contact with the test dough to reduce signal intensity losses arising from absorption within the acrylic plates.

7.2.7. Ultrasonic velocity

Two different procedures for measuring ultrasonic velocity were followed depending on whether the original or the new sample holder was used. For dough chemically leavened in the original sample holder (i.e., SAPP and ADA), ultrasonic velocity was determined by measuring the transit time (θ(t)) of the ultrasonic pulse at a fermentation time t across a dough of thickness (L) relative to the transit time of the reference signal (θ_{ref}). Velocity was calculated as follows: $v(t) = \frac{L}{\theta(t) - \theta_{ref}}$; where L = test dough thickness: 1.64 mm, 2.15 mm, or 2.74 mm. As noted earlier, a pulse's transit time and amplitude were measured at the first dip of each filtered waveform. The transit time for the reference pulse was measured by propagating ultrasound through the apparatus (including the acrylic plates) with no dough sample (Figure 7.3).

For dough chemically leavened in the new sample holder (i.e., KAT and GDL), the velocity of ultrasound was determined by measuring the transit time (θ_∞) of the ultrasonic pulse at a long fermentation time across various dough thicknesses (L). It was assumed that the properties of the dough changed little at long fermentation times (~ 60 min) because the rates of CO_2 production (measured via density measurements) were found to be so small that they were negligible (Figure 7.6). Although in the original sample holder one new dough sample was needed for ultrasonic measurements at different thicknesses (i.e., each experimental thickness required a new dough sample),

due to the configuration of the new sample holder one single dough sample was sufficient to conduct ultrasonic measurements at more than one thickness. This novel procedure was accomplished as follows. Initially, the dough sample (KAT or GDL) is set in the apparatus at a thickness of 4 mm in the ultrasonic apparatus and allowed to ferment for at least 60 min, with ultrasonic measurements of $\theta(t)$ and $A(t)$, as noted earlier, being conducted every 3 min. Ultrasonic measurements of transit time and amplitude corresponding to the longest fermentation time ($t_\infty \sim 60$ min) were regarded as θ_∞ and A_∞ for $L = 4.00$ mm. At this point the dough was gently squashed (by loosening the calipers

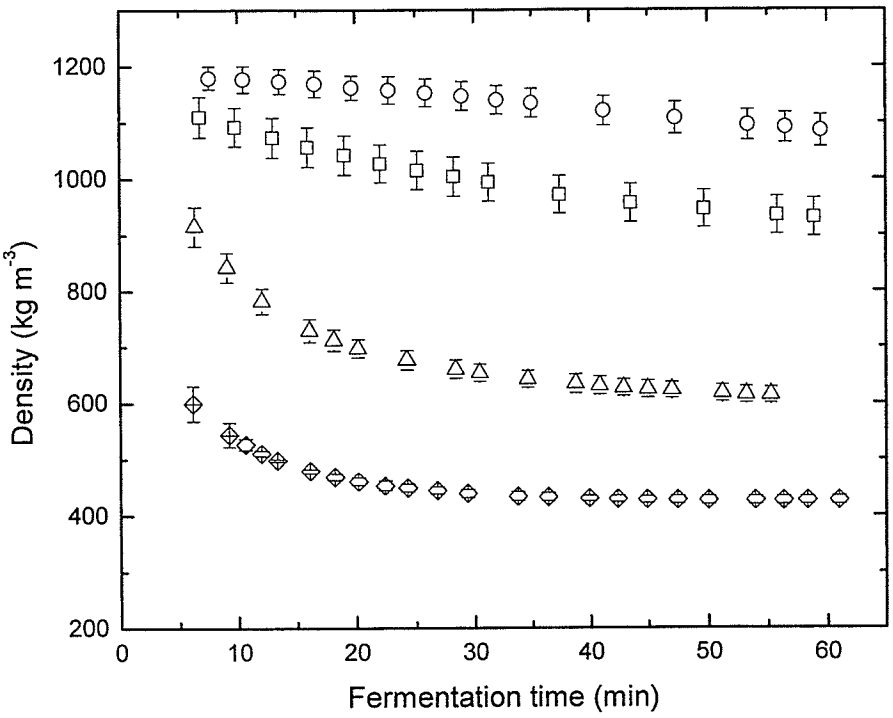

Figure 7.6. The density of chemically leavened doughs as a function of time. Symbols represent the chemical leavening system employed: 5.83 g SAPP 40 + 4.20 g sodium bicarbonate (circles); 1.22 g adipic acid + 1.40 g sodium bicarbonate (squares); 6.22 g potassium tartrate + 2.8 g sodium bicarbonate (triangles); 9.33 g glucono-δ-lactone + 4.20 g sodium bicarbonate (rhombus). Vertical bars represent standard deviation.

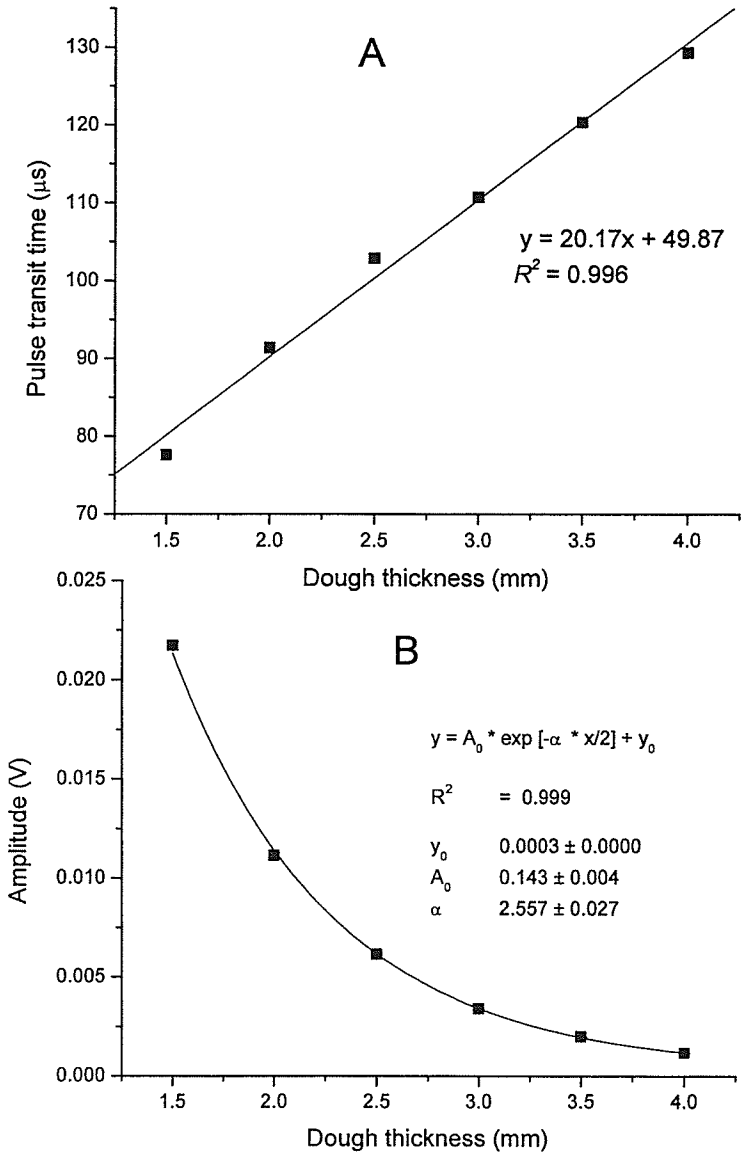

Figure 7.7. Pulse transit time (A) and ultrasonic signal amplitude (B) as a function of sample thickness, after 60 min of fermentation, for chemically leavened doughs containing KAT or GDL, and illustrated here for dough containing GDL. Symbols represent experimental data. The size of the SD (n=2) was comparable to the size of symbols. The solid line in (A) represents best linear fit to the data, where the y-intercept at $L = 0$ represents the transit time across transducers (L denotes sample thickness), and the reciprocal of the slope of the fit is the ultrasonic velocity (x10^3 m s^{-1}). The solid curve in (B) represents a fit to the data of the decaying exponential function: $A(L,t_\infty) = A_0 \exp(-\alpha(t_\infty) * L/2) + y_0$ where $\alpha(t_\infty)$ is the attenuation coefficient at long fermentation times (typically 60 min after the end of mixing), A_0 is a pre-exponential factor, and y_0 is the background contribution.

of Figure 2 of Appendix VI) to establish a new dough thickness of 3.5 mm and the ultrasonic properties measured again, with the ultrasonic measurements of transit time and signal amplitude corresponding to θ_∞ and A_∞ at L = 3.50 mm. This last step was repeated again at thicknesses of 3.00, 2.50, 2.00 and 1.50 mm so as to obtain four more data sets of θ_∞ and A_∞, which are plotted as in Figure 7.7. The velocity of ultrasound was taken from 1/slope (x 1,000 m s^{-1}) of the plot of L versus θ_∞ (Figure 7.7).

7.2.8. Attenuation coefficient

For a longitudinal ballistic pulse, which travels coherently through the dough sample without scattering out of the forward direction, the signal amplitude A as a function of sample thickness L at any fermentation time t is given by the following relationship:

$$A(L,t) = A_0 \exp\left[-\alpha(t)\frac{L}{2}\right] + y_0 \tag{7.1}$$

Here $\alpha(t)$ is the attenuation coefficient, A_0 is the intensity of the ultrasonic signal at the input face of the dough sample (at L = 0), and y_0 is the background contribution. Hence, at long fermentation times, t_∞, the dependence of signal amplitude A on sample thickness L is given by:

$$A(L,t_\infty) = A_0 \exp\left[-\alpha(t_\infty)\frac{L}{2}\right] + y_0 \tag{7.2}$$

Dividing Eq. 7.1 by Eq. 7.2, we have that:

$$\frac{A(L,t) - y_0}{A(L,t_\infty) - y_0} = \exp\left[-[\alpha(t) - \alpha(t_\infty)]\frac{L}{2}\right]$$

Therefore,

$$\alpha(t) = \alpha(t_\infty) - \frac{2}{L}\ln\left[\frac{A(L,t) - y_0}{A(L,t_\infty) - y_0}\right] \tag{7.3}$$

Assuming the background contribution is approximately zero (see below for details on the validity of this assumption), Eq. 7.3 becomes:

$$\alpha(t) \cong \alpha(t_\infty) - \frac{2}{L}\ln\left[\frac{A(L,t)}{A(L,t_\infty)}\right] \tag{7.4}$$

Eq. 7.4 was used to measure the attenuation coefficient as a function of fermentation time of KAT and GDL doughs. Eq. 7.4 suggests that measurements of the attenuation coefficient as a function of fermentation time can be made from a single test dough, *if*, for a given thickness L, the amplitude of the signal as a function of fermentation time, A (L, t), the amplitude of the signal at a long fermentation time, A (L, t_∞), and the attenuation coefficient at a long fermentation time, α (L, t_∞), are all known. All these quantities were measured along with the pulse transit time (for measurements of ultrasonic velocities) in the KAT and GDL doughs according to the protocol described in the preceding section. The typical change in signal amplitude as a function of sample thickness for KAT and GDL doughs is illustrated for GDL dough in Figure 7.7B. Note that, as assumed in Eq. 7.4, the background contribution to the signal amplitude ($L >> 4$ mm) was nearly zero in the fitting analysis, justifying the assumption made to obtain Eq. 7.4. However, Eq. 7.4 was only used to obtain the attenuation coefficient of KAT and GDL doughs.

For SAPP and ADA doughs, Eq. 7.1 was the one used to measure their attenuation coefficient, specifically according to the sequence of steps shown in Figure 3 of Appendix VI. In this procedure, the amplitude of the ultrasonic signal was first plotted as a function of void fraction for various dough thicknesses (i.e., 1.64 mm, 2.15 mm and 2.74 mm). Then, at a specified void fraction, the signal amplitude decay was plotted as a

function of sample thickness and the experimental data fitted with the decaying exponential function shown in Eq. 7.1 in order to obtain the intensity attenuation coefficient α. Intensity attenuation coefficients were then plotted as a function of void fraction (Figure 3C of Appendix VI).

The number of experimental samples (i.e., dough batches) for density and ultrasonic measurements were at least 16. At least 12 dough batches (=2 replicates x 3 thicknesses x 2 chemical leaveners) were prepared for experiments using SAPP and ADA and at least 4 dough batches (= 2 replicates x 2 chemical leaveners) were used for the experiments with KAT and GDL.

7.3. Results and Discussion

7.3.1. Density measurement

Figure 7.6 shows that the density of fermenting dough decreased with fermentation time regardless of the chemical leavening systems employed. Four chemical leavening systems were able to produce doughs whose density ranged from about 1,200 to 430 kg m^{-3}, over a fermentation period of 1 hour. At the onset of fermentation (Figure 7.6) the density of chemically leavened dough decreased quickly, except for dough leavened with SAPP. Because the gas content of dough strongly affects the mechanical properties of dough (Campbell et al., 1998), including the propagation of ultrasound (Elmehdi et al., 2003a, 2004), the density of the dough was expressed in terms of its gas void fraction using the following equivalence:

$$\phi(t) = 1 - \frac{\rho(t)}{\rho_{gf}} \tag{7.5}$$

where $\phi(t)$ is the dough gas void fraction as a function of fermentation time, $\rho(t)$ is the dough density as a function of time [kg m^{-3}], and ρ_{gf} is the gas-free dough density [kg m^{-3}]. Dough density as a function of time, $\rho(t)$, was measured according to the procedure found in the materials and methods section, whereas ρ_{gf} was measured using x-ray micro-tomography according to the procedure explained in Chapter 3.

7.3.2. Ultrasonic velocity

For a material that does not absorb sound too strongly, the longitudinal phase velocity, v, of a pressure wave is a function of the longitudinal modulus, β, and of the density, ρ, of the material according to the following equation:

$$v = \sqrt{\frac{\beta}{\rho}} \tag{7.6}$$

For a solid material, $\beta = \kappa^{-1} + \frac{4}{3}\mu$; where κ is the material's compressibility and μ is the shear modulus. For a liquid, $\beta = \kappa^{-1}$ and $v = \sqrt{\frac{1}{\kappa\rho}}$ because the shear modulus can be neglected. From Equation 7.6 it can be inferred that measurements of ultrasonic velocity in conjunction with independent measurements of density can provide quantitative information on a fundamental mechanical property of the fermenting doughs.

Figure 7.8 shows a plot of ultrasonic velocity as a function of void fraction for the leavening systems studied. It is clear from this plot that ultrasonic velocity was strongly affected not only by changes in the void fraction of the dough but also by the nature of the leavening system employed. For instance, ultrasonic velocities in SAPP or ADA dough were rather different even though there was a considerable overlap in the gas void fractions these two systems covered. Though Elmehdi et al. (2003a) found comparable

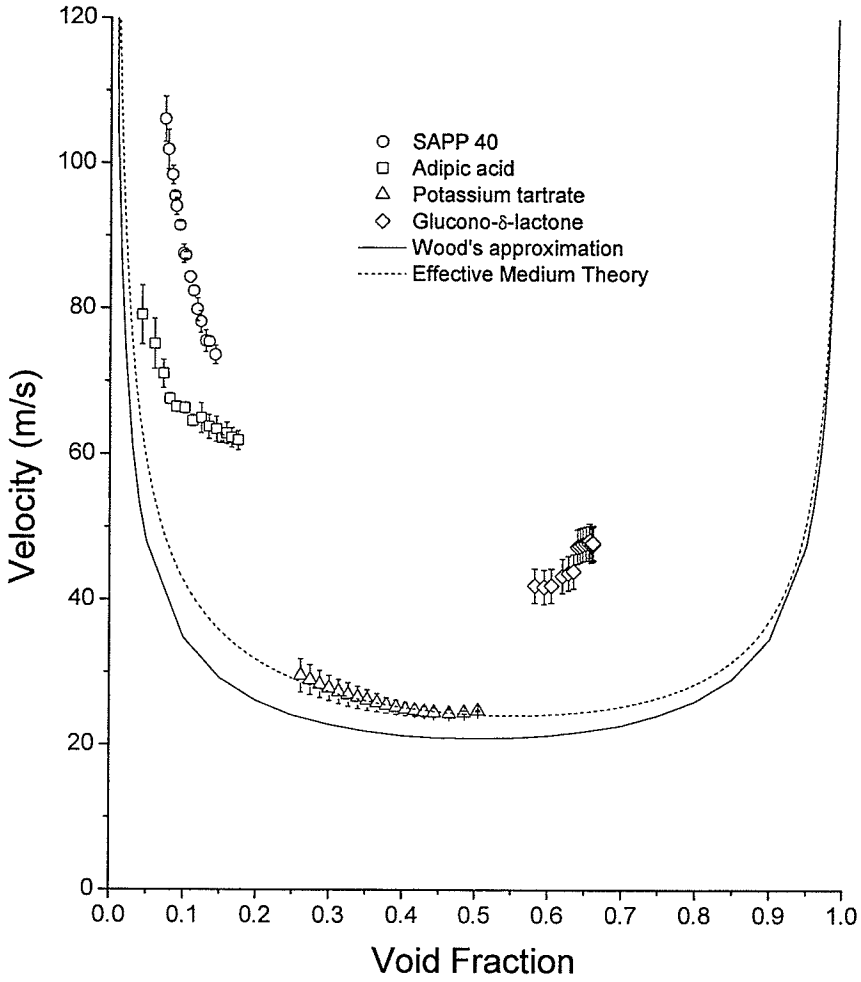

Figure 7.8. Velocity and associated error bars (± 1 SD) of ultrasound through dough that had been leavened using a chemical leavening system. The open symbols represent the chemical leavening system employed: 5.83 g SAPP 40 + 4.20 g sodium bicarbonate (circles); 1.22 g adipic acid + 1.40 g sodium bicarbonate (squares); 6.22 g potassium tartrate + 2.8 g sodium bicarbonate (triangles); 9.33 g GDL + 4.20 g sodium bicarbonate (rhombuses). Solid and dashed curves represent Wood's approximation and the EMT prediction (μ_m = [30 + 27 j] kPa), respectively.

sound velocities in fermenting yeasted doughs (130-85 m s^{-1}), a plot of sound velocity versus void fraction was not communicated. Depending on the leavening system employed, ultrasonic velocity dropped considerably by as much as 36% over 1 h of fermentation (SAPP and ADA dough), or it remained relatively constant in other systems (KAT or GDL dough). The rapid decrease in velocity for SAPP compared to ADA over essentially the same void fraction range suggests that there are mechanisms other than the void fraction which affected the velocity.

To interpret these data we looked at Wood's approximation (Wood, 1941), the simplest effective medium model for studying the propagation of sound waves in a multi-phase material, such as bubbles (inclusions) dispersed in a continuous matrix. According to Wood's approximation, the velocity of sound in a multi-phase material is controlled by the mean compressibility (κ_s) of the material. Mathematically this is equivalent to:

$$\kappa_s = \phi\kappa_i + (1-\phi)\kappa_m \tag{7.7}$$

Here ϕ denotes the gas void fraction, κ the compressibility and subscripts s, i, and m refer to sample, inclusion and matrix, respectively. Then, the velocity of sound in the system was given by the following equation:

$$\frac{1}{\rho_s v_s^2} = \frac{\phi}{\rho_i v_i^2} + \frac{(1-\phi)}{\rho_m v_m^2} \tag{7.8}$$

Since $\rho_s = \rho_i\phi + \rho_m(1-\phi)$ (Povey, 1997), Eq. (7.8) is equivalent to:

$$v_s = \left[\frac{\rho_i v_i^2 \rho_m v_m^2}{\phi\rho_m^2 v_m^2 - \phi^2\rho_m v_m^2 + \rho_m\rho_i v_i^2 - 2\phi\rho_m\rho_i v_i^2 + \phi^2\rho_m\rho_i v_i^2 + \phi^2\rho_i\rho_m v_m^2 + \phi\rho_i v_i^2 - \phi^2\rho_i v_i^2}\right]^{1/2} \tag{7.9}$$

When the inclusion is air, Eq. 7.9 can be re-written as:

$$v_s = \left[\frac{\rho_{air} v_{air}^2 \rho_m v_m^2}{\phi \rho_m^2 v_m^2 - \phi^2 \rho_m v_m^2 + \rho_m \rho_{air} v_{air}^2 - 2\phi \rho_m \rho_{air} v_{air}^2 + \phi^2 \rho_m \rho_{air} v_{air}^2 + \phi^2 \rho_{air} \rho_m v_m^2 + \phi \rho_{air} v_{air}^2 - \phi^2 \rho_{air} v_{air}^2} \right]^{1/2}$$

The resulting expression for the ultrasonic velocity (m s^{-1}) in the system is therefore (Eq. 7.10):

$$v_s = \left[\frac{1.29 * 330^2 * \rho_m v_m^2}{\phi \rho_m^2 v_m^2 - \phi^2 \rho_m v_m^2 + \rho_m * 1.29 * 330^2 - 2\phi \rho_m * 1.29 * 330^2 + \phi^2 \rho_m * 1.29 * 330^2 + \phi^2 * 1.29 * \rho_m v_m^2 + \phi * 1.29 * 330^2 - \phi^2 * 1.29 * 330^2} \right]^{1/2}$$

Letting v_m= 1,600 m s^{-1} (dough matrix velocity taken from ultrasonic velocity measured in dough at high frequencies by Létang et al., 2001) and ρ_m= 1,290 kg m^{-3}, Eq. 7.10 gives the solid curve shown in Figure 7.8. It can be seen that Wood's approximation predicts a velocity of sound at all void fractions lower than the velocities measured experimentally. This implied that there were factors other than the void fraction affecting the velocity of ultrasound in dough. It also suggested that the contribution of the shear modulus of the dough matrix to the properties of the dough could not be neglected (Elmehdi et al., 2004). An effective medium theory that makes use of the velocity and attenuation data to account for the viscoelastic nature of the dough was therefore invoked to describe the individual contributions of the bubbles and the dough matrix to the overall mechanical properties of the leavening doughs.

7.3.3. Attenuation coefficient

Figure 7.9 shows the relationship between the intensity attenuation coefficient and void fraction. Attenuation increased almost linearly with void fraction, particularly for SAPP and GDL dough. Linear fits to the data in Figure 7.9 found the following relationship between α [x 10^3 m^{-1}] and ϕ:

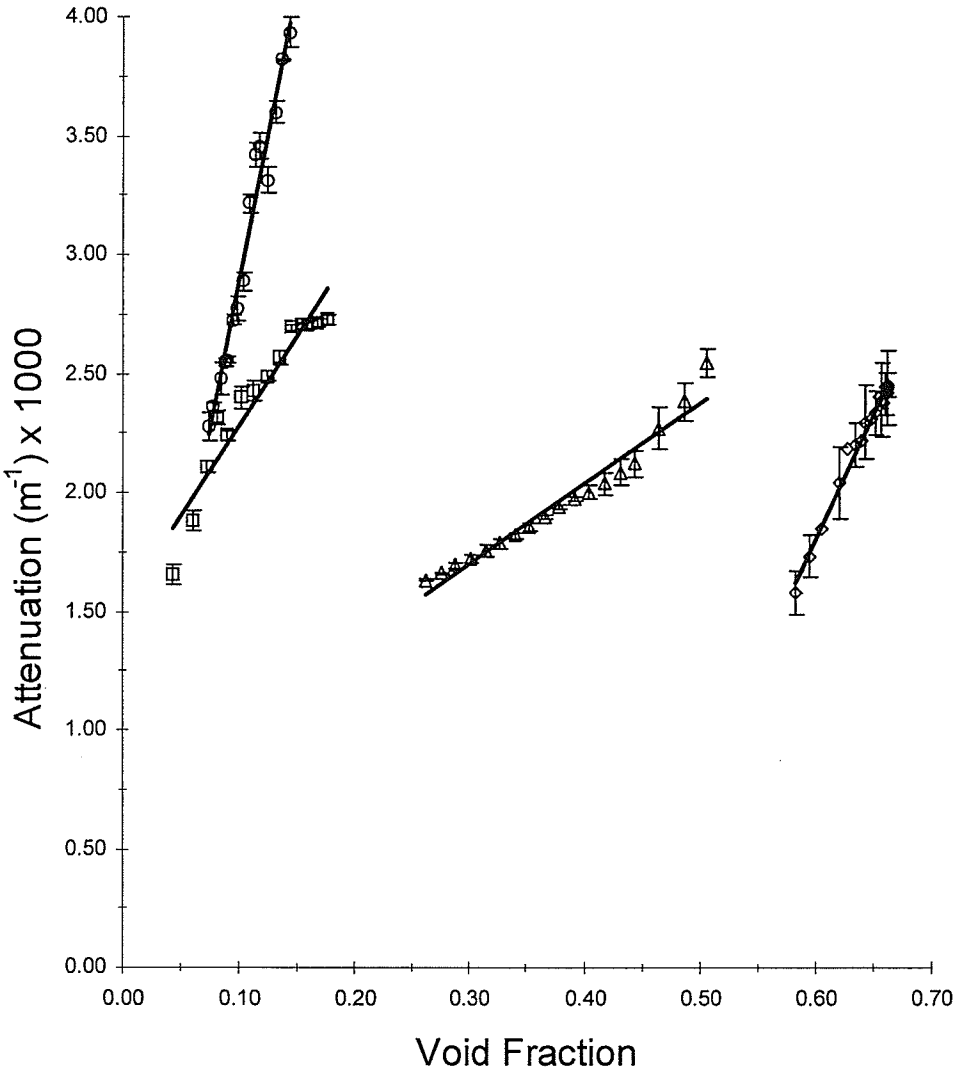

Figure 7.9. Behaviour of attenuation coefficient as a function of void fraction of chemically leavened dough. The symbols represent the chemical leavening system employed: 5.83 g SAPP 40 + 4.20 g sodium bicarbonate (circles); 1.22 g adipic acid + 1.40 g sodium bicarbonate (squares); 6.22 g potassium tartrate + 2.8 g sodium bicarbonate (triangles); 9.33 g GDL + 4.20 g sodium bicarbonate (rhombus). Vertical bars represent standard deviation.

SAPP: $\alpha = 25.20\ \phi + 0.374\ (R^2 = 0.97)$

ADA: $\alpha = 7.612\ \phi + 1.524\ (R^2 = 0.92)$

KAT: $\alpha = 3.383\ \phi + 0.687\ (R^2 = 0.95)$

GDL: $\alpha = 10.43\ \phi - 4.452\ (R^2 = 0.99)$

Because the void fraction of the doughs increased due to the carbon dioxide produced by the chemical leavening systems, the above equations suggest that shifting the chemical leavening reaction equilibrium to the right ($XH + NaHCO_3 \rightarrow NaX + CO_2$ (g) + H_2O; where XH denotes the acidulants) brought about an increase in the dissipative properties of the doughs to sound energy. Though an increase in gas void fraction reflects an increase in bubble size in the doughs due to CO_2 evolution, the accompanying by-products (anionic salts and water) and changes in concentration of reactants (neutralization of acidulants) are expected to affect the properties of the dough's liquid matrix during the course of chemical leavening. Elmehdi et al. (2003a) studied the effects of yeast leavening, where besides CO_2 and water, several organic acids are known to be produced (El-Dash & Johnson, 1970; Johnson & Sanchez, 1973; Wiseblatt & Kohn, 1960; Hoseney et al., 1981, 1988). Over the course of fermentation of a dough mixed under atmospheric conditions, Elmehdi et al. (2003a) found that the change in attenuation coefficient with respect to the change in void fraction was fairly linear ($\Delta\alpha/\Delta\phi$=6.2). The sound attenuating properties of chemically leavened dough as far as the ratio $\Delta\alpha/\Delta\phi$ is concerned spanned a range that included the value of 6.2 found by Elmehdi et al. (2003a). Further, Elmehdi et al.'s (2003a) yeasted dough system (the one mixed at atmospheric pressure) encompassed a range of densities from about 1200 to 650 kg m^{-3}, a range that was also covered by the four chemical leavening systems studied (1200-420 kg m^{-3}).

Hence, the above linear equations suggest that the ultrasonic attenuation coefficient was sensitive to not only the presence of the gas bubbles in the dough but also to the changes in the concentrations of reactants and by-products of the chemical leavening systems in the dough.

Qualitatively, the ranking of the experimental samples in terms of sound attenuation properties ($\Delta\alpha/\Delta\phi$) was the following, in descending order: SAPP > GDL > ADA > KAT. It is worth noting that the absolute attenuation coefficient of the experimental systems was obtained at slightly different frequencies (i.e., 10-35 kHz), depending on the leavening system employed, and hence care must be exercised when interpreting $\Delta\alpha/\Delta\phi$ data. Previous studies have ranked two other physical (i.e., rheological) properties for these four systems, gas retention capacity and consistency, as follows (in descending order): KAT > GDL > ADA > SAPP (gas retention; Chapter 5) and ADA > KAT ~ GDL > SAPP (consistency; Chapter 6). Clearly, no correlation could be established between $\Delta\alpha/\Delta\phi$ and gas retention capacity or between $\Delta\alpha/\Delta\phi$ and dough consistency, suggesting that attenuation alone could not provide sufficient information on the doughs so as to be able to predict their rheological behaviour.

7.3.4. Effective medium theory

The inability of Wood's approximation to predict the changes in ultrasonic velocity as a function of void fraction was indicative that a perspective of the dough as a purely viscous liquid was inadequate, and so the shear modulus of the dough could not be neglected. Sheng (1988) developed an Effective Medium Theory (EMT) that factors in velocity and attenuation data so as to account for the viscoelastic nature of the dough.

The EMT is based on an effective medium model for inclusions (gas cells) dispersed in a viscoelastic medium.

The EMT accounts for the shear modulus of the dough matrix in a model that exhibits the correct microstructure so that the role of microstructure on composite (bubble and matrix) properties can be delineated. In the EMT, the material under evaluation is modeled as elementary structural units embedded in a homogenous effective medium, whose properties (e.g., effective elastic moduli) are to be determined. For a leavening dough, the elementary unit can be taken as being a gas bubble surrounded by an amount of dough matrix that is determined so that the correct volume fraction of bubbles and matrix is preserved; this sets the radii of the "coated sphere" that represents the elementary structural unit. The mathematical problem consists in determining the scattering properties of the coated sphere when it is embedded in an effective homogeneous material whose properties are to be determined. The solution to the problem is found from the condition that the forward scattering amplitude of the scattering units embedded in the effective medium be zero (this is also referred to as the coherent potential approximation). Thus, given the elastic properties of the matrix and inclusions, the moduli of the effective medium representing the average material properties can be determined. Conversely, if the properties of the matrix are unknown, (as in our case), they can be determined by finding the values of the matrix moduli such that the predicted properties of the effective medium containing the coated spheres matches the experimentally measured properties. It is important to recognize that the condition of the effective medium theory is valid in the long wavelength limit where the wavelength of the probing wave (i.e., ultrasonic signal) is much longer than the

characteristic size of the coated spheres (wavelength >> size of bubbles). In this long wavelength limit, the ultrasonic waves cannot resolve individual scattering units (i.e., "the medium appears homogenous to the probing wave"; Sheng (1988)) and therefore there should be, on average, no net scattering of ultrasonic waves out of the input beam direction. The longitudinal modulus and shear modulus of the effective medium, respectively, are denoted β_{eff} and μ_{eff}, which are defined in the EMT as:

$$\beta_{eff} = \frac{\beta_m[4(\mu_m - \mu_i) + 3\beta_i]}{[4(\mu_m - \mu_i) + 3\beta_i](1-\phi) + 3\phi\beta_m} - \frac{4}{3}(\mu_m - \mu_{eff}) \tag{7.11}$$

$$A\left(\frac{\mu_{eff}}{\mu_m}\right)^2 + B\left(\frac{\mu_{eff}}{\mu_m}\right) + C = 0 \tag{7.12}$$

The subscripts i and m denote the inclusions (gas) and the matrix (dough matrix), respectively. The values for the constants A, B and C in equation 7.12 are defined in terms of the void fraction and a group of constants, k_2, k_3 and k_5, which in turn are defined by the following ratios of longitudinal and shear moduli for the matrix and the inclusions:

$$k_2 = \frac{\beta_m}{\mu_m} \qquad k_3 = \frac{\beta_i}{\mu_i} \qquad k_5 = \frac{\mu_m}{\mu_i} \tag{7.13}$$

The complete expressions for A, B and C can be found in Sheng (1988).

Because the attenuation of low intensity ultrasound in dough is significant, the effective longitudinal and shear moduli are complex, with both velocity and attenuation contributing to the real and imaginary parts ($j^2 = -1$) of μ_{eff} and β_{eff}:

$$\beta_{eff} = \beta'_{eff} + j\beta''_{eff}$$

$$\mu_{eff} = \mu_{eff}^{'} + j\mu_{eff}^{''}$$

To account for the dependence of the moduli on both v and α, the velocity of ultrasound, which was initially defined as having only a real component (Eq. 7.6), is made complex (v_c) and related to the complex wavevector, k_c, by $k_c = \omega/v_c$. Here ω is the angular frequency ($\omega = 2\pi f$), f is the ultrasonic frequency, and $k_c = \omega/v - j\alpha/2$. To relate the measurements of ultrasonic velocity (v) and attenuation (α) to the predictions of the EMT, the experimental values of the complex longitudinal modulus (β_{exp}) were calculated from the measurements of v and α from each dough system. The ultrasonic velocity and attenuation was related to the complex longitudinal modulus ($\beta = \beta' + j\beta''$) by (Elmehdi, 2001) :

$$\beta' = \frac{\rho v^2 (1 - \alpha^2 v^2 / 4\omega^2)}{(1 + \alpha^2 v^2 / 4\omega^2)^2} \tag{7.14}$$

$$\beta'' = \frac{\rho v^3 \alpha / \omega}{(1 + \alpha^2 v^2 / 4\omega^2)^2} \tag{7.15}$$

Substituting the ultrasonic data for the velocity and attenuation coefficient, along with the measured density, into Equations 7.14 and 7.15 enabled the calculation of the experimental longitudinal moduli $\beta_{exp}^{'}$ and $\beta_{exp}^{''}$ over the range of void fractions studied (Figures 7.10-7.13). Equations 7.14 and 7.15 can also be rearranged so as to express v and α in terms of β' and β'' (Elmehdi, 2001):

$$v = \sqrt{\frac{2}{\rho}\left(\frac{\beta'^2 + \beta''^2}{\beta' + \sqrt{\beta'^2 + \beta''^2}}\right)} \tag{7.16}$$

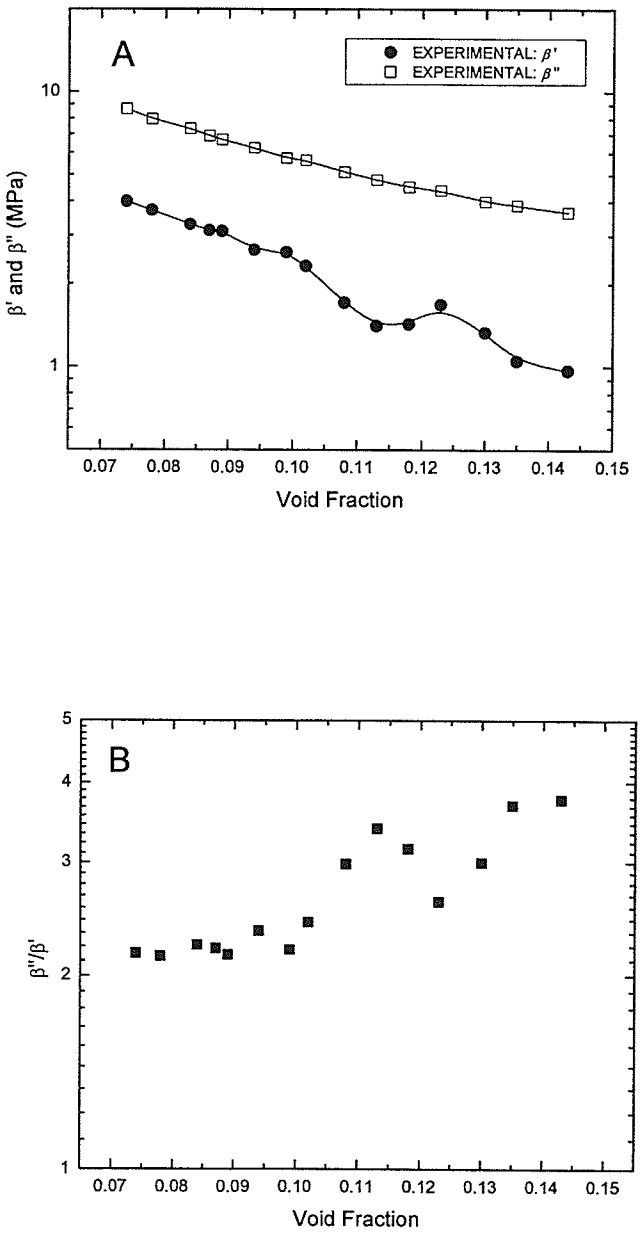

Figure 7.10. Longitudinal moduli (A) and ratio of imaginary and real parts (B) as a function of void fraction in dough that had been chemically leavened with SAPP 40.

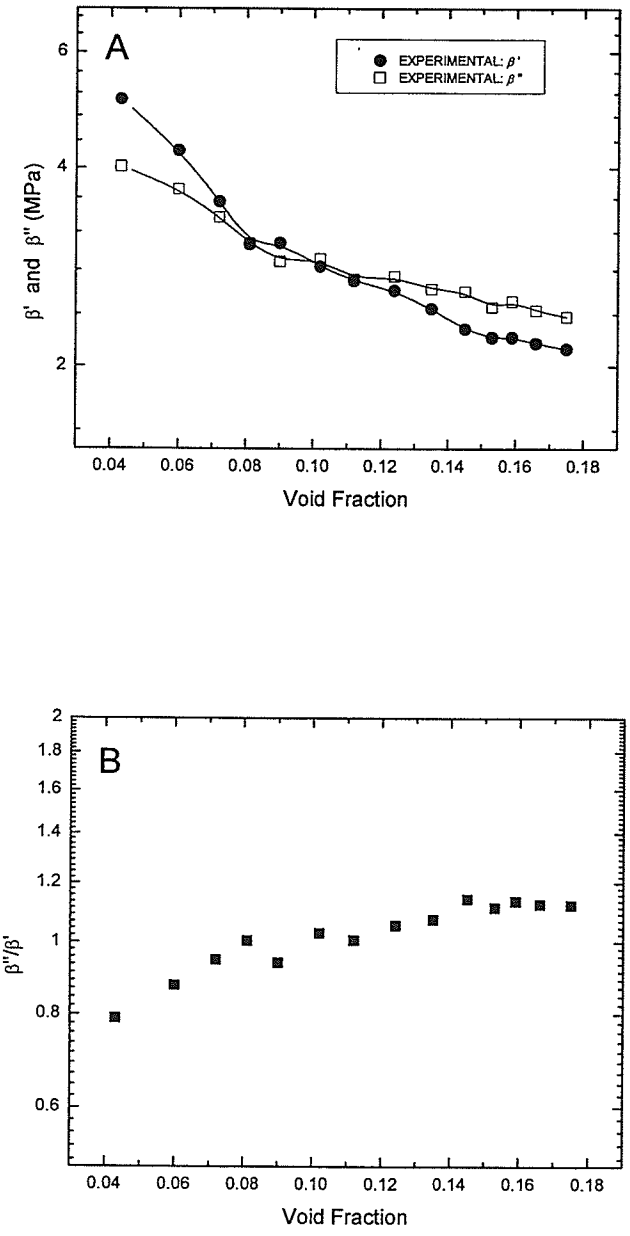

Figure 7.11. Longitudinal moduli (A) and ratio of imaginary to real parts (B) as a function of void fraction in dough that had been chemically leavened with adipic acid.

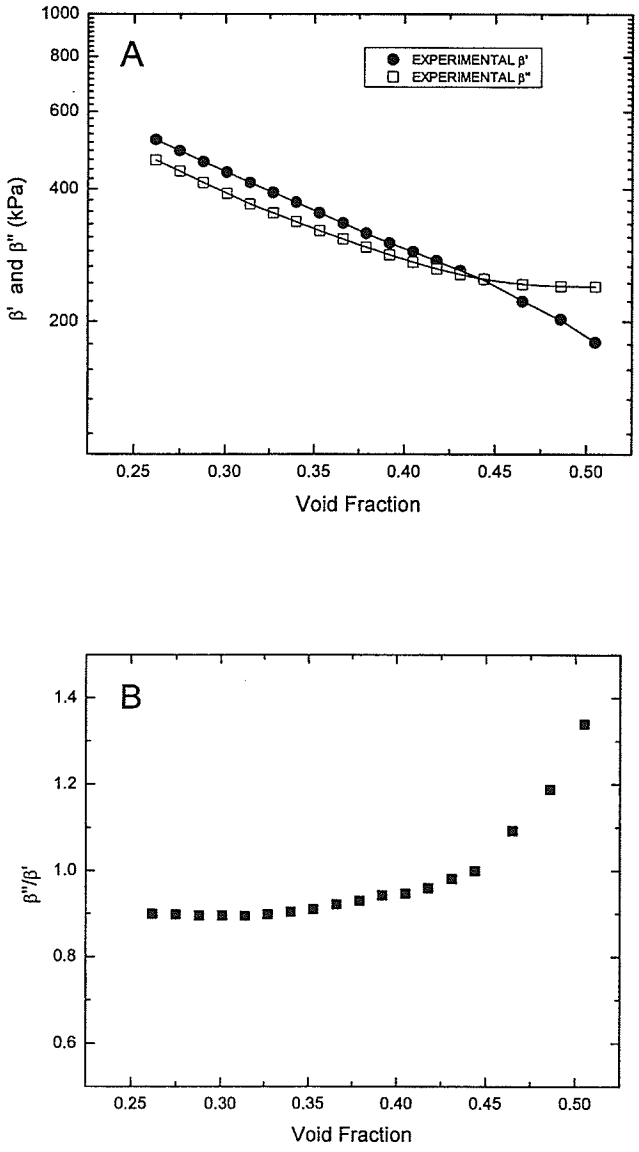

Figure 7.12. Longitudinal moduli (A) and ratio of imaginary and real parts (B) as a function of void fraction in dough that had been chemically leavened with potassium acid tartrate.

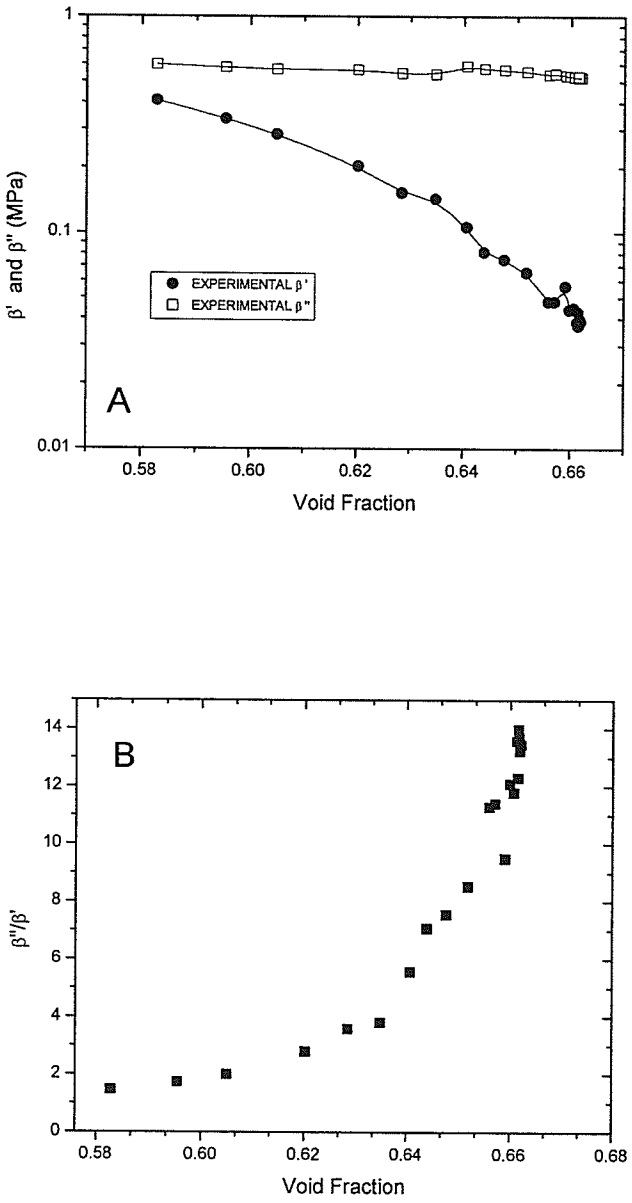

Figure 7.13. Longitudinal moduli (A) and ratio of imaginary and real parts (B) as a function of void fraction in dough that had been chemically leavened with glucono-delta-lactone.

$$\alpha = \omega \sqrt{2\rho \left(\frac{\sqrt{\beta'^2 + \beta''^2} - \beta'}{\beta'^2 + \beta''^2} \right)} \tag{7.17}$$

A first step in fitting the EMT to the experimental data was assigning the values of the longitudinal and shear moduli for the matrix and inclusions using information from the literature. Elmehdi (2001) made a thorough review of the literature and compiled the following literature-based estimates of properties at 50 kHz: $\beta_m' = 3$ GPa and $\beta_m'' = 2.5$ GPa (Létang et al., 1996); $\mu_m' = 30$ kPa (Bloksma, 1990a; Faubion et al., 1985); $\mu_m'' = 27$ kPa (Bloksma, 1990b; Faubion et al., 1985); $\beta_i' = 150$ kPa and $\beta_i'' \sim 4$ Pa (Anderson, 1989); and $\mu_i' = \mu_i'' = 1$ Pa. Using these eight parameters and a matrix density of 1,237 kgm^{-3} (KAT dough), a FORTRAN program predicted the velocity behaviour of ultrasound as a function of ϕ (shown as dashed curve of Figure 7.8). (An insignificant change in this EMT prediction occurred when one of the other three experimental gas-free dough densities was employed instead of KAT).

A first approximation to evaluate the suitability of the values chosen for the longitudinal and shear moduli of the matrix and inclusions is to compare the EMT prediction of velocity as a function of void fraction in relation to the experimental data. Figure 7.8 shows that using the literature-derived shear modulus of the dough matrix ($\mu_m = 30 + j\ 27$ kPa), the EMT predicted well the dependence of sound velocity on gas void fraction in the KAT dough system for most of its void fraction range. However, at higher and at lower void fractions the model does not describe the data, as the experimental velocity for SAPP, ADA and GDL was always higher than predicted using this particular value for μ_m. This discrepancy suggested that, compared to KAT dough, the shear

modulus of the dough liquid matrix of SAPP, ADA and GDL was stiffer. Increasing the elastic moduli of the matrix of the dough should increase the values of the predicted sound velocities made by the EMT (Elmehdi, 2001). Quantitatively, the parameters $\beta_m^{'}$, $\beta_m^{''}$, $\mu_m^{'}$ and $\mu_m^{''}$ needed to be varied iteratively until the predictions of the EMT would fit the ultrasonic data. Although as a first approximation it is reasonable to evaluate the suitability of the EMT to predict only the void fraction dependence of the velocity data, for the EMT to work effectively, the selected values for the said four parameters should be such that the EMT must be able to predict the void fraction dependence of both the ultrasonic velocity and the attenuation data simultaneously.

Provided that ϕ was not zero or nearly zero, it was found that varying the values originally assigned to $\beta_m^{'}$ and $\beta_m^{''}$ (within physically possible ranges) had little effect on the velocity and attenuation coefficients predicted by the EMT. For example, by changing $\beta_m^{'}$ by an order of magnitude to be 30 GPa, a velocity of 35 ms^{-1} at $\phi = 0.15$ was obtained, compared to the value of 34 ms^{-1} in Figure 7.8. Hence, the only parameters that could account for higher than predicted velocities at low void fractions were $\mu_m^{'}$ and $\mu_m^{''}$. Therefore, fitting the predictions of the EMT simultaneously to both velocity versus void fraction and attenuation versus void fraction experimental data, was an unambiguous way of assigning values to $\mu_m^{'}$ and $\mu_m^{''}$ (Elmehdi, 2001). For each value of ϕ, a set of values for $\mu_m^{'}$ and $\mu_m^{''}$ were fitted, so that the families of curves that were generated passed through the experimental data points for β' and β'', or, equivalently, for v and α (Elmehdi, 2001). The results of this fitting analysis to predictions of v and α can be seen in Figures 7.14 to 7.16.

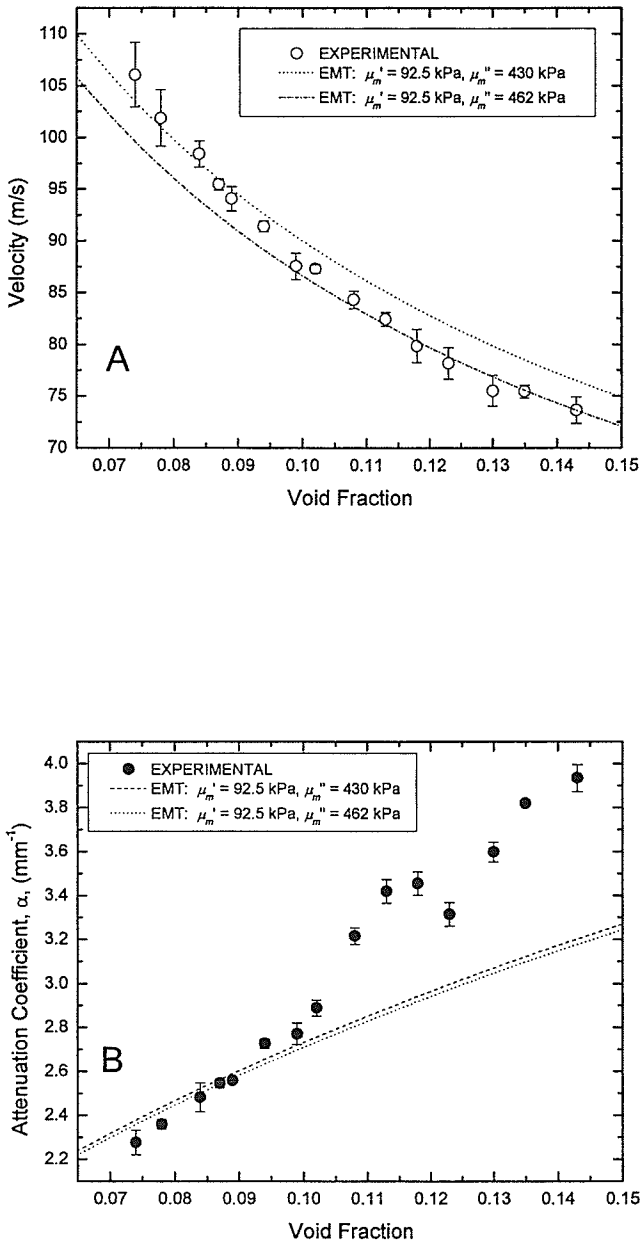

Figure 7.14. Void fraction dependence of velocity of sound (A) and attenuation coefficient (B) in dough that had been chemically leavened with SAPP 40. The curves represent predictions from the effective medium theory at the specified μ_m values.

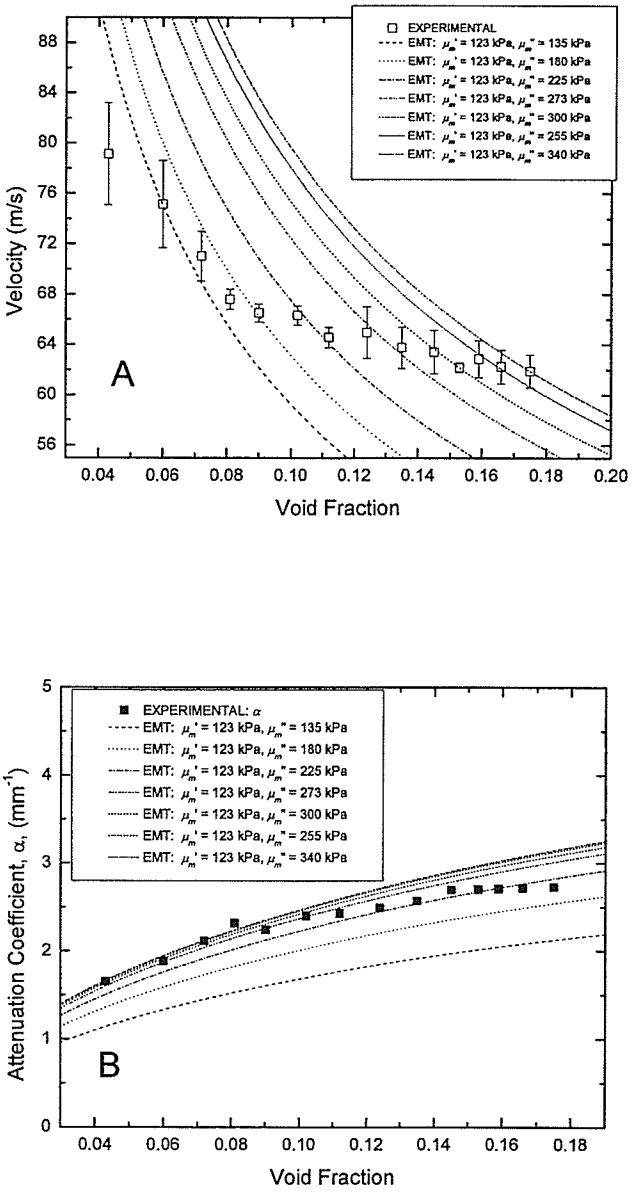

Figure 7.15. Void fraction dependence of velocity of sound (A) and attenuation coefficient (B) in dough that had been chemically leavened with adipic acid. The curves represent predictions from the effective medium theory at the specified μ_m values.

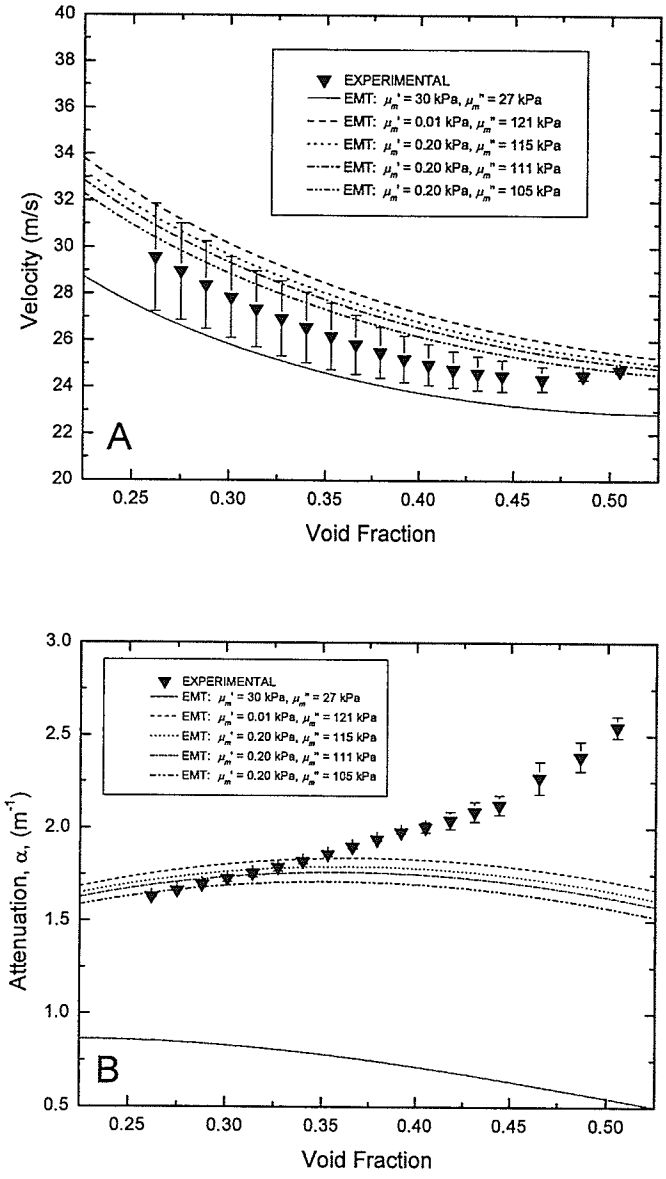

Figure 7.16. Void fraction dependence of velocity of sound (A) and attenuation coefficient (B) in dough that had been chemically leavened with potassium acid tartrate. The curves represent predictions from the effective medium theory at the specified μ_m values.

With the exception of the SAPP dough, Figures 7.14 to 7.16 show that the EMT had difficulty in predicting the void fraction dependence of both the velocity and attenuation data. For example, even though the predictions of the EMT using the literature-derived shear modulus (μ_m=30 + j 27 kPa) were suitable to describe the void fraction dependence of ultrasonic velocity in KAT dough, they did not describe the dependence of the attenuation coefficient on void fraction (Figure 7.16) using these values of μ_m' and μ_m''. Efforts to fit these data for KAT dough using other values of the matrix shear modulus were not successful, especially for the higher void fractions (Figure 7.16). The likely cause of this discrepancy, and the similar difficulties with fitting the velocity and attenuation of GDL and ADA doughs, is that in these aerated doughs, the characteristic size of the inclusions (i.e., bubbles) was so large that the long wavelength effective medium limit was no longer valid. In this regime, it then becomes necessary to account for higher order scattering contributions associated with the low frequency tail of the resonant interaction of ultrasound with the bubbles (Leroy et al., 2007) and these effects are not included in the EMT. Therefore, attempts to model the rheological behaviour of ADA, KAT and GDL doughs by the EMT were not pursued further. Changes in the mechanical properties (β_{exp}' and β_{exp}'') of experimental doughs, as probed by ultrasound, will therefore be discussed in light of the void fraction dependence of β_{exp}' and β_{exp}'' (Figures 7.10-7.13), with the only exception being the SAPP dough, whose void fraction dependence on μ_m' and μ_m'' will be discussed, as in this dough system the EMT was able to decouple the contribution of the dough matrix and of gas cell expansion to the overall mechanical properties of the dough during fermentation. The ability of the EMT to elucidate the contributions of the matrix and gas phase to the properties of the

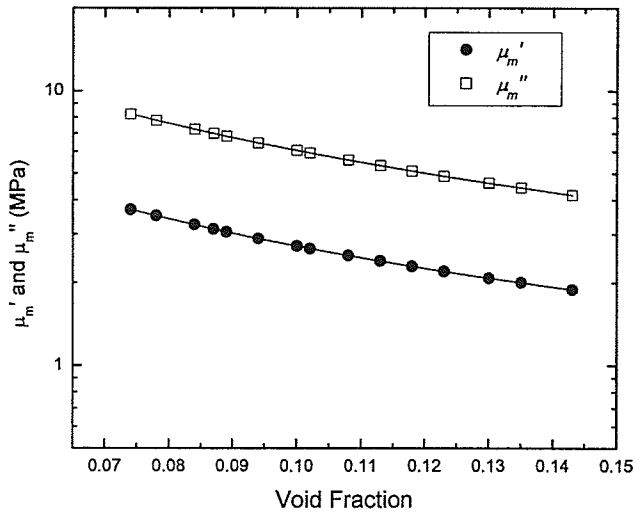

Figure 7.17. The dependence of μ_m' and μ_m'' on void fraction as determined from the effective medium theory. Dough chemically leavened with 5.83 g SAPP 40 and 4.20 g sodium bicarbonate.

SAPP dough can be seen in Figure 7.14A and 7.14B. These two figures show that the predictions of the EMT described reasonably well the ultrasonic properties (i.e., v and α) of SAPP dough, with the only disagreement being that in the high void fraction limit, the matrix properties were more dissipative than the EMT model predicted. As shown in Figure 7.17, the predictions made by the EMT were used to determine the dependence of $\mu_m^{'}$ and $\mu_m^{''}$ on ϕ for the SAPP dough.

The effects of chemical leavening on the mechanical properties of dough are shown in Figures 7.10 to 7.14. From them, one can calculate the absolute value of the longitudinal bulk modulus $\beta_{exp}^{*}\left(=\sqrt{\left(\beta_{exp}^{'}\right)^2+\left(\beta_{exp}^{''}\right)^2}\right)$ as a function of void fraction to observe that, overall, experimental results showed that β_{exp}^{*} decreased with increases in

void fraction (ϕ). β^{*}_{exp} decreased from 10 to 4 MPa when ϕ increased from 7 to 10% (SAPP), from 7 to 3 MPa when ϕ increased from 4 to 18% (ADA), from 0.7 to 0.3 MPa when ϕ increased from 26 to 51% (KAT), and from 0.7 to 0.5 MPa when ϕ increased from 58 to 66% for the GDL dough. The increased in void fraction observed in each of the dough systems was also accompanied by increased losses of mechanical energy ($\beta''_{exp} / \beta'_{exp}$) (Figures 7.10-7.14). The amplification of mechanical energy losses during the course of fermentation, $\Delta\left(\beta''_{exp} / \beta'_{exp}\right)$, on a percentage basis, was 60%, 40%, 50% and 700% for SAPP, ADA, KAT and GDL doughs, respectively. Clearly, expansion of the gas void fraction was associated with a large decrease in dough mechanical strength, though it must be recognized that changes in gas void fraction alone may not account for the observed changes in dough mechanical properties for all systems.

7.3.5. Progressive changes in matrix properties

7.3.5.1. Influence of the relaxation of the dough

One factor that may have affected the ultrasonic data is dough relaxation. Internal stresses in the dough arising from the stretching action of the mixing step are expected to relax over time. Sample preparation procedures following mixing may also contribute to dough relaxation effects. The influence of dough relaxation on ultrasonic velocity was quantified by Elmehdi et al. (2004). They found that ultrasonic velocity dropped by no more than 2 m s^{-1} over the course of 2h, with most of the effects being seeing within the first 15 min following the end of mixing. Therefore, relaxation effects alone cannot explain the observed changes in dough mechanical properties.

7.3.5.2. Influence of water liberated from the chemical leaveners

Because losses of mechanical energy ($\beta''_{exp}/\beta'_{exp}$ or μ''_m/μ'_m) in chemically fermenting dough are expected to increase with moisture content (Elmehdi, 2001; Kidmose et al., 2001), determining the effects of chemical leavening on water production needed to be investigated. Stoichiometry of the chemical leavening reaction dictates that for every mol of CO_2 produced, a mol of water is released into the dough matrix (Heidolph, 1996). To quantify the water produced during dough fermentation, knowledge on the stoichiometry of the chemical neutralization reaction is required (Chapter 4). Stoichiometry indicates that the number of moles of CO_2 and water produced from the leavening system is equivalent to the number of moles of sodium bicarbonate in the formula. The formula of the leavening systems SAPP, ADA, KAT, and GDL contained 50 mmol (= 4.20 g/0.084 g $mmol^{-1}$), 17 mmol (= 1.40 g/0.084 g $mmol^{-1}$), 33 mmol (= 2.80 g/0.084 g $mmol^{-1}$), and 50 mmol (= 4.20 g/0.084 g $mmol^{-1}$) of sodium bicarbonate, respectively. However, since sodium bicarbonate is not 100% neutralized during chemical leavening (Chapter 4), the conversion of sodium bicarbonate into water (or CO_2) was only partial. The percentage of sodium bicarbonate reacting during chemical leavening could be derived from the amount of CO_2 evolved from the system at the same conditions. Data from gas production experiments (Chapter 4) showed that the leavening system made of SAPP was capable of evolving 48% of the available sodium bicarbonate, ADA 80%, KAT 84 %, and GDL 98%. Therefore, for the SAPP, ADA, KAT, and GDL doughs, only 24 mmol (= 50 mmol x 48%), 14 mmol (= 17 mmol x 80 %), 28 mmol (= 33 mmol x 84 %), and 49 mmol (=50 mmol x 98%) of sodium bicarbonate were converted into CO_2, respectively, with an equal number of moles of water being

incorporated into the matrix. This quantity of water, on a percentage basis, would have increased the water content in the dough by 0.24 % [= (24 mmol x 0.018 g $mmol^{-1}$)/178.18 g x 100%], 0.15 % [= (14 mmol x 0.018 g $mmol^{-1}$)/170.77 g x 100%], 0.28% [= (28 mmol x 0.018 g $mmol^{-1}$)/177.14 g x 100%], and 0.48% [= (49 mmol x 0.018 g $mmol^{-1}$)/183.9 g x 100%] for SAPP, ADA, KAT, and GDL doughs, respectively. Considering that a loss of 1% in dough moisture content is associated with an ultrasonic velocity change of ~ 35 ms^{-1} (assuming linearity of the velocity versus frequency data of Létang *et al.*, 2001), the water released would account for an ultrasonic velocity change of only 8 ms^{-1}, 5 ms^{-1}, 10 ms^{-1}, and 17 ms^{-1} in SAPP, ADA, KAT, and GDL doughs, respectively. Therefore, water liberation from the chemical neutralization reaction was likely not responsible for the observed changes in the mechanical properties of fermenting dough.

7.3.5.3. Influence of the reactants and by-products from chemical leavening

An alternative interpretation of the changes observed in the mechanical properties of the experimental dough is that the reactants and reaction by-products from the chemical leaveners affected the properties of the gluten proteins. Gluten protein rheology has the major influence on the rheology of the dough (Belton, 1996; Bushuk, 1985; Ewart, 1989; Abdelrahman & Spies, 1986; Belton & Dobraszczyk, 2006; Bloksma & Bushuk, 1988; Faergestad et al., 2004; Faubion et al., 1985; Xu et al., 2001). An essential consideration to understand how reactants and reaction by-products affected gluten proteins is looking at the course of events taking place during chemical leavening.

Changes in the mechanical properties of the chemically leavened dough are brought about by the evolution of the chemical leavening reaction:

$$XH + H_2O \rightarrow X^- + H_3O^+$$

$$X^- + H_3O^+ + NaHCO_3 \rightarrow NaX + CO_2\,(g) + H_2O$$

where, XH denotes in here sodium acid pyrophosphate 40, adipic acid, potassium acid tartrate, or glucono-δ-lactone, and X^- denotes the pyrophosphate, adipate, tartrate, or gluconate anions. The mechanisms giving rise to the changes in mechanical properties of SAPP, ADA, KAT and GDL doughs are likely related to the transformation of the acids (i.e., adipic acid and glucono-delta-lactone) or the acidic salts (i.e., tetrasodium pyrophosphate and sodium potassium acid tartrate) into the anionic salts (i.e., adipate, gluconate, pyrophosphate and tartrate anions) and carbonic acid. As carbonic acid is dissolved in the dough liquid matrix, the pH of the dough is expected to drop (Scanlon et al., 2002). These events, i.e., changes in the concentration of reactant and by-products, are likely responsible for the observed increase in mechanical energy losses as chemical leavening proceeded.

For SAPP dough, the EMT shows that the matrix of the dough had a viscous-like behaviour throughout the course of fermentation (Figure 7.17), with losses in mechanical energy (i.e., $\mu_m^{''}/\mu_m^{'}$) at the end of fermentation being nearly twice as much as those registered at the onset of fermentation (Figure 7.10). The pH of SAPP dough (pH = 7.2) at the end of fermentation (Table 7.1) suggests that the gluten proteins had a small net positive charge (Kinsella & Hale, 1984; Wu & Dimler, 1963a,); this pH was within expected values (pH=7.3-7.6) according to the literature (Conn, 1981; Heidolph, 1996; Cepeda et al., 2000). At a pH of 7.2, based on the distribution of anionic species of pyrophosphate (McGilvery & Crowther, 1953), it is reasonable to assume that the only anionic species of pyrophosphate present in the dough are $H_2P_2O_7^{2-}$, $HP_2O_7^{3-}$ and $P_2O_7^{4-}$

Table 7.1. The effect of chemical leavening systems on dough pH[a]

Chemical leavening system[b]	pH
Control	5.5
Control + 2.8 g $NaHCO_3$	7.9
SAPP[c]	7.2
ADA[c]	6.1
KAT[c]	5.8
GDL[c]	5.7

[a] Measured after the dough was turned into a slurry. See text for details.
[b] Control = [100 g CWRS flour (14% m.b.) + 67% water + 0.75 % NaCl]; SAPP = [Control + 5.83% sodium pyrophosphate 40 + 4.2% $NaHCO_3$]; ADA = [Control + 1.22% adipic acid + 1.40% $NaHCO_3$]; KAT = [Control + 6.22% potassium acid tartrate + 2.80% $NaHCO_3$]; GDL = [Control + 9.33% glucono-δ-lactone + 4.20% $NaHCO_3$].
[c] Measured at the end of fermentation (~ 60 min after the end of mixing)

(Figure 4.6). In terms of its effects on proteins, the pyrophosphate anion is expected to exert similar ionic (i.e., lyotropic) effects as phosphate anions (PO_4^{-3}) on the rheology of gluten protein (Conn, 1981).

Addition of the phosphate anion to doughs have been shown to weaken the gluten protein network (Holmes & Hoseney, 1987a), possibly due to the non-chaotropicity of this anion (Preston, 1981). The interaction of anionic salts, such as phosphate and tartrate, with gluten proteins is thought to be mediated via their effect on water structure (i.e., based on salt lyotropicity). Kinsella and Hale (1984) explained that non-chaotropic anions accentuate hydrophobic interactions between gluten protein molecules by increasing the ordering of water structure (i.e., by increasing the structure of water molecules). Eliasson and Larsson (1993) indicate that non-chaotropic anions induce weakening of the gluten protein structure by binding itself to the positively charged groups on the surface of the protein, which would also lead to an increase in hydrophobic interactions between and among gluten protein chains, and, thus, protein aggregation.

Hence, salts such as phosphate and tartrate would cause gluten proteins to remain more aggregated and more resistant to hydration during mixing which would impair the formation of subsequent protein-protein interactions or physical entanglements in the dough (Kinsella & Hale, 1984). The deleterious effects of non-chaotropic salts on gluten protein network formation were observed as a reduction in dough strength by Guy et al. (1967) and a drop in gas retention capacity by Holmes and Hoseney (1987a). This increase in protein aggregation was also observed in the study of Preston (1981) in which the extractability and the turbidity of gluten proteins extracted in dilute acetic acid solutions decreased and increased, respectively, with increasing concentrations of non-chaotropic sodium salts. Lyotropic anions with a larger negative charge (e.g., $P_2O_7^{4-}$ compared to $HP_2O_7^{3-}$) are expected to increase the charge density of the protein surfaces to which they bind (Tatham et al., 1983) and hence augment the weakening effects on gluten proteins due to electrostatic repulsions (Preston, 1981). This would explain the higher mechanical losses detected in SAPP dough as the reaction proceeded (i.e., as the reaction proceeds more $P_2O_7^{4-}$ accumulates in the dough since this anion is a reaction by-product). Therefore, the theory of the weakening effects of phosphate ions on gluten proteins supports the viscous-like shear modulus of the dough matrix ($\mu_m'' > \mu_m'$; Figure 7.17) and of the dough ($\beta_{exp}'' > \beta_{exp}'$; Figure 7.10) obtained from interpreting ultrasonic velocity and attenuation measurements of SAPP dough by the EMT.

The difficulty of the EMT to actually predict the matrix properties of the experimental doughs (except for the SAPP dough) as a function of void fraction prompted the use of an alternative means of determining whether or not matrix properties in the dough varied during the course of fermentation. In order to do so, bounds for the

phase velocity in dough were estimated using bounds based on the properties of the dough as per Hashin and Shtrikman (1963). The upper and lower Hashin and Shtrikman bounds can be calculated using the best estimates of the moduli of the two-phase system (i.e., the dough matrix and the gas bubbles). For a two-phase system such as dough, the lower bound is given by Wood's approximation (for the range of void fractions studied) due to the high compressibility of the gas bubbles (Elmehdi et al., 2004). An estimate of the upper Hashin and Shtrikman bound can be calculated from the best estimates of the constituent moduli for the dough. For unyeasted dough, the estimated upper bound would be given by the EMT curve shown in Figure 7.8 (dashed curve) since this curve was calculated using the best estimates of the constituent moduli for the dough based on literature values for $\beta_m^{'}$, $\beta_m^{''}$, $\mu_m^{'}$ and $\mu_m^{''}$. Hence the fact that the measured velocities of doughs were outside the estimated Hashin and Shtrikman bounds can be interpreted as evidence that the properties of the dough matrix changed (i.e., shear modulus increased) as a function of void fraction (maybe less so for SAPP and KAT). The influence of acids or salts on the matrix of dough can be speculated based on the available scientific literature. Two main mechanisms can be highlighted: the pH lowering effects of the leavening acid and the salt-induced effects of the reacted salts on the rheology of dough gluten proteins.

Although the presence of a large concentration of bubbles appears to control the bulk mechanical properties of KAT dough, as one can judge from the upper Hashin and Shtrikman bound (Figure 7.8), the increased dissipative character of the dough as fermentation proceeds (Figure 7.12) may also be due to the conversion of the acidic salt into a reacted salt. As with pyrophosphate, the tartrate anion is a non-chaotropic anion

that is expected to influence gluten proteins via lyotropic effects, though to a lesser degree than the pyrophosphate anion as it ranks higher than tartrate in the lyotropic Hofmeister series (Eliasson & Larsson, 1993; Holmes & Hoseney, 1987a). However, the lyotropic effects of the acidic salt (potassium acid tartrate) and the reacted salt (potassium sodium tartrate) in KAT are expected to be similar due to the presence of the tartrate anion in both these chemical species – this is in contrast to the poly-anionic forms of pyrophosphate being produced in this dough as fermentation progresses. Conversely, the stronger ability of KAT to lower the pH of the dough matrix compared to SAPP (Table 7.1) suggests that the acidic salt (potassium acid tartrate), by virtue of its pH lowering effects, would have a stronger effect on matrix properties than the reacted salt.

Unlike pyrophosphate or tartrate anions, the aliphatic chemical structures of adipate and gluconate anions in ADA and GDL doughs, respectively, would be expected to hamper their ability to exert significant lyotropic effects on gluten proteins. Hence, it would also be expected that as fermentation progresses the conversion of acids into salts would weaken the matrix properties of ADA and GDL doughs, mainly due to the acidification of the dough matrix. This in line with the Extensigraph data reported by Tanaka et al. (1967) who found that acidification of the dough (pH= 5.8-4.2) with acetic acid in the presence of a 3% sodium chloride, brought about a nearly linear decrease in dough extensibility. Similarly, Galal et al. (1978) studied the combined effects of organic acids on dough rheological properties. They noted that the Farinograph dough stability (measured in minutes) for the dough dropped considerably (~ 9 min) after incorporating organic acids (a mix of lactic [80%] and acetic [19%] acids) to the formula. However, for GDL doughs, the large increase in the dissipative properties observed at high void

fractions (Figure 7.13) are likely not due to the transformation of acids into salts (e.g., ADA and GDL are two organic acids that are expected to exert similar effects on gluten proteins; Galal et al., 1978; Heidolph, 1996), but due to large strains at the gas cell wall interface (Babin et al., 2006; Dobraszczyk et al., 2003). Very recently, using x-ray microtomography, Babin et al. (2006) observed that the dough matrix undergoes dramatic structural changes (more so than theoretically predicted; e.g., Bloskma, 1990a), including bubble coalescence, in well aerated dough ($\phi > 40\%$). Structural re-arrangements of the gas cell wall to accommodate the growing bubbles or coalescing bubbles are likely to influence the dough mechanical properties and ultrasound appears to be sensitive to such changes.

Some evidence for the proposed molecular mechanisms explaining the observed changes in dough rheological properties was found in an experiment using doughs prepared with either the leavening acid alone or the fully reacted salts (Figure 7.18). The influence of glucono-delta-lactone on dough mechanical properties was not studied but it was expected to be similar to that of adipic acid, as both are organic acidulants (Galal et al., 1978; Heidolph, 1996). To prepare the reacted salts in this experiment (n=2), the chemical leavening system (leavening acid and sodium bicarbonate) was reacted on the side using a portion of the formula water and then added to the rest of the formula ingredients [flour (100 g), sodium chloride (0.75 g) and the difference in formula water (to make up 69.6 g)], following the procedure outlined in the Materials and Methods. Figure 7.18 shows that a greater reduction in ultrasonic velocity was observed in doughs prepared with the leavening acids than with the reacted salts. Kidmose et al. (2001), using comparable ultrasonic frequencies (37 kHz), found that lower ultrasonic velocities are

associated with weaker doughs (as probed by conventional small strain oscillatory rheometry). Hence, results indicate that the leavening acid had a stronger weakening effect on the dough mechanical properties than its corresponding salts did. The difference between the velocities for the acidic and salt forms of the leavener can be interpreted as the contribution of acidification of dough matrix to the mechanical properties of the dough. The contribution of the gas phase, though certainly important, can be regarded as small due to the low void fractions in these dough systems (<5%). Substantial weakening effects on the dough mechanical properties due to acidification were associated with adipic acid compared to the acidic salts (i.e., SAPP and KAT). Furthermore, Figure 7.18 shows that both the acidic and the reacted salt forms of SAPP or KAT had similar effects on velocity, with slightly stronger weakening effects associated with potassium acid tartrate likely because of its stronger pH lowering effects compared to SAPP (Table 7.1).

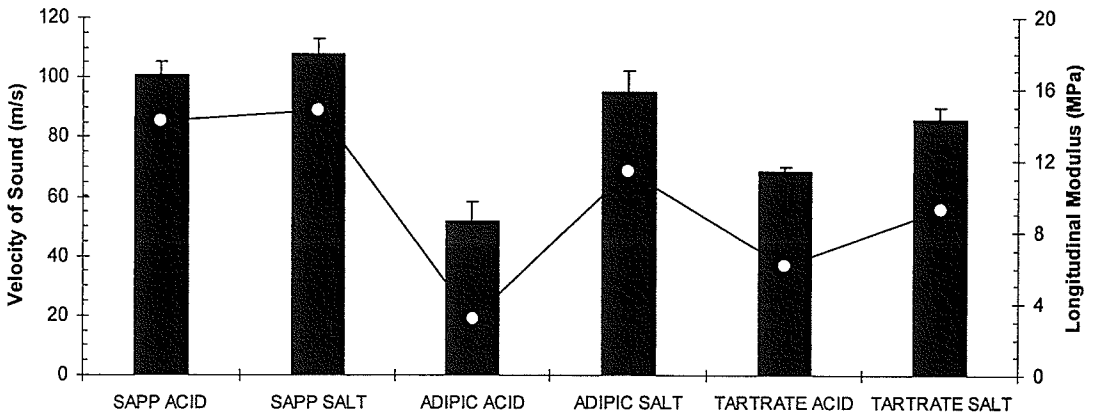

Figure 7.18. Velocity of sound (columns) and longitudinal modulus (circles connected by a line) in non-leavening dough that had been formulated with 5.83 g SAPP 40 (SAPP ACID), 1.22 g adipic acid (ADIPIC ACID), or 2.8 g potassium acid tartrate (TARTRATE ACID) or with a salt resulting from the complete neutralization of the leavening acid with sodium bicarbonate (see text).

Elucidating the structure of dough or ascribing specific mechanisms to the velocity and attenuation data is nevertheless difficult due the complex nature of this inhomogeneous material. A definitive interpretation of the velocity and attenuation data will require more extensive experimentation, particularly the extent to which various types and levels of lyotropic salts and organic acidulants affect dough rheology as probed by ultrasound.

7.4. Conclusions

Measurements of velocity and attenuation of low intensity ultrasound (40 kHz) in chemically leavened dough were able to provide information on its mechanical properties as fermentation actually occurred. Four chemical leavening agents were able to produce dough with a void fraction that ranged from 4 % to nearly 66% when fermented at typical ambient temperature. As void fraction increased, the velocity of ultrasound dropped from nearly 110 m/s to nearly 30 m/s. Changes in void fraction alone (i.e., bubble growth) could not account for all the observed changes in ultrasonic velocity, suggesting that ultrasonic properties were also sensitive to the presence of fermentation by-products (e.g., salts) through the effect of these by-products on the mechanical properties of the dough matrix.

An effective medium theory, which makes use of the velocity and attenuation data to account for the viscoelastic nature of the dough, was capable of describing the individual contributions of the bubbles and the dough matrix to the overall mechanical properties of dough prepared with SAPP. The EMT had its limitations as well. It had difficulty in predicting the increased mechanical energy losses observed in ADA, KAT and GDL doughs as the leaveners continued evolving CO_2. It was surmised that this was

so because the EMT was unable to predict the highly attenuative properties of the doughs, or because the condition that ultrasound wavelength be much longer than the average size of the inclusions (bubble size) was no longer satisfied and so the model would not work. The longitudinal elastic modulus of the dough, calculated from the density, attenuation coefficient and velocity data, was found to be sensitive to changes in the mechanical properties of the dough matrix of ADA, KAT and GDL doughs, all of which were found to increase in viscous-like behaviour as void fraction increased. Addition of SAPP and KAT to doughs weakened the gluten protein network, possibly due to the non-chaotropicity of these anions. Conversely, the stronger ability of GDL and ADA to lower the pH of the doughs was proposed to be the main mechanism by which these leaveners affected dough matrix properties.

The present study confirms the view that ultrasonic velocity and attenuation measurements of fermenting dough could determine non-invasively, non-destructively, and in real time, the mechanical properties of chemically fermenting dough. Low intensity ultrasound has proven capable of providing unprecedented insight into the gas cell formation phenomenon in proving dough. More importantly, this study provides evidence that both the gas cell fraction and the matrix properties are important factors determining the properties of dough, suggesting that breadmaking can not be defined solely in terms of aeration processes. Furthermore, the contribution of gas cell expansion and dough matrix changes during fermentation to the overall mechanical properties of the dough needs to be decoupled if one is to unambiguously characterize the behaviour of the dough.

CHAPTER EIGHT

General Discussion and Conclusions

Identifying and understanding the mechanisms of bubble nucleation, growth and stability in bakery products is of great significance to cereal science and technology since an essential facet of transforming wheat flour into baked goods is the creation of desirable textures (Scanlon & Zghal, 2001). This thesis is a comprehensive investigation of how the aerated structure of dough is created during mixing and bulk fermentation using chemical leavening systems, with a view to gaining a better understanding of the role of gas bubbles and the dough matrix on the overall mechanical properties of dough in breadmaking. The absolutely critical significance of aeration to breadmaking was first demonstrated in the pioneering works of Baker and Mize more than 60 years (Baker & Mize, 1937, 1941, 1946) and can be appreciated in the works of others (Babin et al., 2005, 2006, 2007), but more importantly in the investigations of Campbell and coworkers (Campbell, 1990; Campbell & Mougeot, 1999; Campbell & Shah, 1998; Chin & Campbell, 2005a, 2005b; Chiotellis & Campbell, 2003a, 2003b; Campbell et al., 1991,1993, 1998; Chin et al., 2004, 2005; Martin et al., 2004; Shah et al., 1998) and Elmehdi and coworkers (Elmehdi, 2001; Elmehdi et al., 2003, 2004; Scanlon et al., 2002).

Despite the numerous published works in this field of science, the influence of gas bubbles on the mechanical properties of fermenting dough is still not well understood. Part of the difficulty in understanding the influence of gas bubbles on the properties of dough is the very complex nature of dough and the limited number of experimental techniques capable of sensing the physical presence of gas bubbles in the dough while

monitoring its mechanical properties during fermentation. This thesis has borrowed and attempted to refine the methodologies and techniques developed by the four scientific groups mentioned above (particularly Elmehdi and coworkers) while, at the same time, introducing novel approaches and techniques to study the dynamics of bubble formation and changes in mechanical properties of leavening dough. All experimental lean formula doughs were prepared using Canadian Western red spring wheat milled as a straight-grade flour and with four chemical leavening systems, SAPP, ADA, KAT and GDL, which contained sodium bicarbonate and sodium acid pyrophosphate 40 (SAPP 40), adipic acid, potassium acid tartrate (cream of tartar) and glucono-δ-lactone, respectively. To investigate the creation of the aerated structure of dough, various individual studies were conducted, each of which had the following specific objectives: 1) developing techniques to measure the bubble size distribution and void fraction of dough, 2) developing a technique capable of quantifying gas evolution from flour-water-salt mixtures containing chemical leavening systems and relating gas evolution to the kinetics of molecular reactions occurring in the flour-water-salt mixtures, 3) improving and using a dynamic dough density technique for measuring the gas retention capacity of doughs formulated with chemical leavening systems, 4) comparing two novel methods for measuring dynamic dough density in chemically leavened dough, and 5) measuring mechanical properties of chemically leavened dough using the ultrasonic technique developed by Elmehdi (2001), so that the properties of the dough composed of bubbles and dough matrix could be predicted from knowledge of the properties of these individual components. While the order in which each study appears in this thesis is not accidental, as it reflects the fact that knowledge generated from one study was employed

in a subsequent one, a coherent integration of the findings of these five studies is still necessary and will be conducted in this chapter.

The main focus of this thesis has been to measure the physical properties of fermenting doughs and attempt to model these properties, and in particular, to decouple the contributions of gas bubbles and dough matrix to the overall mechanical properties of dough during leavening. The hypothesis tested in this thesis was that the combined use of a low-intensity ultrasound transmission technique and an adequate 'effective medium' model to interpret the ultrasonic data (Sheng, 1988) would enable one to delineate the effects of bubbles from those of the dough matrix on the overall mechanical properties of a fermenting dough. The effective medium theory (EMT) has proven useful in interpreting ultrasonic information obtained in non-fermented doughs (Elmehdi, 2001).

In the EMT, the material under evaluation is modeled as an elementary structural unit embedded in a homogenous effective medium, whose properties (i.e., effective elastic moduli) are to be determined. For a leavening dough, the elementary unit can be regarded as being a gas bubble surrounded by an amount of dough matrix that is determined so that the correct volume fraction of bubbles and matrix is preserved; this sets the radii of the "coated sphere" that represents the elementary structural unit (Figure 8.1). The idea behind using the EMT model is predicting the scattering properties of the coated sphere when it is embedded in an effective homogeneous material whose properties are to be determined. The solution to the problem is found from the condition that the forward scattering amplitude of the scattering units in the effective medium be zero. Thus, given the elastic properties of the matrix and inclusions, the moduli of the effective medium representing the average material properties can be measured.

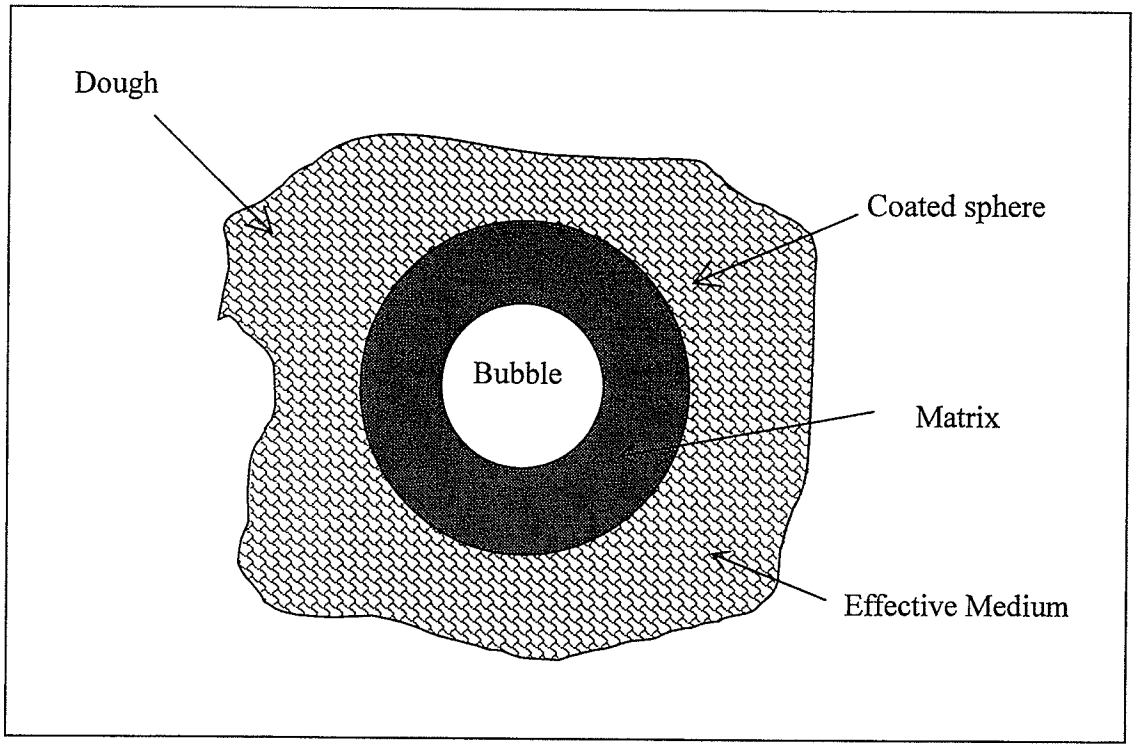

Figure 8.1. A schematic illustration showing the essential components of the Effective Medium Theory (EMT) proposed by Sheng (1988).

Conversely, if the properties of the matrix are unknown, (as in my experiments), they can be determined by finding the values of the matrix moduli such that the predicted properties of the effective medium containing the coated spheres matches the experimentally measured properties. If such correct properties for the dough matrix and the gas bubbles are found, one will be capable of gaining knowledge on the gas void fraction dependence of the shear modulus of the dough. For the sake of illustration, this knowledge and, more importantly a technology capable of providing it, is much needed as it would help us to identify the properties that the dough matrix needs to possess during the later stages of fermentation if this dough matrix is to resist the forces driving coalescence and thus create the highly aerated structure in bread. It is worth noting that the condition of the effective medium theory is valid only when the wavelength of the probing wave is much longer than the characteristic size of the coated spheres.

To monitor the degree of aeration of the experimental doughs during fermentation their void fraction was measured as a function of fermentation time. To determine void fraction (ϕ), the density of the doughs was measured (alongside the ultrasonic experiments) as a function of time using the Dynamic Dough Density (DDD) system described in Chapter 5, while their matrix density (also called the gas-free dough density) (ρ_m) necessary to calculate void fraction from density measurements was quantified using non-invasive microcomputed tomography (μCT) according to the methodology discussed in Chapter 3. According to the latter study, the matrix density of dough chemically leavened with SAPP, ADA, KAT or GDL was found to be 1289, 1212, 1237, and 1262 kg m^{-3}, respectively.

For the EMT model to work, a variety of mechanical properties on the 'coated spheres" needed to be obtained, including the dependence of the ultrasonic velocity (v) and (absolute) attenuation coefficient (α) on the gas void fraction (ϕ) of the dough, and on the magnitudes of the complex mechanical moduli of the dough matrix (matrix) and the inclusions (gas bubbles) (β_m, β_i, μ_m, and μ_i, where β and μ are complex quantities, and the subscripts m and i denote matrix and inclusions, respectively). Note that $\mu_m (= \mu_m^{'} - j\mu_m^{''})$ was an experimental variable that I will attempt to obtain from the EMT model.

Results showed that the ultrasonic velocity and attenuation were strongly affected by changes in the void fraction but also by the nature of the leavening system employed. Ultrasonic velocity, depending on the leavening system, dropped by as much as 50% over 50 minutes of bubble growth for some systems while remaining relatively constant in others. The attenuation always increased with fermentation time. Changes in void fraction alone (i.e., bubble growth) could not account for the observed changes in ultrasonic velocity and attenuation, suggesting that ultrasonic properties were also sensitive to the presence of fermentation by-products (e.g., salts) through the effect of these by-products on the dough matrix and its mechanical properties. Comparison of the experimental velocities as a function of void fraction against the predictions of Wood's approximation highlighted the importance of integrating the shear modulus of the dough matrix into the mechanical properties of the dough (Wood's approximation ignores the shear component of the dough matrix). The effective medium theory, which made use of the velocity and attenuation data to account for the viscoelastic nature of the dough, was capable of describing the individual contributions of the bubbles and the dough matrix to

the overall mechanical properties of SAPP doughs. It was found that the ratio of the imaginary part to the real part of the shear modulus (i.e., $\mu_m^{"}/\mu_m^{'}$), which is an indication of the viscoelastic character of dough, changed little ($\mu_m^{"}/\mu_m^{'} \sim 2.2$) over the range of void fractions studied (Figure 7.17).

With the exception of the SAPP dough, the fitting analysis conducted in Chapter 7 shows that the EMT had difficulty in predicting the void fraction dependence of both the velocity and attenuation data. The ultrasonic data indicated that the likely cause of the difficulties with fitting the velocity and attenuation of ADA, KAT and GDL is that in these aerated doughs, the characteristic size of the inclusions was so large that the long wavelength effective medium limit was no longer valid. In this regime, it would be necessary to account for higher order scattering contributions associated with the low frequency tail of the resonant interaction of ultrasound with the bubbles (Leroy et al., 2007); these effects are not included in the EMT. Therefore, attempts to model the rheological behaviour of ADA, KAT and GDL doughs by the EMT were not pursued further. Rather, changes in the mechanical properties of ADA, KAT and GDL doughs as a function of void fraction were measured in terms of the complex longitudinal elastic modulus of the dough ($\beta^* = \beta' - j\beta''$). This complex modulus, calculated from the density, attenuation coefficient and velocity data, was able to characterize the mechanical properties of the dough matrix of ADA, KAT and GDL doughs. In these three dough systems, it was observed that their viscous-like behaviour became more accentuated as void fraction increased. Because an increase in viscous-like behaviour in the dough can be interpreted as a loss in gas trapping capacity (Abdelrahman & Spies, 1986; Navickis et al., 1982), which in turn reflects a decrease in dough strength (Abdelrahman & Spies,

1986; Faubion et al., 1985; Hibberd, 1970b; Holmes & Hoseney, 1987a), the ultrasonic technique ranked the strength of the dough at the onset of fermentation as follows (in decreasing order): ADA (0.78) > KAT (0.90) > GDL (1.5) > SAPP (2.2) where the number in parentheses denotes the ratio of the imaginary part to the real part ($\beta''_{exp} / \beta'_{exp}$) of the longitudinal elastic modulus (β_{exp}). This ranking was in good agreement with the ranking made independently using very large strain assessments in the Tweedy 1 mixer where dough strength, as measured during dough development at 1 atm, was found to decrease due to the chemical leaveners as follows (in decreasing order): ADA (1840) > KAT (2030) ~ GDL (2060) > SAPP (2500), where the number in parentheses signifies the number of revolutions required by the mixer to deliver an energy input of 40 kJ kg^{-1} dough. By contrast, a lean formula dough (without a chemical leavening system) only required 1760 revolutions to be mixed to the same specific energy in the Tweedy 1 mixer.

The development of the mechanical properties, that in large measure govern the gas retention properties of the experimental dough systems (Figure 8.4), is largely determined during mixing. In terms of molecular events occurring during mixing, shear stresses untangle, dissagregate and depolymerize the gluten proteins (glutenin and gliadin) of the dough as water hydrates the tightly packed gluten proteins (Kinsella & Hale, 1984). Intermolecular protein interactions are eventually formed as the gluten molecules are drawn out into thin films and re-oriented in the plane of the shear stress. The new secondary forces linking the protein chains (i.e., electrostatic, van der Waals, hydrophobic, and dipole-dipole interactions, hydrogen bonding, and covalent disulfide cross-links) are responsible for stabilizing the structure and hence the mechanical properties of the dough (i.e., its gas retention capacity and strength) (Kinsella & Hale,

1984). Kinsella & Hale (1984) proposed that the sequence of physicochemical events occurring during mixing of dough is disrupted when lyotropic salts are present. The ability of non-chaotropic anions (e.g., pyrophosphate and tartrate; Holmes & Hoseney, 1987a) to increase the ordering of water around the gluten protein chains has been associated with a reduction in dough consistency (Preston, 1989; Kinsella & Hale, 1984; Wellner et al., 2003).

Increased water structure accentuates hydrophobic interactions between gluten protein molecules so that gluten proteins remain more aggregated and more resistant to hydration which would impair the formation of subsequent protein-protein interactions or physical entanglements during mixing. From all the secondary forces playing a role in dough stability, hydrophobic interactions between gluten protein chains (Guy et al., 1967; He et al., 1992; Wellner et al., 2003) are particularly important. The amino acid composition of gluten proteins shows that they have 35% hydrophobic amino acids (14% proline), 35% hydrophilic amino acid, and 7% charged amino acids (Wu & Dimler, 1963a). Since dough consistency was reduced more in dough with 0.38 *M* SAPP $\left[=\frac{5.83\ \text{g sodium acid pyrophosphate}}{222\ \text{g mol}^{-1}\ \text{sodium acid pyrophosphate} * 100\ \text{g flour}} * \frac{100\ \text{g flour}}{0.0696\ \text{dm}^3\ \text{water}}\right]$ than in dough with 0.48 *M* KAT $\left[=\frac{6.22\ \text{g adipic acid}}{188\ \text{g mol}^{-1}\ \text{adipic acid} * 100\ \text{g flour}} * \frac{100\ \text{g flour}}{0.0696\ \text{dm}^3\ \text{water}}\right]$ the inference is that a gram molecule of pyrophosphate anions were able to increase the molecular ordering of water around the gluten proteins more so than a gram molecule of tartrate anions (i.e., pyrophosphate ranked higher in non-chaotropicity). Even though the concentration of the adipate and gluconate anions in ADA and GDL doughs (0.12 M and 0.75 M, respectively) covered the range spanned by the SAPP and KAT doughs, these

anions exerted smaller lyotropic effects on dough rheology during mixing (i.e., GDL and ADA dough ranked higher in consistency in the Tweedy 1 mixer) and fermentation (i.e., higher $\beta''_{exp} / \beta'_{exp}$) than did the pyrophosphate and tartrate anions. The lower pH detected in doughs leavened with ADA and GDL (6.1 and 5.7) compared to SAPP and KAT (7.2 and 5.8), suggested that ADA and GDL, two organic acidulants, influenced dough rheology chiefly by virtue of their pH lowering effects, whereas SAPP and KAT, two acidic salts, did so mainly by making use of their lyotropic salts. The molecular basis for the weakening effects of the organic acidulants on dough gluten proteins may be due to an appreciable increase in repulsions between ionizable side chains in the amino acids of the gluten proteins. The increase intermolecular repulsions would change protein conformation by reducing inter- and intra molecular protein interactions during dough development as proposed in the work of Galal et al. (1978) where the effects of organic acids on dough development were assessed using a Farinograph.

Hence, an important piece of information that helps to interpret the ultrasonic data is having an understanding of physicochemical events taking place in the doughs during chemical fermentation at the molecular level since ultrasound, while capable of measuring bulk mechanical properties in dough, has also shown sensitivity to the intermolecular bonding of the dough matrix (Elmehdi, 2001). The fact that the mechanical properties of lean formula dough were weakened after the chemical leavening systems were added (Tweedy 1 mixer experiments; Chapter 6), and that the dough matrix properties of these leavened systems changed during chemical fermentation (ultrasonic experiments; Chapter 7) supported the view that the rheological properties of the gluten proteins of dough were affected by the type of molecular species being formed during

chemical leavening. Hence, information on the reaction kinetics of chemical leavening reactions was crucial to determine the molecular species interacting with the gluten proteins in the dough, since the chemical leavening reaction yielding CO_2 is also accompanied by the transformation of the leavening acid into reacted salts (reaction by-products).

Experimental results using the Gassmart showed that the evolution of CO_2 over time in the chemical leavening systems, which was a measurement of their reaction kinetics, was well characterized by exponential functions, with one (SAPP and ADA doughs) or two (KAT and SAPP doughs) time-constants, depending upon the type of leavening acid employed. Using the fittings obtained on carbon dioxide evolution as a function of time summarized in Tables 4.3 (ADA and GDL) and Table 4.4 (SAPP and KAT) in combination with Appendix I (to express carbon dioxide evolution in SI units), one can determine the CO_2 evolved per kg of dough matrix as a function of time for the four leavening systems. Using the dough matrix densities obtained from the μCT studies, one can further find the CO_2 dissolved in the dough matrix per m^3 of dough matrix as a function of time at 27 °C (Figure 8.2), based on the assumption that all the CO_2 evolved remains in the matrix of the dough (i.e., we assume no CO_2 transfer to the gas bubbles and no CO_2 loss to the atmosphere).

To quantify the extent to which CO_2 was lost from the doughs during fermentation, the density of the leavening systems as a function of fermentation time data (obtained in a previous experiment) was plotted alongside the expected density data had the experimental doughs retained 100% of the CO_2 evolved after the first density reading was taken (Figure 8.3). The first density reading was arbitrarily chosen as a yardstick to

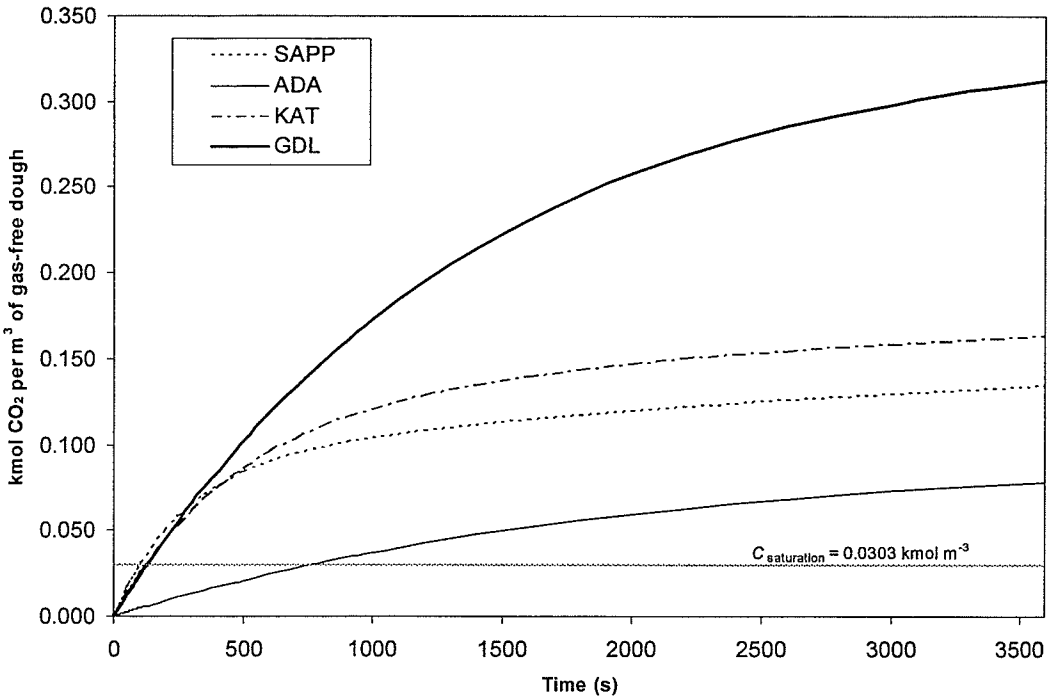

Figure 8.2. Carbon dioxide accumulation in the dough matrix of chemically leavened doughs based on the predictions made by the carbon dioxide evolution models described in Chapter 4. At 27 °C, the model described by Bloksma (1990a) shows that the concentration of carbon dioxide required to saturate the dough matrix is given by the horizontal dashed line. See text for details.

find the difference between empirical and expected density data during fermentation since density measurement began at about the same time after the end of mixing for all the chemically leavened dough systems studied.

To evaluate the overall gas retention properties of the experimental dough, the ratio of the CO_2 retained to the CO_2 evolved was found and expressed as a function of the dough's void fractions. The number of kmol of CO_2 retained by the dough during fermentation per m^3 of gas-free dough was obtained from the experimental data on the density of the doughs as a function of fermentation time shown in Figure 8.3. Since a portion of the gas in the dough was entrained during mixing, not all the overall gas retained by the doughs came from the chemical leavening systems. Based on experiments using reacted chemical leavening systems (where no CO_2 was evolved), the contribution of dough mixing to aeration was found to be small (less than 5%; Figure 7.18), so that a rough estimate of the contribution of mixing to the aeration of doughs containing actual chemical leaveners was taken to be 5%. The gas evolved by the chemical leavening systems, and to be added to this 5% void fraction, was obtained from the data shown in Figure 8.2. Both the CO_2 retained (from Figure 8.3) and the CO_2 evolved (from Figure 8.2) by a given chemically leavened dough was measured at equivalent fermentation times, so that the percentage of kmol CO_2 retained per kmol CO_2 evolved could be related to the gas void fraction of the dough at that fermentation time (Figure 8.4).

One issue related to the data displayed in Figure 8.4 is that it takes account of all gas that would have been evolved by the leavening system. If the dough was well developed during mixing, much of this gas would be retained by the time that the first density and ultrasound measurements were taken. It is apparent from Figure 8.4 that

GDL doughs retained a large percentage of the gas evolved at this stage, whereas SAPP systems did not. To examine how much gas was retained (relative to gas evolved) over the time in which data was being acquired, the data of Figure 8.3 was used to construct a master curve of the ratio of CO_2 retained to CO_2 evolved as a function of void fraction during the fermentation experiment only (Figure 8.5). Figure 8.5 provides information on the amount of CO_2 retained (obtained from density measurements), and the amount of CO_2 evolved between two consecutive void fraction measurements. See Appendix VII for the calculations used to construct Figure 8.5.

Figure 8.2 shows that the doughs are not saturated with CO_2 for at least 2 min in the doughs prepared with SAPP, KAT or GDL while the dough saturated with ADA was not saturated for at least 13 min. For the sake of contrast, the leavening systems employed in this thesis produced more CO_2 than yeast would have produced under similar conditions, at least during the initial stages of fermentation, since Shah et al. (1998) estimated that a dough with 2% yeast will require at least 20 min of fermentation before the dough matrix can become saturated with CO_2 (provided the dough is fermented at 27 °C and that no gas leaves the dough matrix). Hence, it is reasonable to assume that fermentation of the experimental doughs occurred under conditions of saturation, with the exception of ADA doughs.

Because ADA dough was fermented under conditions of sub-saturation, the model of Shah et al. (1998) can be used to calculate the average concentration of CO_2 in ADA dough from information on the growth experienced by an average gas bubble in this dough system. Determining the concentration of CO_2 in the liquid phase of dough can be cross-referenced with the data in Figure 8.2 to estimate the time at which this CO_2

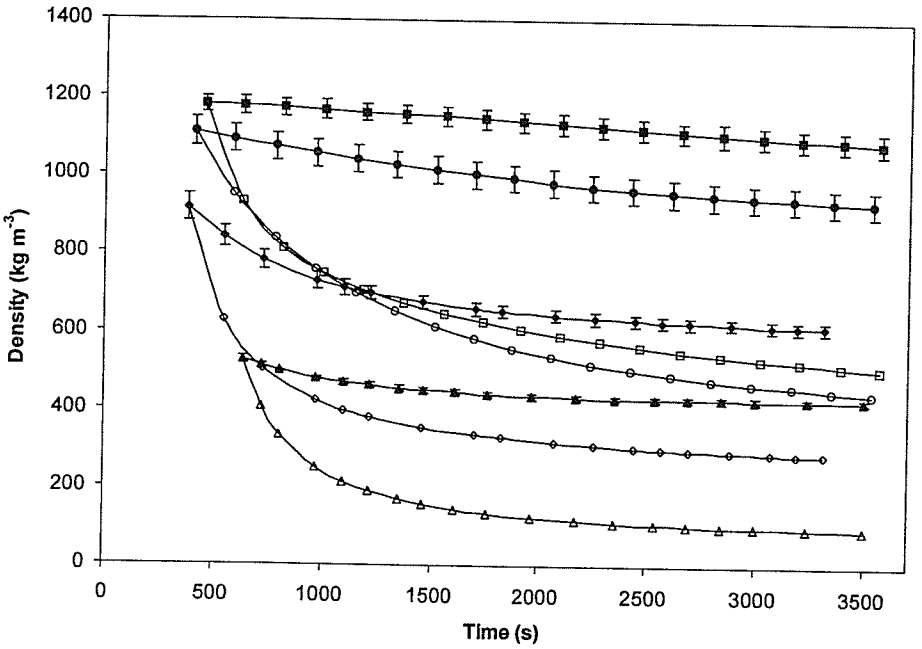

Figure 8.3. Leavening time dependence of density in doughs chemically leavened with SAPP (squares), ADA (circles), KAT (rhombus) and GDL (triangles) at 27 °C. Filled symbols denote empirical data and open symbols represent expected densities assuming 100% gas retention after the first density measurement was made.

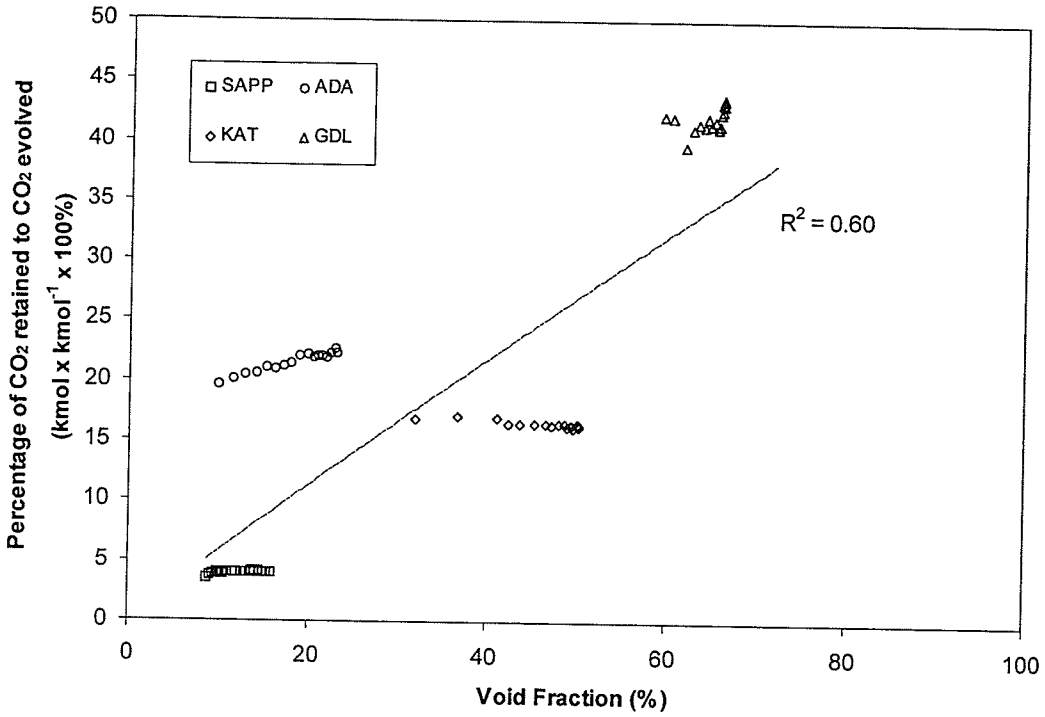

Figure 8.4. The percentage of CO_2 retained to CO_2 evolved (F_R) by dough that had been leavened with one of four chemical leavening systems at 27 °C. The contribution of mixing to aeration of the dough was assumed to be 5% gas void fraction for all leavening systems. The dashed line is a best-fit exponential curve: $F_R = A(\phi)^n$; where A=0.66 and n = 0.95. See text for details.

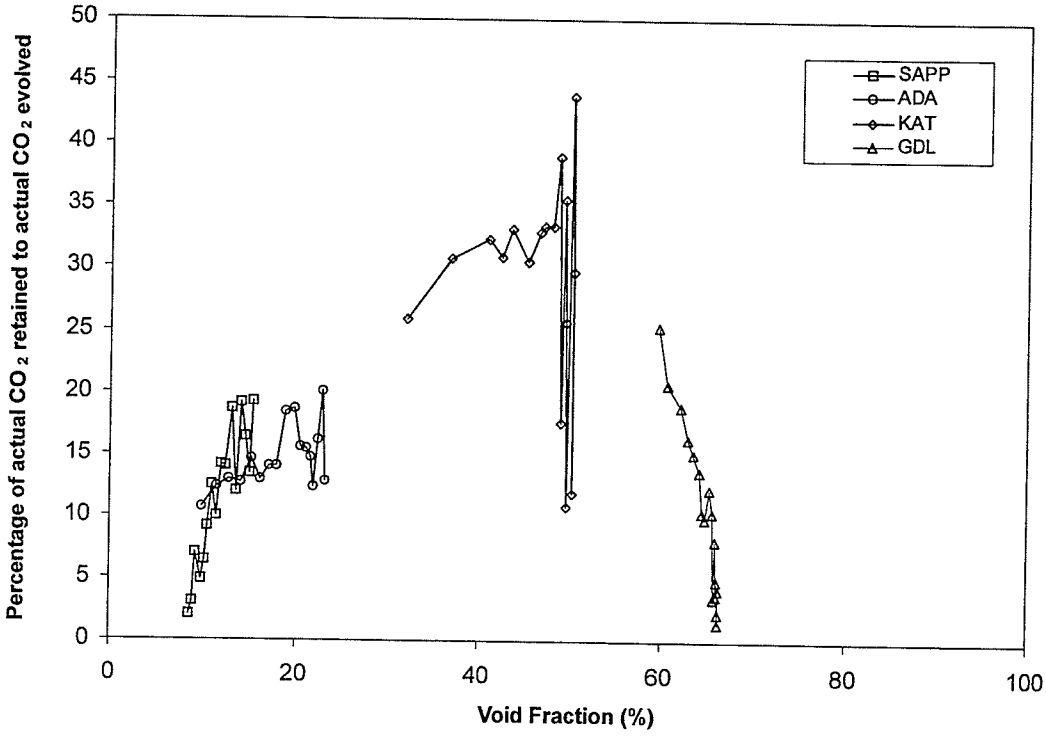

Figure 8.5. The ratio of CO_2 retained per unit time by the dough to the CO_2 evolved per unit time by the chemical leavening systems in the experimental doughs at 27 °C. See Appendix VII for details on calculations.

concentration was achieved during fermentation, so that we can get an estimation of how much CO_2 was neither transferred to the gas bubbles nor remained in the dough liquid matrix (i.e., gas loss to the atmosphere). Shah et al. (1988) proposed that under sub-saturation conditions small bubbles (diameter <10 μm) do not grow due to large internal pressure. Larger bubbles (diameter ≥10 μm) can grow but they only do so until they reach an upper size limit, D_{lim}, which depends on the concentration of CO_2 dissolved in the matrix and the surface tension. Provided that the surface tension is ignored (a reasonable approximation, see below), D_{lim} can be calculated:

$$\frac{D_{lim}}{D_0} = \sqrt[3]{\frac{P_\infty}{P_\infty - HC_\infty}} \tag{8.1}$$

where D_0 is the initial bubble diameter (m), P_∞ is the pressure in the dough (10^5 Pa), H is Henry's law constant (3.30×10^{-6} J kmol^{-1} at 27 °C), and C_∞ is the concentration of CO_2 in the liquid phase of dough (kmol m^{-3} gas-free dough). [Ignoring the contribution of the Young-Laplace equation to the excess pressure, ΔP (= P_b - P_∞), inside a bubble, P_b, seems to be reasonable because $\Delta P = 4\gamma/D \approx 2$ kPa or about 2% greater than P_∞, provided that surface tension, γ, is equal to 0.04 N m^{-1} (Kokelaar & Prins, 1995), and the mean bubble diameter, D, is 109×10^{-6} m (Chapter 3). The excess pressure in a small bubble (D = 10×10^{-6} m), however, should not be ignored since $\Delta P \approx 20$ kPa, or about 20% greater than P_∞]. Further, Equation 8.1 can be re-arranged as follows:

$$C_\infty = \frac{P_\infty}{H}\left(1 - \left(\frac{D_0}{D_{lim}}\right)^3\right) \tag{8.2}$$

Taking the initial mean bubble diameter in ADA doughs to be that found in slack doughs (=109×10^{-6} m; Chapter 3) and assuming that the shape of the bubble size distribution did not change (i.e., all bubble sizes grew proportionally), the upper size limit, D_{lim}, is found

to be 145 x 10^{-6} m (for a total void fraction increase of 13%, based on data in Figure 8.3). Using these data in Eq. 8.2., it can be found that C_∞ was 0.0175 kmol m^{-3} gas-free dough. Figure 8.2 shows that this concentration was achieved only 7 min (400 s) after the onset of fermentation, so it is apparent that gas losses to the atmosphere were substantial in dough chemically leavened with ADA. Holmes and Hoseney (1987a) showed that a decrease in gas retention in dough (based on assessments of the loaf volume of the bread) occurs when dough consistency (as measured in a dough recorder mixer) is decreased due to the incorporation of the chemical leavening ingredient. Since the Tweedy 1 mixer found that ADA dough had a higher dough consistency than SAPP, KAT, and GDL doughs (Chapter 6), it can be inferred that CO_2 losses to the atmosphere during fermentation were even more substantial in the latter three dough systems.

Since Equation 8.2 is only valid for when bubble expansion in fermenting doughs occurs under conditions of sub-saturation, an alternative means to assess the gas retention properties of SAPP, KAT and GDL doughs was sought. Determining the degree to which the doughs were capable of holding the gas produced during leavening (Figure 8.3) was important as this could be related to the dough rheological properties measured by ultrasound during fermentation of the doughs. Figure 8.3 shows that all chemical leavening systems were permeable to CO_2, with KAT and GDL exhibiting the least density difference (329 and 333 kg m^{-3}, respectively), and possibly the least overall permeation to CO_2, as shown by the difference between empirical and expected density data at the end of fermentation, followed by ADA (487 kg m^{-3}) and SAPP (578 kg m^{-3}). This ranking, in fact, was in line with the ranking provided by the empirical values for the mass diffusion coefficient of carbon dioxide in the fermenting dough samples (D_L),

according to the mathematical analysis of experimental density data acquired in Chapter 5. The empirical D_L values were 4.5 x 10^{-9} m^2 s^{-1} (GDL), 4.2 x 10^{-9} m^2 s^{-1} (KAT), 1.8 x 10^{-9} m^2 s^{-1} (ADA), and 2.1 x 10^{-10} m^2 s^{-1} (SAPP).

Hence, it appears that those dough systems that captured more of the CO_2 evolved by the chemical leaveners did so because they were able to transfer most of evolved CO_2 to the gas bubbles (D_L was measured in terms of bubble expansion). Because the surface area of the bubbles is so much larger than that of the dough specimen, a higher D_L (e.g., by changing the type of chemical leavening system employed to leaven a dough) would be expected to favour gas retention properties solely in terms of the rates of CO_2 mass transfer [$Q \approx k_L(\pi D^2)(C_\infty - C^*)$; where $k_L = 2\ (D_L / D)$, and k_L denotes the overall mass transfer coefficient, D is the bubble diameter, C_∞ is the CO_2 concentration in the dough matrix, and C^* is the CO_2 concentration at the interface; Shah et al., 1998]. Figure 8.4 shows that the doughs with the best 'overall' gas retention capacity were ranked as follows (in descending order): GDL > ADA > KAT > SAPP. This is agreement with the ranking obtained from the empirical D_L and also with the ranking obtained from measurements of $\beta''_{exp} / \beta'_{exp}$ by the ultrasonic technique. Interestingly, as suggested earlier by the analysis of the experimental data using Shah et al's (1998) model, Figure 8.4 shows that ADA doughs possessed better gas retention properties than SAPP, KAT, and GDL doughs *during* the course of chemical fermentation (as judged by the steeper upward slope of the data of ADA dough).

Figure 8.5 shows that the gas retention capacity of SAPP improved as bubbles became bigger. Hence, the experimental results support the view that bubble growth was limited to some extent by the interfacial area for mass transfer. This can be observed in

SAPP dough, which despite having the poorest overall gas retention capacity, was able to retain more CO_2 gas as the void fraction increased.

Based on the changes in the viscoelastic properties of SAPP with increasing void fraction ($\beta''_{exp}/\beta'_{exp}$) and the theoretical effects of non-chaotropic salts produced by the reaction of SAPP, it was concluded in Chapter 7 that the mechanical properties of the dough (matrix + bubbles) became weaker (e.g., a substantial decrease in dough consistency that can be attributed to an increase in viscous-like behaviour) with increasing void fraction. This weakening effect on the mechanical properties of the dough appears to be associated with the growth of the gas bubbles as the effective medium theory indicated that the viscoelastic behaviour of the dough matrix (μ''_m/μ'_m) in the SAPP system remained relatively constant as the bubbles expanded. The fact that assigning a single value to the complex shear modulus of the dough matrix of SAPP (μ^*_m= 92.5 kPa $- j$ 430 kPa) described the changes in velocity and absolute attenuation well with increasing void fraction supports the view that bubble growth controlled the mechanical properties of this 'effective medium' (SAPP dough).

Conversely, the "actual" gas retention capacity of ADA doughs changed little with increasing bubble sizes (Figure 8.5) and this is in agreement with the finding that the viscoelastic character of ADA doughs ($\beta''_{exp}/\beta'_{exp}$) changed only moderately with increasing void fraction (the doughs adopted a slightly more pronounced viscous-like character) (Figure 7.11). The ability of ADA dough to maintain its mechanical properties relatively invariant as its gas bubbles expanded (Figure 8.5) appears to be related to its dough strength. The Tweedy 1 mixer ranked ADA doughs first in terms of dough strength (at the onset of fermentation, i.e., after mixing) compared to the other three

leavening systems.).The ultrasonic technique also ranked ADA doughs as the strongest dough system (compared to the other three systems) based on the magnitude of $\beta''_{exp}/\beta'_{exp}$ at the onset of fermentation. The fact that the CO_2 mass diffusion in ADA doughs likely occurred under sub-saturated conditions meant that as fermentation progressed a portion of the CO_2 remained in the dough matrix and did not diffuse through the matrix to the gas bubbles or to the atmosphere. It can be speculated that the reduced 'traffic' of CO_2 diffusive species through the matrix of ADA dough may also have helped ADA doughs to maintain its viscous-like character relatively unaltered ($\beta''_{exp}/\beta'_{exp} \sim$ 0.8-1.2; Figure 7.11) as the bubbles expanded, compared to doughs whose bubbles expanded under saturated conditions (SAPP, KAT, and GDL doughs).

Figure 8.5 shows that the "actual" gas retention capacity of KAT doughs changed little up to a void fraction of 50% and thereafter varied dramatically. This can be associated with the onset of bubble coalescence. An independent study using the internationally recognized DDD system developed by Campbell (Campbell et al., 2001) (Chapter 6) demonstrated that bubble coalescence began when KAT dough reached a void fraction of about 50%. Symptoms of bubble coalescence in GDL dough were detected when the dough reached a void fraction of about 70% (Chapter 6). The wide range of void fractions at which the first signs of coalescence were detected in Chapter 6 suggested that bubble coalescence could not be ascribed as an event that takes place at a given void fraction, but rather takes place over a range of void fractions. This view is supported by the X-ray microtomography data recently published by Babin et al. (2006) in which bubble coalescence in a lean formula dough (100 g flour + 60g water + yeast) became evident when the void fraction was about 40% (3g yeast) or 50% (1.5g yeast),

even though early signs of coalescence began when the void fraction was as small as 30% (3 g yeast) or 35% (1.5 g yeast). Therefore, the conventional view that bubble coalescence starts at a void fraction of 70% is open to question (Bloksma, 1990a, Scanlon & Zghal, 2001).

Very interestingly, low intensity ultrasound was also able to detect a rapid increase in viscous losses ($\beta''_{exp}/\beta'_{exp}$) at void fractions close to 50% in KAT doughs (Figure 7.12) and immediately after the first void fraction measurement was made in GDL dough (Figure 7.13), viscous losses which may also be related to bubble coalescence. Babin et al. (2006) used an index of connectivity I_{co} (ratio of the volume occupied by the largest gas bubble to the total gas void fraction) to follow the expansion of the dough gas phase, with I_{co} values ranging from zero to one. I_{co} values closer to zero would be found in doughs in which bubbles are discretely distributed whereas I_{co} values closer to one would be typical of doughs where bubbles have undergone considerable coalescence (forming "a continuous cavity" at I_{co} = 1; Babin et al., 2006). Hence an increase in viscous losses for KAT and GDL doughs may be related to an increase in I_{co} as the largest bubbles in these systems began to coalesce. Babin et al. (2006) found that the time at which the first signs of coalescence were detected corresponded to the point at which I_{co} rose precipitously from a value of close to zero to a value of close to 0.8 when the void fraction increased from 35% to 50% and from 30% to 40% for lean dough + 1.5g yeast and for lean dough + 3g yeast, respectively. The higher the rates of gas evolution in the dough, the narrower the range of void fraction at which the I_{co} rose abruptly.

The analysis of Figure 8.2 has shown that saturation of KAT or GDL doughs was reached after 2 min of fermentation, whereas Bloksma (1990a) and Shah et al. (1998)

have shown that saturation of a dough with 2% yeast would be achieved 20 min into fermentation. Given the fact that KAT and GDL evolved CO_2 at a rate that was about one order of magnitude higher than of yeasted dough, it can be expected that the transition from a $I_{co} \sim 0$ to a $I_{co} \sim 0.8$ (the transition to observe the onset of bubble coalescence) would be reached suddenly within a very narrow void fraction range. Even though I did not measure I_{co}, Figure 8.5 does show that after the gas retention capacity of KAT changed little between ϕ =32%-49%, the onset of coalescence occurred abruptly at a given void fraction ($\phi \sim 50\%$). In GDL doughs, on the other hand, the signs of coalescence commenced as soon as the first void fraction determination was made (ϕ = 60%) and continued throughout fermentation (until $\phi \sim$ 66%).

Hence, an interpretation of the gas retention capacity of KAT and GDL doughs shown in Figure 8.5 in light of Babin et al. (2006) work would suggest that large bubbles (I_{co} closer to 1) may have been formed in these doughs systems when the void fractions were only 50% and 60%, respectively. The sharp increase in the index of connectivity expected to occur in KAT and GDL doughs at these two void fractions (50% and 60%, respectively) were captured by ultrasound as a rapid rise in viscous losses (i.e., a drop in the ratio $\beta''_{exp}/\beta'_{exp}$) (Figures 7.12 and 7.13). Therefore, while the experimental results found that the EMT model had difficulty in modeling the mechanical properties of the dough matrix, the ratio $\beta''_{exp}/\beta'_{exp}$ has proven to be sensitive to the onset of bubble coalescence in chemically leavened doughs. Part of the difficulty encountered by the EMT in modeling the rheological behaviour of KAT and GDL doughs may be associated with the formation of large bubbles (having a $I_{co} \sim 0.8$) in these systems due to bubble coalescence. It is worth noting that the EMT is valid as long as the wavelength of the

ultrasonic signal is much larger than the characteristic size of the "coated spheres". Further information is needed on the changes in bubble size distribution during leavening in these highly aerated systems to determine the void fraction at which the experiments are no longer conducted in the long range wavelength limit.

In conclusion, I was able to show how velocities and absolute attenuation coefficients could be obtained over a wide range of void fraction range (4-66%), thus providing new rheological information on the properties of fermenting doughs. An effective medium theory model was used to delineate the effect of matrix and bubbles on these ultrasonic results, and showed that even in these simpler chemically leavened dough systems, profound changes in matrix properties occur as a result of the conversion of acid and base to salt and the concomitant effect on the properties of the dough.

CHAPTER NINE

Contributions to knowledge and Recommendations for future work

Summary of Research

This thesis is a comprehensive investigation of how the aerated structure of dough is created during mixing and bulk fermentation using chemical leavening systems. Low-intensity ultrasound (40 kHz) was used to probe the mechanical properties of the fermenting doughs and the ultrasonic data interpreted in light of the effective medium theory proposed by Sheng (1988) with a view to gaining a better understanding of the role of gas bubbles and the dough matrix on the overall mechanical properties of dough in breadmaking. All experimental lean formula doughs were prepared using Canada Western Red Spring wheat milled as a straight-grade flour and with four chemical leavening systems containing sodium bicarbonate and one of four acidulants (sodium acid pyrophosphate 40, adipic acid, potassium acid tartrate (cream of tartar), and glucono-δ-lactone). The fact that to date there exist very few comprehensive reports in the cereal chemistry literature on the use of chemical leavening agents to leaven bread dough was an important motivation to develop novel techniques to characterize and measure the rates of carbon dioxide production and retention in chemically leavened doughs. The major contributions to new knowledge made by this thesis can be summarized in terms of the five individual studies that were conducted to understand the bubble formation phenomenon in the fermenting doughs.

9.1. The bubble size distribution in wheat flour dough

The objective of this paper was to use non-invasive microcomputed tomography

(μCT) to unambiguously determine the bubble size distribution in 'stiff' and 'slack' doughs, with a view to understanding the influence of dough consistency on the size distribution of gas bubbles entrained during standard mixing conditions. Morphological characterization of the stiff and slack doughs indicated that bubbles were entrained whose size distributions were well defined by a two-parameter lognormal distribution, with geometric mean x_g and geometric standard deviation σ_g. The bubble size distributions in the stiff and slack doughs were found to have similar geometric means, 100 and 109 μm, but very distinct dispersions, as their geometric standard deviations were 1.79 and 1.62, respectively. Furthermore, results indicated that the distribution of distances between the centers of adjacent bubbles was normally distributed, with the stiff and slack doughs having a mean of 338 and 460 μm and standard deviation of 88 and 156 μm, respectively. Overall, this paper shows, how the bubble size distribution in dough can be determined using x-ray microcomputed tomography and powerful software, by adapting methodologies developed by medical sciences for studying the skeletal morphology of small animals, to cereal science.

9.2. The use of a pressuremeter to measure the kinetics of carbon dioxide evolution in chemically leavened wheat flour dough

This study developed a methodology to measure and characterize the the rates of CO_2 production from chemical leaveners in a format that is meaningful to both the technologist (i.e., the dough rate of reaction or DRR) and the researcher (e.g., kmol CO_2 per kg of dough per second). Results for the fermenting doughs show that the DRR curves based on the Gassmart system had equivalent trends and the same percentages of evolved carbon dioxide as those reported in the literature. Experimental results

demonstrated that the evolution of CO_2 over time from the chemical leavening systems as the temperature, type and level of leavener was manipulated was well characterized by exponential functions, having one (ADA and GDL) or two (SAPP and KAT) time-constants.. Increasing the fermentation temperature from 27 to 39 °C increased the rate of the chemical leavening reactions. A first-order reaction kinetics model was found to be suitable for describing the neutralizing properties in GDL and ADA, whereas a first-order reaction kinetics model for irreversible parallel reactions better described the leavening properties of KAT and SAPP. Overall, this work presented an original methodology to carry out the dough rate of reaction (DRR) test using a conventional pressuremeter, the Gassmart apparatus, while, at the same time, it provided fundamental information on the actual rates of CO_2 production in leavening dough.

9.3. The measurement of dough specific volume and carbon dioxide transport in chemically leavened dough systems

Another area of research was dedicated to measuring the dynamic specific volume (DSV) of chemically leavened dough (i.e., its gas retention properties) using a technique based on digital image analysis. Using the experimental leavening systems at a concentration of 1.4 to 4.2 g sodium bicarbonate per 100 g of flour was adequate to consistently raise the specific volume of bread dough so that gas void fractions spanned between 5 and 67 %. The linear relationship between the expansion of the dough during fermentation and the square-root of fermentation time, in the early region of the chemical leavening expansion curve, suggested that initially the growth of the gas phase with time was diffusion limited. To interpret this diffusion-controlled region, the analysis for diffusion-controlled bubble growth for a viscoelastic liquid proposed by Venerus *et al.*

(1998) was invoked. The results of the mathematical analysis yielded empirical values for the mass diffusion coefficient of carbon dioxide in the fermenting dough samples (D_L). The empirical D_L values were $4.5 \pm 3 \times 10^{-9}$ m^2 s^{-1} (GDL), $4.2 \pm 1.6 \times 10^{-9}$ m^2 s^{-1} (KAT), $1.8 \pm 0.5 \times 10^{-9}$ m^2 s^{-1} (ADA), and $2.1 \pm 1.5 \times 10^{-10}$ m^2 s^{-1} (SAPP). These values were in relatively good agreement with other predictions made in the literature. Overall, the experimental results indicated that the predictability of the chemical leavening systems makes them useful tools for measuring the gas retention properties of chemically leavened dough.

9.4. Effects of chemical leavening systems on dough development during mixing and on dough aeration during proving: a comparison of the Canadian and British techniques for measuring dynamic dough density in fermenting dough

This section of the thesis was devoted to making a comparison of Campbell's DDD system and Bellido's DDD system using chemical leaveners as the source of CO_2. Since the experimental doughs were mixed in the well-characterized Tweedy 1 mixer located in Dr. Grant Campbell's laboratory at the University of Manchester, England. The effect of chemical leavening systems on dough development during mixing was also investigated. Results show that, overall, the addition of the chemical leaveners to the dough brought about a decrease in dough strength as measured in the Tweedy 1 mixer. The effects of chemical leaveners on dough rheology were associated with changes in dough gluten strength and with aeration of the dough during mixing. Dough strength experiments, as measured during development of doughs mixed under vacuum and under atmospheric pressure, showed that the strength of the experimental doughs was lessened by the chemical leaveners as follows (in decreasing order): ADA > KAT ~ GDL > SAPP. Dough consistency and degree of aeration (i.e., density) data obtained from mixing the

experimental doughs under various mixer headspace pressures further suggested that while the chemical leaveners affected dough development during mixing due to their ability to produce carbon dioxide, the leaveners also influenced the properties of the dough protein matrix due to the conversion of acids and bases to salt products. Density measurements in Campbell's DDD system were suitable to identify the point at which gas cell coalescence came to happen. Based on the experimental results it was proposed that bubble coalescence cannot be ascribed as an event that takes place at a given void fraction, but rather takes place over a range of void fractions. Independent studies using x-ray microtomography (Babin et al., 2005) confirm that this view is physically sound.

9.5. Low-intensity (40 kHz) ultrasound study on gas bubble growth in chemically leavened dough

This study used the low-intensity ultrasound (40 kHz) transmission technique developed by Elmehdi (2001) to measure changes in the ultrasonic velocity and attenuation in chemically fermenting dough systems, thereby monitoring changes in rheology as gas bubble growth actually occurred. Results showed that the ultrasonic velocity and attenuation were strongly affected by changes in the void fraction but also by the nature of the leavening system employed. Changes in void fraction alone (4-66%) could not account for the observed changes in ultrasonic velocity and attenuation, suggesting that ultrasonic properties were also sensitive to the presence of fermentation by-products (e.g., salts) through the effect of these by-products on the mechanical properties of the dough matrix. An effective medium theory model was used to delineate the effect of matrix and bubbles on these ultrasonic results, and showed that even in these simpler chemically leavened dough systems, profound changes in matrix properties occur

as a result of the conversion of acid and base to salt and the concomitant effect on the properties of the dough.

Recommendations for future work

All the techniques presented in this thesis can be regarded as novel or considerably refined versions of their corresponding progenitor, and as such they are expected to be capable of providing a deeper insight into the properties of leavening dough, be it leavened by chemical leavening systems or by yeast. A few examples of future work that can be done are the following:

1. In terms of the x-ray microtomography technique, an important investigation will be to determine the changes in bubble size distribution in chemically leavened doughs with fermentation time and compare these results against real-time measurements of mechanical properties via ultrasound. The pixel resolution of the radiographs will need to be sacrificed in order to reduce the time required to scan fermenting dough specimens if the SCANCO Medical VIVACT 40 X-ray microtomography scanner (Bassersdorf, Switzerland) is to be used again. For example, while a four-frame averaging was used to improve the signal to noise ratio in the SCANCO Medical VIVACT X-ray microtomography scanner, a two-frame averaging will reduce scanning times by half. Also, while the protocol presented in this thesis requires that the x-ray source and detector rotate around the sample at rotation steps of 0.35° over 180°, the rotation step could be cut down to say 0.70°. These new settings would allow scanning a dough sample in about 100 s (instead of 420 s), though it must be recognized that the quality of the reconstructed 3D images will be lowered. An even better alternative is to perform the proposed experiments using a scanner with a

higher intensity x-ray beam, such as the one available at the European Synchrotron Radiation Facility (Grenoble, France), which with an exposure time for a single radiograph of 20 ms, allows the acquisition of a scan of 400 radiographs over 180° in less than 30 s.

2. With respect to the experiments conducted in Chapter 4, an important contribution to baking technology will be to measure the DRR (dough rate of reaction) for a wider group of chemical leavening systems (see Table 2.3 for a comprehensive list of commonly used leaveners in the baking industry). Of particular interest to corroborate the sensitivity of the technique developed in Chapter 4 will be to comprehensively measure the DRR of the various grades of sodium acid pyrophosphate, since chemical companies claim that they can manufacture this leavening acid in various grades (i.e., SAPP 21, SAPP 26, SAPP 28, SAPP 37, SAPP 40 and SAPP 43). In the trade, the number following the abbreviation SAPP represents the percentage of CO_2 that is expected to be evolved by the leavening acid 8 min after the end of mixing. It is worth noting again that the DRR test results published in the literature provide insufficient materials and method information to replicate the experimental results. Further, the few reports available do not disclose the characteristics of the DRR instrumentation.

3. The unique capabilities of chemical leavening systems to produce gas in bakery products where yeast would normally underperform (e.g., refrigerated doughs, frozen doughs, microwaveable doughs, extruded doughs) suggests that the technique outlined in Chapter 4 should be able to facilitate the development of bakery products containing chemical leavening systems. It is recommended that the mathematical

formulae included in Chapter 4 to transform *pressure* versus *time* data into DRR data, be written in a computer program and that this program be installed in the PC running the Gassmart apparatus software. This recommendation will facilitate the characterization of the leavening capacity of chemical leavening systems when used alone or in combination.

4. As far as the technique developed to measure density and to estimate the diffusion coefficient of carbon dioxide in dough, it will be useful to conduct these experiments with a wider range of chemical leaveners and/or the addition of bakery ingredients whose improvement mechanism has not been fully elucidated (surfactants, lipids and enzymes). By doing so, it will be possible to determine whether such bakery ingredients (also termed bakery improvers) exert their improving action during leavening or not, and if so, whether this action is related to their ability to facilitate the transportation of CO_2 from the liquid matrix to the gas bubbles. An improvement of the model for diffusion-induced bubble growth in viscoelastic materials proposed by Venerus et al. (1998) will be to account for the bubble size distribution in the dough. While the difficulty of accomplishing this last objective is clear due to the complex effects that bubbles sizes may have on the rates of gas diffusion across the bubbles' interfaces (Campbell & Mougeot, 1999), the mathematical model for bubble growth during fermentation elaborated by Shah et al. (1998) for a single bubble and later expanded by Chiotellis and Campbell (2003b) to account for the size distribution of bubble in dough, is expected to serve as a useful framework.
5. In terms of the ultrasonic technique, a useful investigation will be to measure the frequency dependence of the ultrasonic velocity and the attenuation coefficients so as

to identify the range of frequencies at which resonant effects are manifested in the fermenting doughs, particularly the GDL doughs since bubbles are expected to be large in this system towards the end of fermentation (possibly of comparable size to the size of the ultrasonic pulse wavelength). The resonant frequency regime is expected to occur in the megahertz frequency range for dough immediately after mixing (Leroy et al., 2006), but this range should move towards lower frequencies as bubbles become increasingly larger during leavening. The results obtained from these experiments can be compared to those obtained in the experiments suggested in item 2 of this section. The experimental techniques described in Chapter 6 for measuring the velocity and attenuation in KAT and GDL should be useful to collect the data required for measuring the bubble size distributions in dough via ultrasound. Since the conversion of acid and base into salts have been shown in this thesis to affect the properties of the dough matrix, I recommend to use glucono-δ-lactone as the sole leavening acid to produce a wide range of void fractions in fermenting. To slow down the rate of reaction of this leavening system, I suggest reducing the temperature of the dough during mixing (e.g., by using cold water, ice) or to conduct the experiments in a cool environment at constant temperature (i.e., <12 °C). Acquiring this ultrasonic data in the transmission mode should be feasible if the experiments are conducted in the sample holder described in Figure 1 of Appendix VI as this apparatus is capable of obtaining the ultrasonic velocity and the (absolute) attenuation coefficient data of the same dough sample as a function of fermentation time. This sample holder is further capable of providing information on the density of the dough since it has been

constructed with Plexiglas, much in the same fashion as the sample holder used in the experiments shown in Chapter 5.

Bibliography

AACC (2000). Approved Methods of the American Association of Cereal Chemists, 10th Edition. Method 02-32, neutralizing value of acid-reacting materials; Method 02-52, hydrogen ion activity [pH]-electrometric method; Method 12-10, residual carbon dioxide in baking power; Method 12-20, total (gasometric) carbon dioxide in baking power; Method 12-21, total carbon dioxide in prepared mixes and self-rising flour; Method 22-11, measurement of gassing power by the pressuremeter method; Method 89-01, yeast activity, gas production. St. Paul, MN: AACC International.

Abdelrahman, A., & Spies, R. (1986). Dynamic rheological studies of dough systems. In H. Faridi & J.M. Faubion (Eds.). *Fundamentals of Dough Rheology* (pp.87-103). St. Paul. MN: American Association of Cereal Chemists, Inc.

Akdogan, H, & Ozilgen, M. (1992). Kinetics of microbial growth, gas production, and dough volume increase during leavening. *Enzyme and Microbial Technology, 14*, 141-143.

Amemiya, J. I., & Menjivar, J. A. (1992). Comparison of small and large deformation measurements to characterize the rheology of wheat flour doughs. *Journal of Food Engineering, 16*, 91-108.

Anderson, H.L. (1989). A Physicist's Desk Reference. New York, NY: American Institute of Physics. Cited by Elmehdi, H.M. (2001) in "An Ultrasonic Investigation of the Effect of Voids on the Mechanical Properties of Bread Dough and the Role of Gas Cells in Determining the Cellular Structure of Freeze-Dried Breadcrumb" (pp. 100). *PhD Thesis*. University of Manitoba, Canada.

Atwell, W.A. (1985). Refrigerated dough. U.S. Patent 4,526,801.

Autio, K., Flander, L., Kinnunen, A., & Heinonen, R. (2001). Bread quality relationship with rheological measurements of wheat flour dough. *Cereal Chemistry, 78*, 654-657.

Babin, P., Della Valle, G., Dendievel, R., Lassoued, N., & Salvo. L. (2005). Mechanical properties of bread crumbs from tomography based finite element simulations. *Journal of Materials Science, 40*, 5867-5873.

Babin, P., Della Valle, G., Chiron, H., Cloetens, P., Hoszowska, J., Pernot, P., Réguerre, Salvo, L., & Dendievel, R. (2006). Fast X-ray tomography analysis of bubble growth and foam setting during breadmaking. *Journal of Cereal Science, 43*, 393-397.

Babin, P., Della Valle, G., Dendievel, R., Lourdin, D., & Salvo, L. (2007). X-ray tomography study of the cellular structure of extruded starches and its relations with expansion phenomenon and foam mechanical properties. *Carbohydrate Polymers, 68*, 329-340.

Bagley, E.B., Dintzis, F.R., & Chakrabarti, S. (1998). Experimental and conceptual problems in the rheological characterization of wheat flour doughs. *Rheologica Acta, 37*, 556-565.

Baird, D.G., & Labropoulos, A.E. (1982). Invited review - food dough rheology. *Chemical Engineering Communications, 15*, 1-25.

Bailey, C.H. (1939). Measuring fermentation rate and gas losses in dough. *Cereal Chemistry, 16*, 665-674.

Bailey, C.H. (1955). Gas pressure in fermented doughs. *Cereal Chemistry, 32*, 152-156.

Baker, J.C., & Mize, M.D. (1937). Mixing doughs in vacuum and in the presence of various gases. *Cereal Chemistry, 14*, 721-734.

Baker, J.C., & Mize, M.D. (1941). The origin of the gas cell in bread dough. *Cereal Chemistry, 18*, 19-34.

Baker, J.C., & Mize, M.D. (1946). Gas occlusion during dough mixing. *Cereal Chemistry, 23*, 39-51.

Barackman, R.A. (1954). Chemical leavening agents. *Transactions of the American Association of Cereal Chemists, 12*, 43-55.

Belton, P.S. (1999). On the elasticity of wheat gluten. *Journal of Cereal Science, 29*, 103-107.

Belton, P. S., & Dobraszczyk, B. J. (2006). Letter to the editor. *Journal of Cereal Science, 43*(2), 258.

Betschart, A.A. (1988). Nutritional quality of wheat and wheat foods (3rd ed.). In Y. Pomeranz (Ed.). *Wheat: Chemistry and Technology* (Vol. 2, pp. 91-130). St. Paul, MN: American Association of Cereal Chemists, Inc.

Bier, M., Bakker, B.M., & Westerhoff, H.V. (2000). How yeast cells synchronize their glycolytic oscillations: a perturbation analytic treatment. *Biophysical Journal, 78*, 1087-1093.

Bloksma, A.H. (1972a). Rheology of wheat flour dough. *Journal of Texture Studies, 3*, 3-17.

Bloksma, A.H. (1972b). The relation between the thiol and disulfide contents of dough and its rheological properties. *Cereal Chemistry, 49*, 104-118.

Bloskma, A.H. (1981). Effect of surface tension in the gas-dough interface on the rheological behaviour of dough. *Cereal Chemistry, 58*, 481-486.

Bloksma, A.H. (1986). Rheological aspects of structural changes during baking. In J. M. V. Blanshard, P. J. Frazier, & T. Gaillard (Eds.). *Chemistry and Physics of Baking* (pp.170-178). London, UK: The Royal Society of Chemistry.

Bloksma, A. H. (1990a). Rheology of the breadmaking process. *Cereal Foods World, 35*, 228-236.

Bloksma, A.H. (1990b). Dough structure, dough rheology, and baking quality. *Cereal Foods World, 35*, 237-244.

Bloksma, A. H. (1990c). Correction. *Cereal Foods World, 35*(9), 960-960.

Bloksma, A.H., & Bushuk, W. (1988). Rheology and chemistry of dough (3rd ed.). In Y. Pomeranz (Ed.). *Wheat: Chemistry and Technology* (Vol. 2, pp. 131-218). St. Paul, MN: American Association of Cereal Chemists, Inc.

Bloksma, A.H., & Nieman, W. (1975). The effect of temperature on some rheological properties of wheat flour doughs. *Journal of Texture Studies, 6*, 343-361.

Boudart, M. (1968). *Kinetics of Chemical Processes*. Cliffs, N.J: Prentice-Hall, Inc. (246 pp.)

Bushuk, W. (1966). Distribution of water in dough and bread. *Bakers Digest*, 40(5), 38-40.

Bushuk, W. (1985). Rheology: theory and application to wheat flour doughs. In H. Faridi (Ed.). *Rheology of Wheat Products* (pp. 1-26). St. Paul, MN: The American Association of Cereal Chemists, Inc.

Bushuk,W. (1998). Interactions in wheat doughs. In Hamer, R.J., & Hoseney, R.C. (Eds.). *Interactions, the Keys to Cereal Quality* (pp.1–14). St Paul, MN: American Association of Cereal Chemists, Inc.

Bushuk, W., & MacRitchie, F. (1988). Wheat proteins: Aspects of structure that are related to breadmaking quality. In R.D. Phillips & J.W. Finley (Eds.). *Protein Quality and the Effects of Processing* (pp. 337-361). New York, NY: Marcel Dekker.

Bushuk, W., Tsen, C.C., & Hlynka, I. (1968). The function of mixing in breadmaking. *Bakers Digest, 42*(4), 36-38, 40.

Campbell, G.M. 1991. The aeration of bread dough during mixing. *PhD Thesis.* University of Cambridge, UK.

Campbell, G.M., & Herrero-Sanchez, R. (2001). Bubble growth during proving of bread dough; Simulation and experimental validation of the effect of proving temperature. In *Proceedings of 6th World Chemical Engineering Congress*. University of Melbourne, Melbourne.

Campbell, G. M., & Mougeot, E. (1999). Creation and characterisation of aerated food products. *Trends in Food Science & Technology, 10*, 283-296.

Campbell, G.M., & Shah, P. (1999). Entrainment and disentrainment of air during bread dough mixing, and their effect on scale-up of dough mixers. In G.M. Campbell, C. Webb, S. S. Pandiella and Niranjan K. (Eds.). *Bubbles in Food* (pp. 11-20). St. Paul, MN: Eagan Press.

Campbell, G.M.; Rielly, C.D.; Fryer, P.J.; Sadd, P.A. (1991). The measurement of bubble size distributions in an opaque food fluid. *Transactions of the Institution of Chemical Engineers, Part C, Food and Bioproducts Processing, 69*, 67-76.

Campbell, G.M., Rielly, C.D., Fryer, P.J., & Sadd, P.A. (1993). Measurement and interpretation of dough densities. *Cereal Chemistry, 70*, 517-521.

Campbell, G.M., Rielly, C.D., Fryer, P.J., & Sadd, P.A. (1998). Aeration of bread dough during mixing: effect of mixing dough at reduced pressure. *Cereal Foods World, 43*, 163-167.

Campbell, G.M., Rielly, C.D., Fryer, P.J., & Sadd, P.A. (1999). Reconstruction of bubble size distributions from slices. In G.M. Campbell, C. Webb, S.S. Pandiella & K. Niranjan, (Eds.), *Bubbles in Food* (pp. 207-220). St. Paul, Minnesota: Eagan Press.

Campbell, G. M., Herrero-Sanchez, R., Payo-Rodriguez, R., & Merchan, M. L. (2001). Measurement of dynamic dough density and effect of surfactants and flour type on aeration during mixing and gas retention during proofing. *Cereal Chemistry, 78*, 272-277.

Campos, D.T., Steffe, J.F., & Ng, P.K.W. (1997). Rheological behaviour of undeveloped and developed wheat dough. *Cereal Chemistry, 74*, 489-494.

Carlson, T., & Bohlin, L. (1978). Free surface energy in the elasticity of wheat flour dough. *Cereal Chemistry, 55*, 539-544.

Cepeda, M., Waniska, R.D., Rooney, L.W., & Bejosano, F.P. (2000). Effects of leavening acids and dough temperature in wheat flour tortillas. *Cereal Chemistry, 77*, 489-494.

Challis, R.E., Povey, M.J.W., Mather, M.L., & Holmes, A.K. (2005). Ultrasound techniques for characterizing colloidal dispersions. *Reports on Progress in Physics, 68*, 1541-1637.

Charalambides, M. N., Wanigasooriya, L., Williams, J.G., Goh, S. M., & Chakrabarti, S. (2006). Large deformation extensional rheology of bread dough. *Rheologica Acta, 46*, 239-248.

Chen, C.H., & Bushuk, W. (1970). Nature of proteins in triticale and its parental species. I. Solubility characteristics and amino acid composition of endosperm proteins. *Canadian Journal of Plant Science, 50*, 9-14.

Chin, I. L., & Campbell, G. M. (2005a). Dough aeration and rheology: Part 1. Effects of mixing speed and headspace pressure on mechanical development of bread dough. *Journal of the Science of Food and Agriculture, 85*, 2184-2193.

Chin, N. L., & Campbell, G. M. (2005b). Dough aeration and rheology: Part 2. Effects of flour type, mixing speed and total work input on aeration and rheology of bread dough. *Journal of the Science of Food and Agriculture, 85*, 2194-2202.

Chin, N. L., Martin, P. J., & Campbell, G. M. (2004). Aeration during bread dough mixing I. Effect of direction and size of a pressure step-change during mixing on the turnover of gas. *Transactions of the Institution of Chemical Engineers, Part C, Food and Bioproducts Processing, 82*, 261-267.

Chin N.L., Martin P.J., & Campbell G.M. (2005). Dough aeration and rheology: Part 3. Effect of the presence of gas bubbles in bread dough on measured bulk rheology and work input rate. *Journal of the Science of Food and Agriculture, 85*, 2203-2212.

Chiotellis, E., & Campbell, G. M. (2003a). Proving of bread dough I - Modelling the evolution of the bubble size distribution. *Transactions of the Institution of Chemical Engineers, Part C, Food and Bioproducts Processing, 81*, 194-206.

Chiotellis, E., & Campbell, G. M. (2003b). Proving of bread dough II - Measurement of gas production and retention. *Transactions of the Institution of Chemical Engineers, Part C, Food and Bioproducts Processing, 81*, 207-216.

Cochran, S.A., Cin, D.A., & Veach, S.K. (1990). Microwaveable baked goods. U.S. Patent 4,957,750.

Cohen, A. C. (1988). Three-parameter estimation. In E.L. Crow & K. Shimizu (Eds.), *Lognormal Distributions: Theory and Applications* (pp. 113-138). New York: Marcel Dekker, Inc.

Collado, M., & De Leyn, I. (2000). Relationship between loaf volume and gas retention of dough during fermentation. *Cereal Foods World, 45*, 214-218.

Collatz, F.A. (1943). Report of hydrogen-ion concentration of flour and cereal products by electrometric measurements. *Cereal Chemistry, 26*, 107-112.

Conn, J.F. (1981). Chemical leavening systems in flour products. *Cereal Foods World, 26*, 119-123.

Cooper, D.M.L., Maytas, J.R., Katzenber, M.A., & Hallgrímsson, B. (2004). Comparison of microcomputed tomographic and microtomographic measurements of cortical bone porosity. *Calcified Tissue International*, 74, 437-447.

Cooper, D.M.L., Turinsky, A.L., Sensen C.W., & Hallgrímsson, B. (2003). Quantitative 3D analysis of the canal network in cortical bone by micro-computed tomography. *The Anatomical Record*, 27: 169-179.

Corbin, D., & Corbin, S. (1992). Process of making a microwaveable bakery product. U.S. Patent 5,110,614

Corbin, D., & Corbin, S. (1993). Method of making a microwaveable bakery product. U.S. Patent 5,266,345.

Cowan, M.L., Page, J.H., & Weitz, D.A. (2002). Novel techniques in ultrasonic correlation spectroscopy for characterizing the dynamics of strongly scattering materials. In Maev R. G. (Ed.). *Acoustical Imaging* (Vol. 26, pp.247-254). New York, NY: Kluwer Academic/Plenum Publishers.

Crow, E.L. (1988). Applications in atmospheric sciences. In E.L. Crow & K. Shimizu (Eds.), *Lognormal Distributions: Theory and Applications* (pp. 331-354). New York: Marcel Dekker, Inc.

David, P. (2003). Breadmaking quality of Durum wheat: effects of semolina particle size, fermentation time and glutenin molecular size. *M.Sc. thesis*. University of Manitoba, Canada.

de Cindio, B., & Correra, S. (1995). Mathematical modelling of leavened cereals goods. *Journal of Food Engineering, 24*, 379-403.

Delcourt, T., Lascar, F., & Grand, C. 2006. Histoire. In *Micro Encyclopédie Larousse* (pp. 410- 428). Paris, France: Larousse.

Dobraszczyk, B. J. (1997a). Development of a new dough inflation system to evaluate doughs. *Cereal Foods World, 42*, 516-519.

Dobraszczyk, B. J. (1997b). The rheological basis of dough stickiness. *Journal of Texture Studies, 28*, 139-162.

Dobraszczyk, B. J. (2004). The physics of baking: Rheological and polymer molecular structure-function relationships in breadmaking. *Journal of Non-Newtonian Fluid Mechanics, 124*, 61-69.

Dobraszczyk, B. J., & Morgenstern, M. P. (2003). Rheology and the breadmaking process. *Journal of Cereal Science, 38*, 229-245.

Dobraszczyk, B. J., & Roberts, C. A. (1994). Strain hardening and dough gas cell-wall failure in biaxial extension. *Journal of Cereal Science, 20*, 265-274.

Dobraszczyk, B. J., Smewing, J., Albertini, M., Maesmans, G., & Schofield, J. D. (2003). Extensional rheology and stability of gas cell walls in bread doughs at elevated

temperatures in relation to breadmaking performance. *Cereal Chemistry, 80*, 218-224.

Dus, S.J., & Kokini, J.L. (1990). Prediction of the nonlinear viscoelastic properties of a hard wheat-flour dough using the Bird-Carreau constitutive model. *Journal of Rheology, 34*, 1069-1084.

Edwards, N.M., Dexter, J.E., Scanlon, M.G., & Cenkowski, S. (1999). Relationship of creep-recovery and dynamic oscillatory measurements to durum wheat physical dough properties. *Cereal Chemistry, 76*, 638-645.

El-Dash, A.A., & Johnson, J.A. (1970). Influence of yeast fermentation and baking on the content of free amino acids and primary amino groups and their effect on bread aroma stimuli. *Cereal Chemistry, 47*, 247-258.

Eliasson, A, & Larsson, K. (1993). In *Cereals in Breadmaking: A Molecular Colloidal Approach* (pp.77). New York: Marcel Dekker, Inc.

Elion, E. (1933). A simple volumetric method for measuring gas production during dough fermentation. *Cereal Chemistry, 10*, 245-249.

Elion, E. (1939). Some remarks on the varying influence of compressed yeasts of different industrial origin on the gas retention of dough, as recorded by a new instrument, the Chefaro balance. *Cereal Chemistry, 16*, 598-610.

Elion, E. (1940). The importance of gas-production and gas-rentention measurements during the fermentation of dough. *Cereal Chemistry, 17*, 573-581.

Elmehdi, H.M. (2001). An Ultrasonic Investigation of the Effect of Voids on the Mechanical Properties of Bread Dough and the Role of Gas Cells in Determining the Cellular Structure of Freeze-Dried Breadcrumb. *PhD Thesis*, University of Manitoba, Canada.

Elmehdi, H. M., Page, J. H., & Scanlon, M. G. (2003a). Monitoring dough fermentation using acoustic waves. *Transactions of the Institution of Chemical Engineers, Part C, Food and Bioproducts Processing, 81*, 217-223.

Elmehdi, H. M., Page, J. H., & Scanlon, M. G. (2003b). Using ultrasound to investigate the cellular structure of bread crumb. *Journal of Cereal Science, 38*, 33-42.

Elmehdi, H. M., Page, J. H., & Scanlon, M. G. (2004). Ultrasonic investigation of the effect of mixing under reduced pressure on the mechanical properties of bread dough. *Cereal Chemistry, 81*, 504-510.

Elmehdi, H. M., Page, J. H., & Scanlon, M. G. (2007). Evaluating dough density changes during fermentation by different techniques. *Cereal Chemistry, 84*, (in print).

Ensminger, D. (1973). *Ultrasonics - The Low- and High-Intensity Applications.* (pp.18-33.

Ewart, J. A. D. (1989). Hypothesis for how Linear Glutenin Holds Gas in Dough. *Food Chemistry, 32*, 135-150.

Faergestad, E. M., Tronsmo, K. M., Aamodt, A., Bjerke, F., Magnus, E. M., & Dingstad, G. (2004). Effects of protein size distribution and dough rheology on hearth bread characteristics baked at different processes and scales. *Journal of Food Science, 69*, 524-535.

Falcone, P.M., Baiano, A., Zanini, F., Mancini, L., Tromba, G., Dreossi, D., Montanari, F., Scuor, N., & del Nobile, M.A. (2005). Three-dimensional quantitative analysis of bread crumb by x-ray microtomography. *Journal of Food Science, 70*, 265-272.

Fan, J., Mitchell, J. R., & Blanshard, J. M. V. (1999). A model for the oven rise of dough during baking. *Journal of Food Engineering, 41*, 69-77.

Faubion, J.M., & Faridi, H.A. (1986). Dough rheology: Its benefits to cereal chemists. In H. Faridi & J.M. Faubion (Eds.). *Fundamentals of Dough Rheology* (pp. 1-9). St. Paul. MN: American Association of Cereal Chemists, Inc.

Faubion, J.M., & Hoseney, R.C. (1990). The viscoelastic properties of wheat flour doughs. In H. Faridi & J.M. Faubion (Eds.). *Dough Rheology and Baked Product Texture* (pp. 29-66). New York, NY: Van Nostrand Reinhold Publishers.

Faubion, J.M., Dreese, P.C., & Diehl, K.C. (1985). Dynamic rheological testing of wheat flour doughs. In H. Faridi (Ed.). *Rheology of Wheat Products* (pp. 91-116). St. Paul, MN: The American Association of Cereal Chemists, Inc.

Ferry, J.D. (1961). *Viscoelastic Properties of Polymers.* New York, NY: John Wiley & Sons, Inc.

Fu, B. X., Sapirstein, H. D., & Bushuk, W. (1996). Salt-induced disaggregation/ solubilization of gliadin and glutenin proteins in water. *Journal of Cereal Science, 24*, 241-246.

Fu, J., Mulvaney, S. J., & Cohen, C. (1997). Effect of added fat on the rheological properties of wheat flour doughs. *Cereal Chemistry, 74*, 304-311.

Galal, E.M., Varriano-Marston, E., & Johnson, J.A., (1978).Rheological dough properties as affected by organic acids and salt. *Cereal Chemistry, 55*, 683-691.

Gan, Z., Ellis, P. R., Vaughan, J. G., & Galliard, T. (1989). Some effects of non-endosperm components of wheat and of added gluten on wholemeal bread microstructure. *Journal of Cereal Science, 10*, 81-91.

Gan, Z., Angold, R. E., Williams, M. R., Ellis, P. R., Vaughan, J. G., & Galliard, T. (1990). The microstructure and gas retention of bread dough. *Journal of Cereal Science, 12*, 15-24.

Gan, Z., Ellis, P. R., & Schofield, J. D. (1995). Mini Review: Gas cell stabilisation and gas retention in wheat bread dough. *Journal of Cereal Science, 21*, 215-230.

Gelinas, P. (1997). Collaborative study on yeast activity, gas production (AACC Method 89-01). *Food Microbiology, 14*, 55-62.

Geng, Q., & Hayes-Jacobson, S. M. (2001). Leavened dough extrusion process. U.S. Patent 6,180,151.

Geng, Q., & Hayes-Jacobson, S. M. (2003). Leavened dough extrusion. U.S. Patent 6,607,763.

Gibson, L.J., & Ashby, M.F. (1997). *Cellular Solids: Structure and Properties* (2nd Edition). Cambridge, UK: University Press. (528 pp).

Guy, E.J., Vettel, H.E., & Pallansch, M.J. (1967). Effect of the salts of the lyotropic series on the Farinograph characteristics of milk-flour dough. *Cereal Science Today*, 12, 200-203.

Hammes, G.G. (1978). *Principles of Chemical Kinetics* (pp.1-23). New York, NY: Associated Press, Inc.

Han, C.D., & Yoo, H.J. (1981). Studies on structural foam processing -4. Bubble growth during mold filling. *Polymer Engineering and Science, 21*, 518-533.

Hansen, L.M., Anderson, B.R., Lorence, & M.W., Reinke, J.D. (2003). Freezer to oven dough products. U.S. Patent 6,589,583.

Hashin, Z., & Shtrikman, S. (1963). A variational approach to the theory of the elastic behaviour of multiphase materials. *Journal of the Mechanics and Physics of Solids, 11*, 127-140.

Hayman, D., Hoseney, R. C., & Faubion, J. M. (1998a). Bread crumb grain development during baking. *Cereal Chemistry*, 75, 577-580.

Hayman, D., Sipes, K., Hoseney, R. C., & Faubion, J. M. (1998b). Factors controlling gas cell failure in bread dough. *Cereal Chemistry, 75*, 585-589.

He, H., & Hoseney, R. C. (1991). Gas retention of different cereal flours. *Cereal Chemistry, 68*, 334-336.

He, H., Roach, R. R., & Hoseney, R. C. (1992). Effect of nonchaotropic salts on flour bread-making properties. *Cereal Chemistry, 69*, 366-371.

Health Canada. (2007). Health Canada. [online database] *Food and Drugs Act* – Division 3 "Baking Powder". URL: http://www.hc-sc.gc.ca/fn-an/legislation/acts-lois/fda-lad/index_e.html (May 13, 2007).

Heidolph, B.B. (1996). Designing chemical leavening systems. *Cereal Foods World, 41*, 118-126.

Hibberd, G.E. (1970a). Dynamic viscoelastic behaviour of wheat flour doughs. Part II: Effects of water content in the linear region. *Rheologica Acta, 9*, 497-500

Hibberd, G.E. (1970b). Dynamic viscoelastic behaviour of wheat flour doughs. Part III: The influence of starch granules. *Rheologica Acta*, 9, 501-505.

Hibberd, G.E., & Parker, N.S. (1975). Measurements of the fundamental rheological properties of wheat-flour doughs. *Cereal Chemistry, 52*, 1-23.

Hibberd, G.E., & Parker, N.S. (1979). Nonlinear creep and creep recovery of wheat-flour doughs. *Cereal Chemistry, 56*, 232 – 235.

Hibberd, G.E., & Wallace, W.J. (1966). Dynamic viscoelastic behaviour of wheat flour doughs. Part I. Linear aspects. *Rheologica Acta*, 5, 193-198.

Hlynka, I. (1962). Influence of temperature, speed of mixing, and salt on some rheological properties of dough in the Farinograph. *Cereal Chemistry, 39*, 286-303.

Hlynka, I., & Anderson, J.A. (1955). Laboratory dough mixer with an air-tight bowl. *Cereal Chemistry, 32*, 83-87.

Holmes, J.T., & Hoseney, R.C. (1987a). Chemical leavening: Effect of pH and certain ions on breadmaking properties. *Cereal Chemistry, 64*, 343-348

Holmes, J.T., & Hoseney, R.C. (1987b). Frozen doughs: Freezing and thawing rates and the potential of using a combination of yeast and chemical leavening. *Cereal Chemistry, 64*, 348-351.

Hood, L.F., & Liboff, M. (1982). Starch Ultrastructure. In D.B. Bechtel (Ed.). *New Frontiers in Food Microstructure* (pp. 341-372). St. Paul, MN: The American Association of Cereal Chemists.

Hoseney, R. C. (1998). *Principles of Cereal Science and Technology* (2nd Ed.) (pp. 29-64, 275-305). St. Paul, MN: American Association of Cereal Chemists, Inc.

Hoseney, R. C., & Finney, P.L. (1974). Mixing, a contrary view. *Bakers Digest, 48*(2), 22-28, 66.

Hoseney, R.C., Hsu, K.H., & Junge, R.C. (1981). A simple spread test to measure the rheological properties of dough. *Cereal Chemistry, 56*, 141-143.

Hoseney, R.C., Wade, P., & Finley, J.W. (1988). Soft wheat products (3rd ed.). In Y. Pomeranz (Ed.). *Wheat: Chemistry and Technology* (Vol. 2, pp. 407-456). St. Paul, MN: American Association of Cereal Chemists, Inc.

Huang, V.T., & Panda, F.A. (2004). Chemical leavener system comprising acidulant precursors. U.S. Patent 6,824,807.

Huebner, F.R. (1970). Comparative studies on glutenins from classes of wheat. *Journal of Agricultural and Food Chemistry*, 18, 256-259

Innophos. (undated). Bakery applications of phosphates.

Janssen, A. M., Van Vliet, T., & Vereijken, J. M. (1996a). Rheological behaviour of wheat glutens at small and large deformations. Effect of gluten composition. *Journal of Cereal Science, 23*, 33-42.

Janssen, A. M., Van Vliet, T., & Vereijken, J. M. (1996b). Fundamental and empirical rheological behaviour of wheat flour doughs and comparison with bread making performance. *Journal of Cereal Science, 23*, 43-54.

Jantzi, S.C., Walker, A.E., Shelton, D.R., & Walker, C.E. (1999). A new method for measuring CO_2 evolution in chemically leavened dough systems. Abstract of poster N° 84 presented at the Annual Meeting of the American Association of Cereal Chemists. Seattle, Washington. October 31 – November 3.

Javanaud, C. (1988). Applications of ultrasound to food systems. *Ultrasonics, 26*, 117-123.

Johannesson, K.A., & Mitson, R.B. (1983). Fisheries acoustics: a practical manual for aquatic biomass estimation. *FAO Fisheries Technical Paper 240* (pp. 249). Rome: Food and Agriculture Organization of the United Nations.

Johnson, J.A. & Sanchez, C. R.S. (1973). The nature of bread flavor. *Bakers Digest, 47* (10), 48-50.

Junge, R.C., Hoseney, R.C., & Varriano-Marston, E. (1981). Effect of surfactants on air incorporation in dough and the crumb grain of bread. *Cereal Chemistry, 58*, 338-342.

Kaczmarek, M. (2001). Ultrasound – A useful tool to investigate complex materials. *Periodica Poytechnica Services Chemical Engineering, 43*, 111-129.

Kemp, G. (2005). Lactate accumulation, proton buffering, and pH change in ischemically exercising muscle. *American Journal of Physiology: Regulatory, Integrative and Comparative Physiology, 289*, 895-901.

Kidmose, U., Pedersen, L., & Nielsen, M. (2001). Ultrasonics in evaluating rheological properties of dough from different wheat varieties and during ageing. *Journal of Texture Studies*, *32*, 321-334.

Kim, H.R., & Bushuk, W. (1995). Salt sensitivity of acetic acid-extractable proteins of wheat flour. *Journal of Cereal Science*, *21*, 241-250.

Kinsella, J.E., & Hale, M.L. (1984). Hydrophobic associations and gluten consistency: effects of specific ions. *Journal of Agricultural and Food Chemistry*, *32*, 1054-1056.

Kolmogoroff, A.N. (1941). Über das logarithmisch normale verteilungsgesetz der dimensionen der teilchen bei zerstückelung. *C. R. Academy of Sciences* (Doklady) *URSS*, *XXXI*, 99-101. Cited by Shimizu, K., & Crow, E.L. (1988), in History, genesis, and properties. In E.L. Crow & K. Shimizu (Eds.), *Lognormal Distributions: Theory and Applications* (pp. 1). New York: Marcel Dekker, Inc.

Kokelaar, J.J., & Prins, A. (1995). Surface rheological properties of bread dough components in relation to gas bubble stability. *Journal of Cereal Science*, *22*, 53-61.

Kokelaar, J.J., vanVliet, T., & Prins, A. (1996). Strain hardening properties and extensibility of flour and gluten doughs in relation to breadmaking performance. *Journal of Cereal Science, 24*, 199-214.

Kuhn, J.L., Goldstein, S.A., Feldkamp, L.A., Goulet, R.W., & Jesion, G. (1990). Evaluation of a microcomputed tomography system to study trabecular bone structure. *Journal of Orthopaedic Research, 8*, 833-842.

Kulmyrzaev, A., Cancelliere, C., & McClements, D.J. (2000). Characterization of aerated foods using ultrasonic reflectance spectroscopy. *Journal of Food Engineering*, *46*, 235-241.

Kulp, K. (1973). Physicochemical properties of wheat starch as related to bread. *Bakers Digest*, *47*, 34-38.

Kusunose, C., Fujii, T., & Matsumoto, H. 1999. Role of starch granules in controlling expansion of dough during baking. *Cereal Chemistry*, *76*, 920-924.

Lagrain, B., Boeckx, L., Wilderjans, E., Delcour, J.A., & Lauriks, W. (2006). Non-contact ultrasound characterization of bread crumb: application of the Biot-Allard model. *Food Research International*, *39*, 1067-1075.

Lajoie, M.S., & Thomas, M.C. (1991). Versatility of bicarbonate leavening bases. *Cereal Foods World*, *36*, 420-424.

Landis, Q., & Frey, C.N. (1943). Direct determination of fermentation rates in dough. *Cereal Chemistry*, 20, 368-376.

Laughlin, D.L., & DeMars, J.A. (1999). Method of preparing dough. U.S. Patent 5,858,440.

Laughlin, D.L., DeMars, J.A., & Vargas, G.C. (1999). Method of preparing dough. U.S. Patent 5,855,945.

Laughlin, D.L., DeMars, J.A., & Vargas, G.C. (2000). Method of preparing dough. U.S. Patent 6,165,533.

Launay, B., & Bure, J. (1974). Stress relaxation in wheat flour doughs following a finite period of shearing. I. Qualitative study. *Cereal Chemistry, 51*, 151 – 162.

Lawrence, C., Rodger, A., & Compton, R. (1996). *Foundations of Physical Chemistry* (pp. 46-62). New York, NY: Oxford University Press

Lee, H. O., Luan, H., & Daut, D. (1992). Use of an ultrasonic technique to evaluate the rheological properties of cheese and dough. *Journal of Food Engineering, 16*, 127-150.

Lee, S. Y., Pyrak-Nolte, L. J., & Campanella, O. (2004). Determination of ultrasonic-based rheological properties of dough during fermentation. *Journal of Texture Studies, 35*, 33-51.

Leroy, V. Fan, Y., Strybulevych, A.L., Bellido, G.G., Page, J.H., & Scanlon, M.G. (2007). Investigating the bubble size distribution in dough using ultrasound. In G. M. Campbell *et al.* (Eds.). *Bubbles in Food 2: Novelty, Health & Luxury*. AACC Press. *In Press*.

Létang, C., Piau, M., & Verdier, C. (1996). Caractérisation ultrasonore et propriétés rhéologiques de mélanges farine eau. *Les Cahiers de Rhéologie*, 15, 319-326.

Létang, C., Piau, M., & Verdier, C. (1999). Characterization of wheat flour-water doughs. Part I: Rheometry and microstructure. *Journal of Food Engineering, 41*, 121-132.

Létang, C., Piau, M., Verdier, C., & Lefebvre, L. (2001). Characterization of wheat-flour-water doughs: A new method using ultrasound. *Ultrasonics, 39*, 133-141.

Lim, K.S., & Barigou, M. (2004). X-ray micro-computed tomography of cellular food products. *Food Research International*, 37, 1001-1012.

Limpert, E., Stahel, W.A., & Abbt, M. (2001). Log-normal distributions across the sciences: keys and clues. *BioScience, 51*, 341-352.

Lindinger, M.I., Kowalchuk, J.M., & Heigenhauser, J.F. (2005). Applying physicochemical principles to skeletal muscle acid-base status. *American Journal of Physiology: Regulatory, Integrative and Comparative Physiology*, 289, 891-894.

Lineback, D.R., & Rasper, V.F. (1988). Wheat carbohydrates (3rd ed.). In Y. Pomeranz (Ed.). *Wheat: Chemistry and Technology* (Vol. 2, pp. 277-372). St. Paul, MN: American Association of Cereal Chemists, Inc.

Liu, Z., & Scanlon, M. G. (2003). Predicting mechanical properties of bread crumb. *Transactions of the Institution of Chemical Engineers, Part C, Food and Bioproducts Processing, 81*, 224-238.

Lubetkin, S.D. (1995). The fundamentals of bubble evolution. *Chemical Society Reviews, 24*, 243-250.

MacRitchie, F. (1976). The liquid phase of dough and its role in baking. *Cereal Chemistry, 53*, 318-326.

MacRitchie, F. (1986). Physicochemical processes in mixing. In J. M. V. Blanshard, P. J. Frazier, & T. Gaillard (Eds.). *Chemistry and Physics of Baking* (pp.132-146). London, UK: The Royal Society of Chemistry.

Mani, K., Eliasson, A.-C., Lindahl, L., & Tragardh, C. (1992). Rheological properties and bread making quality of wheat flour doughs made with different dough mixers. *Cereal Chemistry, 69*, 222-225.

Malloch, J.G. (1939). A convenient apparatus for gas production determinations by the Blish method. *Cereal Chemistry*, 16, 178-182.

Marston, P. E. (1986). Dough development for breadmaking under controlled atmospheres. *Journal of Cereal Science, 4*, 335-344.

Martin, P. (2004). Controlling the breadmaking process: The role of bubbles in bread. *Cereal Foods World, 49*, 72-75.

Martin, P. J., Chin, N. L., & Campbell, G. M. (2004a). Aeration during bread dough mixing II. A population balance model of aeration. *Transactions of the Institution of Chemical Engineers, Part C, Food and Bioproducts Processing, 82*, 268-281.

Martin, P.J., Chin, N.L., Campbell, G.M., & Morrant, C.J. (2004b). Aeration during bread dough mixing. III. Effect of scale-up. *Transactions of the Institution of Chemical Engineers, Part C, Food and Bioproducts Processing, 82*, 282-290.

Matsumoto, H., Nishiyama, J., Mita, T., & Kuninori, T. (1975). Rheology of fermenting dough. *Cereal Chemistry, 52*, 82-88.

Matsumoto, H. (1988). The rheology of yeasted dough and the tension of the cell membrane. In H. Faridi & J.M. Faubion (Eds.). *Fundamentals of Dough Rheology* (pp.55-62). St. Paul. MN: American Association of Cereal Chemists, Inc.

McClements, D.J. (1995). Advances in the application of ultrasound in food analysis and processing. *Trends in Food Science and Technology, 6*, 293-299.

McClements, D.J. (1997). Ultrasonic characterization of foods: Principles methods and applications. *Critical Reviews in Food Science and Nutrition, 37*, 1-46.

McClements, D.J. (1998). Particle sizing of food emulsions using ultrasonic spectrometry: principles, techniques and applications. In M.J.W. Povey & T.J. Mason (Eds.). *Ultrasound in Food Processing* (pp. 85-104). London, UK: Blackie Academic & Professional.

McDermott, E.E., & Pace, J. 1961. Modification of the properties of flour protein by thiolated gelatin. *Nature, 192*, 657.

McGilvery, J.D., & Crowther, J.P. (1953). The hydrolysis of the condensed phosphates. II. (A) The role of the hydrogen ion in the hydrolysis of sodium pyrophosphate. II (B). The dissociation constants of pyrophosphoric acid. *Canadian Journal of Chemistry. 32*, 174-185.

McKinley, G.H., Anna, S.L., Tripathi, A., & Yao, M. (1999). Extensional rheometry of polymeric fluids and the uniaxial elongation of viscoelastic filaments. Presented at the 15th Annual Meeting of the International Polymer Processing Society. June.

Mehta, K. (2007). The use of low intensity ultrasound to investigate the effect of mixing time and ingredients on the mechanical properties of bread dough. M.Sc. Thesis, University of Manitoba, Canada.

Menjivar, J.A. Fundamental aspects of dough rheology. (1989). In H.A. Faridi & J.M. Faubion (Eds.). *Dough Rheology and Baked Product Texture* (pp. 1-28). Van Nostrand Reinhold, NY: Klumer Academic Pub.

Miller, R.A., Graf, E., & Hoseney, R.C. (1994). Leavened dough pH determination by an improved method. *Journal of Food Science, 59*, 1086-1090.

Mills, E. N. C., Wilde, P. J., Salt, L. J., & Skeggs, P. (2003). Bubble formation and stabilization in bread dough. *Food and Bioproducts Processing, 81*(C3), 189-193.

Mitchell, J.R., Fan, J.-T., & Blanshard, J.M.V. (1999). Simulation of bubble growth in heat processed cereal systems. In G.M. Campbell, C. Webb, S. S. Pandiella and Niranjan K. (Eds.). *Bubbles in Food* (pp. 107-112). St. Paul, MN: Eagan Press.

Moore, W.J. (1962). *Physical Chemistry* (3rd ed.). (pp. 253-322). Englewood Cliffs, N.J.: Prentice-Hall International, Inc.

Narayanaswamy, V., & Daravingas, G.V. (2001). Refrigerated and shelf-stable bakery dough products. U.S. Patent 6,261,613.

Navickis, L. L., & Nelsen, T. C. (1992). Mixing and extensional properties of wheat-flour doughs with added corn flour, fibers, and gluten. *Cereal Foods World, 37*, 30-35.

Navickis, L.L. Anderson, R.A., Bagley, E. B., & Jasberg, B.K. (1982). Viscoelastic properties of wheat flour doughs: variation of dynamic moduli with water and protein content. *Journal of Texture Studies*, 13, 249-264.

Ornebro, J., Nylander, T., & Eliasson, A. C. (2000). Interfacial behaviour of wheat proteins. *Journal of Cereal Science, 31*, 195-221.

Orth, R.A., & Bushuk, W. (1972). A comparative study of the proteins of wheats of diverse baking qualities. *Cereal Chemistry, 49*, 268-275.

Orth, R.A., & Shellenberger, J.A. (1988). Origin, production, and utilization of wheat (3rd ed.). In Y. Pomeranz (Ed.). *Wheat: Chemistry and Technology* (Vol. 2, pp. 1-14). St. Paul, MN: American Association of Cereal Chemists, Inc.

Osborne, T.B. (1907). In *The Proteins of the Wheat Kernel* (pp. 119). Washington, DC: Carnegie Institution of Washington.

Page, J.H., Sheng, P., Schriemer, H.P., Jones, I., Jing, X., & Weitz, D.A. (1996). Group velocity in strongly scattering media. *Science, 271*, 13-16.

Page, J.H., Cowan, M.L., & Weitz, D.A. (2000). Diffusing acoustic wave spectroscopy of fluidized suspensions. *Physica, 279*, 130-133.

Page, J.H., Cowan, M.L., Weitz, D.A., & van Tiggelen, B.A. (2003). Diffusing acoustic wave spectroscopy: fluid fluctuation spectroscopy with multiply scattered ultrasonic wave. In B.A. van Tiggelen & S. Skipetrov (Eds.). *Wave Scattering in Complex Media: From Theory to Application* (pp. 151-174). Dordrecht, The Netherlands: Klumer Academic Publishers: NATO Science Series.

Parfitt, A.M., Drezner, M.K., Glorieux, F.H., Kanis, J.A., Malluche, H., Meunier, P.J., Ott, S.M., & Recker, R.R. (1987). Bone morphometry: standardization of nomenclature, symbols and units. *Journal of Bone and Mineral Research, 2*, 595-610.

Parks, J.R., Avrom, R.H., Barnett, J.C., & Wright, F.H. (1960). Methods for measuring reactivity of chemical leavening systems. *Cereal Chemistry, 37*, 503-518.

Perry, M.R., & Colman, M.A. (2001). Packaged dough product. U.S. Patent 6,242,024.

Perry, M.R., & Colman, M.A. (2003). Leavened dough or batter packaging system. U.S. Patent 6,635,291.

Phan-Thien, N., & Safari-Ardi, M. (1998). Linear viscoelastic properties of flour-water doughs at different water concentrations. *Journal of Non-Newtonian Fluid Mechanics, 74*, 137-150.

Phan-Thien, N., Safari-Ardi, M., & Marales-Patiño, A. (1997). Oscillatory and simple shear flows of a flour–water dough: a constitutive model. *Rheologica Acta*, 36, 38–48.

Pomeranz, Y. (1988). Chemical compostion of kernel structures (3rd ed.). In Y. Pomeranz (Ed.). *Wheat: Chemistry and Technology* (Vol. 1, pp. 97-158). St. Paul, MN: American Association of Cereal Chemists, Inc.

Ponte, J.G., Glass, Jr., R.L., & Geddes, W.F. (1960). Studies on the behaviour of active dry yeast in breadmaking. *Cereal Chemistry, 37*, 263-279.

Povey, M.J.W. (1997). *Ultrasonic Techniques for Fluids Characterization* (pp. 214). Academic Press: San Diego, CA.

Povey, M.J.W. (1998). Rapid determination of food materials properties. In M.J.W. Povey & T.J. Mason (Eds.). *Ultrasound in Food Processing* (pp. 30-65). London, UK: Blackie Academic & Professional.

Preston, K.R. (1981). Effects of neutral salts upon wheat gluten protein properties. I. Relationship between the hydrophobic properties of gluten proteins and their extractability and turbidity in neutral salts. *Cereal Chemistry, 58*, 317-324.

Preston, K.R. (1984). Gel filtration and characterization of neutral salt extracted wheat gluten proteins varying in hydrophobic properties. *Cereal Chemistry, 61*, 76-83.

Preston, K. R. (1989). Effects of neutral salts of the lyotropic series on the physical dough properties of a Canadian red spring wheat flour. *Cereal Chemistry, 66*, 144-148.

Ramkumar, D. H. S., Bhattacharya, M., Menjivar, J. A., & Huang, T. A. (1996). Relaxation behavior and the application of integral constitutive equations to wheat dough. *Journal of Texture Studies, 27*(5), 517-544.

Redfern, S. (1950). An automatic electrical recording pressuremeter. *Cereal Chemistry, 27*, 451-463.

Reid, C.E., & Passin, T.B. (1992). *Signal Processing in C*. New York, NY: John Wiley & Sons, Inc. (325 pp.).

Robergs, R.A., Ghiasvand, F., and Parker, D. Biochemistry of exercise-induced metabolic acidosis. (2004). *American Journal of Physiology: Regulatory, Integrative and Comparative Physiology, 287*, 502-516.

Ross, K.A., Pyrak-Nolte, L.J., & Campanella, O.H. (2004). The use of ultrasound and shear oscillatory tests to characterize the effect of mixing time on the rheological properties of dough. *Food Research International, 37*, 567-577.

Safari-Ardi, M., & Phan-Thien, N. (1998). Stress relaxation and oscillatory tests to distinguish between doughs prepared from wheat flours of different varietal origin. *Cereal Chemistry, 75*, 80-84.

Sahi, S. S. (1994). Interfacial properties of the aqueous phases of wheat-flour doughs. *Journal of Cereal Science, 20*, 119-127.

Sahi, S. S. (2003). The interfacial properties of the aqueous phases of full recipe bread doughs. *Journal of Cereal Science, 37*, 205-214.

Sahlstrom, S., Park, W., & Shelton, D.R. (2004). Factors influencing yeast fermentation and the effect of LMW sugars and yeast fermentation on hearth bread quality. *Cereal Chemistry, 81*, 328-335.

Salt, L. J., Wilde, P. J., Georget, D., Wellner, N., Skeggs, P. K., & Mills, E. N. C. (2006). Composition and surface properties of dough liquor. *Journal of Cereal Science, 43*, 284-292.

Sapirstein, HD., David, P., Preston, K.R., & Dexter, J.E. (2007). Durum wheat breadmaking quality: effects of gluten strength, protein composition, semolina particle size and fermentation time. *Journal of Cereal Science, 45*, 150-161.

Sarkar, A. K. (1993). Flour milling (4th Ed.). In *Grains & Oilseeds: Handling, Marketing, Processing* (Vol. 2, pp. 603-654). Winnipeg, MB: Canadian International Grains Institute.

Scanlon, M.G. (2007). Personal communications.

Scanlon, M.G., & Zghal, M.C. (2001). Bread properties and crumb structure. *Food Research International, 34*, 841-864.

Scanlon, M.G., Elmehdi, H.M., & Page, J.H. (2002). Probing gluten interactions with low-intensity ultrasound. In P.K.W. Ng and C.W. Wrigley (Eds.). *Wheat Quality Elucidation: The Bushuk Legacy* (pp. 170-182). St Paul, MN: American Association of Cereal Chemists, Inc.

Shah, P., Campbell, G. M., McKee, S. L., & Rielly, C. D. (1998). Proving of bread dough: Modelling the growth of individual bubbles. *Food and Bioproducts Processing, 76*(C2), 73-79.

Shah, P, Grant, G.M., Dale, C., & Rudder A. (1999). Modelling bubble growth during proving of bread dough: predicting the output from the Chopin Rheofermentometer. In G.M. Campbell, C. Webb, S. S. Pandiella and Niranjan K. (Eds.). *Bubbles in Food* (pp. 95-106). St. Paul, MN: Eagan Press.

Sheng, P. (1988). Microstructures and physical properties of composites. In J.L. Ericksen, D. Kinderlehrer, R. Kohr, & J.-L. Lions. (Eds.). *Homogenization and Effective Moduli of Materials and Media* (pp.196). New York, NY: Springer-Verlarg.

Sherwood, R.C., Hildebrand, F.C., & McClellan, B.A. (1940). Modification of the Bailey-Johnson method for measurement of gas production in fermenting dough. *Cereal Chemistry*, 17, 621-626.

Shewry, P. R., Popineau, Y., Lafiandra, D., & Belton, P. (2001). Wheat glutenin subunits and dough elasticity: findings of the EUROWHEAT project. *Trends in Food Science & Technology*, *11*, 433-441.

Shewry., P.R., Halford, N.G., Belton, P.S., & Tatham, A.S. (2002). The structure and properties of gluten: an elastic protein from wheat grain. *Philosophical Transactions of the Royal Society of London, B*, 133-142.

Shimiya, Y., & Nakamura, K. (1997). Changes in size of gas cells in dough and bread during breadmaking and calculation of critical size of gas cells that expand. *Journal of Texture Studies, 28*, 273-288.

Shimiya, Y., & Yano, T. (1988). Rates of shrinkage and growth of air bubbles entrained in wheat flour dough. *Agricultural and Biological Chemistry*, *52*, 2879-2883.

Shimizu, K., & Crow, E.L. (1988). History, genesis, and properties. In E.L. Crow & K. Shimizu (Eds.), *Lognormal Distributions: Theory and Applications* (pp. 1-26). New York: Marcel Dekker, Inc.

Singh, H., & MacRitchie, F. (2001). Mini review: application of polymer science to properties of gluten. *Journal of Cereal Science*, 33, 231-243.

Singh, M., & Khatkar, B.S. (2005). Structural and functional properties of wheat storage proteins: A review. *Journal of Food Science and Technology*, *42*, 455-471.

Smith, J.R., Smith, T.L., & Tschoegl, N.W. (1970). Rheological properties of wheat flour doughs III. Dynamic shear modulus and its dependence on amplitude, frequency, and dough composition. *Rheologica Acta*, *9*, 239-252.

Szabó, Z.G. (1969). Kinetic characterization of complex reaction systems. In C.H. Bamford, & C.F.H. Tipper (Eds.). *Comprehensive Chemical Kinetics* (Vol. 2, pp. 1-80). Amsterdam, The Netherlands: Elsevier Publishing Company.

Tanaka, K., Furukawa, K., & Matsumoto, H. (1967). The effect of acid and salt on the farinogram and extensigram of dough. *Cereal Chemistry*, *44*, 675-680.

Taranto, M.V. Structural and textural characteristics of baked goods. (1983). In M. Peleg & E.B. Bagley (Eds.). *Physical Properties of Foods* (pp. 229-265). Westport, CT: AVI Publishing Co, Inc.

Tatham, A.S., Hider, R.C., Drake, A.F. (1983). The effect of counterions on melittin aggregation. *Biochemistry Journal*, *211*, 683-686.

Trater, A. M., Alavi, S., & Rizvi, S. S. H. (2005). Use of non-invasive X-ray microtomography for characterizing microstructure of extruded biopolymer foams. *Food Research International, 38*, 709-719.

Tronsmo, K. M., Magnus, E. M., Baardseth, P., Schofield, J. D., Aamodt, A., & Faergestad, E. M. (2003). Comparison of small and large deformation rheological properties of wheat dough and gluten. *Cereal Chemistry, 80*, 587-595.

Underwood, E.E. (1970). In *Quantitative Stereology* (pp. 274). Reading, Massachusetts: Addison-Wesley Publishing Co.

USDA (2006). United States Department of Agriculture [online database]. *National Agricultural Statistics Service*. URL: http://www.usda.gov/nass/pubs/agr05/acro05.htm. (May 15, 2007).

Uthayakumaran, S., Newberry, M., Keentok, M., Stoddard, F. L., & Bekes, F. (2000). Basic rheology of bread dough with modified protein content and glutenin-to-gliadin ratios. *Cereal Chemistry, 77*, 744-749.

van Vliet, T. (1999). Physical factors determining gas cell stability in a dough during bread making. In G.M. Campbell, C. Webb, S. S. Pandiella and Niranjan K. (Eds.). *Bubbles in Food* (pp. 95-106). St. Paul, MN: Eagan Press.

van Vliet, T., Janssen, A. M., Bloksma, A. H., & Walstra, P. (1992). Strain hardening of dough as a requirement for gas retention. *Journal of Texture Studies, 23*, 439-460.

Venerus, D.C., Yala, N., & Bernstein, B. (1998). Analysis of diffusion-induced bubble growth in viscoelastic liquids. *Journal of Non-Newtonian Fluid Mechanics, 75*, 55-75.

Verdier, C., & Piau, M. (1996). Analysis of the morphology of polymer blends using ultrasound. *Journal of Physics D-Applied Physics, 29*, 1454-1461.

Verdier, C, Longin, P.Y., & Piau, M. (1998). Dynamic shear and compressional behavior of polydimethylsiloxanes: Ultrasonic and low frequency characterization. *Rheologica Acta, 37*, 234-244.

Wang, C.E., & Kokini, J.L. (1995). Prediction of the nonlinear viscoelastic properties of gluten doughs. *Journal of Food Engineering, 25*, 297-309

Weegels, P.L., Groeneweg, F., Esselink, E., Smit, R., Brown, R., & Ferdinando, D. (2003). Large and fast deformations crucial for the rheology of proofing dough. *Cereal Chemistry, 80*, 424-426.

Wellner, N., Bianchini, D., Clare-Mills, E.N., & Belton, P. (2003). Effect of selected Hofmeister anions on the secondary structure and dynamics of wheat prolamins in gluten. *Cereal Chemistry, 80*, 596-600.

Whitworth, M.B., & Alava, J.M. (1999). The imaging and measurement of bubbles in bread doughs. In G.M. Campbell, C. Webb, S.S. Pandiella & K. Niranjan, (Eds.), *Bubbles in Food* (pp. 221-232). St. Paul, Minnesota: Eagan Press.

Wikstrom, K., & Bohlin, L. (1999). Extensional flow studies of wheat flour dough. I. Experimental method for measurements in contraction flow geometry and application to flours varying in breadmaking performance. *Journal of Cereal Science, 29*, 217-226.

Wiseblatt, L., & Kohn, F.E. (1960). Some volatile aromatic compounds in fresh bread. *Cereal Chemistry, 37*, 55-66.

Wolfson, R., & Pasachoff, J.M. (1987). In *Physics* (pp. 355, 382). Toronto: Little, Brown, and Company (Canada) Limited.

Wood, A.B. (1941). *A Textbook of Sound.* London, UK: G. Bell and Sons (pp. 361).

Working, E.B., & Swanson, E.C. (1946). An automatic device for the measurement of gas production and gas retention in doughs. *Cereal Chemistry*, 23, 210-216.

Wrigley, C. (2006). Global warming and wheat quality. *Cereal Foods World, 51*, 34-36.

Wu, Y.V., & Dimler, R.J. (1963a). Hydrogen-ion equilibria of wheat gluten. *Archives of Biochemistry and Biophysics, 102*, 230-237.

Wu, Y.V., & Dimler, R.J. (1963b). Hydrogen ion equilibria of wheat glutenin and gliadin. *Archives of Biochemistry and Biophysics, 103*, 310-318.

Xu, J. Y., Bietz, J. A., Felker, F. C., Carriere, C. J., & Wirtz, D. (2001). Rheological properties of vital wheat gluten suspensions. *Cereal Chemistry, 78*, 181-185.

Yong, S.H., Anderson, G.R., & Levin, L. (1983a). Dough product containing an organic acid leavener. U.S. Patent 4,388,336.

Yong, S.H., Edmonson, D., Evans, Leah, G., Hohle, D.G., Jensen, S.H., O'Keefe, & L.S., Laatsch, D.S. (1983b). Refrigerated dough and method of manufacture. U.S. Patent 4,381,315.

Zghal, M. C. (2006). Personal communications.

Zohary, D., & Hopf, M. (2000). *Domestication of Plants in the Old World: the Origin and Spread of Cultivated Plants in West Asia, Europe, and the Nile Valley* (3rd Ed.). (pp.16-59). New York, NY: Oxford University Press.

APPENDIX I

Conversion of the units shown in DRR curves into fundamental units of gas production

Conversion of the DRR values shown in Table 4.3 and 4.4 into fundamental units (e.g., kmol CO_2 per kg of dough per second) can also obtained. For any given temperature, the time dependence of carbon dioxide production per unit mass of dough (i.e., kmol CO_2 per kg of dough), $\bar{c}$ or $\bar{z}$, can be obtained from the empirical equations shown in Table 4.3 and in Table 4.4 for ADA and GDL and SAPP and KAT, respectively, after adjusting the dimensional units of the pre-exponential coefficients as follows.

For ADA and GDL:

$$\bar{a} = \frac{a * Sodium\ Bicarbonat\ e\ Level\ (\%)}{8.4 \times 10^{6} \times Dough\ Mass\ (kg)}$$

where, $\bar{a}$ is the maximum level of CO_2 production in kmol CO_2 per kg of dough.

For SAPP and KAT:

$$\bar{z}_{\infty} = \frac{z_{\infty} * Sodium\ Bicarbonat\ e\ Level\ (\%)}{8.4x10^{6} \times Dough\ Mass\ (kg)}$$

$$\bar{a} = \frac{a * Sodium\ Bicarbonat\ e\ Level\ (\%)}{8.4x10^{6} \times Dough\ Mass\ (kg)}$$

$$\bar{b} = \frac{b * Sodium\ Bicarbonat\ e\ Level\ (\%)}{8.4x10^{6} \times Dough\ Mass\ (kg)}$$

where, $\bar{z}_{\infty}$ is the maximum level of CO_2 production (kmol CO_2 per kg of dough), and $\bar{a}$ and $\bar{b}$ are pre-exponential coefficients (kmol CO_2 per kg of dough).

Further, the rate of carbon dioxide production for ADA and GDL and SAPP and KAT can be obtained by taking the first derivative of $\bar{c}$ and $\bar{z}$, respectively, with respect to time:

$$\frac{d\bar{c}}{dt} = \frac{d(\bar{a} * (1 - e^{-kt}))}{dt} = \bar{a}\, k\, e^{-kt}$$

$$\frac{d\bar{z}}{dt} = \frac{d(\bar{z}_{\infty} - \bar{a}e^{-k_1 t} - \bar{b}e^{-k_2 t})}{dt} = \bar{a}k_1 e^{-k_1 t} + \bar{b}k_2 e^{-k_2 t}$$

The maximum rate of carbon dioxide production is given by the initial slope of the exponential curve (immediately after the onset of fermentation):

$$\left(\frac{d\bar{c}}{dt}\right)_{max} = \bar{a}\, k$$

$$\left(\frac{d\bar{z}}{dt}\right)_{max} = \bar{a}k_1 + \bar{b}k_2$$

For instance, it can be found that the maximum rate of carbon dioxide production in GDL (HL) at 27 °C is 1.94 x 10^{-6} kmol CO_2 kg^{-1} s^{-1} and that of SAPP (HL) at 27 °C is 4.14 x 10^{-6} kmol CO_2 kg^{-1} s^{-1}. These values are not substantially different to those reported in yeasted doughs (1.6 x 10^{-5} kmol CO_2 kg^{-1} s^{-1}) by Chiotellis and Campbell (2003a). However, it must be recognized that the rate of carbon dioxide production in chemically leavened dough is not constant but rather drops exponentially with time, according to the aforementioned equations.

APPENDIX II

Calculations used to determine gas void fraction in chemically leavened dough for constructing Figure 5.7

It is important to note that gas-free specific volume determinations were carried out only in doughs that were chemically leavened with either SAPP 40 or adipic acid when sodium bicarbonate was used at two different concentrations, a high (4.20 g/100g flour) and a low (1.40 g/100g flour) concentration. All other gas-free specific volume measurements were derived from these four measurements. The gas-free specific volume corresponding to dough leavened with 2.80 g of sodium bicarbonate per 100 g flour for these two systems was interpolated from the measurements using high and low levels of sodium bicarbonate. Further, as shown in Table 1, the gas-free specific volume in dough prepared with GDL or potassium acid tartrate was assumed to be equal to that of adipic acid. GDL, potassium acid tartrate and adipic are all organic acids which upon reaction form sodium salts that have anions with relatively similar lyotropic properties (Preston, 1981; Holmes and Hoseney, 1987a). Salt lyotropicity is an important factor for protein aggregation and disaggregation reactions during dough development (Preston, 1989; Hoseney and Holmes, 1987a), as it may affect the overall protein packing upon hydration and thereby the specific volume or density of the gas-free dough (Elmehdi et al., 2004).

Table 1. Gas-free specific volume (g/cm^3) of chemically leavened dough

	Sodium bicarbonate level		
	1.40 g/100g flour	2.80 g/100g flour	4.20 g/100g flour
SAPP 40	0.7849	0.7794	0.7756
Adipic acid	0.8251	0.8084	0.7924
GDL	0.8251	0.8084	0.7924
Potassium acid tartrate	0.8251	0.8084	0.7924

The specific volumes (Tables 4.3 to 4.6) and the gas-free specific volume (Table 6.1) of chemically leavened dough at the end of fermentation were used to calculate gas-void fractions as per Eq. II-2. These void fractions were then plotted as a function of sodium bicarbonate levels (Figure 5.7).

The gas void fraction of fermenting dough at a given time ($\phi(t)$) can be derived from information on its density ($\rho(t)$) and its gas-free density (ρ_{gf}) as per the following equation:

$$\phi(t) = 1 - \frac{\rho(t)}{\rho_{gf}} \qquad \text{(II-1)}$$

Equation II-1 can also be expressed in terms of specific volumes for the final void fraction:

$$\phi_f = 1 - \frac{\psi_{gf}}{\psi_f} \qquad \text{(II-2)}$$

where ψ_f is the specific volume of dough at long fermentation time (~ 60 min after the end of mixing) and ψ_{gf} the specific volume of the gas-free dough.

To determine a dough sample's gas-free specific volume, the void fraction of the experimental dough and its specific volume were needed. The void fraction was determined using x-ray microtomography as per the experimental technique and methodology described in the Materials and Methods section of Chapter 3. To avoid carbon dioxide evolution in the dough, the chemical leavening systems were reacted separately in a portion of the dough's formula water until no gas evolution (i.e., no bubbling) was observed. The reacted (neutralized) salts were then added, along with the other ingredients, to the mixer to prepare the corresponding dough as per the mixing protocol described in Figure 5.1. The specific volume of this mixed dough was derived

from the reciprocal of its density, determined using a 25-mL specific gravity bottle as per the experimental technique described in the Materials and Methods section of Chapter 3. Specific volume was reported as the average of triplicate measurements (three sub-samples obtained from the same dough batch).

APPENDIX III

Calculations employed to construct Figure 5.8

Gas production (cm^3 of CO_2) was calculated using the ideal gas law:

$$V = \frac{nRT}{P} \qquad \text{(III-1)}$$

Where V denotes the volume of CO_2 evolved should the reaction proceed to completion, P is atmospheric pressure (10^5 Pa), n number of moles of carbon dioxide evolved (equal to the number of moles of sodium bicarbonate that had been neutralized), T fermentation temperature (300, 306, or 312 K), and R the universal gas constant (8.315 J mol^{-1} K^{-1}).

Since for every mole of sodium bicarbonate a mole of carbon dioxide is yielded upon its neutralization (Chapter 4), the number of moles of carbon dioxide (n) added to the dough was a function of added levels of sodium bicarbonate as follows:

Low level (LL): n_{LL} = 1.40 g/84 g mol^{-1} = 1.67 x 10^{-2} moles CO_2

Medium level (ML): n_{ML}= 2.80 g/84 g mol^{-1} = 3.33 x 10^{-2} moles CO_2

High level (HL): n_{HL} = 4.20 g/84 g mol^{-1} = 5 x 10^{-2} moles CO_2

Further, as the conversion of sodium bicarbonate into carbon dioxide is not 100% efficient, the actual conversion percentages needed to be determined to estimate actual CO_2 production levels for constructing Fig. 5.8. This information was obtained from gas pressure measurements using the Gassmart apparatus (data taken from Chapter 4) for fermentation temperatures of 27 and 39 °C, whereas the data for 33 °C was interpolated. The actual percentage of conversion of sodium bicarbonate into CO_2 or the maximum percentage of CO_2 production in dough is shown in Table 1.

Table 1. Gassmart study results on maximum CO_2 production (%) in chemically leavened dough formulated with various levels of sodium bicarbonate and fermented at various temperatures*.

	1.40 g $NaHCO_3$/100 g flour			2.80 g $NaHCO_3$/100 g flour			4.20 g $NaHCO_3$/100 g flour		
Sample	300 K	306 K	312 K	300 K	306 K	312 K	300 K	306 K	312 K
SAPP 40	43.4	42.7	41.9	43.4	42.7	41.9	43.4	42.7	41.9
Adipic	66.0	65.5	65.0	67.1	69.3	71.4	67.8	72.6	77.3
GDL	94.8	92.4	90.0	96.6	94.1	91.6	98.4	95.8	93.2
K tartrate	81.3	81.3	81.3	79.1	79.1	79.1	76.9	76.9	76.9

(*) The values corresponding to 306 K were interpolated from the other two readings.

On the other hand, the actual amount (cm^3) of carbon dioxide retained in the dough ($V_{retained}$) during fermentation was a function of the mass of dough and the specific volumes of dough prior to and at the end of fermentation as follows:

$$V_{retained} = V_f - V_i = (\psi_f - \psi_i) \times m \qquad \text{(III-1)}$$

V_f = volume of gas (cm^3 of CO_2) in the dough at the end of fermentation

V_i = volume of gas (cm^3 of CO_2) in the dough at the end of mixing

ψ_f = specific volume of dough at the end of fermentation ($cm^3\ g^{-1}$)

ψ_i = specific volume of dough at the beginning of fermentation ($cm^3\ g^{-1}$)

m = flour + water + NaCl + sodium bicarbonate + acidulant

= 100 + 69.6 + 0.75+ sodium bicarbonate + sodium bicarbonate/NV * 100

Table 2 shows the mass of dough, m, associated with the different experimental treatments.

Table 2. Mass of dough (g) used to calculate carbon dioxide retention in dough (based on the level of sodium bicarbonate in the dough)

Sample	1.40 g $NaHCO_3$/100 g flour	2.80 g $NaHCO_3$/100 g flour	4.20 g $NaHCO_3$/100 g flour
SAPP 40	173.7	177.0	180.4
Adipic	173.0	175.6	178.2
GDL	174.9	179.4	183.9
K tartrate	174.9	179.4	183.9

APPENDIX IV

Calculations for determining the upper limit for the initial concentration of carbon dioxide gas in the bubble

Shah et al. (1998) proposed a mathematical model for predicting the growth of individual bubbles in dough.

The total pressure inside a bubble of diameter D is P_b and the surface tension S. The surface tension causes the pressure inside the bubble to be above the pressure in the liquid, as per the Young-Laplace equation:

$$P_b = P_\infty + \frac{4S}{D} \qquad \text{(IV-1)}$$

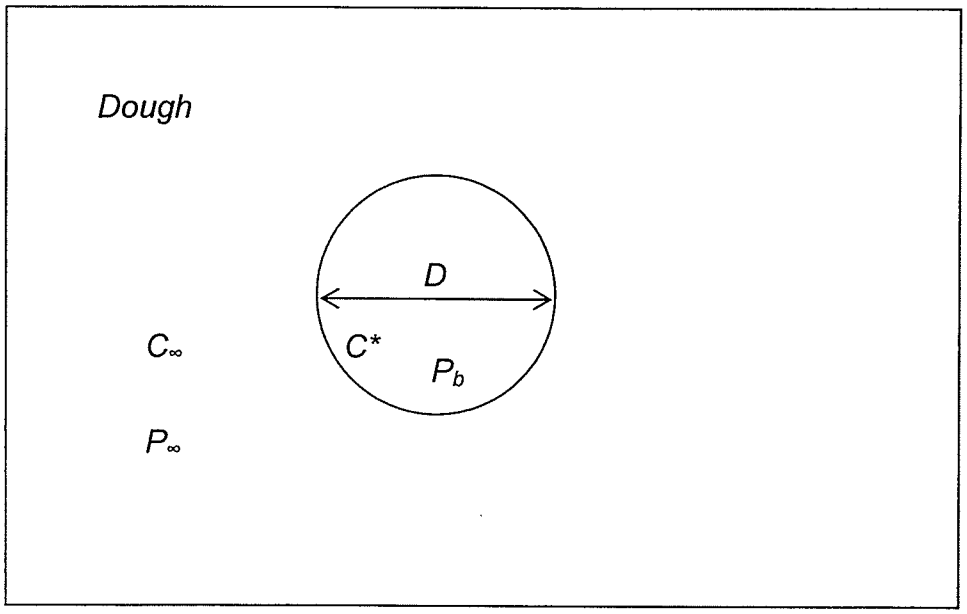

Figure 1. A schematic diagram showing some of the parameters used by Shah et al. (1998) to model the growth of a single bubble containing gaseous carbon dioxide in a matrix containing dissolved carbon dioxide.

Although a term can be added to account for the yield stress of the dough, the growth of the bubble is so slow that it can be assumed that the major contribution to the excess pressure in the bubble is surface tension (Bloksma, 1990a).

Initially, when $D=D_0$, there is nitrogen but essentially no CO_2 in the bubble, so that a concentration driving force for mass transfer of CO_2 is established which permits diffusion of gas into the gas cell interior.

Initially, the bubble only contains n_0 moles of nitrogen. From the ideal gas law:

$$n_0 = \frac{P_{b_0} V_0}{RT} = \frac{(P_\infty + 4S/D_0)\pi D_0^3}{6RT} \tag{IV-2}$$

Since

$$P_{b_o} = P_\infty + \frac{4S}{D_0} \tag{IV-3}$$

Further, nitrogen is assumed to remain in the bubble and not to diffuse out so that the bubble always contains n_0 moles of nitrogen. For a bubble of diameter D containing a total of n moles of gas:

$$n = \frac{(P_\infty + 4S/D)\pi D^3}{6RT} \tag{IV-4}$$

At the long fermentation times, the partial pressure of carbon dioxide in the bubble can be calculated from Equations IV-2 and IV-4 as follows:

$$P_b^{CO_2} = \left(\frac{n - n_0}{n}\right) P_b = \frac{P_\infty (D^3 - D_0^3) + 4S(D^2 - D_0^2)}{D^3} \tag{IV-5}$$

Shah et al. (1998) found that the initial diameter of a bubble can grow up to five times when C_∞ is below saturation (C_∞ < 1.917 kg CO_2 per m^3 dough). As a result, for our initial diameter of 100 μm (based on information from Chapter 3), then we find that:

$$P_b^{CO_2} = \frac{1x10^5 * [(500x10^{-6})^3 - (100x10^{-6})^3] + 4 * 0.040 * [(500x10^{-6})^2 - (100x10^{-6})^2]}{(500x10^{-6})^3}$$

$$P_b^{CO_2} = 99{,}504 Pa$$

Nomenclature

C^* = solute concentration at interface, kmol m^{-3}
C_∞ = solute concentration in dough, kmol m^{-3}
D_0 = Initial bubble diameter, m
D = bubble diameter, m
n = number of moles of gases (nitrogen and carbon dioxide) in a bubble, kmol
n_0 = initial number of moles of gas (nitrogen) in a bubble, kmol
P_b = solute pressure in bubble, Pa
P_{b_b} = initial solute (nitrogen) pressure in bubble, Pa
$P_b^{CO_2}$ = partial pressure of carbon dioxide in bubble, Pa

P_∞ = solute pressure in dough, Pa
R = universal gas constant, J $kmol^{-1}$ K^{-1}
T = absolute temperature, K
V_0 = initial bubble volume, m^{-3}
S = surface tension, N m^{-1}

APPENDIX V

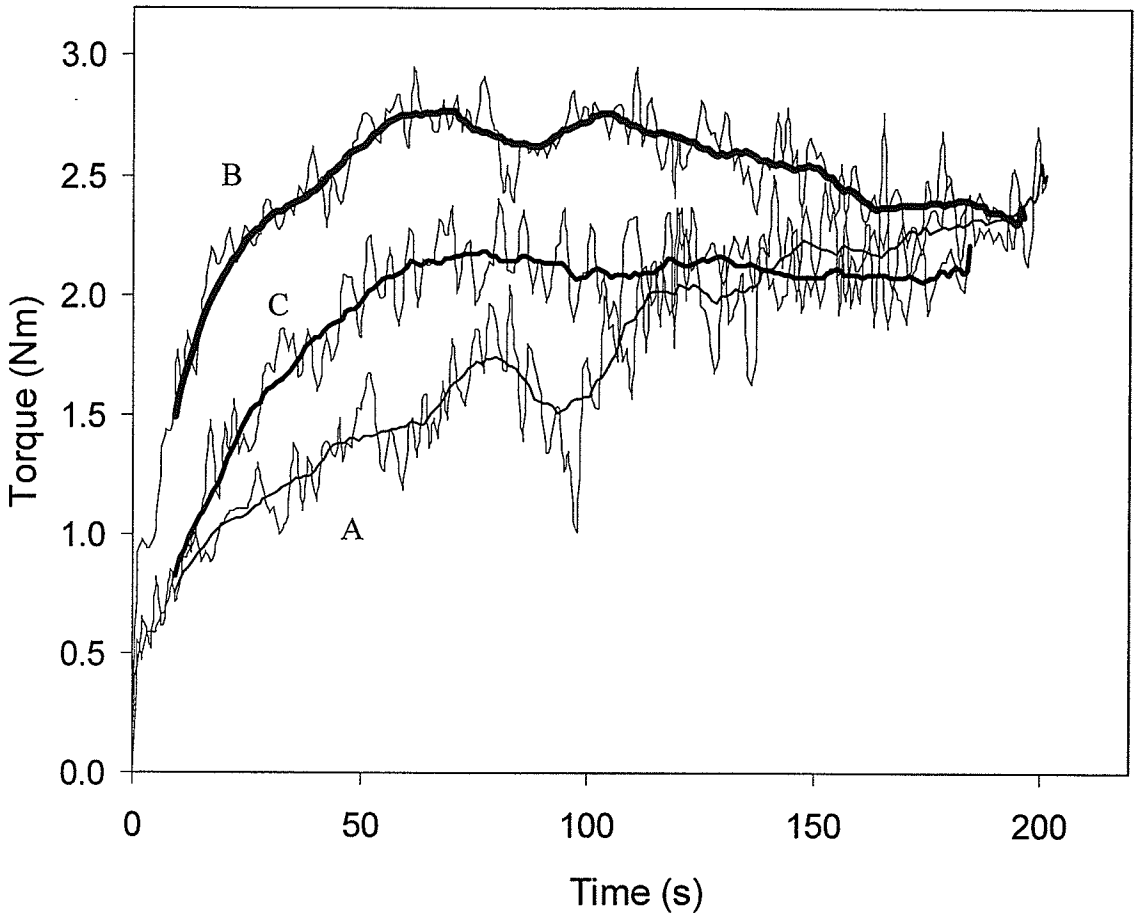

Figure 1. Representative Tweedy 1 mixing curves of strong English flour dough formulated with no added leavener (CONTROL) and mixed under vacuum (7.5 cm Hg) (A), at atmospheric pressure (75 cm Hg) (B), and at over-pressure (150 cm Hg) (C). Original trace of torque (———) and 20 s moving average (▬▬▬). Total work input, measured as TSE, was 40 kJ kg^{-1}.

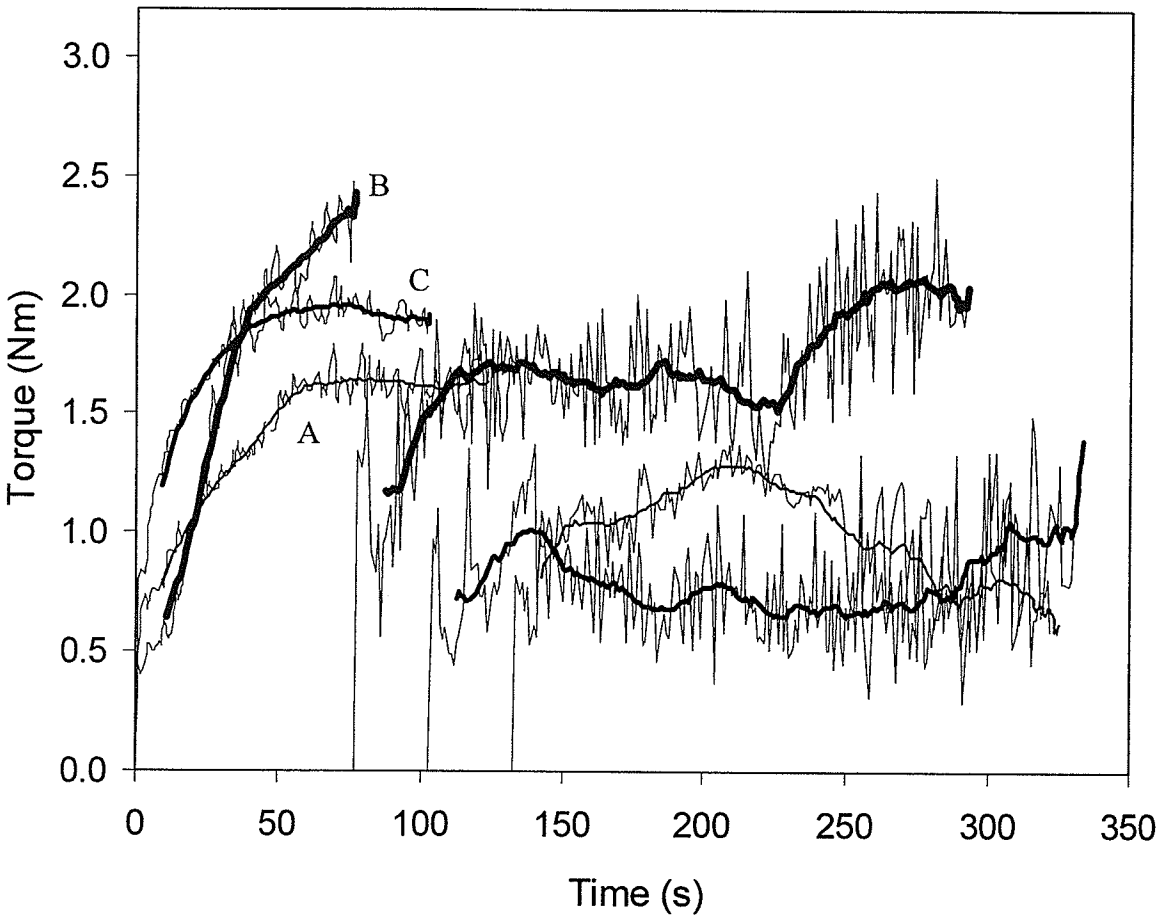

Figure 2. Representative Tweedy 1 mixing curves of strong English flour dough formulated with SAPP and mixed under vacuum (7.5 cm Hg) (A), at atmospheric pressure (75 cm Hg) (B), and at over-pressure (150 cm Hg) (C). Original trace of torque (———) and 20 s moving average (▬▬▬). The leavening system was added to the other dough ingredients after the mixer delivered an initial work input of either 10 kJ (B) or 20 kJ (A & C) per kilogram of dough (shown as a break in the originally recorded torque). Total work input, measured as TSE, was 40 kJ kg^{-1}.

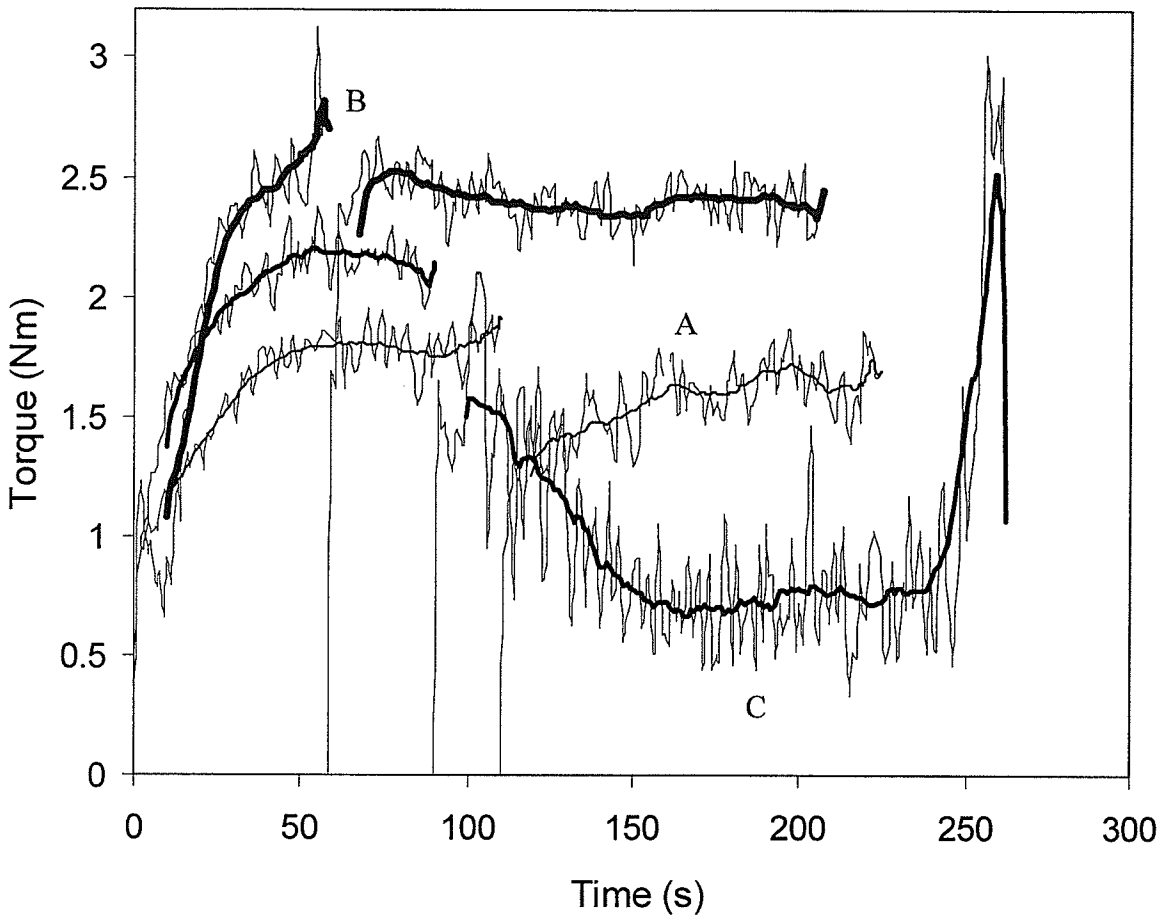

Figure 3. Representative Tweedy 1 mixing curves of strong English flour dough formulated with ADA and mixed under vacuum (7.5 cm Hg) (A), at atmospheric pressure (75 cm Hg) (B), and at over-pressure (150 cm Hg) (C). Original trace of torque (———) and 20 s moving average (———). The leavening system was added to the other dough ingredients after the mixer delivered an initial work input of either 10 kJ (B) or 20 kJ (A & C) per kilogram of dough (shown as a break in the originally recorded torque). Total work input, measured as TSE, was 40 kJ kg^{-1}.

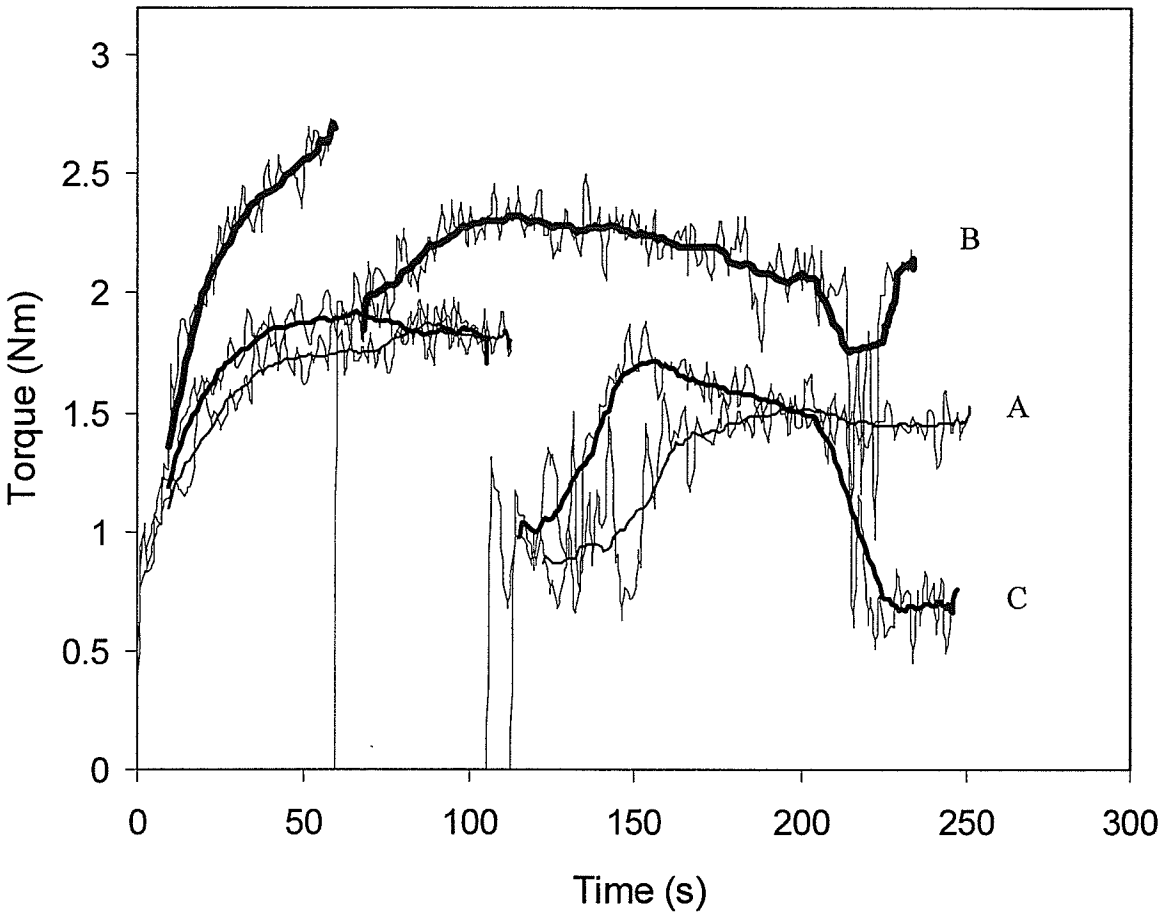

Figure 4. Representative Tweedy 1 mixing curves of strong English flour dough formulated with KAT and mixed under vacuum (7.5 cm Hg) (A), at atmospheric pressure (75 cm Hg) (B), and at over-pressure (150 cm Hg) (C). Original trace of torque (——) and 20 s moving average (——). The leavening system was added to the other dough ingredients after the mixer delivered an initial work input of either 10 kJ (B) or 20 kJ (A & C) per kilogram of dough (shown as a break in the originally recorded torque). Total work input, measured as TSE, was 40 kJ kg^{-1}.

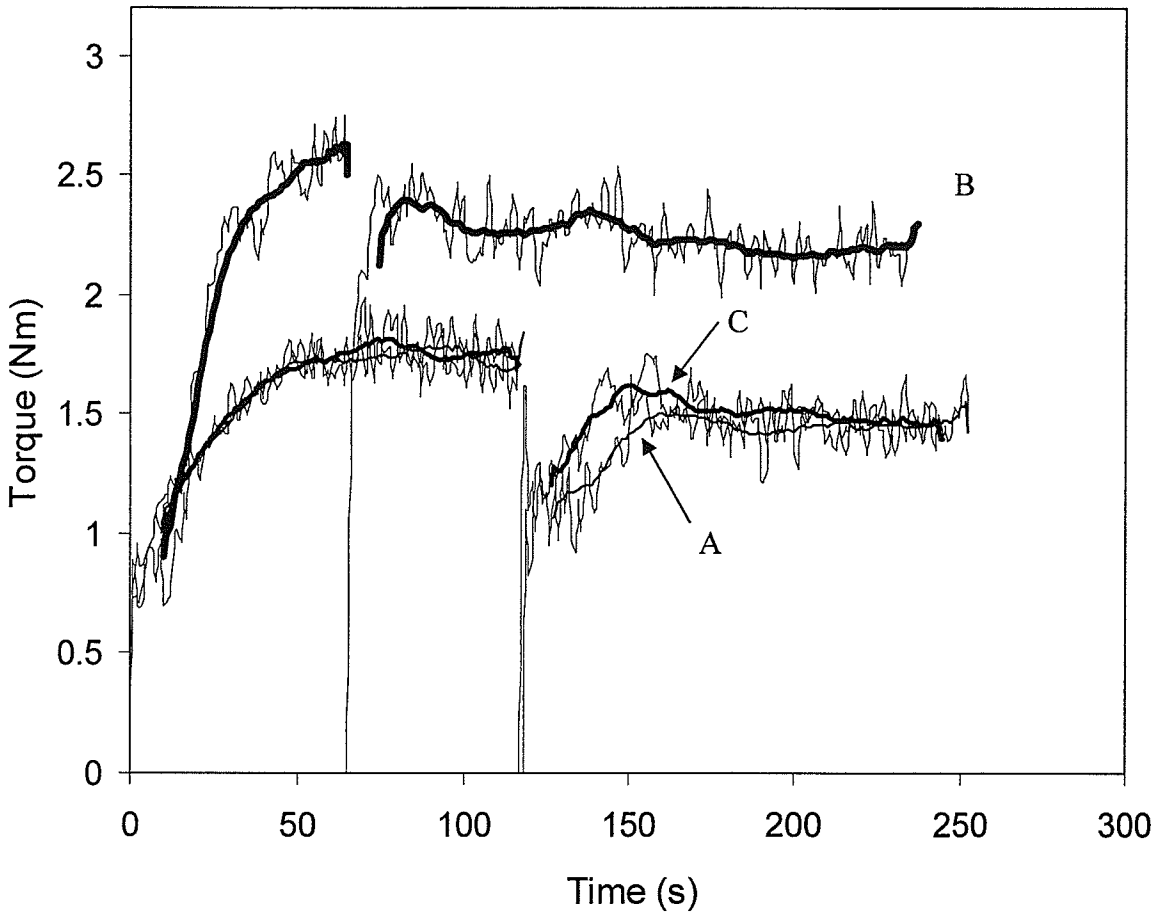

Figure 5. Representative Tweedy 1 mixing curves of strong English flour dough formulated with GDL and mixed under vacuum (7.5 cm Hg) (A), at atmospheric pressure (75 cm Hg) (B), and at over-pressure (150 cm Hg) (C). Original trace of torque (——) and 20 s moving average (——). The leavening system was added to the other dough ingredients after the mixer delivered an initial work input of either 10 kJ (B) or 20 kJ (A & C) per kilogram of dough (shown as a break in the originally recorded torque). Total work input, measured as TSE, was 40 kJ kg^{-1}.

Appendix VI

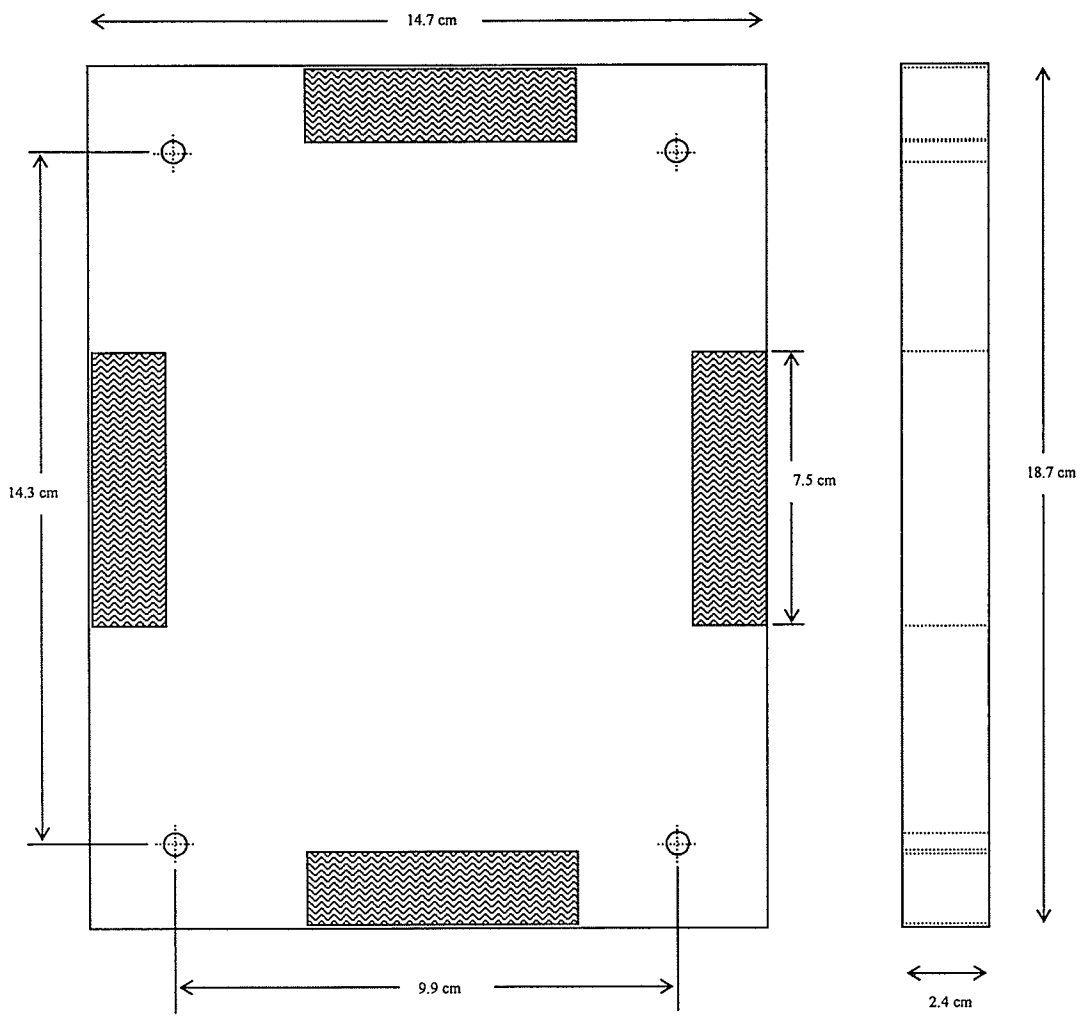

Figure 1. Front (left) and side (right) view of sample holder used for density measurements. An identical sample holder was also used for ultrasonic measurements of dough containing SAPP and ADA. Only one of two acrylic blocks (made of Plexiglas®) is drawn. Shaded areas represent spacers (7.5 x 2.0 cm). The four circles show the position where the tightening screws passed through.

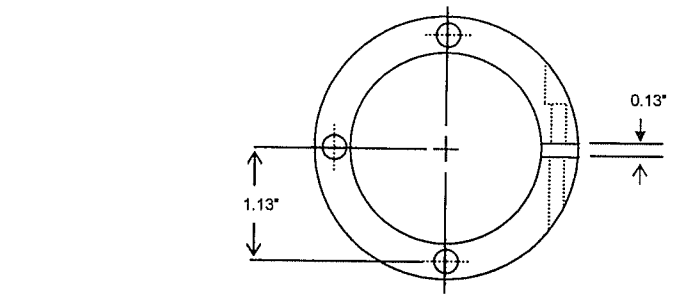
0.13"
1.13"

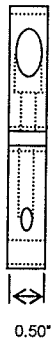
0.50"

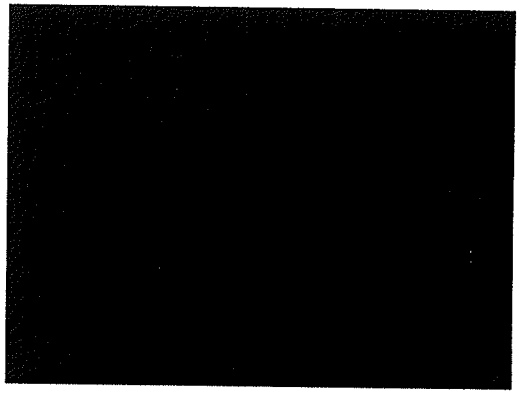

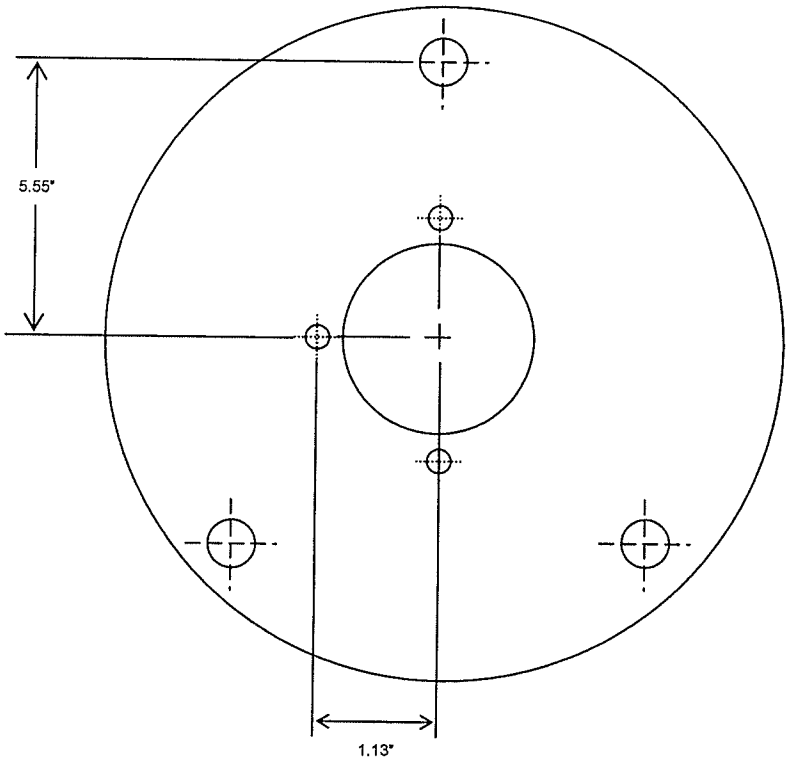
5.55"
1.13"

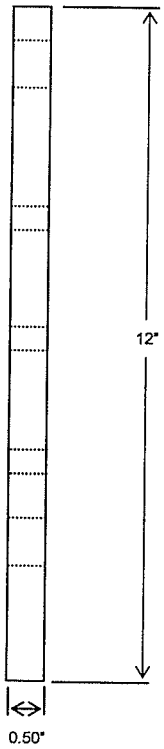
12"
0.50"

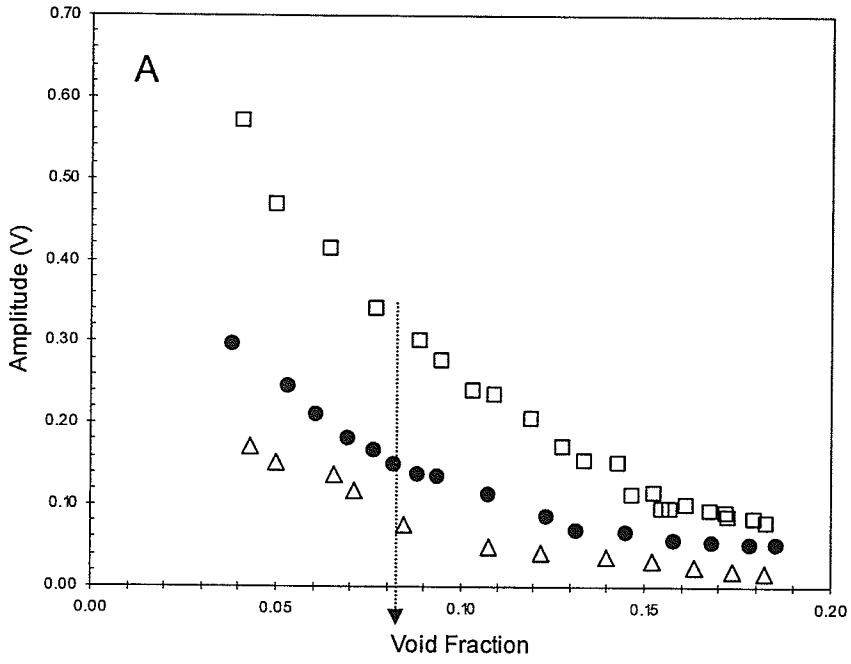
A
Amplitude (V)
0.70
0.60
0.50
0.40
0.30
0.20
0.10
0.00
0.00
0.05
0.10
0.15
0.20
Void Fraction

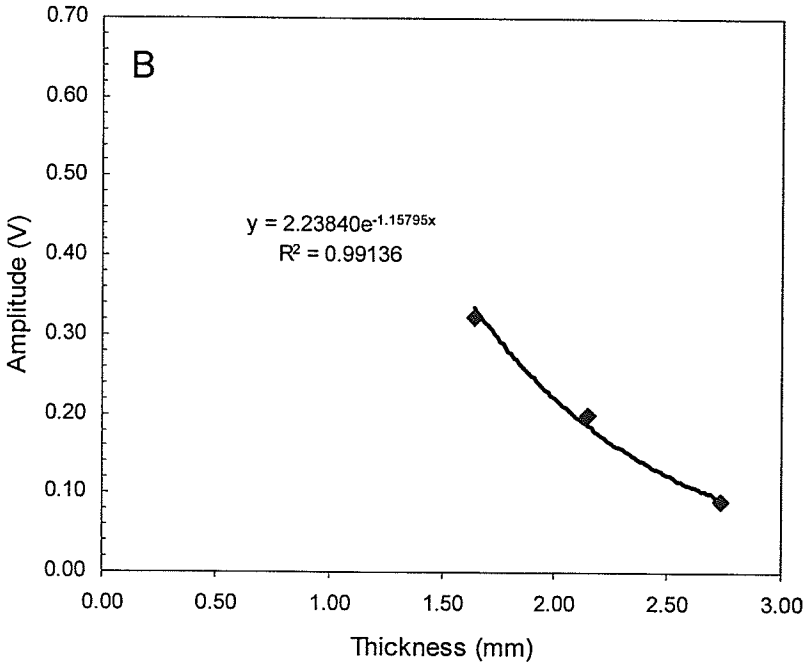
B
y = 2.23840e-1.15795x
R² = 0.99136
Amplitude (V)
0.70
0.60
0.50
0.40
0.30
0.20
0.10
0.00
0.00
0.50
1.00
1.50
2.00
2.50
3.00
Thickness (mm)

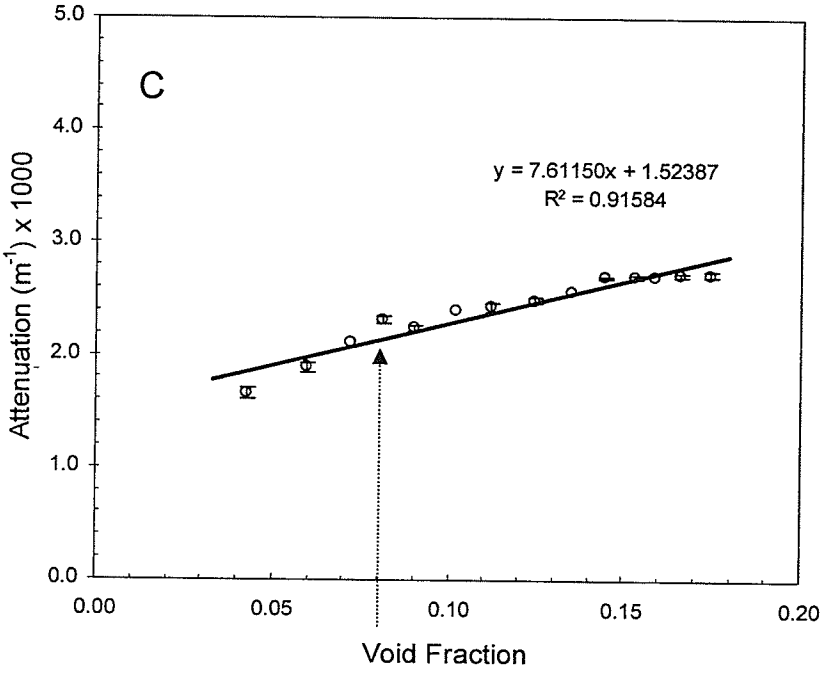

Figure 3. Sequence of steps (A→ B → C) followed to calculate the attenuation of ultrasonic signal through dough systems that had been chemically leavened with SAPP or ADA; illustrated here for dough chemically leavened with SAPP [5.83 g of SAPP 40 and 4.20 g sodium bicarbonate]. First, (A) the amplitude of the ultrasonic signal was plotted as a function of void fraction for various dough thickness: 1.64 mm (open squares), 2.15 mm (filled circles), and 2.74 mm (open triangles). Second, (B) at a specified void fraction, the signal amplitude decay was plotted as a function of sample thickness. Here the symbols represent experimental data and the curve was a fit to the data of the decaying exponential function A (L) = A_0 exp (-α L/2) + y_0 where L represents sample thickness and y_0 represents the background contribution. Finally, (C) the attenuation coefficient (α) was plotted as a function of void fraction (C).

APPENDIX VII

Calculations used to determine the CO_2 retained to CO_2 evolved for constructing Figure 8.5

The data shown in Figure 8.5 was taken from the data shown in Figures 8.3 (CO_2 gas retention) and 8.2 (CO_2 gas evolution). From these two figures, the CO_2 retained and CO_2 evolved, respectively, in a given time period can be obtained from the following relationship:

$$n_{t_2-t_1} = \left(\frac{1}{\rho_{t_2}} - \frac{1}{\rho_{t_1}}\right) * \rho_{gf} * \frac{P}{RT} * \frac{1}{1000} \qquad \text{(VII-1)}$$

$$n^*_{t_2-t_1} = n^*_{t_2} - n^*_{t_1} \qquad \text{(VII-2)}$$

where $n_{t_2-t_1}$ and $n^*_{t_2-t_1}$ are the number of kmol of CO_2 retained and the number of kmol of CO_2 evolved by a chemically leavened dough per unit volume of gas-free dough (kmol CO_2 m^{-3} of gas-free dough) between consecutive fermentation times t_1 and t_2, respectively, ρ_{t_1} and ρ_{t_2} are the experimental dough densities at consecutive fermentation times t_1 and t_2, ρ_{gf} is the density of the gas-free dough (kg m^{-3}), P is atmospheric pressure (10^5 Pa), T fermentation temperature (300 K), and R the universal gas constant (8.315 J mol^{-1} K^{-1}). See Figure 8.2 and 8.3 for graphic representations of the kmol of CO_2 evolved per m^3 of gas-free dough *versus* fermentation time, and the density of the experimental doughs *versus* fermentation time, respectively. To create Figure 8.5, the ratio of $n_{t_2-t_1}$ to $n^*_{t_2-t_1}$ was taken and then expressed as a function of the void fraction of the dough at time t_2. This procedure was repeated for all fermentation times.

For instance, Figure 8.3 shows that between fermentation times t_1 = 723 s and t_2 = 967 s (third and forth data points, respectively), the density of KAT dough changed from

782 to 729 kg m^{-3}, whereas the number of kmol of CO_2 evolved increased from 4.70×10^{-2} to 3.29×10^{-2} (as shown in Figure defined above) changed from 915 to 628 kg m^{-3}.

$$n_{t_2-t_1} = \left(\frac{1}{729} - \frac{1}{782}\right) * 1237 * \frac{10^5}{8.315 * 300} * \frac{1}{1000} = 4.61 \times 10^{-3} \text{ kmol } CO_2 \text{ m}^{-3} \text{ gas-free dough}$$

$$n^*_{t_2-t_1} = 4.70 \times 10^{-2} - 3.29 \times 10^{-2} = 1.41 \times 10^{-2} \text{ kmol } CO_2 \text{ m}^3 \text{ gas-free dough}$$

$$\frac{n_{t_2-t_1}}{n^*_{t_2-t_1}} * 100\% = 32.7\%$$

At time $t_2 = 967$ s, the void fraction of the dough is:

$$\phi(t = 967 \text{ s}) = 1 - \frac{\rho(t = 967 \text{ s})}{\rho_{gf}}$$

$$\phi(t = 967 \text{ s}) = 1 - \frac{729}{1237}$$

$$\phi(t = 967 \text{ s}) = 41.1\%$$

The data point (41.1%, 32.7%) is shown in Figure 8.5 as the third data point.